Il me sera très difficile de remercier tout le monde car c'est grâce à l'aide de nombreuses personnes que j'ai pu mener cette thèse à son terme.

Je voudrais tout d'abord remercier profondément le Prof. Dominique Lison et le Dr. Sybille van den Brule pour leur aide. Je suis ravi d'avoir travaillé en leur compagnie car outre leur appui scientifique, ils ont toujours été là pour me soutenir et me conseiller au cours du doctorat, de l'élaboration de cette thèse et en général pendant ces années. Ils ont pris le temps de m'écouter et de discuter avec moi. Leurs remarques m'ont permis d'envisager mon travail sous un autre angle, de grandir professionnellement et personnellement et à oser. Pour tout cela je les remercie.

Je tiens à remercier les membres du jury pour leur participation scientifique et critiques constructives ainsi que le temps qu'ils ont consacré à ma recherche et l'élaboration de ce manuscrit.

Au cours de ces années j'ai eu le grand honneur de faire partie de l'équipe LTAP. Les discussions que j'ai pu avoir pendant les réunions d'équipe, au laboratoire, le midi ou aussi en dehors du travail m'ont beaucoup apporté. Je tiens à remercier particulièrement et vraiment énormément le Sceptical Office, Francine, Saloua, Géraldine, Barbie, François H. et Sandra. Chacun d'eux m'a donné quelque chose d'unique et spécial d'une manière différente, laissant une marque importante en moi. Bien sûr de nombreuses autres personnes m'ont apporté leur coup de main ou simplement un mot d'encouragement ou un sourire: Micaela, Francesco, Violaine, Virginie, Lisa, Pedro, Mathilde, Jeremy, Eleonora, Doriana, Astrid, Marie-Astrid, Emily, Xavier, Geneviève, Youssef, Mihaly, Vincent, Sabrina, Teresinha, Patricia et surement beaucoup d'autres que je ne pourrai pas citer. Je remercie donc toutes ces personnes que j'ai eu l'opportunité et le grand plaisir de rencontrer pendant ma thèse.

Il m'est impossible d'oublier Nadtha pour toutes nos discussions et moments inoubliables passé ensemble qui m'ont accompagné tout au long de mon chemin à Bruxelles. Nadtha n'a pas été seulement une collègue et une amie, mais pour moi a été et est comme une sœur.

Cristina, plutôt une amie que une collègue, avec qui j'ai partagé beaucoup des aventures et j'ai vraiment changé les idées, qui m'a beaucoup soutenu et aidé pendant un période de ma vie.

Je tiens aussi à remercier le Prof. Marbaix, le Dr. Pascal, le Prof. Tetley, le Dr. Thorley et le Dr. Katsumiti pour leur aide précieuse pour ma recherche et pour leur aide et gentillesse.

Je remercie toutes les personnes avec qui j'ai habité (les Puckois) et avec qui j'ai partagé de moments que m'ont permis de m'échapper du travail ou me détendre ou profiter de la vie en général et que donc m'ont soutenu d'une autre manière. Un grand merci à Marc, Alexandra, Miriam, Heini, Mony, Catherine, Cami, Ed, Francesca, Luca, Melinda, les Pinerolesi, Giulia, Lucia, Antonia, Alessio, Charlotte, etc. Ils sont devenus des amis à qui je souhaite tout le courage qu'ils m'ont apporté.

Et enfin, heureusement que ma famille a été à mon côté et qui m'ont soutenue pendant ces nombreuses années à l'étranger. Mes frères m'ont poussé à voir les choses différemment, à être prétentieuse et faire l'impossible pour réaliser les objectives et rêves visés et fixés, et encore plus. Mes parents ont donné et fait tout pour moi et nous, afin que nous puissions réaliser nos rêves. Et je ne pourrai jamais assez les remercier pour tout cela. La générosité est un de leurs grandes caractéristiques.

J'en oublie certainement encore et je m'en excuse.

Encore un grand merci à tous pour m'avoir conduit à ce jour mémorable.

President

Pr. Véronique PREAT	Université catholique de Louvain, Faculté de pharmacie et des sciences biomédicales (FASB), Brussels, Belgium.

Promoter

Pr. Dominique LISON	Université catholique de Louvain, Louvain centre for Toxicology and Applied Pharmacology (LTAP), Brussels, Belgium.

Co-promoter

Dr. Sybille VAN DEN BRULE	Université catholique de Louvain, Louvain centre for Toxicology and Applied Pharmacology (LTAP), Brussels, Belgium.

External jury members

Dr. Sophie LANONE	Institut Mondor de Recherche Biomedicale (IMRB), Inserm U955, Créteil, France.
Dr. Craig POLAND	Institute of Occupational Medicine (IOM), Edinburgh, UK.

Internal jury members

Pr. Jean-Baptiste DEMOULIN	Université catholique de Louvain, Faculté de pharmacie et des sciences biomédicales (FASB), Brussels, Belgium.
Pr. Peter HOET	Katholieke Universiteit Leuven, Pneumonology, Leuven, Belgium.

TABLE OF CONTENT

I. INTRODUCTION

1.1. NANOTECHNOLOGY **11**

1.2. CARBON NANOTUBES **15**

1.2.1. Carbon nanotubes : properties, applications, and toxicity **17**

1.3. CARBON NANOTUBES AND PULMONARY TOXICITY **47**

1.3.1. Inflammation (alveolitis) **47**

1.3.2. Asthma **48**

1.3.3. Cancer **49**

1.3.4. Fibrosis **50**

1.4. REFERENCES INTRODUCTION **52**

II. OBJECTIVES **57**

III. RESULTS

3.1. ADDRESSING NM-RELATED INTERFERENCES IN IN VITRO CYTOTOXICITY ASSAYS

3.1.1. Context and general experimental design **63**

3.1.2. Integrating nanomaterial-related interferences in in vitro cytotoxicity assays: a reliable and fast method **67**

3.1.3. How does this work contribute to nanotoxicology knowledge? **91**

3.2. TOWARDS PREDICTING THE LUNG FIBROGENIC ACTIVITY OF CARBON NANOTUBES:IN VITRO CELL ASSAY VALIDATION

3.2.1. Context and general experimental design **93**

3.2.2. Towards predicting the lung fibrogenic activity of nanomaterials: experimental validation of an in vitro fibroblast proliferation assay **97**

3.2.3. How does this work contribute to nanotoxicology knowledge? **113**

3.3. TOWARDS PREDICTING THE LUNG FIBROGENIC ACTIVITY OF CARBON NANOTUBES: MECHANISMS

3.3.1. Context and general experimental design **115**

3.3.2. Towards predicting the lung fibrogenic activity of MWCNT: key role of endocytosis, kinase receptors and ERK 1/2 signaling **117**

3.3.3. How does this work contribute to nanotoxicology knowledge? **137**

3.4. REVIEW ON CARBON NANOTUBES AND LUNG FIBROSIS MECHANISMS

3.4.1. Context and general review desing **139**

3.4.2. Mechanisms of carbon nanotube induced fibrosis: towards building an Adverse Outcome Pathway (AOP) **143**

3.4.3. How does this work contribute to nanotoxicology knowledge? **169**

IV. GENERAL CONCLUSIONS, PERSPECTIVES AND RECOMMENDATIONS **175**

ABBREVIATION LIST

A549	Human lung type II epithelial cell
AOP	Adverse outcome pathway
ATII	Primary human alveolar type II epithelial cell
BALB-3T3	Mouse embryonic fibroblast
BEAS-2B	Human bronchial epithelial cell
BSA	Bovine serum albumin
CB	Carbon black
CNT	Carbon nanotube
DNA	Deoxyribonucleic acid
EC	European Commission
ECM	Extracellular matrix
ENM	Engineered nanomaterial
FBS	Fetal bovine serum
GM-CSF	Granulocyte-macrophage colony-stimulating factor
HFL-1	Human lung fibroblast
IL	Interleukin
J774	Mouse peritoneal macrophage
LA4	Mouse alveolar epithelial cell
MLg	Mouse lung fibroblast
MW	Multi-wall
NIOSH	National Institute for Occupational Safety and Health
NM	Nanomaterial
NO	Nitric oxide
PDGF	Platelet-derived growth factor
REL	Recommended exposure limit
SW	Single-wall
TEM	Transmission electron microscopy

TGF	Transforming growth factor
THP-1	Human monocytic cell
TNF	Tumor necrosis factor
TT1	Transformed human alveolar type-I-like epithelial cell
VEGF	Vascular endothelial growth factor
WST	Water soluble tetrazolium salt

ABSTRACT

Carbon nanotubes (CNT) are molecular-scale tubes of graphene sheets rolled into cylinders with peculiar characteristics that make them highly attractive for numerous industrial applications. Thus, investigating the health hazards of CNT is of great importance in view of the increased potential for human exposure within occupational, environmental, and consumer environments. Several studies have already shown that CNT can induce inflammatory, fibrotic or carcinogenic reactions in the lung of experimental animals. These toxic responses appear, however, determined by the physico-chemical characteristics of CNT.

This work focuses on lung fibrosis, a process involving the proliferation and activation of fibroblasts. The main objectives were (1) to understand the mechanisms mediating the fibrogenic activity of CNT by investigating their direct and indirect (via macrophages and epithelial cells) effects on fibroblasts and (2) to develop valid in vitro models to predict the fibrogenic activity of CNT. An additional objective was to assess and to identify physico-chemical properties of CNT that determine their fibrogenic activity. As CNT have been shown to interact with several toxicological assays, we first designed an adapted protocol of the WST-1 cell viability assay to avoid or take into account interferences of nanomaterials.

Our data demonstrate that the direct in vitro activity of CNT on fibroblast proliferation strongly reflects their fibrogenic activity in vivo, supporting a predictive value of this in vitro endpoint. Kinase receptors, ERK 1/2 signaling and endocytosis were identified as mechanisms involved in fibroblast proliferation induced by fibrogenic CNT. In addition, we showed that CNT indirectly stimulate fibroblast differentiation, via epithelial cells and macrophages, highlighting the contribution of these cells in the development of fibrosis. We found that the release of IL-6 from epithelial

cells is another useful biomarker, in addition to the proliferative activity of CNT on fibroblasts, to predict the toxic potential of CNT.

The results also confirm that the length and diameter of CNT constitute important physico-chemical determinants of their capacity to induce lung fibrosis.

Finally, we have organized, analyzed and integrated all the current knowledge concerning the mechanisms of action of CNT relevant for their pro-fibrotic activity in a tentative adverse outcome pathway (AOP). This provides a global picture of the complex network of events contributing to the fibrogenic activity of CNT, and allows identifying predictive in vitro endpoints useful for the toxicological assessment of new and emerging CNT.

I. INTRODUCTION

1.1. NANOTECHNOLOGY

The concept of nanotechnology, a word derived in part from the Greek term “nano” meaning ”dwarf”, was seeded for the first time by the physicist Richard Feynman in December 1959 during his lecture “There’s Plenty of Room at the Bottom” at the American Physical Society at Caltech. In this famous lecture, Feynman considered the possibility of direct manipulation of individual atoms as a more powerful form of synthetic chemistry than those used at the time, and imagined that a day things could be miniaturized.

“*I don’t know how to do this on a small scale in a practical way, but I do know that computing machines are very large; they fill rooms. Why can’t we make them very small, make them of little wires, little elements, and by little, I mean little?”*

Currently, nanotechnology is an emerging science with a multidisciplinary approach that studies materials with morphological features on the nanoscale, where unique phenomena enable novel applications that may have benefits to the entire society. However, defining nanomaterials (NM) is not simple, and in October 2011 the European Commission (EC) published a definition for these materials after more than six years of scientific considerations. According to EC definition, a nanomaterial is:

- *A natural, incidental or manufactured material containing particles, in an unbound state or as an aggregate or as an agglomerate and where, for 50 % or more of the particles in the number size distribution, one or more external dimensions is in the size range 1 nm - 100 nm.*
- *In specific cases and where warranted by concerns for the environment, health, safety or competitiveness the number size distribution threshold of 50 % may be replaced by a threshold between 1 and 50 %.*

- *By derogation from the above, fullerenes, graphene flakes and single wall carbon nanotubes with one or more external dimensions below 1 nm should be considered as nanomaterials.*

NM are interesting because they present a higher surface area per mass unit than conventional materials and may possess new properties. As a result, the implementation of these properties can be exploited to provide products with enhanced applications, from machines to medicine. The advent of nanotechnology is considered to be the biggest engineering innovation since the Industrial Revolution. Engineered nanomaterials (ENM) are used in many commercial products and industrial practices, and can be found in everyday objects, including electronic components, scratch-free paint, sports equipment, cosmetics, food color additives, and surface coating. Moreover, NM have found a wide-spectrum of applications in biomedical area and healthcare, especially in medical imaging and diagnosis, pharmaceuticals, drug delivery and therapy (O'Brien and Cummins, 2008). The global NM market was valued at $3.4 billion in 2014 and is expected to reach $11.8 billion by 2020 showing a compound annual growth rate of 23.1% (Mordor-Intelligence-LLP, 2015).

However, recent studies have shown that the distinctive characteristics of NM, in particular their high number and surface area per unit mass, not only make these materials superior to traditional bulk counterparts for industrial and biomedical applications, but may also affect their potential toxicity (Arora et al., 2012). Thus, as suggested by Shvedova et al. (Shvedova et al., 2009), we can illustrate NM as the two heads of Janus, who in Roman mythology was used to symbolise one condition to another, one vision to another, and one universe to another (Figure 1).

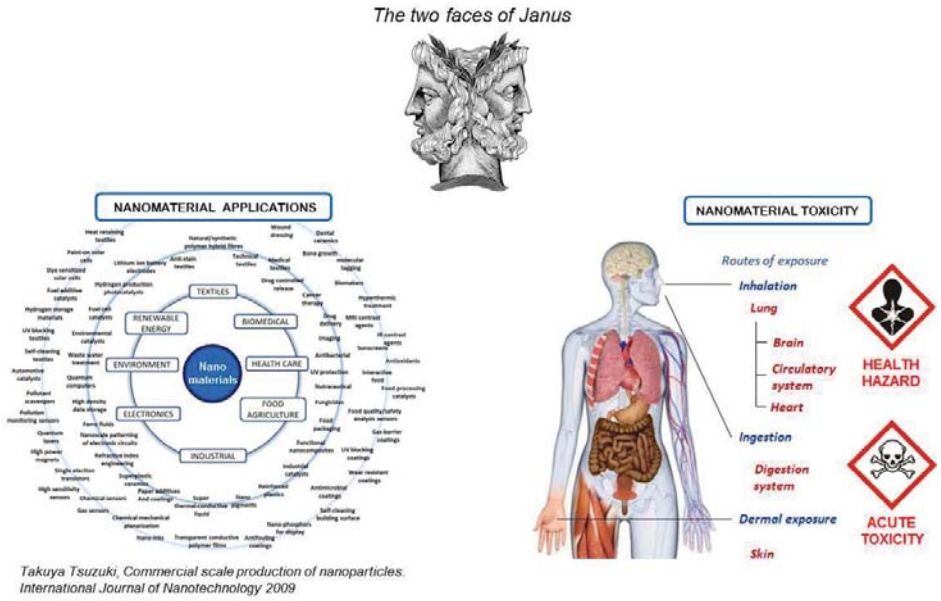


Figure 1. The two faces of Janus-like properties of nanomaterials.

Indeed, several papers have shown potential adverse effects caused by exposure to different types of ENM (Borm et al., 2006; Elsaesser and Howard, 2012) and there is little understanding of their toxicological properties and their long-term impact on human health. The potential for NM exposure is not just in the industrial workplaces, as generally thought, but also in the home environment (Li et al., 2010). The release of NM into the environment can occur through many processes, such as spilling and washing consumer products incorporating NM; during synthesis and production; as an accidental release during transport or use; from industries that exploit nanotechnology, for example waste-water treatment and drug delivery. In general, the principal route of exposure to NM is via inhalation. Exposure to metal NM, as well as carbon-based NM, in the workplace environment has become a common event (Oberdorster et al., 2005; Lee et al., 2015; Shepard and Brenner, 2014). Oral ingestion and dermal exposure

are less well documented. The gastrointestinal tract represents a likely route of entry for many NM, both directly through intentional ingestion or indirectly via NM dissolution from food containers or by secondary ingestion of inhaled particles. Moreover, environmental contamination can increase unintentional ingestion of NM via water, food animals and fish (Bergin and Witzmann, 2013). Uptake via the dermal route, either by injection into the dermal layer or absorption through the pores of the skin, are mainly mediated by exposure from therapeutic or cosmetic applications (Hadrup et al., 2015; Gulson et al., 2015; Smijs and Bouwstra, 2010).

1.2. CARBON NANOTUBES

Carbon nanotubes (CNT) are among the most widely used NM due to their interesting properties, such as mechanical strength, electrical and thermal conductivity, which make them useful for several industrial and biomedical applications. Since their description in 1991 (Iijima 1991), worldwide CNT production and issued patents have grown and currently CNT are incorporated in several commercial products, including rechargeable batteries, sporting goods, boat hulls, water filters (De Volder et al., 2013). However, as discussed for NM, the same physico-chemical properties that make CNT interesting for several applications have also been observed to induce harmful effects. Moreover, CNT are frequently associated to asbestos, due to their needle-like fiber shape, raising concerns that exposure to CNT may lead to fibrosis and pleural diseases, including mesothelioma (Poland et al., 2008). Currently, CNT have been observed to induce harmful and toxic effects both in in vivo and in in vitro studies using lung and skin models. Given these risks, rigorous regulations have been introduced. The National Institute for Occupational Safety and Health (NIOSH) has recommended an occupational exposure limit (REL) of 1 $\mu g/m^3$ together with other strategies for controlling workplace exposures and for implementing a medical surveillance program on exposed workers (NIOSH, 2013). These issues have been addressed in the review below (Ghiazza et al., 2014), which focuses on CNT synthesis, physico-chemical properties, and applications, in particular regarding their use in nanomedicine, and briefly addressed toxicity and physico-chemical properties modulating CNT toxicity.

1.2.1.

Carbon nanotubes:

properties, applications, and toxicity.

Published in “Health and environmental risks of nanomaterials; 2014”

8

Carbon nanotubes: properties, applications, and toxicity

M. GHIAZZA, University of Torino, Italy, G. VIETTI, Catholic University of Louvain, Belgium and I. FENOGLIO, University of Torino, Italy

DOI: 10.1533/9780857096678.3.147

Abstract: Carbon nanotubes (CNTs) are promising candidates for a wide range of applications that are expected to improve our lifestyles, such as alternative forms of energy production, energy storage, and drug delivery. At the same time, there are concerns about their possible adverse effects on human health, since there is evidence that exposure to CNTs induces toxic effects in experimental models. However, CNTs are not a single substance but a growing family of different materials possibly eliciting different biological responses. As a consequence, the hazards associated with the exposure of humans to the different forms of CNTs may be different. Understanding the structure–toxicity relationships would help towards the assessment of the risk related to these materials. Here, we present a snapshot of the current state-of-the art of CNT production, applications, and safety.

Key words: carbon nanotubes, physico-chemical properties, nanomedicine, toxicity, biocompatibility, safety.

8.1 Introduction

Since their discovery in 1991 (Iijima, 1991), the interest of the scientific community and of industry in carbon nanotubes (CNTs) has increased dramatically. Carbon nanotubes exhibit properties that include high thermal and electrical conductivity, mechanical resistance, low density, and tuneable semiconductivity, which renders them useful in a variety of industrial applications, such as components in electronics, energy-storage devices, solar cells, sensors, and as filler in polymeric composites in mechanical applications (Endo *et al.*, 2008). Today, the annual global market in CNTs is estimated to be of the order of hundreds of tons. Carbon nanotubes are mainly used as components of electrodes in lithium batteries or as filler for electrical discharge in composites (Endo *et al.*, 2008). Since the physical properties of CNTs largely depend upon their structure, researchers are endeavouring to produce different types of engineered CNTs with tailored physico-chemical features. Carbon nanotubes should therefore be considered not a single substance but a family of different materials.

Carbon nanotubes have attracted a great interest for their application in medicine (Lacerda *et al.*, 2006, 2007; Boczkowski and Lanone, 2007; Liu *et al.*,

© 2014 Woodhead Publishing Limited

2009; Ji *et al.*, 2010; Zhang *et al.*, 2010). Like fullerenes, CNTs have been shown to rapidly cross the cell membranes (Raffa *et al.*, 2008) and therefore they have been proposed as nanovectors. For this application, CNTs need to be modified to increase their compatibility in water and to bind other entities such as drugs or biomolecules (Cheung *et al.*, 2010). Furthermore, some authors have proposed using CNTs in the manufacture of alternative artificial hard tissues (Sato *et al.*, 2008), tissue scaffold materials for bone formation (Zanello *et al.*, 2006), microcatheters (Koyama *et al.*, 2006), and as substrates for neuronal growth in nervous system disorders (Hu *et al.*, 2004; Roach *et al.*, 2010).

Carbon nanotubes are currently at the centre of a debate on their potential toxicity, and several reviews have been published (Kane and Hurt, 2008; Kostarelos, 2008; Lison and Muller, 2008; Shvedova *et al.*, 2009; Pacurari *et al.*, 2010). A consensus has yet to be reached, since conflicting results have been obtained in toxicological studies. The lack of standardized protocols and the variability of CNTs employed in different studies are the main reasons for this discrepancy (Muller *et al.*, 2005; Kagan *et al.*, 2006; Elgrabli *et al.*, 2008; Poland *et al.*, 2008; Takagi *et al.*, 2008; Ma-Hock *et al.*, 2009; Sakamoto *et al.*, 2009; Fubini *et al.*, 2010). In fact, there is evidence that the responses of cells to CNTs are modulated by their physico-chemical properties. Looking at this evidence from a different viewpoint, the possibility of reducing the toxicity of CNTs by modifying their physico-chemical properties opens the way to the possible design of safe CNTs.

In this review, we look at research associated with the relationships among CNTs, their structure, and their effects on health, as well as the development of tailored synthetic methods aimed not only at increasing the technological performance of CNTs but also reducing their possible impact on human health.

8.2 Physico-chemical properties of carbon nanotubes and their applications

The discovery of CNTs increased the number of possible applications of traditional graphenic materials such as graphite, carbon fibres, fullerenes, and carbon black because of the versatility of these materials. The possibility to tailor the physico-chemical properties of CNTs through synthesis or post-synthesis protocols is one of the reasons for the level of interest in CNTs in various industrial sectors. A discussion of the applications of CNTs is beyond the scope of this review and readers are referred to relevant works in the literature (Endo *et al.*, 2008; Nessim, 2010). Here, we provide an overview of the most interesting properties of CNTs and related applications (summarized in Table 8.1). Medical applications will be discussed separately in section 8.3.

Table 8.1 Physico-chemical properties of carbon nanotubes and applications

Physico-chemical properties	Main industrial applications
Mechanical strength/density	Composites, portable electronic devices
Conductivity	Electronics, electrical materials
Semiconductivity	Electronics, biosensors
Heat capacity/thermal conductivity	Electronics
Hydrophilicity/charge	Medicine, composites
Emission of electrons	Field emission displays

8.2.1 Structural and chemical properties of carbon nanotubes

Carbon nanotubes are made of one (single-walled) or more (multi-walled) graphene sheets rolled-up to form tubes. Single-walled CNTs (SWCNTs) may exhibit external diameters ranging from 0.4 to 4 nm, while multi-walled CNTs (MWCNTs) may reach diameters up to 100 nm. Depending upon the method of synthesis, CNTs may vary from hundreds of nanometres to millimetres in length. The graphene layers may be wrapped to form different geometries. Depending on the arrangement of the sp^2 carbon hexagons, the tubes may be of 'zigzag', 'armchair' or 'chiral' form (Terrones and Terrones, 2003; Galano, 2010). Current synthetic methods generate a mixture of the various forms of SWCNTs or MWCNTs, with each single graphene layer having a different geometry.

A perfectly crystalline carbon nanotube is formed only by hexagonal rings of sp^2 hybridized carbons. However, the CNTs currently produced are far from perfect and various amounts and kinds of defects are possible, including non-hexagonal rings, atom vacancies (topological defects), carbon with sp^3 hybridization, incomplete bonding, and oxygenated functionalities (Ebbesen and Takada, 1995; Charlier, 2002; Galano, 2010). Defects are generated during the nanotube growth process or during post-synthesis treatments. However, defects may also be introduced on purpose, such as following irradiation by charged particles, or removed by annealing processes (see below). A particular kind of defect is the substitution of carbon atoms with other elements like nitrogen (Ayala *et al.*, 2010). Commercially available CNTs may also contain amorphous carbon, fullerenes, graphitic particles, metals derived from the catalysts used in their synthesis (e.g. Fe, Co, Ni, Y), and inert materials (alumina or silica) used as support for the catalysts. The impurities may reach up to 20–30% w/w of the product. However, purification procedures may be applied yielding materials with a carbon content of up to 99%.

8.2.2 Electrical, mechanical, and thermal properties of carbon nanotubes and applications

Metallic CNTs are exceptionally good conductors of electricity. In addition, semiconducting CNTs are considered promising substitutes for silicon in electronic devices (Sharma and Ahuja, 2008). Their nanometric diameter, low density, and anisotropic character make CNTs promising candidates for a wide number of electronic applications, including transistors, conducing continuous fibres (Lu *et al.*, 2012), and nanocomposites (Rahmat and Hubert, 2011). The electrical properties of CNTs, together with their high aspect ratio, also make them useful in the production of sensors (Collins *et al.*, 2000). While metallic CNTs are currently used commercially as a substitute for graphite in energy storage devices, the use of semi-metallic SWCNTs is some way off. Indeed at present, current methods of synthesis provide a mixture of metallic and semi-metallic CNTs and laborious post-synthesis separations are necessary to separate the different CNT forms. Another important potential application of CNTs is as field emitters in cathodes and field emission displays (FED).

Carbon nanotubes are also promising materials for mechanical applications due to their superior mechanical properties, in particular their strength/density ratio, which is higher than that of carbon fibres, and flexibility (Endo *et al.*, 2008). However, the application of CNTs as reinforcing agents in composites is not yet a reality. The performance of CNT-based composites is lowered by a weak CNT–polymer interface and by intrinsic properties of CNTs such as short length and the presence of defects in the tube structure (Endo *et al.*, 2008). Because of their remarkable mechanical properties, CNTs are also attracting interest in medicine for the production of implantable materials or devices. This application will be discussed in section 8.3.3.

Like graphite, CNTs have low heat capacity and high thermal conductivity. Indeed, experimental measurements on single CNTs indicate a thermal conductivity higher than that of diamonds, in the range between 3000 and 3500 W/mK (Balandin, 2011). This property is useful in electrical applications, particularly in microprocessors, since it reduces thermal dissipation (Endo *et al.*, 2008), and may be exploited to produce thermally conductive composites to replace metal parts in several applications, including in motors and generators (Han and Fina, 2011). The thermal conductivity of CNTs strictly depends upon their structural properties, including diameter, length, and chirality of the tubes, the number of structural defects, as well as the presence of any impurities (Pettes and Shi, 2009; Balandin, 2011).

Finally, CNTs are also interesting as microporous materials. The presence of a pore decreases the density of CNTs and increases their surface area, making them useful as electrodes in energy storage for portable electronic devices (Zhai *et al.*, 2011). Carbon nanotubes are also good sorbents for gases and therefore they have been proposed for hydrogen storage. Although the storage capacity of SWNTs

and MWNTs for hydrogen is low at room temperature (Endo *et al.*, 2008; Orinakova and Orinak, 2011), it may be enhanced by the introduction of defects and heteroatoms, functionalization (Orinakova and Orinak, 2011), and decoration with transition metals, in particular palladium (Wu *et al.*, 2012).

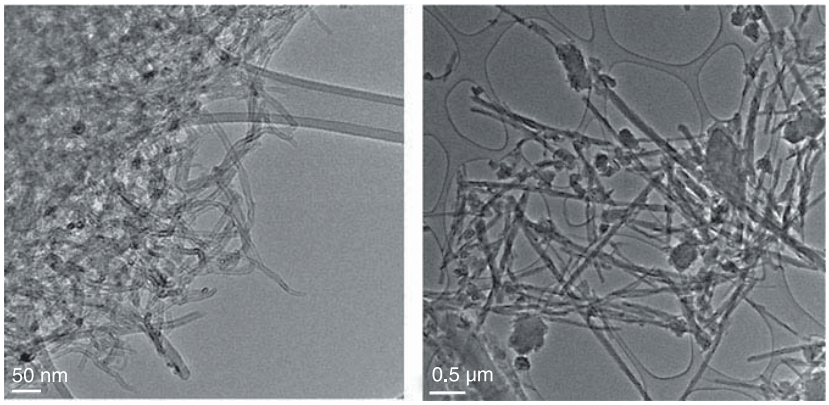
8.2.3 Synthesis and modifications of carbon nanotubes

Carbon nanotubes may be produced in two forms: on substrate and as powders (substrate-free). The first form includes vertically aligned CNTs (VACNTs). In both electronic devices and sensors, semi-conducting CNTs need to interface with a substrate. Therefore, VACNTs are the most interesting product for these applications.

A large number of synthesis methods have been proposed, although the most suitable methods for bulk production are laser ablation, arc discharge, and chemical vapour deposition (CVD). This last method may be used for the synthesis of both substrate and substrate-free CNTs. Arc discharge and laser ablation are based on the vaporization of carbon in an inert atmosphere from a graphite cathode heated by an applied current or by a laser, respectively. Both SWCNTs and MWCNTs may be produced with this method. The properties of CNTs may be modulated by varying the current intensity or the wavelength of the laser, and by introducing catalysts in the cathode. Carbon nanotubes of high crystallinity may be produced by these methods, since the synthesis occurs at high temperature. However, amorphous carbon, catalysts, and fullerenes are present in the final product. The CVD method consists in the catalytic decomposition of a carbon-containing gas on a homogeneous or heterogeneous catalyst. The CNTs may be produced by this method up to millimetres in length. However, since the temperatures used in the process are lower than for arc discharge and laser ablation, the CNTs may exhibit a high number of defects. A particularly efficient method to produce SWCNTs is the HiPCO process based on the use of CO as carbon source. A detailed description of the various methods of synthesis may be found in Nessim (2010).

The yield and properties of CNTs may, to some extent, be modulated by the conditions used during their synthesis. Nevertheless, mixture CNTs with different morphological and structural properties are generally obtained. The transmission electron microscope (TEM) images of two commercially available samples of CNTs are shown in Fig. 8.1. The samples are composed of CNTs of different length mainly organized in bundles. Several amorphous carbon aggregated nanoparticles are detectable.

To produce high-grade CNTs, post-synthesis treatments need to be applied. Briefly, post-synthesis treatments are used (or have been proposed) for the following purposes: (1) improvement of crystallinity by removing structural defects, generally performed by thermal annealing (graphitization) processes; (2) introduction of defects, such as by irradiation with ions (Krasheninnikov and



(a) (b)

8.1 Morphology of carbon nanotubes. Representative TEM images of two different samples of MWCNTs of different diameter. (a) Thin MWCNTs organized in bundles. The MWCNTs in (b) are thick and appear as straight fragments of different length. Aggregates of amorphous carbon nanoparticles are visible. Courtesy of G. Agostini and F. Cesano.

Nordlund, 2010); (3) separation of metallic and semi-metallic CNTs; (4) separation of CNTs with different chirality (Tu *et al.*, 2009); and (5) removal of contaminants. Purification methods include physical separation of CNTs from impurities, gas- or liquid-phase oxidation, and thermal processes (Meyer-Plath *et al.*, 2012). Physical separations are based on sonication, filtration, centrifugation or chromatographic separation of aqueous dispersions of CNTs (Hou *et al.*, 2008; Han and Fina, 2011). Chemical and thermal processes often result in modification of the structure of CNTs. Thermal processes may in fact increase the crystallinity of CNTs while oxidants (e.g. nitric acid or hydrogen peroxide) lead to the introduction of oxygenated surface functionalities at the surface.

Carbon nanotubes may be modified to improve their compatibility with aqueous media or to increase the dispersion in polymeric matrices. Covalent binding to other molecules is also possible (Hirsch, 2002). A rich literature on the chemistry of CNTs is available. Exhaustive reviews on this topic may be found in Banerjee *et al.* (2005) and Tasis *et al.* (2006).

8.3 Carbon nanotubes in nanomedicine

The use of nanomaterials in medicine is increasing rapidly and offers hope for the development of new strategies for the diagnosis and treatment of diseases. Nanomaterials used in nanomedicine include a wide range of organic substances

(e.g. liposomes, dendrimers, solid lipid nanoparticles, polymers). Some preparations based on inorganic materials (gold, iron oxides) have been approved or are in trial. Several other inorganic materials (quantum dots, metal or metal oxide nanoparticles, carbon nanotubes) are currently used for medical applications. Among them, CNTs appear very promising not only as drug and bio-molecule delivery system but also as therapeutic and contrasting agents (Vashist *et al.*, 2011) and as scaffold in tissue engineering or implantable devices (Saito *et al.*, 2009). The major obstacle to the widespread application of CNTs in medicine is their safety. Being completely insoluble in any solvent at any pH, CNTs are thought to remain unaltered in biological fluids and therefore be potentially biopersistent.

Studies on the distribution of CNTs in the various organs are limited (Shevdova, 2009). Nevertheless, the type and degree of functionalization of carbon nanotubes appears critical in determining their toxico/pharmacokinetic profile (Al-Jamal *et al.*, 2012). Previous studies (Wang *et al.*, 2008; Ruggiero *et al.*, 2010; Guo *et al.*, 2007) have found rapid clearance of highly functionalized CNTs (hydroxylated, ammonium, and carboxylated glucosamine CNT) from the systemic blood circulation through renal excretion with minimal accumulation in the reticuloendothelial system (RES). Al-Jamal and co-workers reported that increasing the degree of chemical functionalization in a controlled manner can enhance renal clearance (Al-Jamal *et al.*, 2012). Moreover, they showed that a low degree of chemical functionalization will favour RES organ accumulation.

Some authors have suggested that CNTs may be attached and degraded by endogenous oxidants. Two different routes of degradation were reported: the first is an enzymatic route through a degradation by several peroxidases, such as myeloperoxidase (MPO; Kagan *et al.*, 2010), lactoperoxidase, and eosinophil peroxidase (Shvedova *et al.*, 2012a), while the second route follows a non-enzymatic degradation when CNTs are in contact with simulated phagolysosomial fluid (Liu *et al.*, 2010). In a recent study using MPO-deficient mice, Shvedova *et al.* (2012b) showed that myeloperoxidase contributes to the *in vivo* pulmonary oxidative biodegradation of SWCNTs. Surface functionalization affects the biodegradability of CNTs (Bianco *et al.*, 2011). Indeed, not all types of functionalization seem to favour the degradation of CNTs. Carboxylated CNTs, for example, are markedly affected structurally and partially degraded with respect to non-functionalized CNTs, which are more resistant. The rate of degradation is associated with both the degree of surface functional groups and type of CNTs, with MWCNTs being more resistant than SWCNTs and thus requiring a longer time to be degraded. However, whether such degradation processes would be sufficient to prevent adverse side-effects of CNTs, as well as how efficient the process on the various types of CNTs (SWCNTs vs. MWCNTs, short vs. long) remains unclear.

8.3.1 Carbon nanotubes as nanovectors

Among drug delivery systems, CNTs have emerged as one of the most promising nanovectors for highly efficient delivery of drugs and biomolecules. The rich chemistry of CNTs allows covalent and non-covalent conjugation of various molecules on the side walls and also the encapsulation of drugs and bioactive molecules inside CNTs. Carbon nanotubes are intrinsically hydrophobic and thus cannot be employed directly for drug and biomolecule delivery. Tailored synthesis and surface functionalization must be developed for improving their biocompatibility and dispersibility. Most of the CNT-based drug delivery systems, both with MWCNTs and SWCNTs, have been used for the delivery of anticancer drugs, such as doxorubricin, epirubicin, folate, and platinum-based anticancer drugs (Vashist *et al.*, 2011). Carbon nanotube drug delivery systems have also been assessed for treating many inflammatory and autoimmune diseases (e.g. dexamethasone, dapsone, ketoprofene) (Vashist *et al.*, 2011). Recently, CNTs, in particular amino-functionalized CNTs or polyethylenimine grafted CNTs, have been proposed for the delivery of biomolecules, such as DNA, RNA, and proteins. The first study focusing on the possible utilization of CNTs as a novel gene delivery vector was that of Pantarotto *et al.* (2004a). Generally, DNA and proteins are linked to CNTs by electrostatic interactions or through amino groups inserted at the side walls of CNTs (Awasthi *et al.*, 2009) in order to improve both CNT dispersibility in aqueous solvents and promote gene/protein transfection without using viral vectors, which are very efficient but not completely safe. The development of efficient drug and biomolecule delivery systems requires protection of the biomolecule from degradation, good membrane penetration, and low immunogenicity (Klumpp *et al.*, 2006). In this context, CNTs appear to be most suitable due to their capability to cross the cell membrane by endocytosis without any associated toxicity (Pantarotto *et al.*, 2004b; Singh *et al.*, 2005; Kam *et al.*, 2006; Ji *et al.*, 2010) and to protect drugs and molecules that can be stored inside the tube (Pastorin, 2009).

8.3.2 Thermal and photodynamic therapy

Thermal and photodynamic therapies are very promising approaches to cancer treatment and therefore are currently under investigation since they are considered non-invasive, harmless, and highly efficient techniques (Ji *et al.*, 2010). The traditional photodynamic therapy combines a photosensitizer and near infrared (NIR) light irradiation to destroy cells by generating reactive oxygen species (ROS), such as singlet oxygen ($^1O_2$), superoxide anions (O_2^-), and hydroxyl radicals (·OH), which are the main cytotoxic substances (Lee *et al.*, 2007). Recently, a new therapy based not on the capability of photosensitizers to generate ROS but on the heat generation capability of CNTs combined with a NIR light irradiation technique, has received significant attention. This technique developed

the ability of SWCNTs to absorb NIR radiation (700–110 nm) and to convert it into heat. In 2005, two research groups used this thermal therapy based on a combination of SWCNTs and NIR light irradiation in cancer therapy (Kam *et al.*, 2005; Panchapakesan *et al.*, 2005). Both studies showed a selective destruction of cancer cells in the presence of SWCNTs combined with NIR irradiation while the surrounding healthy cells remained viable (Lee *et al.*, 2007). Other studies report that this approach could be particularly useful for treating small tumours, tumour margins, and micrometastases (Biris *et al.*, 2009). Moon *et al.* (2009) showed complete destruction of tumours 20 days post-treatment in mice treated with PEG-SWCNTs and NIR irradiation. Moreover, they showed that most of the injected SWCNTs were almost completely excreted from the bodies of the mice after two months through the biliary and urinary pathway.

8.3.3 Tissue engineering and implantable materials/devices

Another interesting application of CNTs, exploiting their exceptional mechanical, electrical, and anisotropical properties, is as components in medical devices or scaffolds in tissue engineering (Saito *et al.*, 2009). Carbon nanotubes are good candidate biomaterials for use as scaffold in bone, neuronal and cardiovascular tissue regeneration, or incorporation into other scaffold materials to provide structural reinforcement or confer new properties such as electrical conductivity to direct cell growth. Indeed, various cell types, such as mesenchymal stem cells, osteoblastic and neuronal cells, have been shown to grow extremely well on carbon nanotubes (Zanello *et al.*, 2006; Akasaka *et al.*, 2010; Huang *et al.*, 2011).

Carbon nanotubes are often combined with polymeric substances to improve their physical and chemical characteristics. Carbon nanotubes have been combined with collagen (Endo *et al.*, 2008), but also with chitosan fibres to guide axon re-growth after nerve injuries (Huang *et al.*, 2011) and/or with silk to promote the proliferation and differentiation into neuronal cells of human embryonic stem cells (hESCs) (Chen *et al.*, 2012). Huang *et al.* (2011) have shown that CNT–chitosan composites have superior tensile strength and electrical conductivity compared with chitosan alone and that the composite was not cytotoxic. To improve the neural cell affinity of CNT–chitosan fibres, laminin was incorporated onto the fibre surfaces of the composite, thus increasing cell adhesion. Fan and co-workers (2012) have shown that super-aligned CNT yarn-patterned substrates have a strong effect on neurite growth of the rat hippocampal neurons. Moreover, CNT yarns also minimize branching of neurite growing along the yarns, which is important to neuronal regeneration.

Chen and colleagues (2012) combined CNTs with silk for improving the proliferation and differentiation of human embryonic stem cells (hESCs). The CNT–silk composite was able to induce a higher expression of two proteins (beta-III tubulin and nestin) involved in neuronal differentiation, and longer axons with

higher density. Thus CNT–silk composite can promote neuronal differentiation of hESCs, providing a good opportunity for nerve repair treatments in spinal cord injury and multiple sclerosis.

Carbon nanotubes also show promise as components of biomaterials for bone repair. Several studies have reported that CNTs promote the proliferation of osteoblastic cells *in vitro* (Zanello *et al.*, 2006; Saito *et al.*, 2008) but there have been few reports of bone tissue compatibility of CNTs *in vivo* (Usui *et al.*, 2008; Ogihara *et al.*, 2012). These latter two studies examined bone tissue compatibility of CNTs implanted alone (Usui *et al.*, 2008) and as CNT–alumina ceramic composites (Ogihara *et al.*, 2012) in mice. Both studies demonstrated that CNTs had good bone tissue compatibility, suggesting their use as prostheses in arthroplasty and devices for bone repair (Ogihara *et al.*, 2012).

Finally, CNT-filled nanocomposites have been proposed as microcatheters (Koyama *et al.*, 2006). Nanotube-based catheters were fabricated by incorporating carbon nanotubes into nylon-12 to improve the mechanical properties and reduce thrombogenicity (Endo *et al.*, 2005; Koyama *et al.*, 2006).

The use of CNTs as components in bulk biomaterials poses less concern for health risks compared to their systemic use. However, for biomaterials destined to remain in the body for a long time and subjected to mechanical stress, the possible release of debris needs to be carefully considered.

8.3.4 Carbon nanotubes as antioxidants

Antioxidant substances (e.g. flavonoids and α-lipoic acid) have attracted interest for treating diseases where mitigation of oxidative stress is beneficial, such as in tumours, in cardiovascular diseases or in neurodegenerative disorders (Firuzi *et al.*, 2011). Functionalized fullerenes have also been proposed as antioxidant agents in medicine, since they are potent radical scavengers (Dugan *et al.*, 1997). Indeed, it has been reported that, similar to fullerenes and other carbon-based materials, CNTs are reactive towards free radicals. The use of CNTs in polymeric composites for preserving polymeric matrix from degradation has also been reported (Watts *et al.*, 2003). The susceptibility of CNTs to radical attack is well known and has been exploited to introduce functionalities at their surface (Ying *et al.*, 2003; Banerjee *et al.*, 2005; Tasis *et al.*, 2006). In 2006, Fenoglio *et al.* (2006) reported that purified MWCNTs were able to scavenge hydroxyl radicals. The amount of radicals scavenged by CNTs appeared enough to buffer the oxidative burst of damaged tissues, since a local decrease in reactive oxygen species was observed *in vivo* following the tracheal instillation of MWCNTs in mice (Crouzier *et al.*, 2010). However, CNTs and other graphene materials have been reported to deplete the antioxidant defences of cells by oxidizing glutathione (GSH) through a reaction with oxygen at the surface (Liu *et al.*, 2011). Therefore, CNTs appear to interact with the cellular redox system in several ways, since the overall effect of CNTs on the ROS homeostasis of cells is still to be clarified.

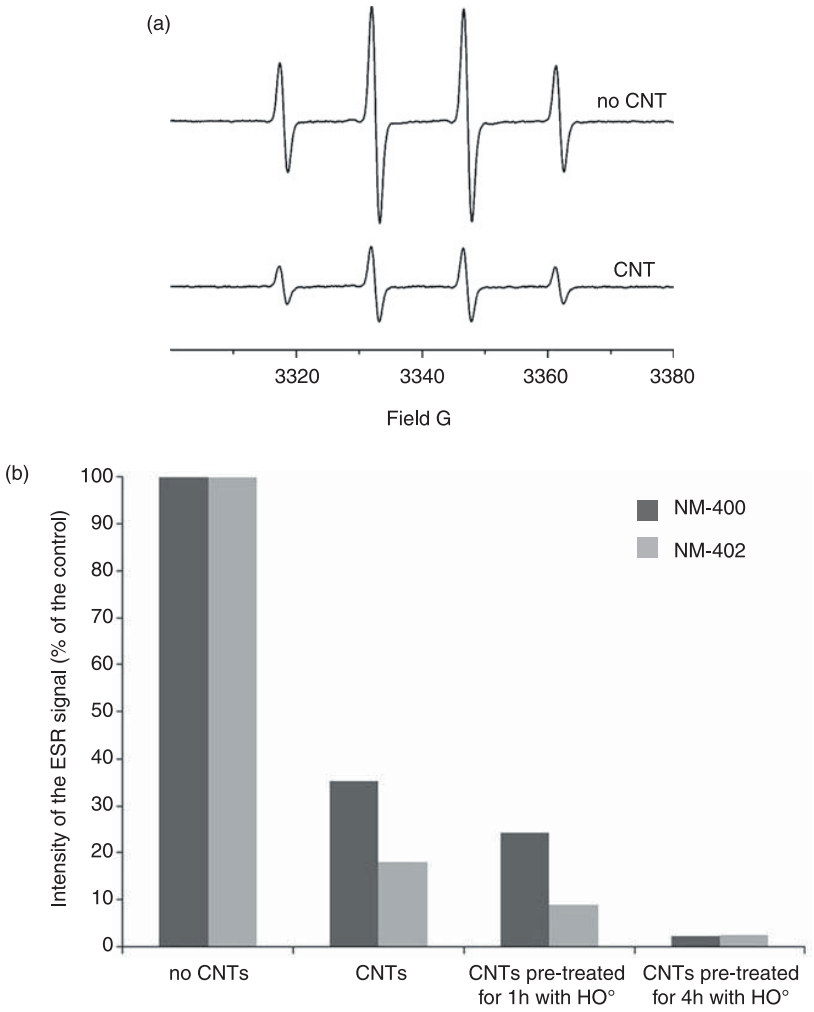
There are indications that the physico-chemical properties of CNTs modulate their antioxidant activity. Theoretical and experimental studies support these findings by showing that the scavenging activity of SWCNTs may be modulated by introducing defects (Fenoglio *et al.*, 2008; Galano, 2010) or by varying their diameter, length, and chirality (Galano, 2009; Martinez and Galano, 2010; Shukla and Mishra, 2010). Moreover, the antioxidant activity may also be modulated by surface functionalization. Recently, Francisco-Marquez *et al.* (2010) reported that the presence of carboxylated functionalities increases the radical scavenging activity of SWCNTs. In contrast, Lucente-Schultz *et al.* (2009) reported that non-functionalized SWCNTs are better radical scavengers than functionalized derivatives. The scavenging activity of a sample of CNTs towards hydroxyl radicals (the most reactive among ROS), evaluated by electron paramagnetic resonance (EPR) spectrometry combined with the spin trapping technique, is shown in Fig. 8.2a. The scavenging potency of two samples of CNTs is shown in Fig. 8.2b. The different antioxidant potency is related to their different origin. The scavenging capacity of both CNTs increases after a pre-treatment with hydroxyl radicals (Fig. 8.2b), suggesting a possible persistent antioxidant activity *in vivo*.

8.4 Carbon nanotube toxicity

The prevention of possible adverse health effects elicited by CNTs is important not just in nanomedicine. The exposure of workers and consumers in both occupational settings and environmentally is becoming more likely with the introduction of CNT-based nanotechnological products and, therefore, validated methodologies for the assessment of risk associated with these materials are urgently required. Unfortunately, some necessary information (e.g. the exposure scenario) is still lacking (Savolainen *et al.*, 2010). Clearly, the risk associated with powdered CNTs is higher than that related to CNTs embedded in a polymeric matrix. Nevertheless, the environmental risk of a CNT-based composite may be high based on the life cycle of the materials and the possible bioaccumulation of CNTs in the environment. Toxicological data are still lacking and a consensus on the hazard represented by CNTs has not been reached. We will summarize here the findings to date for the main endpoints without being exhaustive. More detailed reviews on this topic may be found in the literature (Kane and Hurt, 2008; Kostarelos, 2008; Lison and Muller, 2008; Shvedova *et al.*, 2009; Pacurari *et al.*, 2010).

8.4.1 Lung toxicity

Most experimental studies with CNTs have focused on the respiratory system because inhalation represents the most relevant route of exposure for nanomaterials, especially in occupational settings. *In vivo* studies have reported that CNTs induce inflammatory, fibrotic, and genotoxic effects in the lung of mice and rats upon



8.2 Antioxidant activity of carbon nanotubes. CNTs act as scavengers towards hydroxyl radicals. (a) The signal obtained with the EPR/spin trapping technique in a system generating hydroxyl radicals and the signal obtained in the same system in the presence of CNTs. (b) The scavenging effect of two different samples of CNTs pre-treated for 1 or 4 h with hydroxyl radicals compared with the pristine sample.

intra-tracheal instillation or inhalation exposure (Muller *et al.*, 2005; Shvedova *et al.*, 2005; Chou *et al.*, 2008; Aschberger *et al.*, 2010). Inflammation and pulmonary fibrosis have been associated with an increased risk of lung cancer, thus justifying the assessment of possible genotoxic events accompanying CNT

exposure (Knaapen *et al.*, 2004; Pulskamp *et al.*, 2007; Shvedova *et al.*, 2009). Furthermore, several *in vitro* studies have shown that CNTs can have effects on cell signalling, membrane perturbations, and the production of cytokines, chemokines, and ROS (Chen *et al.*, 2011; Di Giorgio *et al.*, 2011; He *et al.*, 2011; Azad *et al.*, 2012). A strong concern exists about a possible carcinogenic activity of CNTs, and similarities with asbestos fibres have been highlighted (Service, 1998; Sanchez *et al.*, 2009; Donaldson *et al.*, 2010). The induction of neoplastic transformations in pleural mesothelium by CNTs has been reported. However, conflicting data have been obtained (Johnston *et al.*, 2010), as both an ability to induce mesothelioma (Takagi *et al.*, 2008; Sakamoto *et al.*, 2009) and an absence of any carcinogenic response (Muller *et al.*, 2009) were reported. Such variable outcomes may be ascribed to different physical chemical properties among the examined specimens (see section 8.4.5).

8.4.2 Dermal toxicity

Skin is another important route of exposure to toxicants. Several studies have reported skin irritation (e.g. carbon fibre dermatitis and hyperkeratosis) in humans following contact with CNTs, suggesting their possible penetration into the viable epidermis after topical exposure (Shvedova *et al.*, 2003). In an *in vitro* study, Monteiro-Riviere *et al.* (2005) demonstrated that MWCNTs are capable of entering human keratinocytes as well as causing irritation measured as interleukin-8 (IL-8) release. However, there is a lack of evidences that CNTs can cross the stratum corneum or accumulate in dermal tissue following systemic administration. In another *in vitro* study, Murray *et al.* (2009) suggested that metals present as impurities may play a crucial role in the induction of oxidative stress and inflammation in skin following topical exposure to SWCNTs.

8.4.3 Embryotoxicity and neurotoxicity

The relevance of embryotoxicity to risk assessment of nanomaterials is clear. Nevertheless, few studies have focused on this end point. The effects of CNTs on embryonic development have been well studied in aquatic species (Cheng *et al.*, 2007, 2009; Asharani *et al.*, 2008). The zebrafish embryo is an excellent model, as its entire developmental phase takes only about 4 days and takes place outside the mother, allowing direct visualization of the morphological changes. However, the zebrafish model (development and embryo morphology) differs from that of mammals, and findings for one class are not necessarily applicable to another.

Recently, Pietroiusti *et al.* (2011) tested the effect of pristine and oxidized SWCNTs on the development of the mouse embryo. They observed a high percentage of early miscarriages and foetal malformations in females exposed to oxidized SWCNTs. Extensive vascular lesions and increased production of ROS were detected in placentas of malformed gestation products. These results were

confirmed *in vitro*, in an embryonic stem cell test (EST), by identifying oxidized SWCNTs as the more toxic among the tested nanomaterials. Further studies are needed to fully understand the mechanism through which different CNTs can induce embryotoxicity.

As discussed in section 8.3.3, CNTs are applicable in medicine for neuronal regeneration. Yet few *in vivo* studies have been devoted to the evaluation of the toxic effects of CNTs that have accidentally penetrated the body and possibly translocated in the central nervous system. Carbon nanotubes have been reported to elicit toxic effects on dorsal root ganglion (DRG) neurons (Belyanskaya *et al.*, 2009), and to interfere with K^+ channel activity in different cell lines (Park *et al.*, 2003; Xu *et al.*, 2009). It has also been reported that MWCNTs induce cell membrane damage and alter the excitability of chromaffin cells, a neuronal-like model (Gavello *et al.*, 2012).

8.4.4 Repeated and chronic toxicity

Chronic toxicity occurs as a result of a repeated daily exposure to a chemical. The objective of a chronic toxicity study is to determine the effects of a substance following prolonged and repeated exposure. However, as such studies require expensive and time-consuming experiments, limited research has been devoted to the chronic toxicity of CNTs. Furthermore, there is controversy regarding the animal model, the dose and the dose metric, the nanoparticle dispersion protocol, the method and time of exposure.

Qu and co-workers (2012) established a mouse model of chronic exposure to CNTs using intra-peritoneal injection of SWCNTs and MWCNTs. Their results demonstrated that SWCNTs and MWCNTs provoke considerable inflammation, presumably due to their fibre-like shape. Their results also confirmed the length- and size-related structure–activity relationship of CNTs in stimulating inflammatory responses. In contrast, Kobayashi and co-workers (2010) showed no evidence of chronic inflammation, such as angiogenesis or fibrosis, induced by MWCNTs instillation. These results suggest that MWCNTs are processed and cleared by alveolar macrophages.

8.4.5 Physico-chemical properties modulating carbon nanotube toxicity

Toxicological investigations of nanomaterials have demonstrated how some physico-chemical properties affect CNT toxicity. Indeed, there are indications that, depending upon purity, diameter, length, surface charge, functionalization, and aggregation state, CNTs elicit different toxic effects.

Length is considered a crucial factor in CNT toxicity. Schinwald *et al.* (2012) demonstrated that fibres over 4 μm long are pathogenic to the pleura in mice. Other research supports this theory by showing inflammatory and fibrotic effects

only with long (>10 μm) CNTs after exposure to the peritoneal (Kolosnjaj-Tabi *et al.*, 2010) and pleural mesothelial surfaces (Murphy *et al.*, 2011). The deleterious effect of long and straight (>10 μm) CNTs is related to their mechanical interaction with cells: the unsuccessful internalization of long fibres by macrophages may in fact lead to 'frustrated phagocytosis', which activates the inflammatory process. Fibre shape has been proposed as the crucial factor in CNT pleural toxicity (Donaldson *et al.*, 2011). However, other physico-chemical properties are attributable to the mechanism of action of fibres, suggesting that paradigms other than the fibre-shape paradigm ought to be considered (Fubini *et al.*, 2011). Schinwald *et al.* (2012) proposed a threshold length value (4–5 μm) for the induction of acute inflammatory response to pleura in a mouse model. Whether this threshold value will be exploitable for the risk assessment of chronic exposure of humans to CNTs needs further clarification.

The results of Fenoglio *et al.* (2012) suggest that nanotube diameter is an important parameter in toxicological research. A study with two samples of MWCNTs of similar length (<5 μm) and surface reactivity but different diameter (9.4 and 70 nm) showed that thin MWCNTs appeared significantly more toxic than their thicker counterparts *in vivo* (rats, lung) and *in vitro* (murine alveolar macrophages). Similarly, Nagai *et al.* (2011) reported a clear effect of CNT diameter on mesothelial toxicity and carcinogenicity in rats.

The role of defective sites in CNTs has been also investigated in two studies. By keeping all other properties constant, defects generated by grinding appear to activate lung toxicity (Muller *et al.*, 2008) but not carcinogenicity (Muller *et al.*, 2009). Note, however, that in these studies a single kind of defect (i.e. uncompleted bonding generated by grinding) was considered.

The modification of the surface is regarded as an important strategy to decrease the toxicity of nanomaterials. However, in the case of CNTs, the introduction of surface oxygenated functionalities appeared to increase their toxicity in some models (Bottini *et al.*, 2006; Vittorio *et al.*, 2009; Pietroiusti *et al.*, 2011). In contrast, Cheng *et al.* (2008) reported that purified PEGylated SWCNTs, albeit reversibly internalized and translocated into the nucleus, did not exert genotoxicity in mammalian cells in terms of cell cycle distribution and cell division after 5 days of continuous exposure, suggesting that intensive purification and functionalization processes can help improve the biocompatibility of CNTs in biological systems.

Finally, the presence of residual metals dramatically increases the toxicity of CNTs. Redox active metals associated with CNTs (e.g. iron) have been reported to induce oxidative stress mediated toxicity both in an *in vitro* and *in vivo* model (Kagan *et al.*, 2006; Pulskamp *et al.*, 2007). To date, no data on the effect of other impurities (amorphous carbon and inert supports of catalysts) and of tube chirality are available. Table 8.2 provides a list of studies on the effect of physico-chemical properties on the toxicity of CNTs.

Table 8.2 Physico-chemical properties affecting the toxicity of CNTs

Property	Type of CNT	Endpoints/models	Effects	References	Values
Diameter	MWCNT	Cellular viability, phagocytosis, apoptosis/guinea pig alveolar macrophages	Higher toxicity for thick CNTs	Wang *et al.* (2009)	Length: 1–5 μm Diameter: 40–100; 10–20 nm Purity: Ni content different
	MWCNT	Cytotoxicity, uptake/human mesothelial cells Inflammation, cellular viability, carcinogenicity/rats	Higher toxicity for 50 nm CNTs with respect to thick and thin/tangled	Nagai *et al.* (2011)	Length: ~5 μm Diameter: 15 nm (tangled); 50 nm; 100–250 nm Purity: Fe, Cu (amount not reported)
	MWCNT	Cytotoxicity, uptake, oxidative stress induction/murine alveolar macrophages Lung inflammation/rats	Higher toxicity for thin CNTs	Fenoglio *et al.* (2012)	Length: <5 μm Diameter: 9.4 and 70 nm Purity: metal contaminants <0.08%
Length	MWCNT	Lung inflammation and granuloma formation /mice	Long CNTs develop inflammatory and granulomatous response	Poland *et al.* (2008)	Length: 1–5 and 5–20 μm (tangled); 13 and 56 μm Diameter: 15 nm; 10 nm; 85 nm; 165 nm Purity: Fe, Cu, V, Ni, Zn, Co content
	MWCNT	Cytotoxicity, DNA damage/ A459 Lung inflammation/mice	Long and thick CNTs, but not short and thin CNTs, cause DNA damage/ inflammation	Yamashita *et al.* (2010)	Length: 5–15 μm; 1–2 μm Diameter: 20–100 nm; <10
	SWCNT	Lung inflammation, granuloma formation/mice	CNTs > 10 μm induce granuloma formation CNTs < 300 nm excreted from the body	Kolosnjaj-Tabi *et al.* (2010)	Length: >1–2; 1–2 μm; 20–80 nm Diameter: ~1 nm Purity: different Fe content (1.5–25%)

	MWCNT	Pleural inflammation, cellular viability in the mesothelium/ mice	Higher toxicity for longer CNTs	Murphy *et al.* (2011)	Length: 0.5–2, 5–20 and 1–5 μm (tangled); 13 and <56 μm Diameter: 20–30 and 15 nm; 15, 40–50 and 20–100 nm
Defects	MWCNT	Genotoxicity/rat lung epithelial cells Lung inflammation and fibrosis/rats	Defectivity increases the inflammatory and genotoxic potential	Muller *et al.* (2008), Fenoglio *et al.* (2008)	Length: 0.7 μm Diameter: 11 nm Purity: Al, Co, Fe <0.08%
	MWCNT	Carcinogenicity in rats	Carcinogenicity not affected by defects	Muller *et al.* (2009)	Length: 0.7 μm Diameter: 11 nm Purity: Al, Co, Fe <0.08%
Surface functionalities	MWCNT	Cytoxicity/ human T cells	Surface functionalities (oxidized) increase the toxicity	Bottini *et al.* (2006)	Length: 1–5 μm Diameter: 20–40 nm Purity: >95%
	MWCNT	Cytoxicity, oxidative stress/ human neuroblastoma cells	Surface functionalities (oxidized) and impurities increase the toxicity	Vittorio *et al.* (2009)	Length: MWCNT 0.5–2 μm Diameter: >35–40 nm; 20–40 nm Purity: 97–99%
	SWCNT	Embryotoxicity in mice, and mouse embryonic stem cell and NIH3T3	Surface functionalities (oxidized) increase the embryotoxicity	Pietroiusti *et al.* (2011)	Length: 0.85–0.37 μm. Diameter: ~2 nm Purity: Ca, Cr, Fe, Co < 4% (higher in pristine)
	SWCNT	Profibrogenic markers/ BEAS-2B cells; human monomyelocytic leukemia THP-1 cells Fibrosis/mice	Carboxylation SWNT decreases the fibrogenicity	Wang *et al.* (2011)	Length: 10–30 μm Diameter: 20–30 nm Purity: not reported for carboxylated CNTs

(*Continued*)

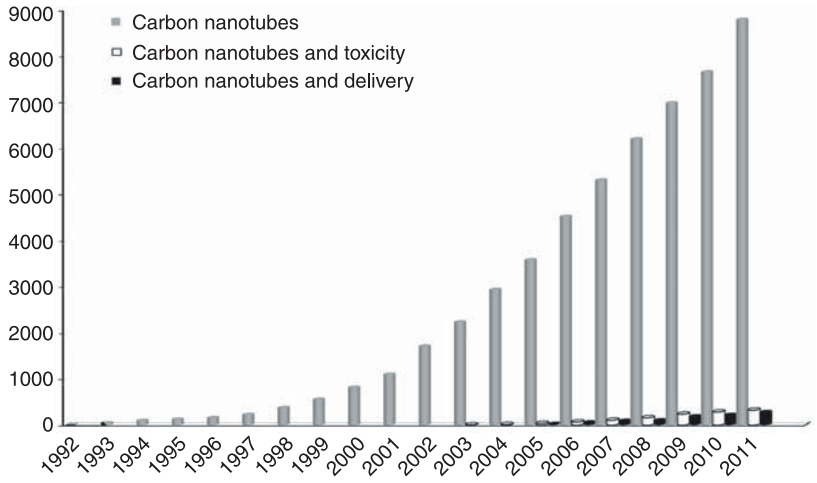
Table 8.2 (Continued)

Property	Type of CNT	Endpoints/models	Effects	References	Values
	SWCNT/ MWCNT	Cytotoxicity/CHO cells, mammalian HeLa cells	No cytotoxicity with ammonium-functionalized-SWCNT:DNA complexes	Pantarotto *et al.* (2004a)	No characterization
	SWCNT	Osteoblast proliferation/ osteosarcoma ROS 17/2.8 cells	Cell growth depends on the type of functionalization	Zanello *et al.* (2006)	Length: from nano- to micrometres Diameter: 1.5 nm
Residual catalyst	SWCNT	Oxidative stress/RAW 264.7 macrophages	Iron increases oxidative stress	Kagan *et al.* (2006)	Diameter: 1–4 nm Purity: Fe 26%–0.23%
	SWCNT/ MWCNT	Cytoxicity, release of inflammatory mediators, oxidative stress/NR8383 and human A549 lung cells	Metals increase oxidative stress	Pulskamp *et al.* (2007)	Diameter: 1–2 nm; 10–20 nm; 30–50 nm Purity: Co, Fe, Ni, Cu and Mo different content
	MWCNT	Genotoxicity/rat lung epithelial cells Lung inflammation, fibrosis/rats	Metals residues contribute to increased toxicity	Muller *et al.* (2008)	Length: 0.7 μm Diameter: 11 nm Purity: Co, Fe ~0.50% and <0.08%
	SWCNT	Oxidative stress, inflammation/ EpiDerm FT engineered skin Collagen accumulation/mice	Metals residues contribute to increased toxicity	Murray *et al.* (2009)	Fe 30% and 0.23%
Catalyst support/ amorphous carbon		No studies			
Chirality		No studies			

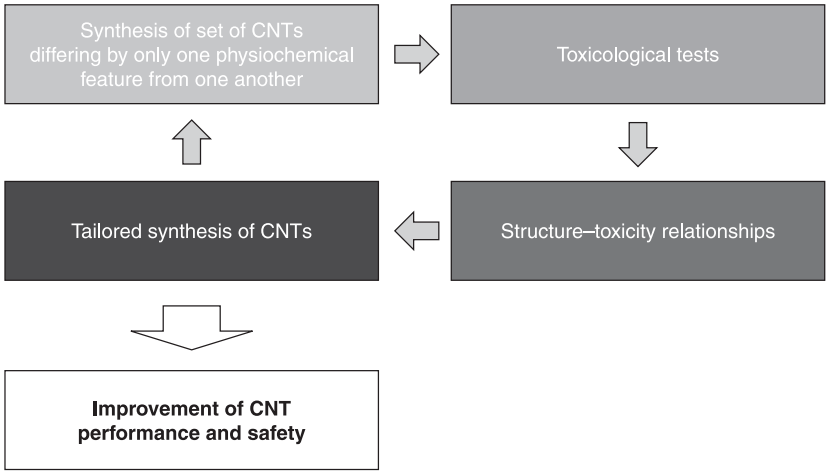
8.5 Conclusion and future trends

The discrepancies in the definition of the toxicological profile of CNTs are due both to a lack of standardized methodologies for risk assessment and variability of the properties of the samples used in toxicological tests, which limit the comparison of data of different studies. On the other hand, due to the huge number of potential applications, the diversity among commercial CNTs is expected to increase, making assessment of the risk associated with their exposure more and more difficult. Clearly, short, monodisperse, functionalized CNTs for drug delivery are different from CNTs used in other industrial areas (e.g. as filler in composites or VACNTs in electronics). The available data strongly suggest different levels of hazard and risk associated with the various forms of CNTs. The growing diversity in nanomaterial properties has been underlined by the Nanomaterial Working Party of the OECD in a 2010 report (ENV/JM/MONO(2010)46) with a note suggesting the need to continuously revise the list of priority nanomaterials for toxicological testing.

There are indications that the toxicity of CNTs may be to some extent modulated by their properties. However, the effects of the different physico-chemical properties (diameter, length, defects, purity, chirality) have been unequivocally demonstrated in a few cases only. Figure 8.3 shows the number of papers published since the discovery of CNTs and those focusing on their toxicity or on medical applications. In 2011, only 3.7% of the papers addressed the safety aspects.



8.3 Publications on carbon nanotubes since their discovery compared with those addressing their toxicity or focusing on medical applications.



8.4 A proposed strategy for the design of safe carbon nanotubes.

Clearly, more effort is required to reduce this gap. Furthermore, more effort is needed to ameliorate the methods of synthesis of CNTs. The availability of synthetic methods suitable for the production of sets of tailored CNTs that can be compared in toxicological studies will enable exploration of structure–toxicity relationships, which, in turn, will open the way to sustainable technologies able to improve both technological performance and safety of CNTs (Fig. 8.4).

8.6 Acknowledgements

The authors would like to thank Dr. Giovanni Agostini and Dr. Federico Cesano, Dip. di Chimica, University of Torino, Italy for providing the TEM scans for this review.

8.7 References

Akasaka, T., Yokoyama, A., Matsuoka, M., Hashimoto, T. and Watari, F. (2010). Thin films of single-walled carbon nanotubes promote human osteoblastic cells (Saos-2) proliferation in low serum concentrations. *Materials Science and Engineering C: Materials for Biological Applications*, 30(3): 391–399.

Al-Jamal, K. T., Nunes, A., Methven, L., Ali-Boucetta, H., Li, S. *et al.* (2012). Degree of chemical functionalization of carbon nanotubes determines tissue distribution and excretion profile. *Angewandte Chemie: International Edition*, 51(26): 6389–6393.

Aschberger, K., Johnston, H. J., Stone, V., Aitken, R. J., Hankin, S. M. *et al.* (2010). Review of carbon nanotubes toxicity and exposure: appraisal of human health risk assessment based on open literature. *Critical Reviews in Toxicology*, 40(9): 759–790.

Asharani, P. V., Serina, N. G. B., Nurmawati, M. H., Wu, Y. L., Gong, Z. *et al.* (2008). Impact of Multi-walled carbon nanotubes on aquatic species. *Journal of Nanoscience and Nanotechnology*, 8(7): 3603–3609.

Awasthi, K., Singh, D. P., Singh, S., Dash, D. and Srivastava, O. N. (2009). Attachment of biomolecules (protein and DNA) to amino-functionalized carbon nanotubes. *New Carbon Materials*, 24(4): 301–306.

Ayala, P., Arenal, R., Ruemmeli, M., Rubio, A. and Pichler, T. (2010). The doping of carbon nanotubes with nitrogen and their potential applications. *Carbon*, 48(3): 575–586.

Azad, N., Iyer, A. K., Wang, L., Liu, Y., Lu, Y. *et al.* (2012). Reactive oxygen species-mediated p38 MAPK regulates carbon nanotube-induced fibrogenic and angiogenic responses. *Nanotoxicology*, 7(2): 157–168.

Balandin, A. A. (2011). Thermal properties of graphene and nanostructured carbon materials. *Nature Materials*, 10(8): 569–581.

Banerjee, S., Hemraj-Benny, T. and Wong, S. S. (2005). Covalent surface chemistry of single-walled carbon nanotubes. *Advanced Materials*, 17(1): 17–29.

Belyanskaya, L., Weigel, S., Hirsch, C., Tobler, U., Krug, H. F. *et al.* (2009). Effects of carbon nanotubes on primary neurons and glial cells. *Neurotoxicology*, 30(4): 702–711.

Bianco, A., Kostarelos, K. and Prato, M. (2011). Making carbon nanotubes biocompatible and biodegradable. *Chemical Communications*, 47(37): 10182–10188.

Biris, A. S., Boldor, D., Palmer, J., Monroe, W. T., Mahmood, M. *et al.* (2009). Nanophotothermolysis of multiple scattered cancer cells with carbon nanotubes guided by time-resolved infrared thermal imaging. *Journal of Biomedical Optics*, 14(2): 14(2): 021007.

Boczkowski, J. and Lanone, S. (2007). Potential uses of carbon nanotubes in the medical field: how worried should patients be? *Nanomedicine*, *2*(4): 407–410.

Bottini, M., Bruckner, S., Nika, K., Bottini, N., Bellucci, S. *et al.* (2006). Multi-walled carbon nanotubes induce T lymphocyte apoptosis. *Toxicology Letters*, 160(2): 121–126.

Charlier, J. C. (2002). Defects in carbon nanotubes. *Accounts of Chemical Research*, 35(12): 1063–1069.

Chen, B., Liu, Y., Song Wei, M., Hayashi, Y., Ding Xun, C. and Li Wei, H. (2011). *In vitro* evaluation of cytotoxicity and oxidative stress induced by multiwalled carbon nanotubes in murine RAW 264.7 macrophages and human A549 lung cells. *Biomedical and Environmental Sciences*, 24(6): 593–601.

Chen, C.-S., Soni, S., Le, C., Biasca, M., Farr, E. *et al.* (2012). Human stem cell neuronal differentiation on silk-carbon nanotube composite. *Nanoscale Research Letters*, 7(1): 126.

Cheng, J., Flahaut, E. and Cheng, S. H. (2007). Effect of carbon nanotubes on developing zebrafish (*Danio rerio*) embryos. *Environmental Toxicology and Chemistry*, 26(4): 708–716.

Cheng, J., Fernando, K. A. S., Veca, L. M., Sun, Y.-P., Lamond, A. I. *et al.* (2008). Reversible accumulation of PEGylated single-walled carbon nanotubes in the mammalian nucleus. *ACS Nano*, 2(10): 2085–2094.

Cheng, J., Chan, C. M., Veca, L. M., Poon, W. L., Chan, P. K. *et al.* (2009). Acute and long-term effects after single loading of functionalized multi-walled carbon nanotubes into zebrafish (*Danio rerio*). *Toxicology and Applied Pharmacology*, 235(2): 216–225.

Cheung, W., Pontoriero, F., Taratula, O., Chen, A. M. and He, H. (2010). DNA and carbon nanotubes as medicine. *Advanced Drug Delivery Reviews*, 62(6): 633–649.

Chou, C.-C., Hsiao, H.-Y., Hong, Q.-S., Chen, C.-H., Peng, Y.-W. *et al.* (2008). Single-walled carbon nanotubes can induce pulmonary injury in mouse model. *Nano Letters*, 8(2): 437–445.

Collins, P. G., Bradley, K., Ishigami, M. and Zettl, A. (2000). Extreme oxygen sensitivity of electronic properties of carbon nanotubes. *Science*, 287(5459): 1801–1804.

Crouzier, D., Follot, S., Gentilhomme, E., Flahaut, E., Arnaud, R. *et al.* (2010). Carbon nanotubes induce inflammation but decrease the production of reactive oxygen species in lung. *Toxicology*, 272(1/3): 39–45.

Di Giorgio, M. L., Di Bucchianico, S., Ragnelli, A. M., Aimola, P., Santucci, S. *et al.* (2011). Effects of single and multi walled carbon nanotubes on macrophages: cyto and genotoxicity and electron microscopy. *Mutation Research: Genetic Toxicology and Environmental Mutagenesis*, 722(1): 20–31.

Donaldson, K., Murphy, F. A., Duffin, R. and Poland, C. A. (2010). Asbestos, carbon nanotubes and the pleural mesothelium: a review of the hypothesis regarding the role of long fibre retention in the parietal pleura, inflammation and mesothelioma. *Particle and Fibre Toxicology*, 7: 5.

Donaldson, K., Murphy, F., Schinwald, A., Duffin, R. and Poland, C. A. (2011). Identifying the pulmonary hazard of high aspect ratio nanoparticles to enable their safety-by-design. *Nanomedicine*, 6(1): 143–156.

Dugan, L. L., Turetsky, D. M., Du, C., Lobner, D., Wheeler, M. *et al.* (1997). Carboxyfullerenes as neuroprotective agents. *Proceedings of the National Academy of Sciences USA*, 94(17): 9434–9439.

Ebbesen, T. W. and Takada, T. (1995). Topological and sp3 defect structures in nanotubes. *Carbon*, *33*(7): 973–978.

Elgrabli, D., Floriani, M., Abella-Gallart, S., Meunier, L., Gamez, C. *et al.* (2008). Biodistribution and clearance of instilled carbon nanotubes in rat lung. *Particle and Fibre Toxicology*, 5: 20.

Endo, M., Koyama, S., Matsuda, Y., Hayashi, T. and Kim, Y. A. (2005). Thrombogenicity and blood coagulation of a microcatheter prepared from carbon nanotube–nylon-based composite. *Nano Letters*, 5(1): 101–105.

Endo, M., Strano, M. S. and Ajayan, P. M. (2008). Potential applications of carbon nanotubes, in A. Jorio, G. Dresselhaus and M. S. Dresselhaus (eds.), Carbon Nanotubes. *Topics in Applied Physics*, 111: 13–62.

Fan, L., Feng, C., Zhao, W., Qian, L., Wang, Y. *et al.* (2012). Directional neurite outgrowth on superaligned carbon nanotube yarn patterned substrate. *Nano Letters*, 12(7): 3668–3673.

Fenoglio, I., Tomatis, M., Lison, D., Muller, J., Fonseca, A. *et al.* (2006). Reactivity of carbon nanotubes: free radical generation or scavenging activity? *Free Radical Biology and Medicine*, 40(7): 1227–1233.

Fenoglio, I., Greco, G., Tornatis, M., Muller, J., Rayrnundo-Pinero, E. *et al.* (2008). Structural defects play a major role in the acute lung toxicity of multiwall carbon nanotubes: physicochemical aspects. *Chemical Research in Toxicology*, 21(9): 1690–1697.

Fenoglio, I., Aldieri, E., Gazzano, E., Cesano, F., Colonna, M. *et al.* (2012). Thickness of multiwalled carbon nanotubes affects their lung toxicity. *Chemical Research in Toxicology*, 25(1): 74–82.

Firuzi, O., Miri, R., Tavakkoli, M. and Saso, L. (2011). Antioxidant therapy: current status and future prospects. *Current Medicinal Chemistry*, 18(25): 3871–3888.

Francisco-Marquez, M., Galano, A. and Martinez, A. (2010). On the free radical scavenging capability of carboxylated single-walled carbon nanotubes. *Journal of Physical Chemistry C*, 114(14): 6363–6370.

Fubini, B., Ghiazza, M. and Fenoglio, I. (2010). Physico-chemical features of engineered nanoparticles relevant to their toxicity. *Nanotoxicology*, 4(4): 347–363.

Fubini, B., Fenoglio, I., Tomatis, M. and Turci, F. (2011). Effect of chemical composition and state of the surface on the toxic response to high aspect ratio nanomaterials. *Nanomedicine*, 6(5): 899–920.

Galano, A. (2009). Influence of diameter, length, and chirality of single-walled carbon nanotubes on their free radical scavenging capability. *Journal of Physical Chemistry C*, 113(43): 18487–18491.

Galano, A. (2010). Carbon nanotubes: promising agents against free radicals. *Nanoscale*, 2(3): 373–380.

Gavello, D., Vandael, D. H. F., Cesa, R., Premoselli, F., Marcantoni, A. *et al.* (2012). Altered excitability of cultured chromaffin cells following exposure to multi-walled carbon nanotubes. *Nanotoxicology*, 6(1): 47–60.

Guo, J., Zhang, X., Li, Q. and Li, W. (2007). Biodistribution of functionalized multiwall carbon nanotubes in mice. *Nuclear Medicine and Biology*, 34(5): 579–583.

Han, Z. and Fina, A. (2011). Thermal conductivity of carbon nanotubes and their polymer nanocomposites: a review. *Progress in Polymer Science*, 36(7): 914–944.

He, X., Young, S.-H., Schwegler-Berry, D., Chisholm, W. P., Fernback, J. E. *et al.* (2011). Multiwalled carbon nanotubes induce a fibrogenic response by stimulating reactive oxygen species production, activating NF-κ B signaling, and promoting fibroblast-to-myofibroblast transformation. *Chemical Research in Toxicology*, 24(12): 2237–2248.

Hirsch, A. (2002). Functionalization of single-walled carbon nanotubes. *Angewandte Chemie: International Edition*, 41(11): 1853–1859.

Hou, P.-X., Liu, C. and Cheng, H.-M. (2008). Purification of carbon nanotubes. *Carbon*, 46(15): 2003–2025.

Hu, H., Ni, Y. C., Montana, V., Haddon, R. C. and Parpura, V. (2004). Chemically functionalized carbon nanotubes as substrates for neuronal growth. *Nano Letters*, 4(3): 507–511.

Huang, Y.-C., Hsu, S.-H., Kuo, W.-C., Chang-Chien, C.-L., Cheng, H. and Huang, Y.-Y. (2011). Effects of laminin-coated carbon nanotube/chitosan fibers on guided neurite growth. *Journal of Biomedical Materials Research A*, 99 (1): 86–93.

Iijima, S. (1991). Helical microtubes of graphitic carbon. *Nature*, 354: 56–58.

Ji, S.-R., Liu, C., Zhang, B., Yang, F., Xu, J. *et al.* (2010). Carbon nanotubes in cancer diagnosis and therapy. *Biochimica et Biophysica Acta*, 1806(1): 29–35.

Johnston, H. J., Hutchison, G. R., Christensen, F. M., Peters, S., Hankin, S. *et al.* (2010). A critical review of the biological mechanisms underlying the *in vivo* and *in vitro* toxicity of carbon nanotubes: the contribution of physico-chemical characteristics. *Nanotoxicology*, 4(2): 207–246.

Kagan, V. E., Tyurina, Y. Y., Tyurin, V. A., Konduru, N. V., Potapovich, A. I. *et al.* (2006). Direct and indirect effects of single walled carbon nanotubes on RAW 264.7 macrophages: role of iron. *Toxicology Letters*, 165(1): 88–100.

Kagan, V. E., Konduru, N. V., Feng, W. H., Allen, B. L., Conroy, J. *et al.* (2010). Carbon nanotubes degraded by neutrophil myeloperoxidase induce less pulmonary inflammation. *Nature Nanotechnology*, 5(5): 354–359.

Kam, N. W. S., O'Connell, M., Wisdom, J. A. and Dai, H. J. (2005). Carbon nanotubes as multifunctional biological transporters and near-infrared agents for selective cancer cell destruction. *Proceedings of the National Academy of Sciences USA*, 102(33): doi: 11600–11605.

Kam, N. W. S., Liu, Z. A. and Dai, H. J. (2006). Carbon nanotubes as intracellular transporters for proteins and DNA: an investigation of the uptake mechanism and pathway. *Angewandte Chemie: International Edition*, 45(4): 577–581.

Kane, A. B. and Hurt, R. H. (2008). Nanotoxicology: the asbestos analogy revisited. *Nature Nanotechnology*, 3(7): 378–379.

Klumpp, C., Kostarelos, K., Prato, M. and Bianco, A. (2006). Functionalized carbon nanotubes as emerging nanovectors for the delivery of therapeutics. *Biochimica et Biophysica Acta: Biomembranes*, 1758(3): 404–412.

Knaapen, A. M., Borm, P. J. A., Albrecht, C. and Schins, R. P. F. (2004). Inhaled particles and lung cancer. Part A: Mechanisms. *International Journal of Cancer*, 109(6): 799–809.

Kobayashi, N., Naya, M., Ema, M., Endoh, S., Maru, J. *et al.* (2010). Biological response and morphological assessment of individually dispersed multi-wall carbon nanotubes in the lung after intratracheal instillation in rats. *Toxicology*, 276(3): 143–153.

Kolosnjaj-Tabi, J., Hartman, K. B., Boudjemaa, S., Ananta, J. S., Morgant, G. *et al.* (2010). *In vivo* behavior of large doses of ultrashort and full-length single-walled carbon nanotubes after oral and intraperitoneal administration to Swiss mice. *ACS Nano*, 4(3): 1481–1492.

Kostarelos, K. (2008). The long and short of carbon nanotube toxicity. *Nature Biotechnology*, 26(7): 774–776.

Koyama, S., Haniu, H., Osaka, K., Koyama, H., Kuroiwa, N. *et al.* (2006). Medical application of carbon-nanotube-fitted nanocomposites: the microcatheter. *Small*, 2(12): 1406–1411.

Krasheninnikov, A. V. and Nordlund, K. (2010). Ion and electron irradiation-induced effects in nanostructured materials. *Journal of Applied Physics*, 107(7): 071301.

Lacerda, L., Bianco, A., Prato, M. and Kostarelos, K. (2006). Carbon nanotubes as nanomedicines: from toxicology to pharmacology. *Advanced Drug Delivery Reviews*, 58(14): 1460–1470.

Lacerda, L., Raffa, S., Prato, M., Bianco, A. and Kostarelos, K. (2007). Cell-penetrating CNTs for delivery of therapeutics. *Nano Today*, 2(6): 38–43.

Lee, C., Kim, H., Cho, Y. and Lee, W. I. (2007). The properties of porous silicon as a therapeutic agent via the new photodynamic therapy. *Journal of Materials Chemistry*, *17*(25): 2648–2653.

Lison, D. and Muller, J. (2008). Letter to the Editor. *Toxicological Sciences*, 101(1): 179–180.

Liu, X., Hurt, R. H. and Kane, A. B. (2010). Biodurability of single-walled carbon nanotubes depends on surface functionalization. *Carbon*, 48(7): 1961–1969.

Liu, X., Sen, S., Liu, J., Kulaots, I., Geohegan, D. *et al.* (2011). Antioxidant deactivation on graphenic nanocarbon surfaces. *Small*, 7(19): 2775–2785.

Liu, Z., Tabakman, S., Welsher, K. and Dai, H. (2009). Carbon nanotubes in biology and medicine: *in vitro* and *in vivo* detection, imaging and drug delivery. *Nano Research*, 2(2): 85–120.

Lu, W., Zu, M., Byun, J.-H., Kim, B.-S. and Chou, T.-W. (2012). State of the art of carbon nanotube fibers: opportunities and challenges. *Advanced Materials*, 24(14): 1805–1833.

Lucente-Schultz, R. M., Moore, V. C., Leonard, A. D., Price, B. K., Kosynkin, D. V. *et al.* (2009). Antioxidant single-walled carbon nanotubes. *Journal of the American Chemical Society*, 131(11): 3934–3941.

Ma-Hock, L., Treumann, S., Strauss, V., Brill, S., Luizi, F. *et al.* (2009). Inhalation toxicity of multiwall carbon nanotubes in rats exposed for 3 months. *Toxicological Sciences*, 112(2): 468–481.

Martinez, A. and Galano, A. (2010). Free radical scavenging activity of ultrashort single-walled carbon nanotubes with different structures through electron transfer reactions. *Journal of Physical Chemistry C*, 114(18): 8184–8191.

Meyer-Plath, A., Orts-Gil, G., Petrov, S., Oleszak, F., Maneck, H.-E. *et al.* (2012). Plasma-thermal purification and annealing of carbon nanotubes. *Carbon*, 50(10): 3934–3942.

Monteiro-Riviere, N. A., Nemanich, R. J., Inman, A. O., Wang, Y. Y. Y. and Riviere, J. E. (2005). Multi-walled carbon nanotube interactions with human epidermal keratinocytes. *Toxicology Letters*, 155(3): 377–384.

Moon, H. K., Lee, S. H. and Choi, H. C. (2009). *In vivo* near-infrared mediated tumor destruction by photothermal effect of carbon nanotubes. *ACS Nano*, 3(11): 3707–3013.

Muller, J., Huaux, F., Moreau, N., Misson, P., Heilier, J. F. *et al.* (2005). Respiratory toxicity of multi-wall carbon nanotubes. *Toxicology and Applied Pharmacology*, 207(3): 221–231.

Muller, J., Huaux, F., Fonseca, A., Nagy, J. B., Moreau, N. *et al.* (2008). Structural defects play a major role in the acute lung toxicity of multiwall carbon nanotubes: toxicological aspects. *Chemical Research in Toxicology*, 21: 1698–1705.

Muller, J., Delos, M., Panin, N., Rabolli, V., Huaux, F. and Lison, D. (2009). Absence of carcinogenic response to multiwall carbon nanotubes in a 2-year bioassay in the peritoneal cavity of the rat. *Toxicological Sciences*, 110(2): 442–448.

Murphy, F. A., Poland, C. A., Duffin, R., Al-Jamal, K. T., Ali-Boucetta, H. *et al.* (2011). Length-dependent retention of carbon nanotubes in the pleural space of mice initiates sustained inflammation and progressive fibrosis on the parietal pleura. *American Journal of Pathology*, 178(6): 2587–2600.

Murray, A. R., Kisin, E., Leonard, S. S., Young, S. H., Kommineni, C. *et al.* (2009). Oxidative stress and inflammatory response in dermal toxicity of single-walled carbon nanotubes. *Toxicology*, 257(3): 161–171.

Nagai, H., Okazaki, Y., Chew, S. H., Misawa, N., Yamashita, Y. *et al.* (2011). Diameter and rigidity of multiwalled carbon nanotubes are critical factors in mesothelial injury and carcinogenesis. *Proceedings of the National Academy of Sciences USA*, 108(49): E1330–E1338.

Nessim, G. D. (2010). Properties, synthesis, and growth mechanisms of carbon nanotubes with special focus on thermal chemical vapor deposition. *Nanoscale*, 2(8): 1306–1323.

Ogihara, N., Usui, Y., Aoki, K., Shimizu, M., Narita, N. *et al.* (2012). Biocompatibility and bone tissue compatibility of alumina ceramics reinforced with carbon nanotubes. *Nanomedicine*, 7(7): 981–993.

Orinakova, R. and Orinak, A. (2011). Recent applications of carbon nanotubes in hydrogen production and storage. *Fuel*, 90(11): 3123–3140.

Pacurari, M., Castranova, V. and Vallyathan, V. (2010). Single- and multi-wall carbon nanotubes versus asbestos: are the carbon nanotubes a new health risk to humans? *Journal of Toxicology and Environmental Health A: Current Issues*, 73(5/6): 378–395.

Panchapakesan, B., Lu, S., Sivakumar, K., Teker, K., Cesarone, G. and Wickstrom, E. (2005). Single-wall carbon nanotube nanobomb agents for killing breast cancer cells. *Nanobiotechnology*, 1(2): 133–139.

Pantarotto, D., Singh, R., McCarthy, D., Erhardt, M., Briand, J. P. *et al.* (2004a). Functionalized carbon nanotubes for plasmid DNA gene delivery. *Angewandte Chemie: International Edition*, 43(39): doi: 5242–5246.

Pantarotto, D., Briand, J. P., Prato, M. and Bianco, A. (2004b). Translocation of bioactive peptides across cell membranes by carbon nanotubes. *Chemical Communications*, 1: 16–17.

Park, K. H., Chhowalla, M., Iqbal, Z. and Sesti, F. (2003). Single-walled carbon nanotubes are a new class of ion channel blockers. *Journal of Biological Chemistry*, 278(50): 50212–50216.

Pastorin, G. (2009). Crucial functionalizations of carbon nanotubes for improved drug delivery: a valuable option? *Pharmaceutical Research*, 26(4): 746–769.

Pettes, M. T. and Shi, L. (2009). Thermal and structural characterizations of individual single-, double-, and multi-walled carbon nanotubes. *Advanced Functional Materials*, 19(24): 3918–3925.

Pietroiusti, A., Massimiani, M., Fenoglio, I., Colonna, M., Valentini, F. *et al.* (2011). Low doses of pristine and oxidized single-wall carbon nanotubes affect mammalian embryonic development. *ACS Nano*, 5(6): 4624–4633.

Poland, C. A., Duffin, R., Kinloch, I., Maynard, A., Wallace, W. A. H. *et al.* (2008). Carbon nanotubes introduced into the abdominal cavity of mice show asbestos-like pathogenicity in a pilot study. *Nature Nanotechnology*, 3(7): 423–428.

Pulskamp, K., Diabate, S. and Krug, H. F. (2007). Carbon nanotubes show no sign of acute toxicity but induce intracellular reactive oxygen species in dependence on contaminants. *Toxicology Letters*, 168(1): 58–74.

Qu, C., Wang, L., He, J., Tan, J., Liu, W. *et al.* (2012). Carbon nanotubes provoke inflammation by inducing the pro-inflammatory genes IL-1 beta and IL-6. *Gene*, 493(1): 9–12.

Raffa, V., Ciofani, G., Nitodas, S., Karachalios, T., D'Alessandro, D. *et al.* (2008). Can the properties of carbon nanotubes influence their internalization by living cells? *Carbon*, 46(12): 1600–1610.

Rahmat, M. and Hubert, P. (2011). Carbon nanotube–polymer interactions in nanocomposites: a review. *Composites Science and Technology*, 72(1): 72–84.

Roach, P., Parker, T., Gadegaard, N. and Alexander, M. R. (2010). Surface strategies for control of neuronal cell adhesion: a review. *Surface Science Reports*, 65(6): 145–173.

Ruggiero, A., Villa, C. H., Bander, E., Rey, D. A., Bergkvist, M. *et al.* (2010). Paradoxical glomerular filtration of carbon nanotubes. *Proceedings of the National Academy of Sciences of USA*, 107(27): 12369–12374.

Saito, N., Usui, Y., Aoki, K., Narita, N., Shimizu, M. *et al.* (2008). Carbon nanotubes for biomaterials in contact with bone. *Current Medicinal Chemistry*, 15(5): 523–527.

Saito, N., Usui, Y., Aoki, K., Narita, N., Shimizu, M. *et al.* (2009). Carbon nanotubes: biomaterial applications. *Chemical Society Reviews*, 38(7): 1897–1903.

Sakamoto, Y., Nakae, D., Fukumori, N., Tayama, K., Maekawa, A. *et al.* (2009). Induction of mesothelioma by a single intrascrotal administration of multi-wall carbon nanotube in intact male Fischer 344 rats. *Journal of Toxicological Sciences*, 34(1): 65–76.

Sanchez, V. C., Pietruska, J. R., Miselis, N. R., Hurt, R. H. and Kane, A. B. (2009). Biopersistence and potential adverse health impacts of fibrous nanomaterials: what have we learned from asbestos? *Nanomedicine and Nanobiotechnology*, 1(5): 511–529.

Sato, Y., Yokoyama, A., Kasai, T., Hashiguchi, S., Ootsubo, M. *et al.* (2008). *In vivo* rat subcutaneous tissue response of binder-free multi-walled carbon nanotube blocks cross-linked by de-fluorination. *Carbon*, 46(14): 1927–1934.

Savolainen, K., Alenius, H., Norppa, H., Pylkkanen, L., Tuomi, T. and Kasper, G. (2010). Risk assessment of engineered nanomaterials and nanotechnologies: a review. *Toxicology*, 269(2/3): 92–104.

Schinwald, A., Murphy, F. A., Prina-Mello, A., Poland, C. A., Byrne, F. *et al.* (2012). The threshold length for fiber-induced acute pleural inflammation: shedding light on the early events in asbestos-induced mesothelioma. *Toxicological Sciences*, 128(2): 461–470.

Service, R. F. (1998). Nanotubes: the next asbestos? *Science*, 281(5379): 941–942.

Sharma, P. and Ahuja, P. (2008). Recent advances in carbon nanotube-based electronics. *Materials Research Bulletin*, 43(10): 2517–2526.

Shukla, P. K. and Mishra, P. C. (2010). Effects of diameter, length, chirality and defects on the scavenging action of single-walled carbon nanotubes for OH radicals: a quantum computational study. *Chemical Physics*, 369(2/3): 101–107.

Shvedova, A. A., Castranova, V., Kisin, E. R., Schwegler-Berry, D., Murray, A. R. *et al.* (2003). Exposure to carbon nanotube material: assessment of nanotube cytotoxicity using human keratinocyte cells. *Journal of Toxicology and Environmental Health A*, 66(20): 1909–1926.

Shvedova, A. A., Kisin, E. R., Mercer, R., Murray, A. R., Johnson, V. J. *et al.* (2005). Unusual inflammatory and fibrogenic pulmonary responses to single-walled carbon nanotubes in mice. *American Journal of Physiology: Lung Cellular and Molecular Physiology*, 289(5): L698–L708.

Shvedova, A. A., Kisin, E. R., Porter, D., Schulte, P., Kagan, V. E. *et al.* (2009). Mechanisms of pulmonary toxicity and medical applications of carbon nanotubes: two faces of Janus? *Pharmacology and Therapeutics*, 121(2): 192–204.

Shvedova, A. A., Pietroiusti, A., Fadeel, B. and Kagan, V. E. (2012a). Mechanisms of carbon nanotube-induced toxicity: focus on oxidative stress. *Toxicology and Applied Pharmacology*, 261(2): 121–133.

Shvedova, A. A., Kapralov, A. A., Feng, W. H., Kisin, E. R., Murray, A. R. *et al.* (2012b). Impaired clearance and enhanced pulmonary inflammatory/fibrotic response to carbon nanotubes in myeloperoxidase-deficient mice. *PLoS One*, 7(3): 0030923.

Singh, R., Pantarotto, D., McCarthy, D., Chaloin, O., Hoebeke, J. *et al.* (2005). Binding and condensation of plasmid DNA onto functionalized carbon nanotubes: toward the construction of nanotube-based gene delivery vectors. *Journal of the American Chemical Society*, 127(12): 4388–4396.

Takagi, A., Hirose, A., Nishimura, T., Fukumori, N., Ogata, A. *et al.* (2008). Induction of mesothelioma in p53+/− mouse by intraperitoneal application of multi-wall carbon nanotube. *Journal of Toxicological Sciences*, 33(1): 105–116.

Tasis, D., Tagmatarchis, N., Bianco, A. and Prato, M. (2006). Chemistry of carbon nanotubes. *Chemical Reviews*, 106(3): 1105–1136.

Terrones, M. and Terrones, H. (2003). The carbon nanocosmos: novel materials for the twenty-first century. *Philosophical Transactions of the Royal Society of London A: Mathematical, Physical and Engineering Sciences*, 361(1813): 2789–2806.

Tu, X. M., Manohar, S., Jagota, A. and Zheng, M. (2009). DNA sequence motifs for structure-specific recognition and separation of carbon nanotubes. *Nature*, 460(7252): 250–253.

Usui, Y., Aoki, K., Narita, N., Murakami, N., Nakamura, I. *et al.* (2008). Carbon nanotubes with high bone-tissue compatibility and bone-formation acceleration effects. *Small*, 4(2): 240–246.

Vashist, S. K., Zheng, D., Pastorin, G., Al-Rubeaan, K., Luong, J. H. T. and Sheu, F.-S. (2011). Delivery of drugs and biomolecules using carbon nanotubes. *Carbon*, 49(13): 4077–4097.

Vittorio, O., Raffa, V. and Cuschieri, A. (2009). Influence of purity and surface oxidation on cytotoxicity of multiwalled carbon nanotubes with human neuroblastoma cells. *Nanomedicine*, 5(4): 424–431.

Wang, J., Deng, X., Yang, S., Wang, H., Zhao, Y. and Liu, Y. (2008). Rapid translocation and pharmacokinetics of hydroxylated single-walled carbon nanotubes in mice. *Nanotoxicology*, 2(1): 28–32.

Wang, L.X., Xia, T., Ntim, S.A., Ji, Z., Lin, S. *et al.* (2011). Dispersal state of multiwalled carbon nanotubes elicits profibrogenic cellular responses that correlate with fibrogenesis biomarkers and fibrosis in the murine lung. *ACS Nano*, 5(12): 9772–9787.

Wang, X., Jia, G., Wang, H., Nie, H., Yan, L. *et al.* (2009). Diameter effects on cytotoxicity of multi-walled carbon nanotubes. *Journal of Nanoscience and Nanotechnology*, 9(5): 3025–3033.

Watts, P. C. P., Fearon, P. K., Hsu, W. K., Billingham, N. C., Kroto, H. W. and Walton, D. R. M. (2003). Carbon nanotubes as polymer antioxidants. *Journal of Materials Chemistry*, 13(3): 491–495.

Wu, H., Wexler, D. and Liu, H. (2012). Effects of different palladium content loading on the hydrogen storage capacity of double-walled carbon nanotubes. *International Journal of Hydrogen Energy*, 37(7): 5686–5690.

Xu, H., Bai, J., Meng, J., Hao, W., Xu, H. and Cao, J.-M. (2009). Multi-walled carbon nanotubes suppress potassium channel activities in PC12 cells. *Nanotechnology*, 20(28): 285102.

Yamashita, K., Yoshioka, Y., Higashisaka, K., Morishita, Y., Yoshida, T. *et al.* (2010). Carbon nanotubes elicit DNA damage and inflammatory response relative to their size and shape. *Inflammation*, 33(4): 276–280.

Ying, Y. M., Saini, R. K., Liang, F., Sadana, A. K. and Billups, W. E. (2003). Functionalization of carbon nanotubes by free radicals. *Organic Letters*, 5(9): 1471–1473.

Zanello, L. P., Zhao, B., Hu, H. and Haddon, R. C. (2006). Bone cell proliferation on carbon nanotubes. *Nano Letters*, 6(3): 562–567.

Zhai, Y., Dou, Y., Zhao, D., Fulvio, P. F., Mayes, R. T. and Dai, S. (2011). Carbon materials for chemical capacitive energy storage. *Advanced Materials*, 23(42): 4828–4850.

Zhang, Y., Bai, Y. and Yan, B. (2010). Functionalized carbon nanotubes for potential medicinal applications. *Drug Discovery Today*, 15(11/12): 428–435.

1.3. CARBON NANOTUBES AND PULMONARY TOXICITY

We focused our attention on the pulmonary toxicity, as inhalation is the most important route of exposure to CNT. The human lung is a vulnerable organ composed by approximately 2300 km of airways and 300 million alveoli, giving rise to a large surface area (Hoet et al., 2004). The small size of CNT allows them to easily penetrate into the deep air spaces of the lung. It has been shown that CNT can induce several toxic effects in the lung, including inflammation (alveolitis), asthma, fibrosis and mesothelioma (Figure 2).

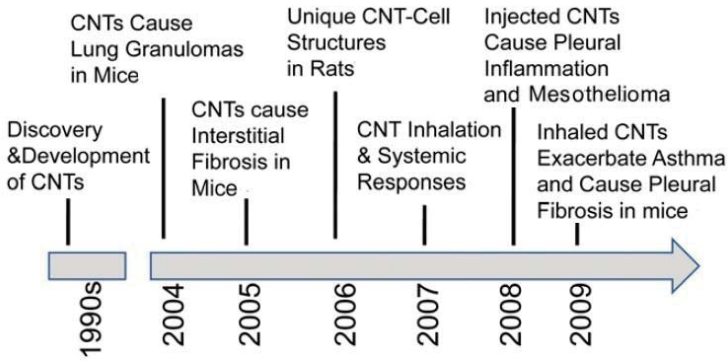


Figure 2. Timeline of selected reports in the literature that indicate toxic effects of CNT in mice or rats. Adapted from Bonner et al. (Bonner, 2010).

1.3.1. Inflammation (alveolitis)

Inflammation (from the Latin, to set on fire) is an adaptive response involving cells and soluble factors that is triggered in response to infection, trauma, ischemia, toxic or other injury. CNT that reach the deep lung can initiate an inflammatory process (alveolitis), in which inflammatory cells that are in the front line of the immune system, principally neutrophils, macrophages and epithelial cells, are activated. The inflammatory response

influences resident lung cells and the ensuing inflammatory cells, thus influencing the immune response and compromising the homeostasis of the lung. Activated inflammatory cells resulting from CNT exposure can release a broad array of mediators. CNT have been shown to induce the release of interleukin (IL)-1 family proteins, a group of cytokines which play a central role in the regulation of inflammatory responses, among which IL-1α and IL-1β are the most studied (Rabolli et al., 2014; He et al., 2011). Also the tumor necrosis factor (TNF)-α, a key cytokine involved in inflammation, is produced by activated macrophages upon CNT exposure (Muller et al., 2005). Shvedova et al. (Shvedova et al., 2005) found that pharyngeal aspiration of single-wall (SW)CNT resulted in pulmonary effects in C57BL/6 mice that combined an acute inflammatory response including early neutrophil accumulation, followed by macrophage influx, and elevation of pro-inflammatory cytokines TNF-α and IL-1β. Katwa et al. (Katwa et al., 2012) demonstrated that MWCNT exposure also triggers the extracellular release of IL-33 in the lung, leading to the activation of mast cells, resulting in a pulmonary inflammation and granuloma formation. In this context, oxidative stress seems to be a major underlying mechanism driving inflammatory responses to CNT, which leads to the activation of different transcription factors with subsequent enhanced synthesis of pro-inflammatory proteins (Palomaki et al., 2011; Sun et al., 2015).

1.3.2. Asthma

Asthma is a common chronic inflammatory disease of the airways characterized by variable and recurring symptoms, reversible airflow obstruction and bronchospasm. Several evidence show that exposure to inhaled CNT can exaggerate pre-existing inflammation, such as allergic asthma. Different authors have shown that multi-wall (MW)CNT exacerbate ovalbumin-induced allergic airways inflammation in mice (Ryman-

Rasmussen et al., 2009; Inoue et al., 2009; Thompson et al., 2015). Interestingly, Ryman-Rasmussen et al. demonstrated that inhaled MWCNT induced significant airway fibrosis in mice pre-treated with ovalbumin, while did not in mice that received ovalbumin or MWCNT alone. These studies suggest that CNT exacerbate allergic reaction and thus, that individuals with allergic asthma are more susceptible to immune responses in a workplace environment.

1.3.3. Cancer

Cancer is a group of diseases involving abnormal cell growth with the potential to invade or spread to other parts of the body. Key biological events of cancer are genetic alterations, uncontrolled proliferation and tissue invasion. CNT pose a cancer risk similar to that of asbestos, due to their similar fiber-shape structure, as first addressed by Robert F. Service in 1998 in his question “are carbon nanotube the next asbestos?” (Service, 1998). Asbestos exposure has been shown to lead to a range of different lung diseases such as lung fibrosis (asbestosis), lung cancer as well as mesothelioma, a specific type of cancer of the lining of the pleural cavity, which is fatal and seen as a hallmark disease of asbestos exposure (Prazakova et al., 2014). Poland et al. (Poland et al., 2008) were the first to address this issue regarding CNT and showed that injection of long MWCNT into the peritoneal cavity of mice (a surrogate for the pleura) induced inflammation and granuloma similar to long asbestos fibers, suggesting that MWCNT can induce mesothelioma. This question was confirmed by other studies that clearly demonstrated the induction of mesothelioma in animal treated with CNT (Nagai et al., 2011; Rittinghausen et al., 2014). Evidence has also emerged regarding the deoxyribonucleic acid (DNA) damaging properties of CNT. Exposure to CNT was shown to induce DNA damage and increase mutation frequency in mesothelial cells

as well as epithelial cells (Karlsson et al., 2008; Visalli et al., 2015; Muller et al., 2008; Lindberg et al., 2013). Moreover, in vitro and in vivo studies show that exposure to SWCNT and MWCNT induced proliferation, migration, and invasion of mesothelial cells similar to that observed in asbestos-exposed cells (Xu et al., 2012; Lohcharoenkal et al., 2013). From these evidence, CNT appear as a risk factor for cancer, although it is still unclear whether CNT could cause these adverse effects in humans.

1.3.4. Fibrosis

Pulmonary fibrosis is a respiratory disease in which scars are formed in the lung tissue, leading to serious breathing problems. The formation and accumulation of fibrous connective tissue is the result of fibroblast activation leading to inspiratory insufficiency. Indeed, fibroblasts are the key actor in fibrosis. In response to different stimuli they can be activated leading to proliferation, differentiation into myofibroblasts and induction of extracellular matrix (ECM) protein production (Wynn, 2011), as shown in Figure 3. Several in vivo studies reported that CNT are able to induce pulmonary fibrosis in murine models as shown in Table 1 in the chapter 3.4. CNT-induced pulmonary fibrosis is thought to result from a chronic inflammatory response (alveolitis) where immune cells are excessively or inappropriately activated, probably due to an inability to clear toxic particles from the lungs via the usual protective mechanisms, accompanied by a persistent release of pro-inflammatory and pro-fibrotic mediators. The two most important pro-fibrotic growth factors are platelet-derived growth factor (PDGF) and transforming growth factor (TGF)-β. PDGF stimulate fibroblast proliferation and acts as a potent chemoattractant for fibroblasts and myofibroblasts, thereby promoting fibrosis, while TGF-β principally stimulates the differentiation of mesenchymal cells which synthesize collagen. Moreover, emerging evidence report that CNT can reach the

interstitial space and, thus, can be in contact with fibroblasts to induce some adverse effect. This is discussed in chapter 3.4.

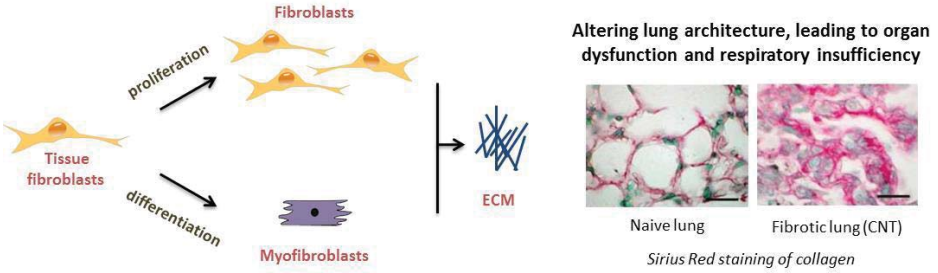


Figure 3. Fibroblasts and lung fibrosis.

1.4. REFERENCES INTRODUCTION

Arora S, Rajwade JM, Paknikar KM. 2012. Nanotoxicology and in vitro studies: the need of the hour. Toxicol Appl Pharmacol 258**,** 151-65.

Bergin IL, Witzmann FA. 2013. Nanoparticle toxicity by the gastrointestinal route: evidence and knowledge gaps. Int J Biomed Nanosci Nanotechnol 3.

Bonner JC. 2010. Nanoparticles as a potential cause of pleural and interstitial lung disease. Proc Am Thorac Soc 7**,** 138-41.

Borm PJ, Robbins D, Haubold S, Kuhlbusch T, Fissan H, Donaldson K, Schins R, Stone V, Kreyling W, Lademann J, Krutmann J, Warheit D, Oberdorster E. 2006. The potential risks of nanomaterials: a review carried out for ECETOC. Part Fibre Toxicol 3**,** 11.

De Volder MF, Tawfick SH, Baughman RH, Hart AJ. 2013. Carbon nanotubes: present and future commercial applications. Science 339**,** 535-9.

Elsaesser A, Howard CV. 2012. Toxicology of nanoparticles. Adv Drug Deliv Rev 64**,** 129-37.

Ghiazza M, Vietti G, Fenoglio I 2014. Carbon nanotubes (CNTs): properties, applications and toxicity. *In:* Njuguna, J, Pielichowski, K, Zhu, H (eds.) *Health and environmental risks of nanomaterials.* Woodhead Publishing U.K.

Gulson B, Mccall MJ, Bowman DM, Pinheiro T. 2015. A review of critical factors for assessing the dermal absorption of metal oxide nanoparticles from sunscreens applied to humans, and a research strategy to address current deficiencies. Arch Toxicol.

Hadrup N, Sharma AK, Poulsen M, Nielsen E. 2015. Toxicological risk assessment of elemental gold following oral exposure to sheets and nanoparticles - A review. Regul Toxicol Pharmacol 72**,** 216-21.

He X, Young SH, Schwegler-Berry D, Chisholm WP, Fernback JE, Ma Q. 2011. Multiwalled carbon nanotubes induce a fibrogenic response by stimulating reactive oxygen species production, activating NF-kappaB signaling, and promoting fibroblast-to-myofibroblast transformation. Chem Res Toxicol 24**,** 2237-48.

Inoue K, Koike E, Yanagisawa R, Hirano S, Nishikawa M, Takano H. 2009. Effects of multi-walled carbon nanotubes on a murine allergic airway inflammation model. Toxicol Appl Pharmacol 237**,** 306-16.

Karlsson HL, Cronholm P, Gustafsson J, Moller L. 2008. Copper oxide nanoparticles are highly toxic: a comparison between metal oxide nanoparticles and carbon nanotubes. Chem Res Toxicol 21**,** 1726-32.

Katwa P, Wang X, Urankar RN, Podila R, Hilderbrand SC, Fick RB, Rao AM, Ke PC, Wingard CJ, Brown JM. 2012. A carbon nanotube toxicity paradigm driven by mast cells and the IL-(3)(3)/ST(2) axis. Small 8**,** 2904-12.

Lee JH, Ahn KH, Kim SM, Kim E, Lee GH, Han JH, Yu IJ. 2015. Three-Day Continuous Exposure Monitoring of CNT Manufacturing Workplaces. Biomed Res Int 2015**,** 237140.

Li JJ, Muralikrishnan S, Ng CT, Yung LY, Bay BH. 2010. Nanoparticle-induced pulmonary toxicity. Exp Biol Med (Maywood) 235**,** 1025-33.

Lindberg HK, Falck GC, Singh R, Suhonen S, Jarventaus H, Vanhala E, Catalan J, Farmer PB, Savolainen KM, Norppa H. 2013. Genotoxicity of short single-wall and multi-wall carbon nanotubes in human bronchial epithelial and mesothelial cells in vitro. Toxicology 313**,** 24-37.

Lohcharoenkal W, Wang L, Stueckle TA, Dinu CZ, Castranova V, Liu Y, Rojanasakul Y. 2013. Chronic exposure to carbon nanotubes induces invasion of human mesothelial cells through matrix metalloproteinase-2. ACS Nano 7**,** 7711-23.

Mordor-Intelligence-Llp. 2015. *Global Nanomaterials Market - Segmented by Product Type, End-User Industry, and Geography - Trends and Forecasts (2015-2020)* [Online].

Muller J, Decordier I, Hoet PH, Lombaert N, Thomassen L, Huaux F, Lison D, Kirsch-Volders M. 2008. Clastogenic and aneugenic effects of multi-wall carbon nanotubes in epithelial cells. Carcinogenesis 29**,** 427-33.

Muller J, Huaux F, Moreau N, Misson P, Heilier JF, Delos M, Arras M, Fonseca A, Nagy JB, Lison D. 2005. Respiratory toxicity of multi-wall carbon nanotubes. Toxicol Appl Pharmacol 207**,** 221-31.

Nagai H, Okazaki Y, Chew SH, Misawa N, Yamashita Y, Akatsuka S, Ishihara T, Yamashita K, Yoshikawa Y, Yasui H, Jiang L, Ohara H, Takahashi T, Ichihara G, Kostarelos K, Miyata Y, Shinohara H, Toyokuni S. 2011. Diameter and rigidity of multiwalled carbon nanotubes are critical factors in mesothelial injury and carcinogenesis. Proc Natl Acad Sci U S A 108**,** E1330-8.

Niosh D. 2013. Current Intelligence Bulletin 65: Occupational Exposure to Carbon Nanotubes and Nanofibers.

O'brien N, Cummins E. 2008. Recent Developments in Nanotechnology and Risk Assessment Strategies for Addressing Public and Environmental Health Concerns. Human and Ecological Risk Assessment 14**,** 568-592.

Oberdorster G, Oberdorster E, Oberdorster J. 2005. Nanotoxicology: an emerging discipline evolving from studies of ultrafine particles. Environ Health Perspect 113**,** 823-39.

Palomaki J, Valimaki E, Sund J, Vippola M, Clausen PA, Jensen KA, Savolainen K, Matikainen S, Alenius H. 2011. Long, needle-like carbon nanotubes and asbestos activate the NLRP3 inflammasome through a similar mechanism. ACS Nano 5**,** 6861-70.

Poland CA, Duffin R, Kinloch I, Maynard A, Wallace WA, Seaton A, Stone V, Brown S, Macnee W, Donaldson K. 2008. Carbon nanotubes introduced into the

abdominal cavity of mice show asbestos-like pathogenicity in a pilot study. Nat Nanotechnol 3**,** 423-8.
Prazakova S, Thomas PS, Sandrini A, Yates DH. 2014. Asbestos and the lung in the 21st century: an update. Clin Respir J 8**,** 1-10.
Rabolli V, Badissi AA, Devosse R, Uwambayinema F, Yakoub Y, Palmai-Pallag M, Lebrun A, De Gussem V, Couillin I, Ryffel B, Marbaix E, Lison D, Huaux F. 2014. The alarmin IL-1alpha is a master cytokine in acute lung inflammation induced by silica micro- and nanoparticles. Part Fibre Toxicol 11**,** 69.
Rittinghausen S, Hackbarth A, Creutzenberg O, Ernst H, Heinrich U, Leonhardt A, Schaudien D. 2014. The carcinogenic effect of various multi-walled carbon nanotubes (MWCNTs) after intraperitoneal injection in rats. Part Fibre Toxicol 11**,** 59.
Ryman-Rasmussen JP, Tewksbury EW, Moss OR, Cesta MF, Wong BA, Bonner JC. 2009. Inhaled multiwalled carbon nanotubes potentiate airway fibrosis in murine allergic asthma. Am J Respir Cell Mol Biol 40**,** 349-58.
Service RF. 1998. Nanotubes: The next asbestos? Science 281**,** 941.
Shepard MN, Brenner S. 2014. An occupational exposure assessment for engineered nanoparticles used in semiconductor fabrication. Ann Occup Hyg 58**,** 251-65.
Shvedova AA, Kisin ER, Mercer R, Murray AR, Johnson VJ, Potapovich AI, Tyurina YY, Gorelik O, Arepalli S, Schwegler-Berry D, Hubbs AF, Antonini J, Evans DE, Ku BK, Ramsey D, Maynard A, Kagan VE, Castranova V, Baron P. 2005. Unusual inflammatory and fibrogenic pulmonary responses to single-walled carbon nanotubes in mice. Am J Physiol Lung Cell Mol Physiol 289**,** L698-708.
Shvedova AA, Kisin ER, Porter D, Schulte P, Kagan VE, Fadeel B, Castranova V. 2009. Mechanisms of pulmonary toxicity and medical applications of carbon nanotubes: Two faces of Janus? Pharmacol Ther 121**,** 192-204.
Smijs TG, Bouwstra JA. 2010. Focus on skin as a possible port of entry for solid nanoparticles and the toxicological impact. J Biomed Nanotechnol 6**,** 469-84.
Sun B, Wang X, Ji Z, Wang M, Liao YP, Chang CH, Li R, Zhang H, Nel AE, Xia T. 2015. NADPH Oxidase-Dependent NLRP3 Inflammasome Activation and its Important Role in Lung Fibrosis by Multiwalled Carbon Nanotubes. Small 11**,** 2087-97.
Thompson EA, Sayers BC, Glista-Baker EE, Shipkowski KA, Ihrie MD, Duke KS, Taylor AJ, Bonner JC. 2015. Role of Signal Transducer and Activator of Transcription 1 in Murine Allergen-Induced Airway Remodeling and Exacerbation by Carbon Nanotubes. Am J Respir Cell Mol Biol 53**,** 625-36.

Visalli G, Bertuccio MP, Iannazzo D, Piperno A, Pistone A, Di Pietro A. 2015. Toxicological assessment of multi-walled carbon nanotubes on A549 human lung epithelial cells. Toxicol In Vitro 29**,** 352-62.

Wynn TA. 2011. Integrating mechanisms of pulmonary fibrosis. J Exp Med 208**,** 1339-50.

Xu J, Futakuchi M, Shimizu H, Alexander DB, Yanagihara K, Fukamachi K, Suzui M, Kanno J, Hirose A, Ogata A, Sakamoto Y, Nakae D, Omori T, Tsuda H. 2012. Multi-walled carbon nanotubes translocate into the pleural cavity and induce visceral mesothelial proliferation in rats. Cancer Sci 103**,** 2045-50.

II. OBJECTIVES

When this project was initiated, there were different gaps and open issues regarding CNT-induced pulmonary fibrosis, which can be summarized as follows:

- *What are the essential key events/mechanisms involved in CNT pro-fibrotic activities?*
- *What are the main CNT physico-chemical properties that determine their fibrotic activities?*
- *How to predict the pro-fibrotic activities of CNT?*

Thus, the key objectives of my thesis were to identify the mechanisms of action and the physico-chemical properties of CNT that determine their pro-fibrotic activities as well as to develop in vitro tests predictive of the pro-fibrotic activities of CNT. To achieve these tasks, most experiments have been conducted in vitro on fibroblasts, since: i) fibroblasts play a key role in the development of pulmonary fibrosis; ii) CNT have been shown to reach the interstitial space upon inhalation, suggesting a new mode of action for CNT compared to other inhaled particles. However, to conduct relevant in vitro studies with CNT, we first had to design adequate protocols to avoid or take into account interferences of the tested material with the assays, as CNT have been reported to interact with classical toxicological tests. Thus, we developed a NM-adapted in vitro assay to assess cell viability and proliferation in response to NM exposure before investigating mechanisms of CNT pro-fibrotic activities.

Our working hypotheses were:

- *fibroblast proliferation play a relevant role in the fibrogenic activity of CNT in the lung and,*
- *stimulation of fibroblast proliferation by CNT can predict CNT in vivo fibrotic activities.*

III. RESULTS

3.1. ADDRESSING NM-RELEATED INTERFERENCES IN IN VITRO CYTOTOXICITY ASSAYS

3.1.1. Context and general experimental design.

To assess the toxic potential of ENM, in vivo and in vitro experiments are performed with animal and cell models. In recent years, researchers have moved towards the development of predictive in vitro tests to reduce animal use, supporting ongoing 3Rs efforts (Replacement, Refinement and Reduction). These approaches may offer the potential faster and more cost-effective assays to assess the toxic potential of ENM. However, several papers have shown that ENM can interact with classical assays, thus raising the question of potentially misleading results and incorrect interpretations. Because of their high adsorption capacity, optical activity and reactivity, ENM seem to have a high potential for influencing common cytotoxicity assays. The group of Worle-Knirsch et al. (Worle-Knirsch et al., 2006) was the first to investigate this issue. They found that SWCNT interact with the tetrazolium salts of MTT, and recommended to verify results with at least two or more independent assays. Several subsequent papers have reported worrying results on interferences between NM and in vitro cytotoxicity assays (Casey et al., 2007; Monteiro-Riviere et al., 2009). A literature survey indicated that ca. 95% of papers from 2010 using biochemical techniques to assess cytotoxicity did not account for potential interferences of NM with assays, and this number had not substantially improved in 2012 (Ong et al., 2014). Some studies have addressed this issue by reporting the development of NM-adapted protocols (Cho et al., 2013; Darolles et al., 2013; Kroll et al., 2012). However, these NM-adapted protocols are not satisfying (see manuscript below). In this context, we have attempted to design a fast and reliable protocol to assess the cytotoxic activity of NM, including CNT. To achieve this purpose, we have

selected the water soluble tetrazolium salt (WST-1) assay, a colorimetric test that quantifies the cellular/mitochondrial activity and thus reflects cell viability with the advantage of being easy and fast to perform. Twelve different NM/particles have been selected and tested to understand how they may interfere with the WST-1 assay. Interference (adsorption or reaction) with the substrate and product of the assay, as well as influence on the optical absorbance have been analyzed (Figure 4). Four different WST-1 protocols have been proposed and tested on macrophages and epithelial cells to understand which one might be the most convenient to reduce possible analytical interferences of NM.

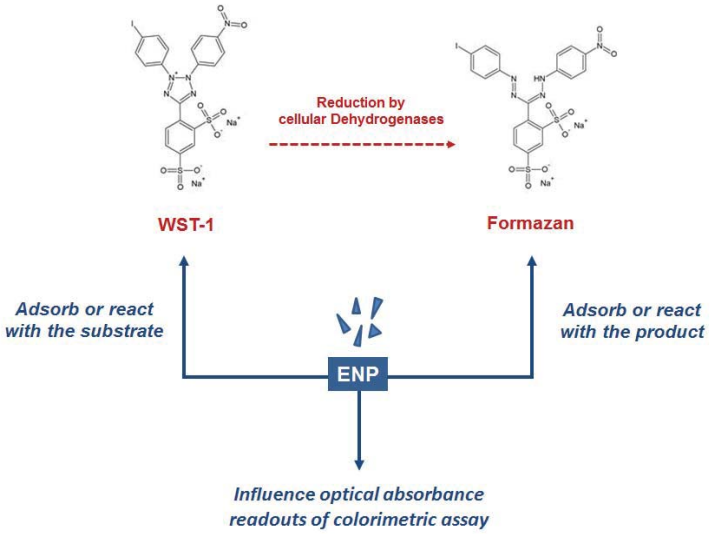


Figure 4. ENM and their possible interferences with the WST-1 assay.

REFERENCES

Casey A, Herwog E, Davoren M, Lyng FM, Byrne HJ, Chambers G. 2007. Spectroscopic analysis confirms the interactions between single walled carbon nanotubes and various dyes commonly used to assess cytotoxicity. Carbon 45**,** 1425-1432.

Cho WS, Duffin R, Bradley M, Megson IL, Macnee W, Lee JK, Jeong J, Donaldson K. 2013. Predictive value of in vitro assays depends on the mechanism of toxicity of metal oxide nanoparticles. Part Fibre Toxicol 10**,** 55.

Darolles C, Sage N, Armengaud J, Malard V. 2013. In vitro assessment of cobalt oxide particle toxicity: identifying and circumventing interference. Toxicol In Vitro 27**,** 1699-710.

Kroll A, Pillukat MH, Hahn D, Schnekenburger J. 2012. Interference of engineered nanoparticles with in vitro toxicity assays. Arch Toxicol 86**,** 1123-36.

Monteiro-Riviere NA, Inman AO, Zhang LW. 2009. Limitations and relative utility of screening assays to assess engineered nanoparticle toxicity in a human cell line. Toxicol Appl Pharmacol 234**,** 222-35.

Ong KJ, Maccormack TJ, Clark RJ, Ede JD, Ortega VA, Felix LC, Dang MK, Ma G, Fenniri H, Veinot JG, Goss GG. 2014. Widespread nanoparticle-assay interference: implications for nanotoxicity testing. PLoS One 9**,** e90650.

Worle-Knirsch JM, Pulskamp K, Krug HF. 2006. Oops they did it again! Carbon nanotubes hoax scientists in viability assays. Nano Lett 6**,** 1261-8.

3.1.2.

Integrating nanomaterial-related interferences in in vitro cytotoxicity assays: a reliable and fast method

Integrating nanomaterial interferences in *in vitro* cytotoxicity assays: a fast and reliable method.

Giulia Vietti[a*], Saloua Ibouraadaten[a], Leen C.J. Thomassen[b], Dominique Lison[a], Sybille van den Brule[a]

[a]Louvain centre for Toxicology and Applied Pharmacology (LTAP), Institut de Recherche Expérimentale et Clinique (IREC), Université catholique de Louvain (UCL), Avenue E. Mounier, 53 (bte B1.52.12), 1200 Brussels, Belgium.
[b]KU Leuven, Faculty of Industrial Engineering, Department of Chemical Engineering, Lab4U; Agoralaan building B box 8, 3590 Diepenbeek, Belgium.

[*]Corresponding author: phone +322 764 53 54
Fax +322 764 53 38
giulia.vietti@uclouvain.be

Abstract

Nanomaterials (NM) are deeply investigated to identify their potential hazards for human health. Because of the increasing variety of NM on the market, development of fast and reliable *in vitro* assays is urgently needed to evaluate and predict NM toxic activities. However, data resulting from *in vitro* tests, e.g. cytotoxicity tests, are often unreliable or contradictory due to interferences between NM and these assays. In this study, we investigated interferences of 12 NM/particles with the WST-1 assay and designed a procedure to control and deal with these interferences. Incubating NM with the WST-1 reagent or product showed that NM mainly interfere with the absorbance at the assay detection wavelength. We then evaluated several adaptations to the WST-1 protocol with macrophages and epithelial cells, and compared the results to cell counting (trypan blue exclusion method). Adaptations included cell washing before WST-1 addition, transfer of WST-1 cell supernatant before absorbance reading, and introduction of condition-matched blanks containing as much NM as in the test wells but no cell activity. We conclude that washing cells after exposure to NM and the use of condition-matched blanks allow a reliable evaluation of cytotoxicity with most NM, and propose here a NM-adapted WST-1 procedure easily amenable to high-throughput.

Keywords

Cell, viability; nanoparticle; carbon nanotube; WST-1; absorbance

1. Introduction

Because of the fast and extensive development of nanomaterials (NM) and their introduction into everyday life products, it is essential to efficiently assess their potential hazards for human health. In view of the large variety of NM to be tested and the necessity to reduce animal experimentation, there is a need to develop and validate fast but reliable *in vitro* tests to predict NM toxic activities (Vietti et al. 2013) and to identify physico-chemical determinants of these hazardous properties (see (Braakhuis et al. 2014) for review). However, many authors have reported conflicting results with conventional *in vitro* cytotoxicity assays (Casey et al. 2007; Darolles et al. 2013; Davoren et al. 2007; Monteiro-Riviere et al. 2009) and this raised the issue of data misinterpretation. It was rapidly realized that interferences between assays and NM could contribute to confound the results of several *in vitro* tests, leading to false positive or negative results, but it is not clear how to exactly cope with this issue.

Interferences between NM and assays, and identification at which NM concentration level and which experimental procedure/step NM can interfere, have been reported in several studies (Holder et al. 2012; Ong et al. 2014). Cobalt oxide nanoparticles (NP), single-wall (SW) and multi-wall (MW) carbon nanotubes (CNT) were shown to interfere with the assay detection wavelength in colorimetric (water soluble tetrazolium salt, WST-1) and fluorescent (Alamar blue, AB) assays (Casey et al. 2007; Darolles et al. 2013). Polar CNT could even quench the fluorescence of resorufin, the product of AB-based assays (Breznan et al. 2015). Interactions of NM with the assay reagent were reported for MTS (3-(4,5-dimethylthiazol-2-yl)-5-(3-carboxymethoxyphenyl)-2-(4-sulfophenyl)-2H-tetrazolium, similar to WST-1) and AB (Ong et al. 2014) and with the MTT (3-(4,5-dimethylthiazol-2-yl)-2,5-diphenyltetrazolium bromide) product (insoluble formazan) (Belyanskaya et al. 2007; Fisichella et al. 2009; Worle-Knirsch et al. 2006). Assessment of membrane integrity can be obscured by adsorption on NM of a variety of molecules to be detected or measured, i.e. lactate dehydrogenase (LDH) (Holder et al. 2012; Kroll et al. 2012). Various NM were also reported to interfere with other assays such as CyQuant, CellTiter-Blue, CellTiter-Glo, neutral red and Commassie blue (Casey et al. 2007; Darolles et al. 2013; Davoren et al. 2007; Mittal et al. 2011; Monteiro-Riviere et al. 2009; Vietti et al. 2013).

Therefore, there is an urgent need to develop appropriate methods to assess NM cytotoxicity (Casey et al. 2007; Mittal et al. 2011). Some authors provided recommendations, including (i) not to use MTT for nanotoxicology (Fisichella et al. 2009), (ii) confirming results with independent tests (Worle-Knirsch et al. 2006), (iii) individually assessing interferences because they are not predictable (Ong et al. 2014). However, only few studies have addressed the issue of NM interferences (Cho et al. 2013; Darolles et al. 2013; Kroll et al. 2012).

Assays such as WST-1 and AB quantify cellular activity and reflect cell viability by the detection of a colored or fluorescent molecule, respectively, produced by dehydrogenases in viable cells. These tests are fast and easy to implement. However, due to the optical, catalytic and adsorption properties of NM, they could interfere with the assay at different levels: (i) absorbance or fluorescence at detection wavelength, (ii) adsorption or transformation of the assay reagent, and (iii) quenching or transformation of the assay product, as already listed in (Holder et al. 2012; Ong et al. 2014). Assessing interferences is therefore a real challenge and appropriate NM-specific adaptations are absolutely necessary to produce data that take all these possible sources of interference into account.

We recently described a NM-adapted WST-1 protocol to assess the proliferating activity of CNT on fibroblasts (Vietti et al. 2013). In the present study, we analyzed different adaptations of the WST-1 protocol to determine the most convenient option to reduce analytical interferences with a large panel of NMs. We show that interferences are mainly due to NM absorbance at the WST-1 detection wavelength and that most of them can be removed by washing the culture wells before adding WST-1 and using appropriate controls/blanks. Thus, by adapting the WST-1 assay, we propose here a fast and reliable procedure to test NM cytotoxicity.

2. Material and methods

2.1. Materials

Micrometric crystalline silica particles Min-U-Sil 5 (µSiO2) were purchased from US Silica (Berkeley Springs, USA); nanometric ZnO (NM110), TiO_2 (NM101, NRCWE-01 to 04), MWCNT (NM400) from the European Commission Joint Research Centre (Ispra, Italy); MWCNT (20-30 nm and 8 nm) from Cheaptubes (Cambridgeport, USA); UfCB from ERACHEM Comilog S.A. (Willebroek, Belgium). Amorphous nanometric silica ($nSiO_2$) was synthesized and purified according to the Stöber synthesis and dialysis procedure as described in (Thomassen et al. 2010). A solution of 0.8 M ultrapure water, 0.2 M NH_4OH, 1.5 M tetraethyl orthosilicate (TEOS, Acros, Geel, Belgium) was prepared in ethanol. Briefly, 1400 ml of ethanol was poured in a 2 l Erlenmeyer. Next, 5.87 ml DDI water and 20.96 ml NH_4OH was added. The solution was stirred vigorously with a magnetic stir bar while 465 ml TEOS was slowly added. The solution was further stirred at 400 rpm during 24 h. To ensure a complete hydrolysis and condensation of TEOS, a total of 91 ml of DDI water was added over the next 48 h. After the dialysis procedure, the silica sample was filtered on Whattmann filter n°5 to retain aggregated and gelled particles. The concentration of the $nSiO_2$ suspension (47.8 g SiO_2/l) was determined by analyses of the silicon content by inductively coupled plasma atomic emission spectroscopy (ICP-AES, Perkin Elmer 4300 DV). Transmission electron microscopy (TEM) Philips CM200 FEG instrument operated at 200 kV

recorded monodispersed non-aggregated nanoparticles with an average diameter of 12.2 ± 3 nm (100 particles measured). Small angle X-ray scattering (SAXS) of $nSiO_2$ suspension was measured at room temperature in a 1 mm quartz capillary on a SAXSess MC2 instrument (Anton Paar, Gentbrugge, Belgium) with line-collimated CuKa radiation and image plate detector. Analysis of SAXS patterns yielded particle size of 14 nm (in a dispersed spherical model with varying electron density). A larger diameter measured by SAXS compared to TEM is expected due to shrinkage of the particles upon vacuum drying in the TEM preparation procedure. Nitrogen sorption isotherms of the powder samples were recorded at -196 °C using a TriStar apparatus (Micromeritics). Samples were pretreated at 250 °C under nitrogen flow during 12 h in a SmartPrep Programmable Degas System (Micromeritics). The total specific surface area, derived from the adsorption branch of the isotherms using the Brunauer-Emmett-Teller (BET) method (P/P0 range 0.05–0.3) is 400 m²/g. The external surface area (alpha-s) is 227 m²/g, corresponding to spherical particles of ca 15 nm, and the micropore volume is 55 µl/g, reflecting a substantial surface roughness. NM and particle characteristics are presented in Table 1.

2.2. Material dispersion

MWCNT 20-30 nm, MWCNT 8 nm, NM400 and UfCB were dispersed as described previously (Vietti et al. 2013). Briefly, samples were suspended to a concentration of 4 mg/ml in filter-sterilized nanopure H_2O supplemented with 1.4 mg/ml bovine serum albumin (BSA, Sigma Aldrich, St Louis, USA). The suspension was sonicated for 16 min without interruption on ice. To keep the final dispersant identical at all NM concentrations, stock suspensions (4 mg/ml) were serially diluted in the same dispersion medium and then sonicated for 15 min in a water bath. NM110, NM101 and NRCWE-01 to 04 were suspended in the same dispersion medium, sonicated 15 min in a water bath and serially diluted as described above. $nSiO_2$ stock suspension was diluted in the dispersion medium. Min-U-Sil was heated at 200°C for 2 h to remove any trace of endotoxin and then suspended in the dispersion medium.

2.3. Cell culture and exposure

The mouse leukemic macrophage cell line (RAW 264.7, a gift from Pr Michiels, de Duve institute, Brussels, Belgium) was cultured in Dulbecco's Modified Eagle's Medium (DMEM, Invitrogen, Paisley, USA) supplemented with 10 % fetal bovine serum (FBS, Invitrogen) and 1 % antibiotic-antimycotic (AA, Invitrogen) and maintained at 37°C under 5 % CO_2. RAW 264.7 cells were harvested and subcultured by scraping, centrifuged 10 min at 400 *g* and resuspended in fresh complete medium (DMEM, 10 % FBS, 1 % AA). Viable cell number was determined with trypan blue solution (Sigma Aldrich) on a Neubauer cell under a light microscope. Cells were seeded in 96-well (for WST-1, AB and LDH activity assays) or 12-well (for trypan blue exclusion method) culture plates in complete medium at a concentration

of 9.10^4 cells/cm² (surface area of the culture well) and incubated at 37°C for 24 h before exposure. RAW 264.7 were subcultured for a maximum of 15 passages.

Mouse type II alveolar epithelial cells (LA-4) obtained from ATCC (catalog n°CCL-196) were cultured in F-12K (Invitrogen) supplemented with 15 % FBS and 1 % AA and maintained at 37°C under 5 % CO_2. For harvesting, LA-4 cells were incubated with 0.25 % trypsin-EDTA (Invitrogen) at 37°C. Trypsin was neutralized by adjunction of complete medium (F-12K, 15 % FBS, 1 % AA). Cell suspensions were centrifuged for 10 min at 400 *g* and resuspended in fresh complete medium. Viable cell number was determined as described above. Cells were seeded in 96-well culture plates in complete medium at a concentration of 15.10^4 cells/cm² and incubated at 37°C for 24 h before exposure. LA-4 were subcultured for a maximum of 15 passages.After 24 h in complete culture medium, cells were washed once with their basal medium (without FBS) and supplied with 200 µl (96-well culture plates) or 2 ml (12-well culture plates) medium containing 1/10 material dilutions. Cells were exposed during 24 h to different concentrations of particles/NM depending on the particle studied. Low toxicity NM were tested to a maximal concentration of 200-400 µg/ml while other NM at relevant concentrations determined in preliminary experiments (data not shown).

2.4. Trypan blue exclusion method

Trypan blue stains the nucleus of non-viable cells because of increased plasma membrane permeability, whereas viable cell membranes are not permeable to trypan blue. Non-stained cells are counted as viable cells under a light microscope. This method requires that adherent cells be detached and suspended before staining. After exposure to NM, RAW 264.7 in 12-well culture plates were washed twice with their basal medium and then supplied with 1 ml medium. Cells were scrapped and cell suspensions were transferred and kept on ice. Viable cell number was determined with trypan blue solution on a Neubauer cell. LA-4 in 96-well culture plates were also washed twice with their basal medium and then supplied with 25 µl 0.25 % trypsin-EDTA and incubated 5 min at 37°C. Trypsin was neutralized by adjunction of 100 µl complete medium and cell suspensions were transferred and kept on ice. Viable cell number was determined with trypan blue solution on a Neubauer cell. Data are presented as relative cell viability (relative cell count) compared to non-exposed cells. Cells were not counted with an automated cell counter because of the unpredictable formation of NM agglomerates/aggregates that can interfere with cell detection.

2.5. LDH activity assay

This test is a spectrophotometric method that measures the release of cytoplasmic LDH into the extracellular space upon cell lysis and damage, as a marker of cytotoxicity. Twenty four h after exposure to NM, LDH activity was measured by the Synchron LX Unicell DXC-800 (Beckman Coulter, Brea, USA) on cell supernatants in the presence of NAD+ 11 mM and lactate 50 mM. Each assay included a “100 % cell death” condition consisting of cells treated

with triton 0.1 % used to calibrate LDH release. Data are presented as relative cell viability compared to non-exposed cells.

2.6. WST-1 assay

WST-1 is a colorimetric assay that quantifies cellular/mitochondrial activity and reflects cell viability by the cleavage of the tetrazolium salt WST-1 by, mainly mitochondrial, dehydrogenases in viable cells. The assay measures the absorbance of the soluble product formazan. In the original protocol (Figure 4, procedure A), WST-1 reagent (Roche Diagnostics, Mannheim, Germany) is directly added to the exposed cells. To reduce interferences to a minimal level, culture medium containing the NM were always removed after exposure, and cells were washed with basal medium before WST-1 addition to eliminate remaining NM/particles adsorbed on cells or sticking to the plastic culture well. Cells were then supplied with 100 µl of their respective medium. In procedures B and C, 100 µl WST-1 diluted 10x (RAW) or 5x (LA-4) in medium were added to all wells, incubated at 37°C during 1-2 h and, then, absorbance was measured directly in the culture well or cell supernatants were transferred to new wells before absorbance reading, respectively. Blanks are wells containing only medium and WST-1. In procedures D and D', part of the wells (blanks) were supplied with 100 µl triton X-100 0.2 % (final concentration 0.1 % in medium, Sigma Aldrich) or $HgCl_2$ 200 µM (final concentration 100 µM in medium), respectively (see below); other wells received 100 µl medium. After 15 min at 37°C, 100 µl WST-1 diluted 10x (RAW) or 5x (LA-4) in medium (1 % AA) were added to all wells and plates were incubated at 37°C. Absorbance was measured at 480 nm and corrected at 680 nm (Spectrophotometer Infinite F200, Tecan, Mannedorf, Switzerland) at different time points (as indicated) or after 60 min for RAW 264.7 and 120 min for LA-4. Data are also presented as relative cell viability compared to non-exposed cells, where cell viability = $(Abs_{480} - Abs_{680})_{test}$ - $(Abs_{480} - Abs_{680})_{blank}$ with $(Abs_{480} - Abs_{680})_{test} = Abs_X$ and $(Abs_{480} - Abs_{680})_{blank} = Abs_Y$ (see Figure 4).

To identify a soluble chemical that completely suppressed WST-1 cell activity while keeping the same amount of NM in the blank wells as in the test sample (procedures D and D'), several cytotoxic agents were tested. RAW 264.7 were seeded in 96-well culture plates in complete medium at a concentration of 9.10^4 cells/cm². After 24 h at 37°C, cells were incubated with 100 µl medium (1 % AA) containing NaN_3 1-25 mM, H_2O_2 5-50 mM, Triton X-100 0.1-2.5 % or $HgCl_2$ 100-500 µM. After 15 min at 37°C, 100 µl WST-1 diluted 10x in medium (1 % AA) were added. The plates were incubated at 37°C and absorbance was measured directly and every 10 min during 1 or 2 hour. Identical tests were performed without cells to assess interferences between cytotoxic agents and WST-1.

2.7. Alamar Blue assay

The Alamar Blue (AB) assay is based on the same principle as WST-1 but uses the resazurin reagent. Resazurin is reduced by living cells to resorufin which fluorescence is

quantified as a marker of cell viability. Modified AB (Invitrogen) assay was conducted as described for procedure B with WST-1 assay. Fluorescence was measured after 2 h incubation with an excitation wavelength of 540 nm and an emission wavelength of 585 nm with the SpectraMax Gemini-XS (Molecular Devices, Sunnyvale, USA). Data are also presented as relative cell viability compared to non-exposed cells, where cell viability was calculated exactly as for WST-1.

2.8. Evaluation of interferences between NM and WST-1 assay components.

Interferences between NM and the WST-1 assay were assessed in 96 well plates containing NM and the WST-1 reagent or product (formazan). 100 µl NM diluted in medium (1 % AA) were incubated with 100 µl WST-1 diluted 10 x in medium or formazan, exactly under the same conditions as for the WST-1 assay described above. Absorbance was measured directly (T0) and after 2 h (T120) incubation at 37°C. Formazan was obtained from RAW 264.7 incubated with WST-1 in medium (1 % AA) until absorbance reached 1.6 to 2 units. The effect of triton and $HgCl_2$ on interferences between NM and WST-1 reagent was also tested under the same conditions.

2.9. Statistics

All graphs show means ± standard error on the mean (SEM) of technical or biological replicates (see legend of figures). Differences were evaluated using one-way analysis of variance (ANOVA), followed by a Dunnett multiple comparisons test or two-way ANOVA, followed by a Bonferroni post-test, as appropriate. Statistical significance was considered at $p < 0.05$. Data analysis was performed with GraphPad Prism version 3.03 (GraphPad Software, San Diego, USA).

3. Results and discussion

3.1. Inconsistency of non-adapted cytotoxicity assays with NM

The cytotoxic activity of 11 NM and 1 micrometric particle (see Table 1) and their possible interferences with *in vitro* cytotoxicity assays were assessed in this study. The relative cell viability of an adherent macrophage cell line (RAW 264.7) was first analyzed after exposure to 6 NM with different elemental composition, structure and dimensions. To assess the cytotoxic activity of these particles, 4 independent assays based on different readouts were tested: WST-1, AB, LDH release and trypan blue exclusion method (cell counting). Cells were washed after exposure to NM, before performing the WST-1 and AB assays. Indeed, in absence of washing, the analytical beam was dimmed by many of the NM (mainly MWCNT and UfCB) and absorbance values above the upper detection limit were recorded (data not shown). Figure 1 clearly shows that results were inconsistent among assays for all NM examined.

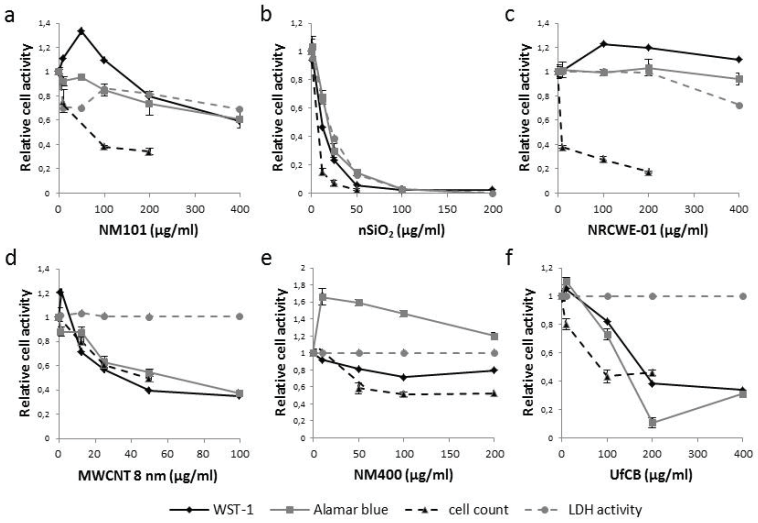


Figure 1: Comparison of dose-responses obtained with 4 cell viability assays to assess NM cytotoxicity. *Relative cell viability was assessed by the WST-1 assay (procedure B, see figure 4), Alamar Blue, LDH activity and trypan blue exclusion method (cell count) on RAW 264.7 exposed 24 h to several NM (mean ± SEM, n=3-4).*

Thus, we selected one of these assays to adapt a protocol amenable to all NM. Though manual cell counting (trypan blue exclusion method) is expected to be a reliable method to assess viable cell number, it is time consuming and not suitable for large throughput, especially as automated cell counting can interfere with NM (agglomerates/aggregates), as already mentioned in (Vietti et al. 2013). Moreover, cell detachment by scrapping (compared to trypsin treatment) may lead to high cell mortality and, therefore, to possible bias for strongly adherent cells such as macrophages (data not shown). Measurement of LDH activity was often described to be affected by NM (Cho et al. 2013; Kroll et al. 2012; Mittal et al. 2011) and does not allow detecting increased cell number, i.e. activation of cell proliferation. AB assay is based on fluorescence detection and is therefore potentially unsuitable for fluorescent NM, such as quantum dots. Finally, interferences have also been described with the WST-1 assay (Casey et al. 2007; Darolles et al. 2013; Wilhelmi et al. 2012) though they appear to be mainly due to NM absorbance at the assay wavelength. Because of its high-throughput potential, we selected WST-1 as the best candidate assay and investigated how to adapt it for NM testing.

3.2. Interferences of NM with WST-1 reagent and product

Absorbance at the assay detection wavelength was assessed after incubation of NM with the WST-1 assay reagent (WST-1) or product (formazan) without cells. WST-1 (diluted in culture medium) or formazan (produced by RAW 264.7 incubated with WST-1) were added to NM suspensions. Absorbance was measured directly (T0) and 2 h (T120) after incubation at 37°C. Absorbance increased dose-dependently with almost all NM at T0 (Figure 2). Starting from a slightly higher value (due to spontaneous WST-1 reduction), absorbance curves at T120 paralleled those at T0, indicating that no additional reaction occurred after 2 h for 10 of the 12 NM/particles tested. These results confirmed that most NM mainly interfere with the WST-1 assay detection wavelength but do not interact with the WST-1 reagent. For NM400 and UfCB, absorbance increased slightly more at T120 compared to T0 above 10 µg/ml. Moreover, above 100 µg/ml for NM400 and 200 µg/ml for UfCB, absorbance exceeded the maximal limit of detection of the plate reader (after incubation with WST-1 and formazan).

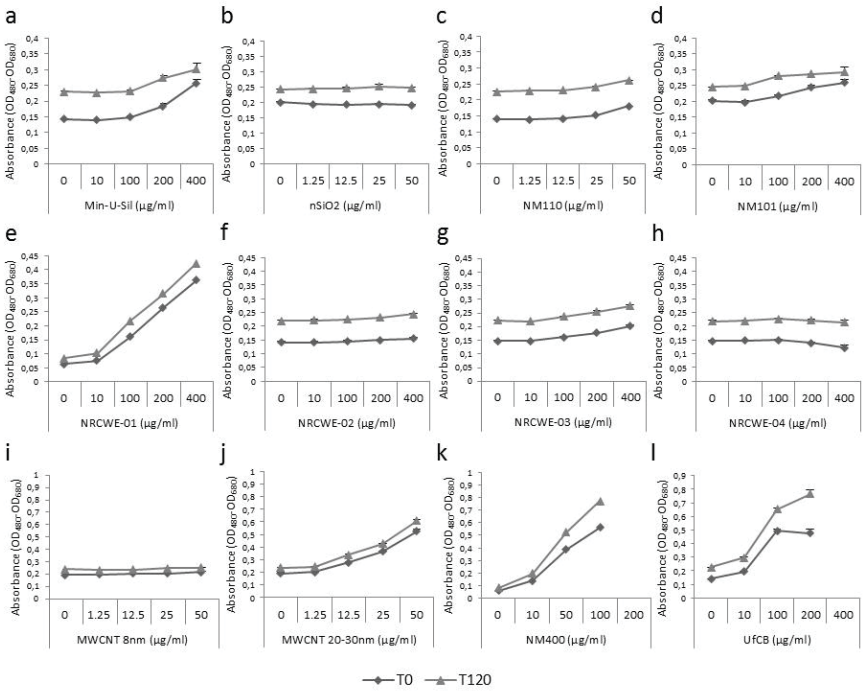


Figure 2: Interferences of NM with absorbance wavelength and WST-1 assay reagent. *Absorbance (OD_{480} - OD_{680}) was measured directly after adding NM to WST-1 and after 120 min incubation at 37°C (mean ± SEM, n=4 technical replicates).*

After incubation with formazan, NM/particles tested had the same profile of absorbance as with WST-1 and curves at T0 and T120 overlapped each other, again indicating that no additional reaction occurred after 2 h (Figure 3). We concluded that most NM mainly interfere with the detection absorbance wavelength of the WST-1 assay.

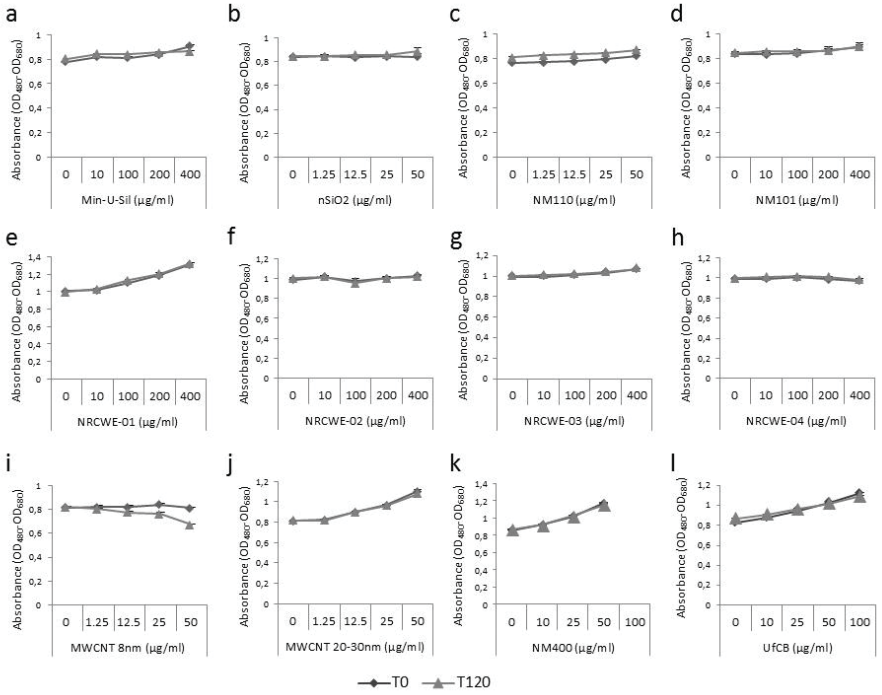


Figure 3: Interferences of NM with absorbance wavelength and WST-1 assay product. *Formazan was obtained from RAW 264.7 incubated with 200 µl WST-1 until absorbance reached 1.6 to 2 units. Cell supernatant/formazan was diluted twice in medium and added to NM. Absorbance (OD_{480} - OD_{680}) was measured directly after NM addition and after 120 min incubation at 37°C (mean ± SEM, n=4 technical replicates).*

3.3. Design of different adaptations to the WST-1 protocol

In Figure 4, we illustrate and outline the different options considered for adapting the original WST-1 assay according to 4 different procedures. In panel A (WST-1) we show the original WST-1 assay, where WST-1 is directly added to the cells after exposure. The blank is a cell-free well containing the medium and WST-1 and its absorbance (Abs_Y) is subtracted from the test well absorbance (Abs_X). Cells can also be washed after exposure (panel B, WST-1 wash), before addition of WST-1. In panel C (WST-1 SN), the protocol is identical to B, but cell culture supernatant is additionally transferred to new wells before absorbance reading. Blanks for procedures B and C are as in the original protocol (procedure A).

Because of the interference of some NM with the detection absorbance wavelength of the WST-1 assay (Figures 2 and 3), the fact that NM400 and UfCB possibly interfere at another level of the assay (Figure 2), and that the amount of NM remaining in the culture wells after washing (including endocytosed NM) is not easily predictable, we sought to design a WST-1 procedure that would completely overcome these issues. Therefore, an experimental blank, identical to the test wells (same amount of material) but without cell activity, was added to the protocol. The strategy was to include additional blanks for each condition (type of NM and concentration), containing the same amount of material as in the test well after washing but where cells are lysed just before WST-1 addition. As described in the material and methods for procedures D and D', the absorbance of these "matched" blanks (Abs_Y) is subtracted from the absorbance of the test well (Abs_X) (procedures A to C). Thus, in procedures D and D', after exposure to NM and a washing step, half of culture wells (blanks) were treated with a cytolytic dose of a soluble agent before addition of WST-1.

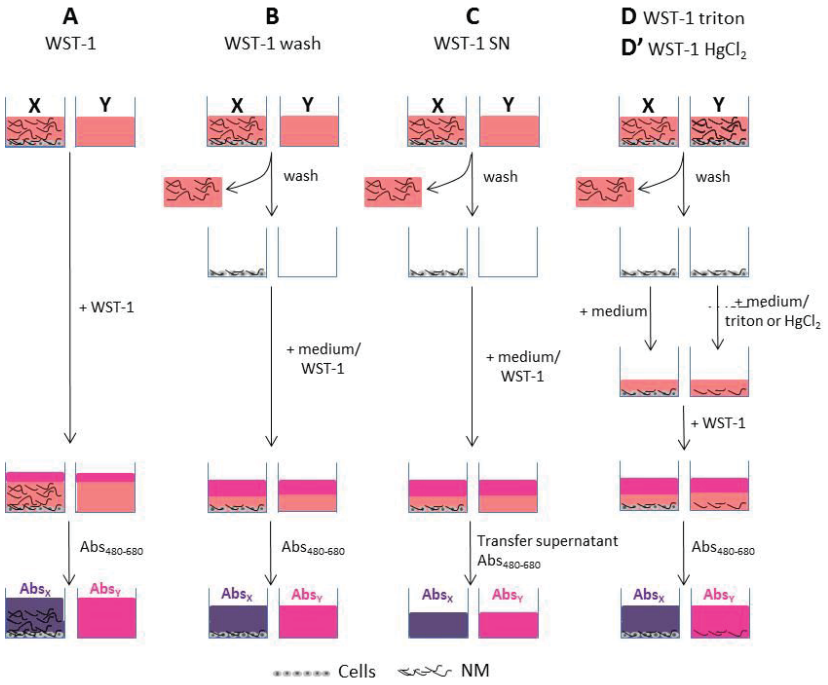


Figure 4: Original vs. modified WST-1 assay protocols*. This figure illustrates 5 different WST-1 protocols to perform after cell exposure to NM. The culture well X is the test sample well and Y is the blank well implemented in the corresponding procedure. After addition of the WST-1 reagent, cells are incubated between 30 min and 4 h at 37°C and absorbance (Abs) is read at 480 nm vs background (680 nm). The endpoint value of the test is the*

subtraction of the blank Abs (Abs_Y) to the test sample Abs (Abs_X). In procedure A (WST-1), WST-1 is directly added to the exposed cells, as recommended by the manufacturer. In B (WST-1 wash), cells are washed before addition of WST-1. In C (WST-1 SN), cells are also washed before adding WST-1 but supernatant is transferred to a new well after WST-1 incubation and before Abs reading. In (A), (B) and (C), blanks are wells containing only the medium and WST-1. In D and D' (WST-1 triton or WST-1 $HgCl_2$, respectively), replicates of test samples are washed simultaneously and part of the wells are treated with triton or $HgCl_2$ to kill cells before addition of WST-1 (blanks).

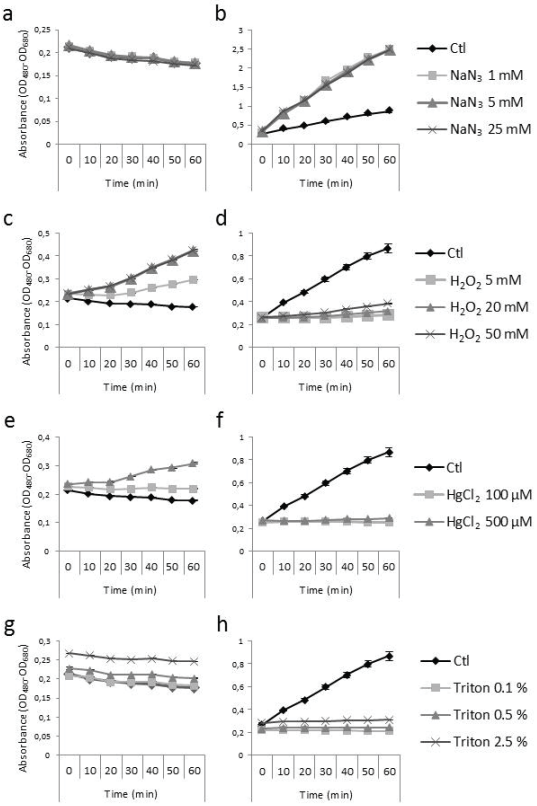


Figure 5: Selection of a cell lytic agent that does not interfere with the WST-1 assay. *(A-B) NaN_3, (C-D) H_2O_2, (E-F) $HgCl_2$ and (G-H) triton were incubated with WST-1 (A, C, E and G) or RAW 264.7 and WST-1 (B, D, F and H). Absorbance was measured every 10 min during 1 h (mean ± SEM, n=6 technical replicates).*

3.4. Selection of the soluble cytolytic agent

We assessed the cytolytic activity of 4 soluble agents (NaN_3, H_2O_2, $HgCl_2$ and triton) and their effect on the WST-1 absorbance in absence or presence of cells at different time points. In

absence of cells, NaN_3 did not modify WST-1 absorbance 1 h after incubation but strongly increased it in the presence of cells (Figures 5 a and b). H_2O_2 increased WST-1 absorbance in absence and presence of cells (Figures 5 c and d). Though $HgCl_2$ 500 µM slightly increased WST-1 absorbance with time (Figure 5 e), both 100 and 500 µM similarly reduced absorbance to a minimal level in presence of cells (Figure 5 f). Finally, triton 0.1 and 0.5 % had not effect on WST-1 absorbance in absence of cells and reduced absorbance to a minimal level in presence of cells (Figures 5 g and h).

Triton 0.1 % was selected for subsequent experiments. Interferences of triton with the absorbance of NM after incubation with WST-1 were first analyzed as in Figure 2. Except for NM400 and UfCB, triton 0.1 % had no effect (data not shown). Triton increased absorbance at the detection wavelength above 100 µg/ml of NM400 and UfCB (see figure 7 h for UfCB). However, since cells are washed before WST-1 application in procedure D, the final NM concentration can consequently be considered much lower than the exposure concentration. Thus, at this stage of the work, we decided to assess the validity of triton for our objective.

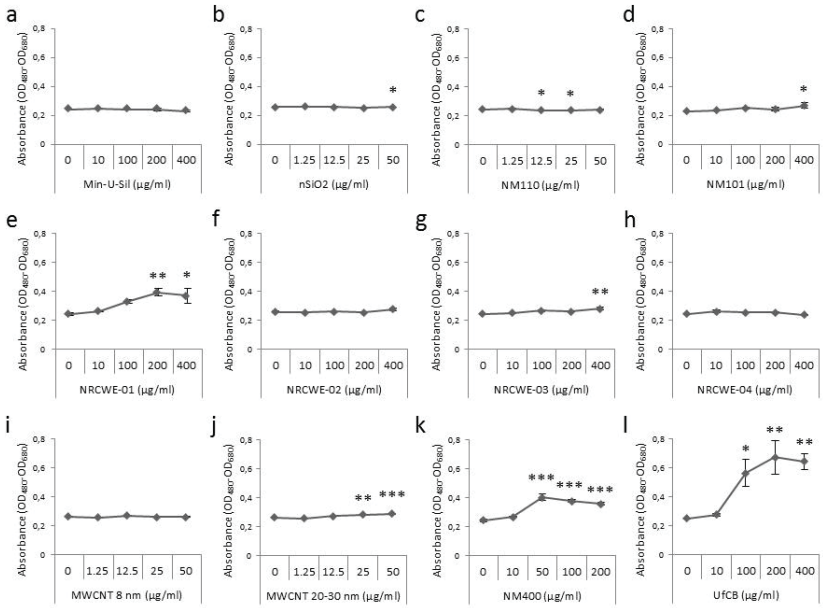


Figure 6: WST-1 assay on triton-treated cells after exposure to NM and washing step. *Absorbance (OD_{480} - OD_{680}) was measured 60 min after adding WST-1 reagent on RAW 264.7 exposed 24 h to NM, washed and treated with triton. * $p \leq 0.05$, ** $p \leq 0.01$ and *** $p \leq 0.001$ relative to vehicle-treated cells (one-way ANOVA followed by Dunnett multiple comparison test between vehicle and NM/particle-treated cells, mean ± SEM, n=4 technical replicates).*

To first assess the relevance of procedure D, RAW 264.7 were exposed for 24 h to NM/particles and absorbance was measured in wells after cell lysis with triton (Abs_Y, blanks). We observed that, even after washing, absorbance was still increased in the presence of some NM such as NRCWE-01, NM400 and UfCB (Figure 6), justifying the relevance of an adapted procedure.

3.5. Comparison of adapted WST-1 procedures for nanotoxicology testing

To examine the validity of the adaptations of the WST-1 assay, procedures B, C and D were compared with RAW 264.7 macrophages exposed to 8 NM (Figure 7). Results for procedures B, C and D were similar for most NM suggesting that washing before WST-1 addition probably eliminated the majority of interferences. However, for TiO_2 NP (NRCWE-01), we found that the relative cell viability measured with procedure B (WST-1 wash) was significantly higher than with procedure D (WST-1 triton) (Figure 7 b). Results obtained for NM110 were slightly different between procedures C and D (Figure 7 c). Finally, UfCB cytotoxicity was shown to be much more severe with procedure D (WST-1 triton) compared to procedures B and C (Figure 7 h).

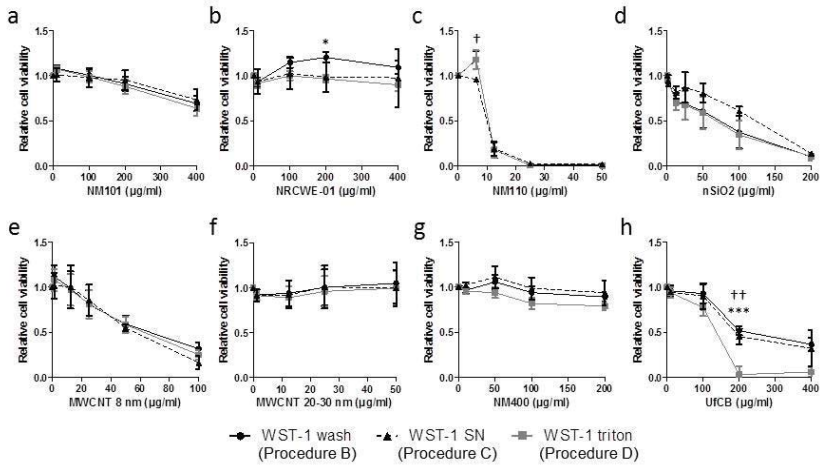


Figure 7: Comparison of adapted WST-1 procedures after RAW 264.7 exposure to NM. *Relative cell viability was assessed on RAW 264.7 exposed 24 h to several NM by adapted WST-1 procedures: (i) WST-1 wash, procedure B, (ii) WST-1 SN, procedure C or (iii) WST-1 triton, procedure D. The statistical difference between procedures was analyzed by two-way ANOVA, followed by a Bonferroni post-test (mean ± SEM, n=3-6 independent experiments). The effect of the procedure was significant for NRCWE-01 ($p \leq 0.05$), NM400 ($p \leq 0.01$) and UfCB ($p \leq 0.001$). * $p \leq 0.05$ and *** $p \leq 0.001$ between WST-1 wash and WST-1 triton; † $p \leq 0.05$ and †† $p \leq 0.01$ between WST-1 triton and WST-1 SN.*

To further assess the validity of the different procedures and the use of triton for blanks, we tested another cell line (type II alveolar epithelial cells LA-4) that can be detached from the culture well by a more gentle procedure (trypsin) than RAW 264.7 macrophages. In this way, we were able to more accurately compare the WST-1 procedures to the cell count by trypan blue exclusion method. Cell count and all WST-1 procedures conducted to equivalent results for NM such as the highly cytotoxic NM110 and the non-cytotoxic MWCNT 8 nm (Figures 8 b and d), indicating that a washing step can efficiently help for accurately assessing the cytotoxicity of some NM with the WST-1 assay. For other NM, an adaptation of the WST-1 protocol was clearly required. Washing was not sufficient to remove all interferences of NRCWE-01 (Figure 8 a) as already suggested in Figure 6 e: transfer of the WST-1 supernatant or the use of triton blank could overcome the remaining interferences to obtain results similar to the trypan blue exclusion method. For $nSiO_2$, we repeatedly observed a discrepancy between trypan blue exclusion method and WST-1 procedures at some $nSiO_2$ concentrations (Figure 8 c), though no interferences were detected between these NP and absorbance detection wavelength, WST-1 and formazan (Figures 2 and 3). This increase of WST-1 activity has also been reported for other silica NP in another study (Wilhelmi et al. 2012) but we can currently not explain this artefact observed with the WST-1 procedure. However, this does not preclude using the WST-1 assay to identify doses that induce a strong cytotoxicity.

Data were less straightforward for MWCNT. As already said, both cell count and all WST-1 procedures led to similar results for MWCNT 8 nm (Figure 8 d). For NM400, only the procedure with triton gave viability results similar to cell count (Figure 8 f). However, although no interferences were detected between MWCNT 20-30 nm and absorbance detection wavelength, WST-1 and formazan (Figures 2 and 3), WST-1 cell viability for MWCNT 20-30 nm results were overestimated compared to cell count above 25 µg/ml (Figure 8 e). Thus, except for one sample of MWCNT, our data suggest that using blank wells with triton (procedure D) is the most appropriate assay adjustment to reliably assess cytotoxicity of NM.

The WST-1 procedure using triton blanks indicated more severe cytotoxicity than any other test for 200 and 400 µg/ml UfCB both with macrophages and epithelial cells (Figures 7 h and 8 g), suggesting that this procedure is not appropriate for CB. Thus, we additionally tested $HgCl_2$ as cytolytic agent in procedure D'. Direct interferences of UfCB with WST-1 in presence of $HgCl_2$ was first assessed. Figure 8 h shows that $HgCl_2$ has no effect on WST-1 absorbance while triton strongly increases absorbance in presence of 200 µg UfCB/ml. This strongly suggests that, because of its detergent/surfactant properties, triton can modify UfCB aggregation state and thus the turbidity of the suspension in culture wells and, in this way, light absorbance. It can lead to the overestimation of the blank absorbance and,

consequently, to underestimate cell viability. As shown in Figure 8 g, while WST-1 triton (procedure D) strongly underestimated cell viability at high UfCB concentration (200 µg/ml), WST-1 $HgCl_2$ (procedure D') led to similar results compared to the trypan blue exclusion method. On the contrary, procedures B and C overestimated cell viability. With other NM, WST-1 procedure using $HgCl_2$ or triton led to similar results.

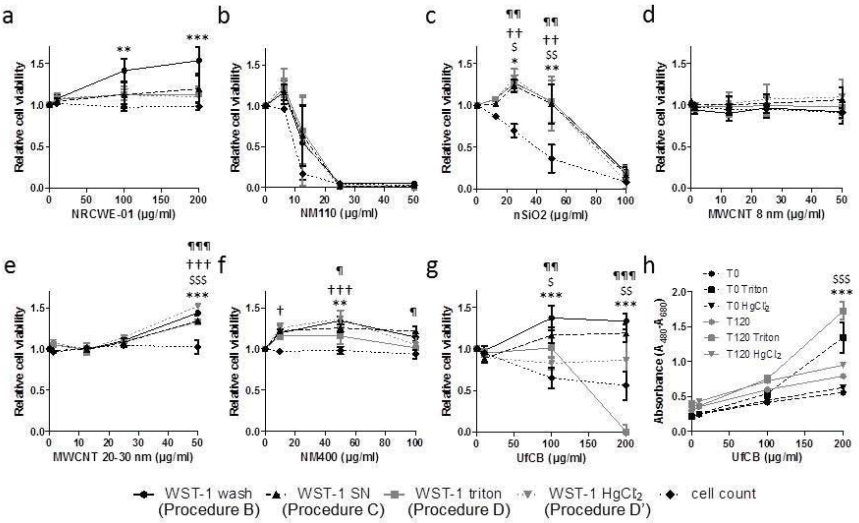


Figure 8: Comparison of adapted WST-1 procedures to trypan blue exclusion method after LA-4 exposure to NM. *(A-G) Relative cell viability was assessed on LA-4 exposed 24 h to NM by the trypan blue exclusion method (cell count) or 4 WST-1 protocols (WST-1 wash, procedure B; WST-1 SN, procedure C; WST-1 triton, procedure D; WST-1 $HgCl_2$, procedure D'). The statistical difference between procedures was analyzed by two-way ANOVA, followed by a Bonferroni post-test comparing WST-1 conditions to cell counts (mean ± SEM, n=3-6 independent experiments). The effect of the procedure on the results was significant for NRCWE-01 ($p \leq 0.0001$), nSiO2 ($p \leq 0.01$), MWCNT 20-30 nm ($p \leq 0.001$), M400 ($p \leq 0.001$) and UfCB ($p \leq 0.001$).* $p \leq 0.05$, ** $p \leq 0.01$ and *** $p \leq 0.001$ between cell count and WST-1 wash; \$ $p \leq 0.05$, \$\$ $p \leq 0.01$ and \$\$\$ $p \leq 0.001$ between cell count and WST-1 triton; † $p \leq 0.05$, †† $p \leq 0.01$ and ††† $p \leq 0.001$ between cell count and WST-1 $HgCl_2$. ¶ $p \leq 0.05$, ¶¶ $p \leq 0.01$ and ¶¶¶ $p \leq 0.001$ between cell count and WST-1 SN. (H) Interferences of UfCB with absorbance wavelength and substrate of WST-1 assay in presence of triton or $HgCl_2$. Absorbance (OD_{480} - OD_{680}) was measured directly after adding UfCB to WST-1 reagent and after 120 min incubation in presence of 0.1 % triton, 100 µM $HgCl_2$ or none of the toxic agents (mean ± SEM, n=4 technical replicates). The statistical difference between procedures was analyzed by two-way ANOVA, followed by a Bonferroni post-test. *** $p \leq 0.001$ between T0 and T0 triton and T120 and T120 triton; \$\$\$ $p \leq 0.001$ between T0 triton and T0 $HgCl_2$ and T120 triton and T120 $HgCl_2$.*

4. Conclusions

In this manuscript, we showed that interferences between most NM and the WST-1 cytotoxicity assay mainly result from the dose-dependent absorbance of NM at the assay detection wavelength. To take these interferences into account for producing reliable cytotoxicity data, we adapted the WST-1 assay by evaluating the relevance of several modifications to the protocol and compared results to the trypan blue exclusion method which is not sensitive to optical interferences. We conclude that most data obtained by washing cells after exposure to NM (procedure B) and transferring cell supernatant after incubation with WST-1 (procedure C) are consistent with cell count results. Moreover, we observed that using the procedure with adapted blank wells lysed with triton or $HgCl_2$ (procedure D or D') is the most reliable for all NM tested. Indeed, this adaptation of the protocol also allows taking into account NM left in the culture well after the washing step and the potential reactivity of NM with the WST-1 substrate. This procedure does, however, not take into account the possible interference of NM with the WST-1 product, formazan. To the best of our knowledge, such interferences between NM and soluble formazan have never been reported, and we found that the NM tested in the present study did not interfere at this level of the WST-1 assay, indicating that this limitation is minimal.

Our data confirms the results of (Kroll et al. 2012) concluding that a washing step should be included in the MTT assay when testing NM. These authors showed that their method was valid until exposure NM concentrations of 10 µg/cm² and not for CB. In our study, the use of specific blank wells (with triton or $HgCl_2$), allows extending the tested concentrations and the type of NM. Thus, we propose here a NM-adapted WST-1 assay easily amenable to high-throughput to fast and reliably assess NM *in vitro* cytotoxicity.

Acknowledgments

Giulia Vietti is research fellow with the Fonds National de la Recherche Scientifique (FNRS). This work was supported by Innoviris (Nano-Iris project).

Declaration of interest

The authors report no declarations of interest.

References

1. Belyanskaya, L, Manser, P, Spohn, P, Bruinink, A, Wick, P. (2007). The reliability and limits of the MTT reduction assay for carbon nanotubes-cell interaction. *Carbon*, 45, 2643-8.
2. Braakhuis, HM, Park, MV, Gosens, I, De Jong, WH, Cassee, FR. (2014). Physicochemical characteristics of nanomaterials that affect pulmonary inflammation. *Part Fibre Toxicol*, 11, 18.
3. Breznan, D, Das, D, MacKinnon-Roy, C, Simard, B, Kumarathasan, P, Vincent, R. (2015). Non-specific interaction of carbon nanotubes with the resazurin assay reagent: Impact on in vitro assessment of nanoparticle cytotoxicity. *Toxicol In Vitro*, 29, 142-7.
4. Casey, A, Herzog, E, Davoren, M, Lyng, FM, Byrne, HJ, Chambers, G. (2007). Spectroscopic analysis confirms the interactions between single walled carbon nanotubes and various dyes commonly used to assess cytotoxicity. *Carbon*, 45, 1425-32.
5. Cho, WS, Duffin, R, Bradley, M, Megson, IL, Macnee, W, Lee, JK, Jeong, J, Donaldson, K. (2013). Predictive value of in vitro assays depends on the mechanism of toxicity of metal oxide nanoparticles. *Part Fibre Toxicol*, 10, 55.
6. Darolles, C, Sage, N, Armengaud, J, Malard, V. (2013). In vitro assessment of cobalt oxide particle toxicity: identifying and circumventing interference. *Toxicol In Vitro*, 27, 1699-710.
7. Davoren, M, Herzog, E, Casey, A, Cottineau, B, Chambers, G, Byrne, HJ, Lyng, FM. (2007). In vitro toxicity evaluation of single walled carbon nanotubes on human A549 lung cells. *Toxicol In Vitro*, 21, 438-48.
8. Fisichella, M, Dabboue, H, Bhattacharyya, S, Saboungi, ML, Salvetat, JP, Hevor, T, Guerin, M. (2009). Mesoporous silica nanoparticles enhance MTT formazan exocytosis in HeLa cells and astrocytes. *Toxicol In Vitro*, 23, 697-703.
9. Holder, AL, Goth-Goldstein, R, Lucas, D, Koshland, CP. (2012). Particle-induced artifacts in the MTT and LDH viability assays. *Chem Res Toxicol*, 25, 1885-92.
10. Kermanizadeh, A, Pojana, G, Gaiser, BK, Birkedal, R, Bilanicova, D, Wallin, H, Jensen, KA et al. (2013). In vitro assessment of engineered nanomaterials using a hepatocyte cell line: cytotoxicity, pro-inflammatory cytokines and functional markers. *Nanotoxicology*, 7, 301-13.
11. Kroll, A, Pillukat, MH, Hahn, D, Schnekenburger, J. (2012). Interference of engineered nanoparticles with in vitro toxicity assays. *Arch Toxicol*, 86, 1123-36.
12. Mittal, S, Sharma, V, Vallabani, NV, Kulshrestha, S, Dhawan, A, Pandey, AK. (2011). Toxicity evaluation of carbon nanotubes in normal human bronchial epithelial cells. *J Biomed Nanotechnol*, 7, 108-9.
13. Monteiro-Riviere, NA, Inman, AO, Zhang, LW. (2009). Limitations and relative utility of screening assays to assess engineered nanoparticle toxicity in a human cell line. *Toxicol Appl Pharmacol*, 234, 222-35.
14. Muller, J, Huaux, F, Moreau, N, Misson, P, Heilier, JF, Delos, M, Arras, M et al. (2005). Respiratory toxicity of multi-wall carbon nanotubes. *Toxicol Appl Pharmacol*, 207, 221-31.
15. Ong, KJ, MacCormack, TJ, Clark, RJ, Ede, JD, Ortega, VA, Felix, LC, Dang, MK et al. (2014). Widespread nanoparticle-assay interference: implications for nanotoxicity testing. *PLoS One*, 9, e90650.
16. Vietti, G, Ibouraadaten, S, Palmai-Pallag, M, Yakoub, Y, Bailly, C, Fenoglio, I, Marbaix, E, Lison, D, van den Brule, S. (2013). Towards predicting the lung fibrogenic activity of nanomaterials: experimental validation of an in vitro fibroblast proliferation assay. *Part Fibre Toxicol*, 10, 52.
17. Wilhelmi, V, Fischer, U, van, BD, Schulze-Osthoff, K, Schins, RP, Albrecht, C. (2012). Evaluation of apoptosis induced by nanoparticles and fine particles in RAW 264.7 macrophages: facts and artefacts. *Toxicol In Vitro*, 26, 323-34.

18. Worle-Knirsch, JM, Pulskamp, K, Krug, HF. (2006). Oops they did it again! Carbon nanotubes hoax scientists in viability assays. *Nano Lett*, 6, 1261-8.

Table 1 Characteristics of NM and particles tested in this study

NM or particle	Code or commercial name	Provider	Phase	Coating	Size[a]	Surface area (BET, m^2/g)	Ref.
μSiO_2	Min-U-Sil 5	US Silica	crystalline	-	D 1.4 µm	-	(Vietti et al. 2013)
$nSiO_2$	-	This study	amorphous	-	D 12 nm	227	-
ZnO[b]	NM110	BASF	Zincite	-	D 9 nm	322	(Kermanizadeh et al. 2013)
TiO_2[b]	NM101	Sachtleben	Anatase	-	D 70 to >100 nm	14	(Kermanizadeh et al. 2013)
TiO_2[b]	NRCWE-01	NRCWE[c]	Rutile	-	D 10 nm	99	(Kermanizadeh et al. 2013)
TiO_2[b]	NRCWE-02	NRCWE[c]	Rutile	+ charge	D 10 nm	84	(Kermanizadeh et al. 2013)
TiO_2[b]	NRCWE-03	NRCWE[c]	Rutile	- charge	D 10 nm	84	(Kermanizadeh et al. 2013)
TiO_2[b]	NRCWE-04	NRCWE[c]	Rutile	-	D 100 nm	ND	(Kermanizadeh et al. 2013)
MWCNT[b]	NM400	Nanocyl	-	-	D 5-35 nm L 0.7-3 µm	298	(Kermanizadeh et al. 2013; Vietti et al. 2013)
MWCNT[d]	MWCNT 8 nm	Cheaptubes	-	-	D <8 nm L 10-30 µm	500	-
MWCNT[d]	MWCNT 20-30 nm	Cheaptubes	-	-	D 20-30 nm L 10-30 µm	110	-
UfCB	ENSACO 250	ERACHEM Comilog S.A.	-	-	-	66.8	(Muller et al. 2005)

[a]L, length; D, diameter (outer diameter for CNT)
[b]Obtained from the European Commission Joint Research Centre (Ispra, Italy) and characterized in (Kermanizadeh et al. 2013).
[c]National Research Centre for the working environment.
[d]Properties provided by the supplier.

3.1.3. How does this work contribute to nanotoxicology knowledge?

Our study confirms the recommendation by the group of Kroll (Kroll et al., 2012), which consists to include a washing step after exposure and before the assay. However, the adapted procedure proposed by the group of Kroll cannot be used with NM concentration higher than 10 µg/cm² or with carbon black (CB). Thus, to extend the tested concentrations and the type of NM, we suggest to use procedure D with specific blank wells, such as Triton X-100 or $HgCl_2$ lysed cells. We recommended to systematically verify possible interferences of any NM prior to evaluating cellular responses whether suitable and adapted models have not been used. Authors should report the results of interference tests in their publications or refer to previous investigations performed. Thus, researchers will be able to figure out whether interferences were appropriately taken into account or not.

Additional information on NM interferences have been recently reported by the group of Guadagnini (Guadagnini et al., 2015). They suggest that an accurate characterization of NM could be not only essential to understand the relevant physico-chemical characteristics of CNT that induce adverse and toxic effects, but could be also necessary to understand and predict which NM may interfere with the readout system. Authors fully characterized a panel of NM and checked interferences with a range of in vitro cytotoxicity assays (WST-1, MTT, LDH, neutral red, propidium iodide, ^{3}H-thymidine incorporation and cell counting), pro-inflammatory response (ELISA for granulocyte-macrophage colony-stimulating factor GM-CSF, IL-6 and IL-8), and oxidative stress (monoBromoBimane, dichlorofluorescein and nitric oxide NO assays). However, it has to be underlined that this study did not fully and systematically analyze interferences as we did. As reported in Figure 5, they suggested that depending on the physico-chemical properties of NM, such as light absorption or scattering, aggregation/agglomeration, surface reactivity or dissolution, these can

interfere with spectrophotometric and fluorimetric analyses, flow cytometry and automatic cell counting, assay reagents and biomolecules.

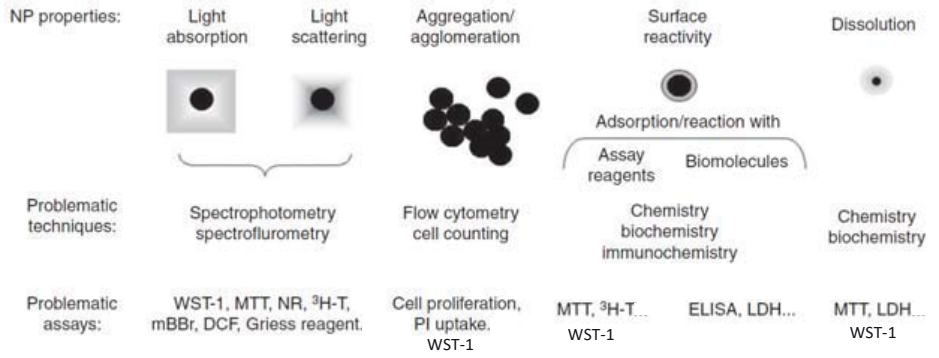


Figure 5. NP and interferences with assays, adapted from (Guadagnini et al., 2015).

In conclusion, we can assume that the physico-chemical characterization of NM is not only useful to identify physico-chemical determinants of their toxicity but also for the preselection of suitable assays.

REFERENCES

Guadagnini R, Halamoda Kenzaoui B, Walker L, Pojana G, Magdolenova Z, Bilanicova D, Saunders M, Juillerat-Jeanneret L, Marcomini A, Huk A, Dusinska M, Fjellsbo LM, Marano F, Boland S. 2015. Toxicity screenings of nanomaterials: challenges due to interference with assay processes and components of classic in vitro tests. Nanotoxicology 9 Suppl 1**,** 13-24.

Kroll A, Pillukat MH, Hahn D, Schnekenburger J. 2012. Interference of engineered nanoparticles with in vitro toxicity assays. Arch Toxicol 86**,** 1123-36.

3.2. TOWARDS PREDICTING THE LUNG FIBROGENIC ACTIVITY OF CARBON NANOTUBES: IN VITRO CELL ASSAY VALIDATION

3.2.1. Context and general experimental design.

As discussed previously, several studies demonstrated that exposure to some CNT can lead to lung fibrosis. However, due to the huge number of CNT with different physico-chemical properties, it appears extremely difficult to estimate which of these CNT are toxic and which properties determine their pro-fibrotic activity. Screening approaches are therefore needed to easily and reliably evaluate and predict their toxicity. Indeed, efforts are currently focused on the development and validation of new alternative test systems (sensitive, specific, rapid) for toxicological research that will reduce, replace, or refine animal use. Moreover, the implementation of new strategies, which provide additional or more accurate information, can strengthen the science on which regulatory decisions are based.

When the present work was initiated, few studies were available on how to predict the fibrotic potential of CNT. An association has been observed between the capacity of CNT to trigger the release of IL-1β from human monocytic cell line (THP-1) or alveolar macrophages and the pro-fibrogenic TGF-β from human bronchial epithelial cell line (BEAS-2B) in vitro and their ability to induce an increase of the same cytokines as well as collagen deposition in the alveolar region of mice (Wang et al., 2011). The capacity of a range of CNT to induce fibroblast proliferation and collagen production from these cells has also been shown to correlate with their in vivo fibrotic activity (Wang et al., 2010; Wang et al., 2011). This observation was important because some studies had highlighted the capacity of CNT to reach the alveolar interstitium (Mercer et al., 2011; Mercer et al., 2013) and thus the possibility for CNT to interact directly with fibroblasts, which seems

to be a particular feature of CNT. Based on this limited information and previous data already obtained by our group showing that CNT induce fibroblast proliferation in vitro, we decided to analyze whether the direct effect of CNT on fibroblast proliferation could be predictive and relevant of the in vivo activity. To confirm our hypothesis, an in vitro fibroblast proliferation assay has been validated experimentally. We examined the influence of different parameters, among which: i) CNT dispersion media, ii) fibroblast type, and iii) different assays. The in vivo experiment was performed on C57BL/6 mice that were pharyngeally aspirated with 100 µg of MWCNT or asbestos. Pulmonary fibrosis was assessed after 2 months by histopathology and quantification of total collagen lung content. The activity of different MWCNT samples (NM400, the crushed form of NM400 named NM400c, NM402 and MWCNTg 2400) and asbestos (crocidolite) was investigated towards the association of the proliferative activity of CNT on fibroblasts in vitro and their ability to induce pulmonary fibrotic responses in vivo.

REFERENCES

Mercer RR, Hubbs AF, Scabilloni JF, Wang L, Battelli LA, Friend S, Castranova V, Porter DW. 2011. Pulmonary fibrotic response to aspiration of multi-walled carbon nanotubes. Part Fibre Toxicol 8**,** 21.

Mercer RR, Scabilloni JF, Hubbs AF, Battelli LA, Mckinney W, Friend S, Wolfarth MG, Andrew M, Castranova V, Porter DW. 2013. Distribution and fibrotic response following inhalation exposure to multi-walled carbon nanotubes. Part Fibre Toxicol 10**,** 33.

Wang X, Xia T, Ntim SA, Ji Z, George S, Meng H, Zhang H, Castranova V, Mitra S, Nel AE. 2010. Quantitative techniques for assessing and controlling the dispersion and biological effects of multiwalled carbon nanotubes in mammalian tissue culture cells. ACS Nano 4**,** 7241-52.

Wang X, Xia T, Ntim SA, Ji Z, Lin S, Meng H, Chung CH, George S, Zhang H, Wang M, Li N, Yang Y, Castranova V, Mitra S, Bonner JC, Nel AE. 2011. Dispersal state of multiwalled carbon nanotubes elicits profibrogenic cellular

responses that correlate with fibrogenesis biomarkers and fibrosis in the murine lung. ACS Nano 5**,** 9772-87.

3.2.2.

Towards predicting the lung fibrogenic activity of nanomaterials: experimental validation of an in vitro fibroblast proliferation assay.

Vietti et al. Particle and Fibre Toxicology 2013, 10:52
http://www.particleandfibretoxicology.com/content/10/1/52

PARTICLE AND FIBRE TOXICOLOGY

RESEARCH Open Access

Towards predicting the lung fibrogenic activity of nanomaterials: experimental validation of an in vitro fibroblast proliferation assay

Giulia Vietti[1*], Saloua Ibouraadaten[1], Mihaly Palmai-Pallag[1], Yousof Yakoub[1], Christian Bailly[2], Ivana Fenoglio[3], Etienne Marbaix[4], Dominique Lison[1] and Sybille van den Brule[1]

Abstract

Background: Carbon nanotubes (CNT) can induce lung inflammation and fibrosis in rodents. Several studies have identified the capacity of CNT to stimulate the proliferation of fibroblasts. We developed and validated experimentally here a simple and rapid in vitro assay to evaluate the capacity of a nanomaterial to exert a direct pro-fibrotic effect on fibroblasts.

Methods: The activity of several multi-wall (MW)CNT samples (NM400, the crushed form of NM400 named NM400c, NM402 and MWCNTg 2400) and asbestos (crocidolite) was investigated in vitro and in vivo. The proliferative response to MWCNT was assessed on mouse primary lung fibroblasts, human fetal lung fibroblasts (HFL-1), mouse embryonic fibroblasts (BALB-3T3) and mouse lung fibroblasts (MLg) by using different assays (cell counting, WST-1 assay and propidium iodide PI staining) and dispersion media (fetal bovine serum, FBS and bovine serum albumin, BSA). C57BL/6 mice were pharyngeally aspirated with the same materials and lung fibrosis was assessed after 2 months by histopathology, quantification of total collagen lung content and pro-fibrotic cytokines in broncho-alveolar lavage fluid (BALF).

Results: MWCNT (NM400 and NM402) directly stimulated fibroblast proliferation in vitro in a dose-dependent manner and induced lung fibrosis in vivo. NM400 stimulated the proliferation of all tested fibroblast types, independently of FBS- or BSA- dispersion. Results obtained by WST1 cell activity were confirmed with cell counting and cell cycle (PI staining) assays. Crocidolite also stimulated fibroblast proliferation and induced pulmonary fibrosis, although to a lesser extent than NM400 and NM402. In contrast, shorter CNT (NM400c and MWCNTg 2400) did not induce any fibroblast proliferation or collagen accumulation in vivo, supporting the idea that CNT structure is an important parameter for inducing lung fibrosis.

Conclusions: In this study, an optimized proliferation assay using BSA as a dispersant, MLg cells as targets and an adaptation of WST-1 as readout was developed. The activity of MWCNT in this test strongly reflects their fibrotic activity in vivo, supporting the predictive value of this in vitro assay in terms of lung fibrosis potential.

Keywords: Carbon nanotubes, CNT, Lung fibrosis, Asbestos, Crocidolite, Dispersion, MLg, WST-1

* Correspondence: giulia.vietti@uclouvain.be
[1]Louvain centre for Toxicology and Applied Pharmacology, Université catholique de Louvain, Avenue E. Mounier, 52 - bte B1.52.12, 1200 Brussels, Belgium
Full list of author information is available at the end of the article

BioMed Central

© 2013 Vietti et al.; licensee BioMed Central Ltd. This is an open access article distributed under the terms of the Creative Commons Attribution License (http://creativecommons.org/licenses/by/2.0), which permits unrestricted use, distribution, and reproduction in any medium, provided the original work is properly cited.

Background

Serious concerns have been raised regarding the potential adverse effects of nanomaterials (NM) on the health of exposed workers, users or consumers, as well as on the environment [1]. Among the variety of already existing NM, carbon nanotubes (CNT) are particularly scrutinized because of their structural resemblance to asbestos, suggesting that they could induce similar harmful effects, including inflammatory and fibrotic lung reactions, pleural mesothelioma and lung cancer [2]. Furthermore, pristine CNT are generally hydrophobic, essentially insoluble in water and, when long enough, expected to be biopersistent. These features contribute to reinforce the concerns about their pathogenic activity [3].

Most experimental studies conducted with CNT have focused on respiratory effects because inhalation represents the most worrying route of exposure to this material. Early studies indicated that they were able to induce inflammatory reactions, granulomas, fibrosis, and biochemical changes in rodent lungs when administered intratracheally or intrapharyngeally [4-6]. In these studies CNT were shown to be more toxic than quartz, well known for its pulmonary toxicity. Results from inhalation studies revealed the capacity of CNT to induce lung fibrosis [7,8] or not [9-11].

Recent data indicated that CNT can stimulate lung fibroblast proliferation in vitro. Wang et al. [12] showed that lung fibroblasts exposed in vitro to single-wall (SW) CNT displayed increased proliferation and collagen production in the absence of cell damage. They also observed that SWCNT stimulated the proliferation of lung epithelial cells. Non-dispersed SWCNT were not active in these assays, pointing to the importance of isolated CNT for these effects [13]. Similar results were obtained with multi-wall (MW)CNT [14-16].

This in vitro activity of CNT is likely relevant to understand their capacity to induce lung fibrosis in vivo because fibroblast proliferation is an essential component of the fibrotic process, together with differentiation in myofibroblasts and excessive production of collagen, leading to the exaggerated deposition of extracellular matrix [17-19]. Though inhaled NM first encounter macrophages and epithelial cells in alveoli, a direct interaction of CNT with fibroblasts is very likely in vivo since it has been shown that they can rapidly reach the alveolar interstitial space and co-localize with inflammatory and fibrotic granulomas containing collagen fibers [4,5,20].

The capacity of CNT (or other NM) to stimulate fibroblast proliferation may, therefore, offer an opportunity to develop an in vitro assay able to predict a fibrotic activity in vivo. Such an in vitro assay would contribute to the efforts for reducing the number of toxicological testings on vertebrates to ensure the protection of human health, including in the context of the European REACH regulations.

In this manuscript, we report on the development of a simple, effective, fast and standardized in vitro assay to determine whether a NM can exert a direct proliferative effect on fibroblasts. The consistency of the proliferative response was confirmed with different endpoints, cell types and dispersion conditions. The association between the proliferative activity of CNT on fibroblasts in vitro and their ability to induce pulmonary fibrotic responses in vivo was established by correlating the respective activities of different samples.

Results

Physicochemical characterization of MWCNT

The morphology of the different MWCNT samples is shown in Figure 1 and their characteristics are reported in Table 1. NM400 and NM402 are similar in length but slightly differ by their diameter and impurity content. MWCNTg 2400 were shorter than NM400 and NM402 and had lower defect and impurity levels. The individual length of crushed NM400 (NM400c) was significantly reduced compared to the pristine NM400, without modifying other characteristics. CNT diameters and lengths were not modified after the dispersion by sonication (Figure 1B).

MWCNT stimulate fibroblast proliferation in vitro and induce lung fibrosis

The (pro-)fibrotic activity of NM400 and NM402 was assessed in vitro on fibroblasts and in vivo in mouse lungs. Primary lung fibroblasts were exposed to NM400 and NM402 pre-dispersed in 2% fetal bovine serum (FBS - 0.2% final FBS concentration during cell exposure), or to human platelet-derived growth factor (PDGF)-BB as a fibrosis-relevant growth factor. Cell proliferation was assessed by counting the number of living cells after 24 h exposure to doses ranging from 1 to 37.5 μg/cm^2. Both CNT samples significantly increased cell number in a dose-dependent manner and the highest concentration induced an effect similar to PDGF (Figure 2A). In parallel, the pulmonary fibrotic response to the same CNT was assessed. Min-U-Sil (SiO_2), a reference micrometric crystalline silica particle, was used as positive control. Fibrosis was assessed by quantifying hydroxyproline lung content as a marker of total collagen accumulation, 2 months after instillation. NM400 and NM402 induced a dose-dependent collagen accumulation and, at the highest doses (50–100 μg/mouse), similar in extent to 2.5 mg Min-U-Sil (Figure 2B). Thus, the tested MWCNT showed a direct effect on lung fibroblasts which might reflect their fibrotic activity in vivo. We next optimized the experimental conditions for the in vitro proliferation assay.

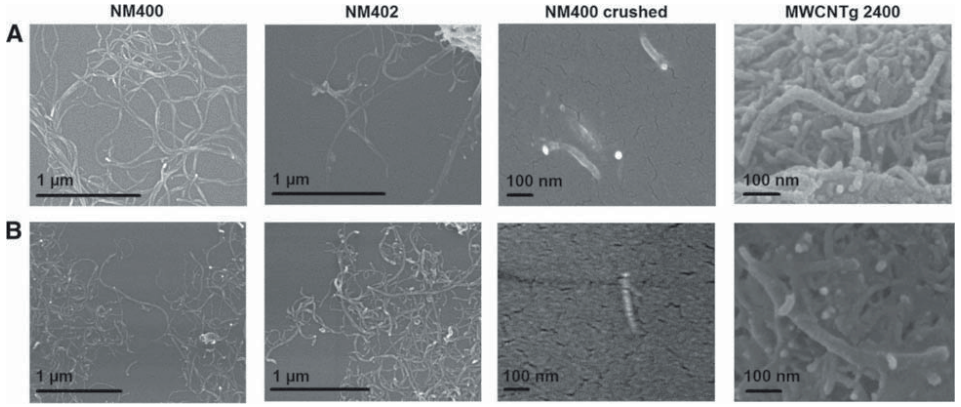


Figure 1 Scanning Electron Microscopy images of different MWCNT. NM400, NM402, NM400c and MWCNTg 2400 images were taken **(A)** before and **(B)** after dispersion by sonication with a scanning electron microscope.

Influence of the dispersion medium on the in vitro effect of MWCNT on fibroblast proliferation

Since NM400 and NM402 similarly increased fibroblast proliferation and induced similar lung fibrosis, subsequent in vitro experiments were mainly performed with NM400. To exclude any FBS-specific effect, e.g. linked to a growth factor activity present in serum and possibly adsorbed on MWCNT, several other dispersion media were compared. NM400 was dispersed in FBS 2% or 10%, bovine serum albumin (BSA) 1.4 mg/ml, or Survanta 150 μg/ml (a natural bovine lung extract used to mimic lung surfactant). The selected BSA concentration is based on the total protein concentration present in FBS 2%. Figure 3 shows that NM400 induced fibroblast proliferation with all dispersion media containing FBS or BSA. The effect was, however, amplified with increasing serum concentration in the dispersion medium. The proliferation of fibroblasts (BALB-3T3) was also increased by CNT dispersed in Survanta (data not shown). These results supported the selection of 1.4 mg BSA/ml to disperse test materials for subsequent experiments, since it excludes that active serum components might confound the proliferation effect.

Table 1 Physicochemical characterization of MWCNT

	NM400	NM402	NM400 crushed	MWCNTg 2400[b]
Diameter (nm)	5 – 35[a]	6 - 20[a]	18 - 35	20 - 50
Length (μm)	0.7 - 3[a]	0.7 - 4[a]	0.14 - 0.5	0.7
Impurities	5.38	3.16	5.22	0.37
% Al	0.24	3.00×10^{-4}	0.24	0.15×10^{-3}
% Co	0.58	2.39	0.50	0.10×10^{-4}
% Fe				
Extent of defects (I_D/I_G)	1.20	1.12	1.20	0.58

Refer to [42] [a] and [24,25] [b].

Selection of a fibroblast cell line

To examine the response of different fibroblast cell types, the effect of NM400 on human fetal lung fibroblasts (HFL-1), mouse embryonic fibroblasts (BALB-3T3) and mouse lung fibroblasts (MLg) was evaluated. At the concentrations tested, NM400 had a similar and significant stimulating effect on the proliferation of all fibroblasts (Figure 4). MLg were chosen for subsequent experiments since the propagation of this cell in culture is more convenient than primary cells and furthermore, the in vitro results obtained with these cells can be directly compared to in vivo experiments performed in mice.

Selection and validation of an optimal proliferation assay

Accumulating evidence show that CNT can interact with conventional in vitro assays leading to potentially biased results [21-23]. This may be avoided by evaluating the in vitro proliferative activity by counting cells, as this readout appears as the least susceptible to CNT interference. However, since manual cell counting is time consuming and not amenable to large throughput, we explored the possibility to use other assays by using cell counting as a reference method. The relevance of other in vitro endpoints, including water-soluble tetrazolium salts (WST)-1, Alamar Blue, CyQuant, [^{3}H]-thymidine incorporation and propidium iodide (PI) staining was further assessed. Alamar blue assay yielded unstable results, and MWCNT interfered with most other assays. We observed that MWCNT can interfere with different

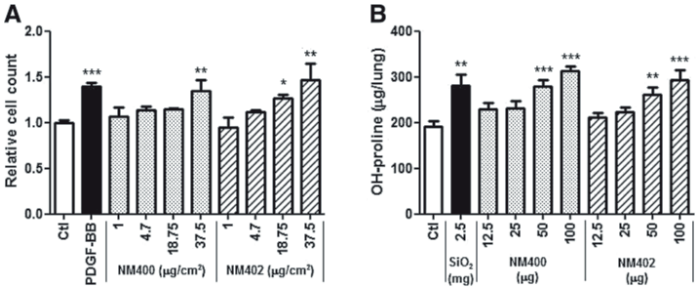


Figure 2 MWCNT stimulate fibroblast proliferation in vitro and induce lung fibrosis in a dose-dependent manner. (A) In vitro effect of MWCNT on primary murine lung fibroblast proliferation assessed by cell counting. Fibroblasts cultured from C57BL/6 mouse lungs were treated with different doses (µg/cm^2 culture well) of MWCNT (NM400 and NM402, final FBS concentration 0.2%) for 24 h. PDGF-BB (50 ng/ml) was used as a positive control. Results are expressed relative to non-treated cell number (Ctl). * $p < 0.05$, ** $p < 0.01$, *** $p < 0.001$ vs non-treated cells (n = 3, t-test or Dunnet multiple comparison test as appropriate). **(B)** In vivo lung fibrotic response to MWCNT (hydroxyproline lung content) assessed 2 months after pharyngeal administration in mice with different doses of MWCNT (NM400 and NM402), or Min-U-Sil (SiO_2) as positive control. * $p < 0.05$, ** $p < 0.01$, *** $p < 0.001$ vs non-treated cells (n = 5-7, t-test or Dunnet multiple comparison test as appropriate).

aspects of the experimental procedures, such as the assay absorbance wavelength (WST-1), DNA nucleosides (thymidine) and DNA intercalating agents (CyQuant) (data not shown). However, we were able to fend off most potential interferences of MWCNT with the WST-1 assay by applying the procedure described in the Methods section. Figure 5B shows that WST-1 activity increased dose-dependently in response to MWCNT, similarly to cell number (Figure 5A), suggesting that this adapted procedure can be used instead of cell counting, particularly if high throughput is sought.

At the same time, increased cell number after exposure to MWCNT was confirmed to be, at least in part, due to enhanced proliferation by using PI staining that evaluates the cell DNA content. The ratio of fibroblasts in S (DNA synthesis) and G_2/M (Gap2 and mitosis) phases 24 h after exposure was calculated from the histogram (event counts vs. PI fluorescence) and was

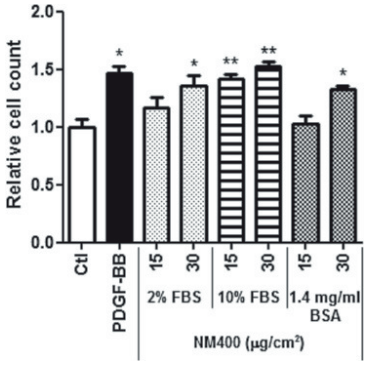


Figure 3 Influence of dispersion medium on the in vitro effect of MWCNT on fibroblast proliferation assessed by cell counting. Primary murine lung fibroblasts were treated for 24 h with different doses of NM400 dispersed in 2 or 10% FBS or 1.4 mg/ml BSA (final concentrations 0.2% FBS and 0.14 mg/ml BSA, respectively). PDGF-BB (50 ng/ml) was used as a positive control. Results are expressed relative to non-treated cell number (Ctl). * $p < 0.05$, ** $p < 0.01$ vs non-treated cells (n = 3, t-test or Dunnet multiple comparison test as appropriate).

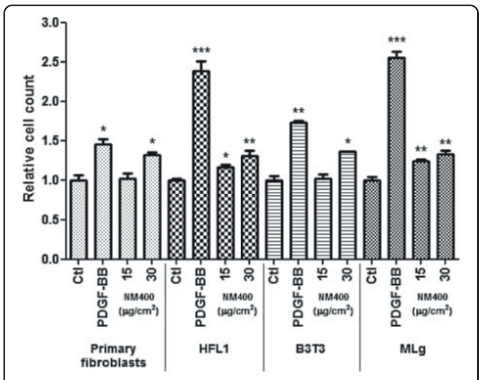


Figure 4 In vitro effect of MWCNT on proliferation of several fibroblast types assessed by cell counting. Primary murine lung fibroblasts and human and mouse fibroblast cell lines (HFL-1, BALB/3T3 and MLg) were treated for 24 h with different doses of NM400 dispersed in 1.4 mg BSA /ml (final concentration 0.14 mg BSA /ml). PDGF-BB (50 ng/ml) was used as a positive control. Results are expressed relative to non-treated cell number (Ctl). * $p < 0.05$, ** $p < 0.01$, *** $p < 0.001$ vs non-treated cells (n = 3, t-test or Dunnet multiple comparison test as appropriate).

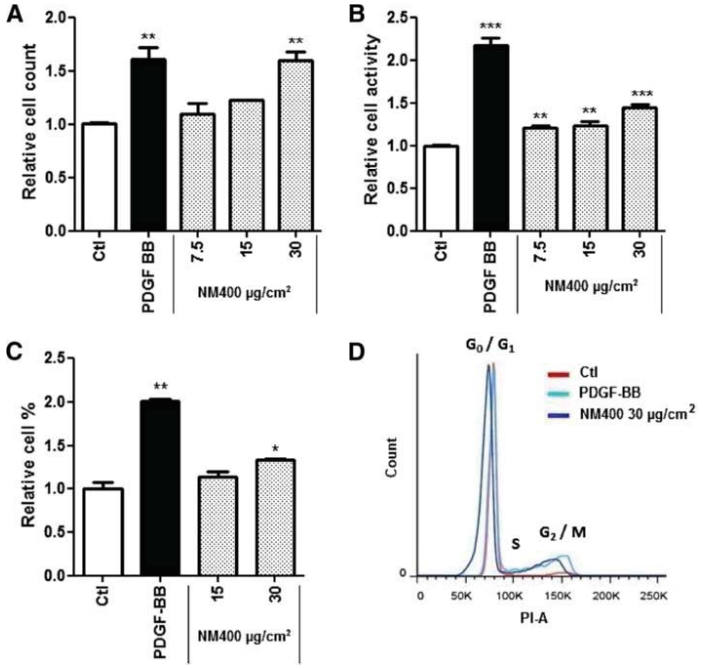


Figure 5 In vitro effect of MWCNT on MLg fibroblast proliferation assessed by different assays. Fibroblasts were treated 24 h with different doses of NM400 dispersed in 1.4 mg BSA /ml (final concentration 0.14 mg BSA /ml). **(A)** Cell counting, **(B)** WST-1 assay and **(C, D)** propidium iodide staining **(C)** % cells in S and G2/M phases and **(D)** histogram plot event counts vs PI were used for in vitro assays. PDGF-BB (30 ng/ml) was used as a positive control. Results are expressed relative to cell number, WST1 activity or % cells in S/G2/M in non-treated cells (Ctl). * $p < 0.05$, ** $p < 0.01$, *** $p < 0.001$ vs non-treated cells (n = 3-4, t-test or Dunnet multiple comparison test as appropriate).

significantly increased after treatment with PDGF and NM400 (Figure 5C and D). Figure 5D shows a representative histogram that illustrates FACS data for each condition. Thus, data obtained by cell counting were confirmed by two other readouts based on completely different principles, and proliferation can be conveniently assessed by the adapted WST-1 assay.

In vitro comparison of different CNT samples

To assess the effect of CNT length on fibroblasts proliferation, we disrupted the "high-aspect ratio" structure of NM400 by grinding (crushed NM400, NM400c). Additionally, we selected MWCNTg 2400 [24,25], characterized by a length (0.7 μm) intermediate between NM400 and NM400c. Crocidolite was included because of its known (pro-)fibrotic activities in vitro and in vivo and of its fiber-like structure (in the micrometer length range). Figure 6 shows that intact NM400 and crocidolite, but not NM400c and MWCNTg 2400, stimulated fibroblast proliferation as shown by the WST-1 assay. NM400 had a stronger proliferative activity on fibroblast cells than crocidolite.

The in vitro effect on fibroblast proliferation appears predictive of the in vivo lung fibrotic response to MWCNT

In parallel, C57BL/6 mice were aspirated with 100 μg of each of these CNT samples; silica (Min-U-Sil) and asbestos (crocidolite) were used as positive controls. Two months after treatment, we observed a significant increase of collagen lung content with the intact NM400, silica and crocidolite, but not with NM400c or MWCNTg 2400 (Figure 7A). The histopathological study, evaluated by Sirius red staining, confirmed the biochemical findings, revealing the accumulation and a greater thickness of the collagen fibers only in the lung of mice instilled with NM400 and crocidolite (Figure 8) tough NM400 led to a stronger fibrotic response than crocidolite. Furthermore, the levels of total transforming growth factor (TGF)-β1, PDGF-BB and osteopontin (OPN), all key mediators of the lung fibrotic process, were significantly increased in

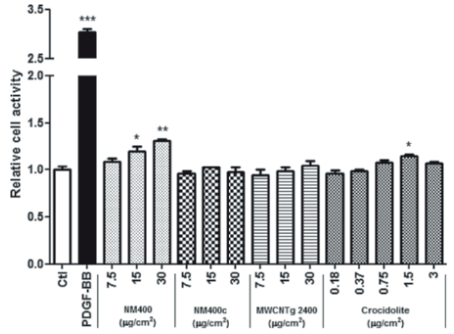


Figure 6 In vitro effect of several MWCNT and crocidolite on MLg fibroblast proliferation. Fibroblasts were treated for 24 h with different doses of MWCNT (NM400, NM400c, MWCNTg 2400) and crocidolite dispersed in 1.4 mg BSA /ml (final concentration 0.14 mg BSA /ml). WST-1 assay were used for in vitro assays. PDGF-BB (30 ng/ml) was used as a positive control. Results are expressed relative to WST1 activity in non-treated cells (Ctl). * $p < 0.05$, ** $p < 0.01$, *** $p < 0.001$ vs non-treated cells (n = 3-4, t-test or Dunnet multiple comparisons test as appropriate).

the bronchoalveolar lavage fluids (BALF) of mice exposed to intact NM400 and to a greater extent than to silica and crocidolite (Figure 7B to D). NM402 also enhanced these cytokines in a dose-dependent manner (data not shown).

Altogether, these results indicate that in vitro fibroblast proliferation and lung fibrosis appear to be mainly induced by intact CNT and to a lower extent by asbestos. Furthermore, they suggest a predictive value of the in vitro proliferative activity in terms of lung fibrosis potential.

Discussion

Several in vivo studies have shown that CNT can induce a fibrotic reaction in the lung (for a review see [2,26,27]). A number of investigators have indicated that the mechanism of CNT-induced pulmonary fibrosis is indirect and mediated via macrophages and/or epithelial cells. Cesta et al. [28] demonstrated that pre-existing respiratory inflammation exacerbates the lung fibrotic response to CNT by increasing PDGF release by macrophages and the PDGF-receptor in fibroblasts. More recently, Li et al. [29] showed that macrophages and epithelial cells exposed to CNT can release interleukin (IL)-1β, TGF-β and PDGF, three key mediators in the development of pulmonary fibrosis. Wang et al. [30] also reported that long MWCNT can activate macrophages and increase their production of TGF-β.

Other investigators have shown the ability of CNT to reach the alveolar interstitium and to directly enter in contact with fibroblasts [5,20]. It is, therefore, relevant to examine whether CNT can act directly on fibroblasts, in addition to the indirect inflammatory pathway. CNT have already been reported to stimulate the in vitro proliferation of lung fibroblasts [12,16], epithelial cells [13] and osteoblasts [31,32]. In the present study, we confirmed the ability of MWCNT to stimulate fibroblast proliferation and we optimized an in vitro assay to assess this activity. The response to MWCNT in this assay appears predictive of their capacity to induce pulmonary fibrosis in vivo, which further supports the biological relevance of this assay.

Whether doses applied in the present study are relevant for human exposure scenarios can be evaluated by the approach suggested by Porter et al. [33] (Figure 9). Mice were exposed to 12.5-100 μg/mouse (alveolar surface area 0.05 m^2), which is equal to 25-200 mg/lung in humans (alveolar surface area 102 m^2). Considering a deposition fraction of 30% [34], a peak MWCNT airborne level of 400 $\mu g/m^3$ measured in a research laboratory [35], and a minute ventilation of 20 l/min [36], a human- equivalent dose would be achieved within 1 to 7.5 months of exposure in a contaminated work place. Assuming a 10-fold lower exposure of 40 $\mu g/m^3$, the experimental dose could be reached after 10 months to 6.2 years of human inhalation exposure. Extrapolation of in vitro concentrations to in vivo dosimetry can be approximated by normalizing the surface area exposed to MWCNT in the tissue culture dish and in the murine airways [16]. Here, the in vivo doses correspond to 0.025-0.2 μg MWCNT/cm^2 culture well, which is less than the in vitro doses used (7.5 - 30 $\mu g/cm^2$). However, three important aspects should be taken into account: (i) in vitro, cells are exposed for only 24 h, while in vivo experiments were performed over 2 months, (ii) in vivo, CNT are not distributed uniformly in the lung and inhaled particles can be found concentrated in some so-called hot spots in the lung [37] and (iii) it should also be considered that CNT do not entirely sediment onto cells in vitro. These aspects can, therefore, contribute to justify the doses used in vitro to explore the possible mechanisms of CNT toxicity in the lung (see Figure 10).

The doses used in the present study both in vitro (7.5 - 30 $\mu g/cm^2$) and in vivo (12.5 - 100 μg) are also higher than those used by other investigators. For example, Wang et al. [12] and Azad et al. [38] used SWCNT with doses of 0.02 - 0.2 $\mu g/cm^2$ in vitro and 10 μg/mouse in vivo, and 5-25 μg/ml in vitro, respectively. However, the mass of an individual CNT differs according to structure (SW vs MW). NM400 and NM402 are composed of 10-20 and 6-15 walls, respectively, leading to a mass per nanotube about 10-fold greater compared to SWCNT, for similar lengths. The rationale for this comparison implies that nanotube number is the relevant dose metrics accounting for the biological activity of CNT, which is a plausible hypothesis [3].

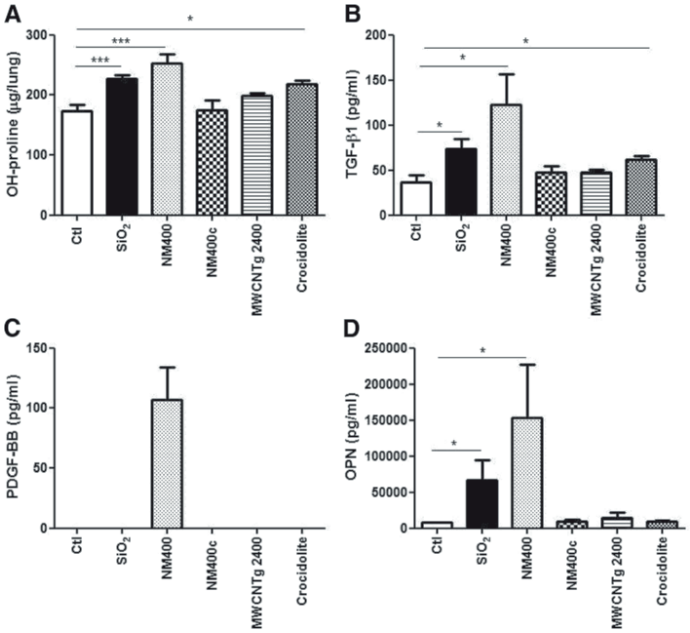


Figure 7 In vivo lung fibrotic response to several MWCNT and crocidolite. (A) Hydroxyproline lung content and cytokine levels in BALF, **(B)** total TGF-β1, **(C)** PDGF-BB and **(D)** OPN (quantified by ELISA) were measured 2 months after pharyngeal aspiration of MWCNT (NM400, NM400c, MWCNTg 2400) and crocidolite in C57BL/6 mice. Min-U-Sil (SiO_2) was used as positive control. * $p < 0.05$, ** $p < 0.01$, *** $p < 0.001$ vs non-treated mice (n = 5-8, t-test).

However, a study by Wang et al. [14] also showed the stimulation of fibroblast proliferation with a MWCNT concentration as low as 5 µg/ml in vitro. Differences in concentrations may also be related to different experimental procedures, such as cell lines, incubation time periods (48 h instead of 24 h) and presence of 10% serum during exposure to CNT (no serum in the present study).

Several authors have reported that the dispersion of CNT is a key determinant of their capacity to stimulate the proliferation of fibroblasts or to induce an interstitial fibrotic reaction in vivo [13,14,16]. Initially, we dispersed CNT in an aqueous solution containing FBS. However, we observed that serum had an additive effect on CNT activity on fibroblast proliferation, suggesting that serum growth factors could adsorb on CNT and be released during cell exposure. Indeed, we showed that the higher the FBS concentration used for dispersion, the stronger the proliferative effect on fibroblasts. It is important to notice that final serum concentrations (0.2% FBS) during exposure to CNT was identical whatever the initial dispersion condition. To avoid the effect of serum, we used a dispersion medium containing BSA, a protein that most likely adsorb onto CNT but has no effect on fibroblast survival or proliferation. Our choice is in agreement with previous studies recommending the use of BSA as a dispersant [14]. Furthermore, the final BSA concentration in exposure medium is lower than the concentration measured in the alveolar fluid of a normal mouse [33].

The pro-fibrotic activity of CNT in vitro was confirmed on different fibroblast cells of various origins, among which primary murine lung fibroblasts, mouse embryonic and lung fibroblast cell lines and human fetal lung fibroblasts, indicating that this activity is not species-specific and providing some support to extrapolate mouse in vivo and in vitro data to humans (parallelogram approach, [39]).

As first reported by Worle-Knirsch et al. [21], some nanospecific (CNT) properties can lead to interferences between NM and commonly used in vitro assays. Therefore, it is strongly recommended to take possible interferences into account and to verify results with other assays. Here, three tests based on totally different readouts were performed in order to confirm the proliferative effect of MWCNT. The data obtained with cell counting and

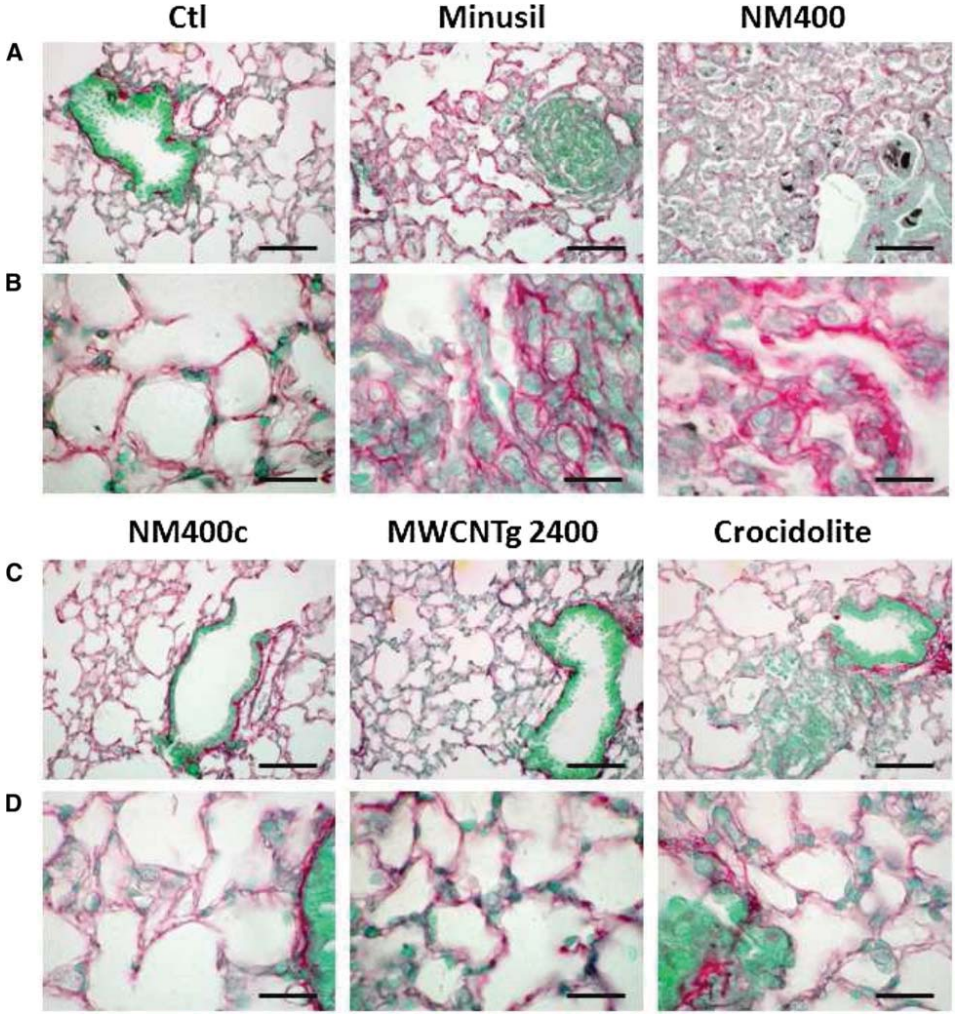


Figure 8 In vivo lung fibrotic response to several MWCNT and crocidolite assessed by histology. Sirius red lung sections were analyzed 2 months after pharyngeal aspiration of MWCNT (100 μg - NM400, NM400c and MWCNTg 2400) and crocidolite (100 μg) in C57BL/6 mice. Min-U-Sil (SiO_2) was used as positive control. Bars correspond to 100 μm **(A, C)** or 20 μm **(B, D)**.

the WST-1 assay indicated a CNT-stimulating effect on fibroblast proliferation. Since a reduction of cell death or apoptosis of fibroblasts could also account for these results, we confirmed the stimulation of fibroblast proliferation by using PI that detects cells in the process of DNA replication or division. The possible interferences between NM and WST-1 absorption wavelength or NM reactivity with WST-1 substrate have been integrated in our protocol by using triton-treated blanks for each condition. Thus, we have optimized the WST-1 assay for NM and results were validated by two other assays. We conclude that stimulation of fibroblast proliferation can be consistently assessed with the NM-adapted WST-1 assay described in this manuscript.

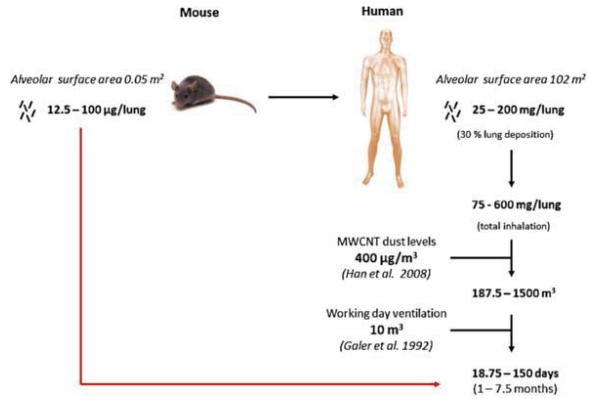


Figure 9 Correlation and relevance of in vivo mouse doses to human MWCNT exposure.

Finally, we validated our in vitro test by relating the results obtained with CNT, asbestos and silica to the development of pulmonary fibrosis in mice. NM400 and NM402 MWCNT and crocidolite induced fibrotic responses. NM400, however, had a stronger effect than crocidolite (asbestos), strengthening the concern about the hazardous properties of CNT. As CNT length is suggested to play an important role in CNT toxicity and particularly the pro-fibrotic potential [30,40] shortened NM400 (NM400c) and MWCNTg 2400 were tested. Interestingly, we observed that nanotube length/structure was critical since these shorter MWCNT did not induce fibroblast proliferation or lung fibrosis in mice contrary to NM400 and NM402. In contrast, in a previous study from our group [24], MWCNTg 2400 were shown to induce lung fibrosis. This apparent discrepancy could be explained by the different protocol conditions of the two studies: animal model (mouse vs rat), dispersion method (BSA + sonication vs Tween), mode of particle administration (aspiration injection vs intratracheal aspiration), dose (100 µg/mouse vs 2 mg/rat). Our results also indicate that metallic contaminants are not necessary for CNT pro-fibrotic activity since NM400c, chemically identical to NM400, was inactive in vitro and in vivo. Furthermore, we observed that NM400 and NM402 do not produce reactive oxygen species (ROS) in absence of cells [41], but instead exhibit a remarkable radical scavenging capacity, suggesting that acellular ROS production by CNT is also not necessary for CNT pro-fibrotic activity.

Conclusions

The present study proposes an experimentally validated in vitro assay suitable for assessing the lung fibrogenic

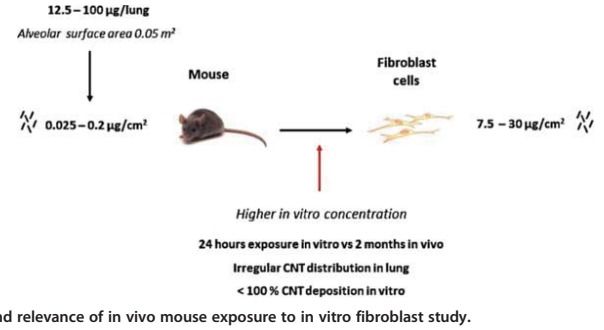


Figure 10 Correlation and relevance of in vivo mouse exposure to in vitro fibroblast study.

activity of NM. The results show that the in vitro proliferative activity of CNT strongly reflects the in vivo fibrosis findings, supporting a predictive value of our in vitro assay. The results obtained in this study also indicate that the structure/length of CNT constitute an important physicochemical determinant in the capacity of these materials to induce lung fibrosis. Several other CNT features have been shown to modulate their pro-fibrotic activity, reinforcing the need of a predictive test. Thus, the value of the present assay will need to be confirmed with a larger range of CNT covering different physicochemical properties and through an inter-laboratory comparison study to address its reproducibility and transferability. A better understanding of the cellular mechanism involved in the proliferative activity of CNT will further contribute to better establish the predictive value of the assay.

Methods

CNT, silica and asbestos

MWCNT NM400 and NM402 were obtained from the European Commission Joint Research Centre (Ispra, Italy) and originate from Nanocyl (Belgium) and Arkema (France), respectively. A fraction of NM400 was crushed in an oscillatory agate ball mill (Fritsch, Idar-Oberstein, Germany), with a vertical vibration of 1 mm applied during 6 h to obtain NM400c. MWCNTg 2400 were obtained as reported previously [24,25]. Briefly, these CNT were modified by grinding and then heated at 2400°C for the elimination of metal clusters and ablation of structural defects. Asbestos (crocidolite) was obtained from the Union internationale contre le Cancer (IUCC, Geneva, Switzerland) and Min-U-Sil (crystalline SiO_2) from the U.S. Silica Company (Berkeley Springs, USA).

Physicochemical characterization of MWCNT

Different analytical techniques were used to characterize MWCNT. Scanning electron microscopy (SEM) was used to study the length and diameter of the samples. CNT have been dispersed in a solution of chloroform (Sigma Aldrich, St Louis, USA) or in dispersion medium after sonication (see below) at room temperature and a drop of the fresh suspension was placed on a sample holder with a carbon coating and air dried. SEM pictures were taken with a scanning electron microscope 7600 F (Jeol, Tokyo, Japan) and NM400c length and diameter were measured with the Analysis program (Olympus, Tokyo, Japan). For NM400 and NM402, refer to [42] and for MWCNTg 2400, refer to [24,25]. Raman spectroscopy was acquired with a DXR SmartRaman Spectrometer (Thermo Scientific, Waltham, USA) operating in the microscopic mode with a 2048 pixel charge-coupled device (CCD) detector. A laser with an incident excitation wavelength of 780 nm and a power of 10 mW, a 50 μm slit aperture and a 10 times magnification objective were used to evaluate the degree of crystallinity of CNT. The concentration of metals in the samples was quantified after mineralization in acid (HNO_3 14 N and HCl 12 N; Merck, Darmstadt, Germany) in a high pressure microwave (Multiwave, Anton Paar GmbH, Graz, Austria). The amount of Fe was measured by atomic absorption spectrometry on a Spectra AA 300 (Varian Zeeman Inc., Palo Alto, USA) equipped with a graphite furnace atomizer and a Zeeman system for correction of nonspecific absorbance. The amount of Al and Co was measured by inductively coupled plasma mass spectrometry (ICP-MS; Agilent 7500G, Santa Clara, USA) with an octapole reaction system.

Material dispersion

MWCNT were weighed in a sterile glass vial and suspended to a concentration of 2.55 mg/ml. Several dispersion media were evaluated. They were prepared with autoclaved nanopure H_2O supplemented either with 2 or 10% fetal bovine serum (FBS, Invitrogen, Paisley, USA), 1.4 mg/ml bovine serum albumin (BSA, Sigma Aldrich, St Louis, USA) or 150 μg/ml Survanta (Abbott Laboratory, Illinois, USA). The suspension was sonicated (Virsonic 300 ultrasonic cell disrupter, Virtis, Gardiner, USA) for 16 min without interruption (power 15%) on ice. In order to keep the final concentration of the dispersant equal at all tested doses, the stock solutions (2.55 mg/ml) were serially diluted (2 fold-dilutions) in the same dispersion medium and then sonicated 15 min in a waterbath. Min-U-Sil and asbestos were directly dispersed with autoclaved nanopure H_2O supplemented with 2% FBS or 1.4 mg/ml BSA.

Fibroblast culture

Primary mouse lung fibroblasts were obtained from eight to twelve-week old female C57BL/6 mice (local breeding facility, Animalerie Centrale, Université catholique de Louvain, Brussels, Belgium), housed in positive pressure air-conditioned units (25°C, 50% relative humidity) on a 12 h light/dark cycle with free access to water and laboratory animal food. Mice were euthanized with an injection of pentobarbital (15 mg/mouse intraperitoneally, Certa, Braine-l'Alleud, Belgium). Whole lungs were perfused with phosphate buffered saline (PBS, Invitrogen) via the right ventricle. Lungs were minced with scissors for 4 min and then digested in 9 ml Hank's buffered salt solution (HBSS, Invitrogen), 0.8 ml Liberase TH (5 mg/ml, Roche, Mannheim, Germany) and 0.25 ml DNase (1 mg/ml, Worthington Biochemical Corporation, Lakewook, USA) at 37°C during 35 min under gentle agitation. The resulting cell suspension was filtered (70 μm), resuspended in Dulbecco's Modified Eagle Medium (DMEM) supplemented with 10% FBS and 1% antibiotic-antimycotic (AA, Invitrogen), transferred into a flat tissue culture flask (2 lungs/75 cm^2) and incubated at 37°C

under 5% CO_2. After 1 day, cells were washed with 10 ml DMEM and supplemented with fresh DMEM, 10% FBS, 1% AA. Cells were harvested 6 days later by adding 3 ml of 0.25% trypsin-EDTA (Invitrogen) and incubated for 10 min at 37°C. Trypsin was neutralized by adjunction of DMEM, 10% FBS and 1% AA. Cell suspensions were centrifuged for 10 min at 400 *g* and resuspended in 5 ml fresh DMEM, 10% FBS, 1% AA. Cell number and viability were determined with Trypan Blue Solution (Sigma Aldrich). Cells were seeded into 96-well or 24-well culture plates in complete medium (10% FBS) at a density of 30 000 or 180 000 cells/well, respectively, and incubated at 37°C under 5% CO_2 for 24 h. Primary fibroblasts were sub-cultured for a maximum of 3 passages and used at passages 2 and 3 (refer to [43] for cell purity).

Mouse lung fibroblasts (MLg cell line) obtained from ATCC (catalog n°CCL-206) were cultured in MEM (Invitrogen) supplemented with 10% FBS and 1% AA and maintained at 37°C under 5% CO_2. Cells were harvested, counted and cultured as previously described for primary fibroblasts. MLg were sub-cultured for a maximum of 15 passages.

BALB-3T3 cells were obtained from Pr. Michiels (Institut De Duve, Université catholique de Louvain, Brussels, Belgium) and cultured in DMEM GlutaMAX (Invitrogen) supplemented with 10% FBS and 1% AA at 37°C under 5% CO_2. Cells were harvested, counted and cultured as previously described for primary fibroblasts. BALB-3T3 were sub-cultured for a maximum of 15 passages.

Human fetal lung fibroblasts (HFL-1 cell line) cells obtained from ATCC (catalog n°CCL-153) were cultured in F12K Nutrient Mixture (Invitrogen) supplemented with 10% FBS and 1% AA and maintained at 37°C under 5% CO_2. Cells were harvested, counted and cultured as previously described for primary fibroblasts. HFL-1 were sub-cultured for a maximum of 15 passages.

Fibroblast exposure

After 24 h at 37°C in complete culture medium (10% FBS), cells were washed once with their basal medium (no FBS, no AA) and then supplied with 200 µl (96-well culture plate) or 1 ml (24-well culture plate) medium with 1% AA containing 1/10 material dilutions. Cells were exposed during 24 h to 1 to 37.5 µg MWCNT or equivalent/cm^2. Exposure to human platelet-derived growth factor (PDGF-BB, R&D System, Minneapolis, USA) at the indicated final concentration was used as a positive control for proliferation assays.

Proliferation assays

Cell proliferation was assessed by cell counting, WST-1 assay and propidium iodide staining.

For cell counting, cells exposed for 24 h to test materials in 96-well plates were washed twice with their basal medium and then incubated with 25 µl 0.25% trypsin-EDTA for 10-15 min at 37°C. Trypsin was neutralized by adjunction of 100 µl of complete medium and cell suspensions were transferred and kept on ice. Cell number and viability were determined with Trypan Blue Solution on a Bürker cell. Data are presented as relative cell count compared to the non-exposed cells.

WST-1 is a colorimetric assay that quantifies mitochondrial activity and reflects cell viability. For this test, cells exposed for 24 h to test materials in 96-well plates were washed twice with their basal medium. Half of the cultures were supplied with 100 µl of medium and the other half with 100 µl medium containing 0.2% Triton X-100 to kill cells. Triton-treated wells were used as blanks since they contain the same amount of test material as test samples but have no mitochondrial activity. This procedure was introduced to eliminate the possible interferences of test materials with the assay either by interacting with the absorbance wavelength and/or with the WST-1 substrate. After 15 min at 37°C, 100 µl WST-1 (diluted 10 times in medium, Roche Diagnostics GmbH, Mannheim, Germany) were added to the cells and absorbance was measured after 60–90 min at 480 nm and at 680 nm (Spectrophotometer Infinite F200, Tecan, Mannedorf, Switzerland). Data are presented as relative cell activity ($Abs_{exposed}$ / $Abs_{non\text{-}exposed}$) where $Abs = (Abs_{480} - Abs_{680})_{no\ Triton} - (Abs_{480} - Abs_{680})_{Triton}$.

For the propidium iodide (PI) staining, cells exposed for 24 h to test materials in 24-well plates were washed once with 500 µl MEM and then incubated with 200 µl 0.25% trypsin-EDTA for 10–15 min at 37°C, until cells detached. Trypsin was neutralized by adding 800 µl MEM, 10% FBS, 1% AA. Cell suspensions were centrifuged for 5 min at 100 *g* (4°C), washed with 1 ml PBS and then re-centrifuged for 5 min at 100 *g* (4°C). Cells were re-suspended in 1 ml EtOH 70% for fixation, by adding first 300 µl PBS and then 700 µl cold EtOH 100% drop wise while gently vortexing to avoid precipitation. Cells were incubated for at least 2 h at 4°C. Cell suspensions were then centrifuged for 5 min at 100 *g* (4°C), washed with 1 ml PBS, and then re-centrifuged for 5 min at 100 *g* (4°C). Then cells were resuspended in 250 µl PI staining solution containing 50 µg/ml PI (P4170, Sigma-Aldrich), Triton X-100 0.1% and 0.1 mg/ml RNase A (R6513, Sigma Aldrich), to ensure that only DNA was stained. Cells were filtered (40 µm), incubated 15 min at 37°C and then stored protected from light at 4°C. The samples (10000 cells) were analyzed by flow cytometry with BD FACS CANTO II (BD Biosciences, San Jose, USA) and the software BD FACS Diva. Pulse processing was used to exclude cell doublets and interference from the analysis. A first gate was applied to the

scatter plot FSC vs SSC to remove cell debris and a second gate to the scatter plot PI-A vs PI-W to remove cell doublets. Cell% in G_0-G_1, S and G_2-M phases were then deduced from the histogram plot event count vs PI derived from gates applied.

Animals and treatments

Eight week-old C57BL/6 female mice were obtained from Taconic Europe (Lille Skensvad, Denmark), housed in positive pressure air-conditioned units (25°C, 50% relative humidity) on a 12 h light/dark cycle with free access to water and laboratory animal food. MWCNT (NM400, NM402, NM400c, MWCNTg 2400), crocidolite and Min-U-Sil were dispersed as previously described. In the first in vivo experiment, NM400 and NM402 suspensions were diluted to 100, 50, 25, 12.5 μg/50 μl H_2O with 2% FBS. In the second experiment, NM400, NM400c, MWCNTg 2400 and crocidolite suspensions were only diluted to 100 μg/50 μl H_2O with 1.4 mg/ml BSA. After anesthesia with a mix of Ketalar, 1 mg/mouse (Warner-Lambert, Zaventem, Belgium), and Rompun, 0.2 mg/mouse (Bayer, Leverkusen, Germany) given intraperitoneally, 50 μl of particle suspensions were injected directly into the lungs by pharyngeal aspiration. At least five mice were included per group. Control animals were treated with an equivalent volume of sterile water with the dispersant (control group). Positive control groups were instilled with 2.5 mg Min-U-Sil particles. Mice were sacrificed 2 months after instillation with an overdose of sodium pentobarbital (15 mg/mouse intraperitoneally). The left lobe was isolated by clamping the corresponding bronchi. This lobe was recovered in 3.65% paraformaldehyde (Sigma-Aldrich) in PBS for later histological analysis. The remaining lobes were lavaged to recover bronchoalveolar lavages (BAL), perfused with NaCl 0.9%, excised and then placed in 3 ml ice-cold PBS for determination of lung hydroxyproline (OH-proline) content.

BAL and biochemical assays

BAL were performed by cannulating the trachea and lavaging the lobes with 1 ml NaCl 0.9%. The lavage was centrifuged (200 *g*, 10 min, 4°C) and the cell-free supernatant (BALF) was used for biochemical measurements. Enzyme-linked immunosorbent assays (ELISA) were performed on BALF according to manufacturer's instructions (R&D System) for active transforming growth factor (TGF)-β1, platelet transforming growth factors (PDGF)-BB and osteopontin (OPN).

Lung homogenates and measurement of lung collagen content

Lungs were homogenized on ice with an Ultra-Turrax T25 homogenizer (Janke & Kunkel, Brussels, Belgium) and stored at −80°C. Lung total collagen was estimated by measuring OH-proline, a specific component of collagen. Part of lung homogenate was hydrolyzed in HCl 6 N at 108°C during 24 h and OH-proline was quantified by high-performance liquid chromatography [44].

Histology

Paraffin-embedded sections were stained with Sirius Red for light microscopy examination. Sirius red binds to total collagen, whereas the fast green stains non-collagenous proteins.

Statistical analysis

Data are presented as means ± standard error on the mean (SEM). Differences were evaluated by using t-test or one-way analysis of variance, followed by Dunnett's Multiple Comparison or Newman-Keuls Multiple Comparison tests, as appropriate. Statistical significance was considered at $p \leq 0.05$. Data analysis was performed with GraphPad Prism 5.00 (GraphPad Software, San Diego, USA).

Abbreviations

AA: Antibiotic-antimycotic; BAL: Bronchoalveolar lavage; BALF: Bronchoalveolar lavage fluid; BSA: Bovine serum albumin; CNT: Carbon nanotube; DMEM: Dulbecco's modified eagle medium; ECM: Extracellular matrix; FACS: Fluorescence-activated cell sorting; FBS: Fetal bovine serum; HBSS: Hank's buffered salt solution; HFL-1: Human fetal lung fibroblast; ICP-MS: Inductively coupled plasma mass spectrometry; IL: Interleukin; IUCC: Union internationale contre le cancer; MLg: Mouse lung fibroblast; MWCNT: Multi-wall carbon nanotube; NM: Nanomaterial; OPN: Osteopontin; PBS: Phosphate buffered saline; PDGF: Human platelet-derived growth factor; PI: Propidium iodide; ROS: Reactive oxigen species; SEM: Scanning electron microscopy; SWCNT: Single-wall carbon nanotube; TGF: Transforming growth factor; WST: Water-soluble tetrazolium salts.

Competing interests

The authors declare that they have no competing interests.

Authors' contributions

GV is research fellow with the Fonds National de la Recherche Scientifique (FNRS, Belgium) and contributed to the experimental design, carried out in vitro and in vivo experiments, analyzed the experimental results and drafted the manuscript. SI participated in in vitro studies and ELISA analysis; MP and YY participated in animal exposure studies; CB participated in particle characterization; IF contributed in the particle characterization; EM carried out lung histology; DL and SV conceived the study, contributed to the experimental design, the evaluation of results and writing of the manuscript. SV also participated in the experimental work. All authors read and approved the final manuscript.

Acknowledgements

We thank Sabine Bebelman, Colette Douchamps and Pascal Van Velthem for helping with the scanning electron microscopy images and the characterization of particles. This work has been supported by the Fonds de la Recherche Scientifique (FNRS) the FP7 Risk Assessment of Engineered Nanoparticles (ENPRA) project and Innoviris (Nano-Iris project).

Author details

[1]Louvain centre for Toxicology and Applied Pharmacology, Université catholique de Louvain, Avenue E. Mounier, 52 - bte B1.52.12, 1200 Brussels, Belgium. [2]Bio and soft matter, Institute of Condensed Matter and Nanosciences, Université catholique de Louvain, Croix du Sud 1 - bte L7.04.02, 1348 Louvain-la-Neuve, Belgium. [3]Interdepartmental Center "G. Scansetti" for Studies on Asbestos and other Toxic Particulates, Università

degli Studi di Torino, Via P. Giuria 7, 10125 Torino, Italy. [4]De Duve Institute, Université catholique de Louvain, Avenue Hippocrate 75 - bte B1.75.02, 1200 Brussels, Belgium.

Received: 23 July 2013 Accepted: 27 September 2013
Published: 10 October 2013

References

1. Gorman J: **Taming high-tech particles: cautious steps into the nanothech future.** *Sci News* 2002, **161:**200–201.
2. Sanchez VC, Pietruska JR, Miselis NR, Hurt RH, Kane AB: **Biopersistence and potential adverse health impacts of fibrous nanomaterials: what have we learned from asbestos?** *Wiley Interdiscip Rev Nanomed Nanobiotechnol* 2009, **1:**511–529.
3. Donaldson K, Aitken R, Tran L, Stone V, Duffin R, Forrest G, Alexander A: **Carbon nanotubes: a review of their properties in relation to pulmonary toxicology and workplace safety.** *Toxicol Sci* 2006, **92:**5–22.
4. Lam CW, James JT, McCluskey R, Hunter RL: **Pulmonary toxicity of single-wall carbon nanotubes in mice 7 and 90 days after intratracheal instillation.** *Toxicol Sci* 2004, **77:**126–134.
5. Shvedova AA, Kisin ER, Mercer R, Murray AR, Johnson VJ, Potapovich AI, Tyurina YY, Gorelik O, Arepalli S, Schwegler-Berry D, *et al*: **Unusual inflammatory and fibrogenic pulmonary responses to single-walled carbon nanotubes in mice.** *Am J Physiol Lung Cell Mol Physiol* 2005, **289:**L698–L708.
6. Muller J, Huaux F, Moreau N, Misson P, Heilier JF, Delos M, Arras M, Fonseca A, Nagy JB, Lison D: **Respiratory toxicity of multi-wall carbon nanotubes.** *Toxicol Appl Pharmacol* 2005, **207:**221–231.
7. Shvedova AA, Kisin E, Murray AR, Johnson VJ, Gorelik O, Arepalli S, Hubbs AF, Mercer RR, Keohavong P, Sussman N, *et al*: **Inhalation vs. aspiration of single-walled carbon nanotubes in C57BL/6 mice: inflammation, fibrosis, oxidative stress, and mutagenesis.** *Am J Physiol Lung Cell Mol Physiol* 2008, **295:**L552–L565.
8. Pauluhn J: **Subchronic 13-week inhalation exposure of rats to multiwalled carbon nanotubes: toxic effects are determined by density of agglomerate structures, not fibrillar structures.** *Toxicol Sci* 2010, **113:**226–242.
9. Mitchell LA, Gao J, Wal RV, Gigliotti A, Burchiel SW, McDonald JD: **Pulmonary and systemic immune response to inhaled multiwalled carbon nanotubes.** *Toxicol Sci* 2007, **100:**203–214.
10. Ma-Hock L, Treumann S, Strauss V, Brill S, Luizi F, Mertler M, Wiench K, Gamer AO, van Ravenzwaay B, Landsiedel R: **Inhalation toxicity of multiwall carbon nanotubes in rats exposed for 3 months.** *Toxicol Sci* 2009, **112:**468–481.
11. Morimoto Y, Hirohashi M, Kobayashi N, Ogami A, Horie M, Oyabu T, Myojo T, Hashiba M, Mizuguchi Y, Kambara T, *et al*: **Pulmonary toxicity of well-dispersed single-wall carbon nanotubes after inhalation.** *Nanotoxicology* 2012, **6:**766–775.
12. Wang L, Mercer RR, Rojanasakul Y, Qiu A, Lu Y, Scabilloni JF, Wu N, Castranova V: **Direct fibrogenic effects of dispersed single-walled carbon nanotubes on human lung fibroblasts.** *J Toxicol Environ Health A* 2010, **73:**410–422.
13. Wang L, Castranova V, Mishra A, Chen B, Mercer RR, Schwegler-Berry D, Rojanasakul Y: **Dispersion of single-walled carbon nanotubes by a natural lung surfactant for pulmonary in vitro and in vivo toxicity studies.** *Part Fibre Toxicol* 2010, **7:**31.
14. Wang X, Xia T, Ntim SA, Ji Z, George S, Meng H, Zhang H, Castranova V, Mitra S, Nel AE: **Quantitative techniques for assessing and controlling the dispersion and biological effects of multiwalled carbon nanotubes in mammalian tissue culture cells.** *ACS Nano* 2010, **4:**7241–7252.
15. Wang X, Xia T, Duch MC, Ji Z, Zhang H, Li R, Sun B, Lin S, Meng H, Liao YP, *et al*: **Pluronic F108 coating decreases the lung fibrosis potential of multiwall carbon nanotubes by reducing lysosomal injury.** *Nano Lett* 2012, **12:**3050–3061.
16. Wang X, Xia T, Ntim SA, Ji Z, Lin S, Meng H, Chung CH, George S, Zhang H, Wang M, *et al*: **Dispersal state of multiwalled carbon nanotubes elicits profibrogenic cellular responses that correlate with fibrogenesis biomarkers and fibrosis in the murine lung.** *ACS Nano* 2011, **5:**9772–9787.
17. Crouch E: **Pathobiology of pulmonary fibrosis.** *Am J Physiol* 1990, **259:**L159–L184.
18. Thannickal VJ, Toews GB, White ES, Lynch JP 3rd, Martinez FJ: **Mechanisms of pulmonary fibrosis.** *Annu Rev Med* 2004, **55:**395–417.
19. Lu P, Takai K, Weaver VM, Werb Z: **Extracellular matrix degradation and remodeling in development and disease.** *Cold Spring Harb Perspect Biol* 2011, **3**.
20. Mercer RR, Hubbs AF, Scabilloni JF, Wang L, Battelli LA, Schwegler-Berry D, Castranova V, Porter DW: **Distribution and persistence of pleural penetrations by multi-walled carbon nanotubes.** *Part Fibre Toxicol* 2010, **7:**28.
21. Worle-Knirsch JM, Pulskamp K, Krug HF: **Oops they did it again! carbon nanotubes hoax scientists in viability assays.** *Nano Lett* 2006, **6:**1261–1268.
22. Casey A, Herwog E, Davoren M, Lyng FM, Byrne HJ, Chambers G: **Spectroscopic analysis confirms the interactions between single walled carbon nanotubes and various dyes commonly used to assess cytotoxicity.** *Carbon* 2007, **45:**1425–1432.
23. Monteiro-Riviere NA, Inman AO, Zhang LW: **Limitations and relative utility of screening assays to assess engineered nanoparticle toxicity in a human cell line.** *Toxicol Appl Pharmacol* 2009, **234:**222–235.
24. Muller J, Huaux F, Fonseca A, Nagy JB, Moreau N, Delos M, Raymundo-Pinero E, Beguin F, Kirsch-Volders M, Fenoglio I, *et al*: **Structural defects play a major role in the acute lung toxicity of multiwall carbon nanotubes: toxicological aspects.** *Chem Res Toxicol* 2008, **21:**1698–1705.
25. Fenoglio I, Greco G, Tomatis M, Muller J, Raymundo-Pinero E, Beguin F, Fonseca A, Nagy JB, Lison D, Fubini B: **Structural defects play a major role in the acute lung toxicity of multiwall carbon nanotubes: physicochemical aspects.** *Chem Res Toxicol* 2008, **21:**1690–1697.
26. Fubini B, Fenoglio I, Tomatis M, Turci F: **Effect of chemical composition and state of the surface on the toxic response to high aspect ratio nanomaterials.** *Nanomedicine (Lond)* 2011, **6:**899–920.
27. Castranova V, Schulte PA, Zumwalde RD: **Occupational nanosafety considerations for carbon nanotubes and carbon nanofibers.** *Acc Chem Res* 2012, **46:**642–649.
28. Cesta MF, Ryman-Rasmussen JP, Wallace DG, Masinde T, Hurlburt G, Taylor AJ, Bonner JC: **Bacterial lipopolysaccharide enhances PDGF signaling and pulmonary fibrosis in rats exposed to carbon nanotubes.** *Am J Respir Cell Mol Biol* 2010, **43:**142–151.
29. Li R, Wang X, Ji Z, Sun B, Zhang H, Chang CH, Lin S, Meng H, Liao YP, Wang M, *et al*: **Surface charge and cellular processing of covalently functionalized multiwall carbon nanotubes determine pulmonary toxicity.** *ACS Nano* 2013, **7:**2352–2368.
30. Wang P, Nie X, Wang Y, Li Y, Ge C, Zhang L, Wang L, Bai R, Chen Z, Zhao Y, Chen C: **Multiwall carbon nanotubes mediate macrophage activation and promote pulmonary fibrosis through TGF-beta/smad signaling pathway.** *Small* 2013. doi: 10.1002/smll.201300607. [Epub ahead of print].
31. Zanello LP, Zhao B, Hu H, Haddon RC: **Bone cell proliferation on carbon nanotubes.** *Nano Lett* 2006, **6:**562–567.
32. Bhattacharya M, Wutticharoenmongkol-Thitiwongsawet P, Hamamoto DT, Lee D, Cui T, Prasad HS, Ahmad M: **Bone formation on carbon nanotube composite.** *J Biomed Mater Res A* 2011, **96:**75–82.
33. Porter DW, Hubbs AF, Mercer RR, Wu N, Wolfarth MG, Sriram K, Leonard S, Battelli L, Schwegler-Berry D, Friend S, *et al*: **Mouse pulmonary dose- and time course-responses induced by exposure to multi-walled carbon nanotubes.** *Toxicology* 2010, **269:**136–147.
34. Phalen RF: *Basic morphology and physiology of the respiratory tract.* Boca Raton: Inhalation Studies: Foundations and Techniques CRC Press; 1984:33–75.
35. Han JH, Lee EJ, Lee JH, So KP, Lee YH, Bae GN, Lee SB, Ji JH, Cho MH, Yu IJ: **Monitoring multiwalled carbon nanotube exposure in carbon nanotube research facility.** *Inhal Toxicol* 2008, **20:**741–749.
36. Galer DM, Leung HW, Sussman RG, Trzos RJ: **Scientific and practical considerations for the development of occupational exposure limits (OELs) for chemical substances.** *Regul Toxicol Pharmacol* 1992, **15:**291–306.
37. Donaldson K, Murphy FA, Duffin R, Poland CA: **Asbestos, carbon nanotubes and the pleural mesothelium: a review of the hypothesis regarding the role of long fibre retention in the parietal pleura, inflammation and mesothelioma.** *Part Fibre Toxicol* 2010, **7:**5.
38. Azad N, Iyer AK, Wang L, Liu Y, Lu Y, Rojanasakul Y: **Reactive oxygen species-mediated p38 MAPK regulates carbon nanotube-induced fibrogenic and angiogenic responses.** *Nanotoxicology* 2013, **7:**157–168.

39. Blaauboer BJ: **The applicability of in vitro-derived data in hazard identification and characterisation of chemicals.** *Environ Toxicol Pharmacol* 2002, **11:**213–225.
40. Poland CA, Duffin R, Kinloch I, Maynard A, Wallace WA, Seaton A, Stone V, Brown S, Macnee W, Donaldson K: **Carbon nanotubes introduced into the abdominal cavity of mice show asbestos-like pathogenicity in a pilot study.** *Nat Nanotechnol* 2008, **3:**423–428.
41. Ghiazza M, Vietti G, Fenoglio I: **Carbon nanotubes (CNTs): properties, applications and toxicity**. In *Health and environmental risks of nanomaterials*. Edited by Njuguna J, Pielichowski K, Zhu H. UK: Woodhead Publishing. in press.
42. Kermanizadeh A, Pojana G, Gaiser BK, Birkedal R, Bilanicova D, Wallin H, Jensen KA, Sellergren B, Hutchison GR, Marcomini A, Stone V: **In vitro assessment of engineered nanomaterials using a hepatocyte cell line: cytotoxicity, pro-inflammatory cytokines and functional markers.** *Nanotoxicology* 2013, **7:**301–313.
43. Huaux F, Noel S, Dhooghe B, Panin N, Lo Re S, Lison D, Wallemacq P, Marbaix E, Scholte BJ, Lebecque P, Leal T: **Dysregulated proinflammatory and fibrogenic phenotype of fibroblasts in cystic fibrosis.** *PLoS One* 2013, **8:**e64341.
44. Biondi PA, Chiesa LM, Storelli MR, Renon P: **A new procedure for the specific high-performance liquid chromatographic determination of hydroxyproline.** *J Chromatogr Sci* 1997, **35:**509–512.

doi:10.1186/1743-8977-10-52
Cite this article as: Vietti *et al.*: Towards predicting the lung fibrogenic activity of nanomaterials: experimental validation of an in vitro fibroblast proliferation assay. *Particle and Fibre Toxicology* 2013 **10**:52.

Submit your next manuscript to BioMed Central and take full advantage of:

- **Convenient online submission**
- **Thorough peer review**
- **No space constraints or color figure charges**
- **Immediate publication on acceptance**
- **Inclusion in PubMed, CAS, Scopus and Google Scholar**
- **Research which is freely available for redistribution**

Submit your manuscript at
www.biomedcentral.com/submit

BioMed Central

3.2.3. How does this work contribute to nanotoxicology knowledge?

In this study, we validated an experimental in vitro assay useful for assessing and predicting the lung fibrogenic effect of CNT. Some other experimental studies have been available since the publication of this work, contributing to further understand how to predict the lung fibrotic effects of CNT. Regarding the in vitro fibroblast model, another study has shown a correlation between in vitro and in vivo data. The in vitro upregulation of TGF-β expression by fibroblasts upon exposure to long SWCNT was associated with the in vivo lung fibrosis outcome, providing further evidence for a role of fiber length in CNT-induced lung fibrosis (Manke et al., 2014). In the next chapter, we confirm the relevance of this in vitro proliferation assay with another set of CNT samples (Vietti et al., 2015). Other cell models than fibroblasts have been investigated to study the pro-fibrotic potential of CNT. As mentioned above, inflammatory cells, such as macrophages, and epithelial cells have been explored for this purpose. CNT were able to trigger the release of IL-1β by THP-1 or alveolar macrophages in vitro and induced lung fibrosis in vivo (Wang et al., 2011; Li et al., 2013; Wang et al., 2015; Sun et al., 2015). The release of TGF-β and PDGF has also been observed in a co-culture of THP-1 with BEAS-2B exposed to CNT and associated with an increase of collagen and of these growth factors in vivo (Li et al., 2013). Two other studies observed a good correlation between the release of the pro-fibrogenic TGF-β from BEAS-2B exposed to CNT in vitro and the induction of a fibrotic response in vivo (Wang et al., 2011; Wang et al., 2015). Altogether these results suggest that the fibrogenic activity of CNT can be predicted by investigating in vitro: i) the effect of CNT on fibroblast activation; ii) the release of relevant pro-inflammatory or pro-fibrotic mediators from macrophages and epithelial cells. It is, therefore, difficult to draw a single definitive and trustworthy

predictive in vitro assay for CNT lung fibrosis, suggesting that several tests might provide a more relevant connection between in vitro CNT activities and in vivo effects.

REFERENCES

Li R, Wang X, Ji Z, Sun B, Zhang H, Chang CH, Lin S, Meng H, Liao YP, Wang M, Li Z, Hwang AA, Song TB, Xu R, Yang Y, Zink JI, Nel AE, Xia T. 2013. Surface charge and cellular processing of covalently functionalized multiwall carbon nanotubes determine pulmonary toxicity. ACS Nano 7**,** 2352-68.

Manke A, Luanpitpong S, Dong C, Wang L, He X, Battelli L, Derk R, Stueckle TA, Porter DW, Sager T, Gou H, Dinu CZ, Wu N, Mercer RR, Rojanasakul Y. 2014. Effect of fiber length on carbon nanotube-induced fibrogenesis. Int J Mol Sci 15**,** 7444-61.

Sun B, Wang X, Ji Z, Wang M, Liao YP, Chang CH, Li R, Zhang H, Nel AE, Xia T. 2015. NADPH Oxidase-Dependent NLRP3 Inflammasome Activation and its Important Role in Lung Fibrosis by Multiwalled Carbon Nanotubes. Small 11**,** 2087-97.

Vietti G, Ibouraadaten S, Palmai-Pallag M, Yakoub Y, Piret JP, Marbaix E, Lison D, Van Den Brule S. 2015. Towards predicting the lung fibrogenic activity of MWCNT: Key role of endocytosis, kinase receptors and ERK 1/2 signaling. Nanotoxicology**,** 1-13.

Wang X, Duch MC, Mansukhani N, Ji Z, Liao YP, Wang M, Zhang H, Sun B, Chang CH, Li R, Lin S, Meng H, Xia T, Hersam MC, Nel AE. 2015. Use of a pro-fibrogenic mechanism-based predictive toxicological approach for tiered testing and decision analysis of carbonaceous nanomaterials. ACS Nano 9**,** 3032-43.

Wang X, Xia T, Ntim SA, Ji Z, Lin S, Meng H, Chung CH, George S, Zhang H, Wang M, Li N, Yang Y, Castranova V, Mitra S, Bonner JC, Nel AE. 2011. Dispersal state of multiwalled carbon nanotubes elicits profibrogenic cellular responses that correlate with fibrogenesis biomarkers and fibrosis in the murine lung. ACS Nano 5**,** 9772-87.

3.3. TOWARDS PREDICTING THE LUNG FIBROGENIC ACTIVITY OF CARBON NANOTUBES: MECHANISMS

3.3.1. Context and general experimental design.

The study of biological mechanisms is a priority for researchers interested in particle toxicology. Mechanistic insight is required for understanding the pathology that underlies the adverse response to particle exposure as well as to develop biomarkers useful for predicting the adverse outcomes associated with particle exposure. Knowledge and insight gained from mechanistic toxicology investigations have also been useful in risk assessment. Current risk assessment processes use mechanistic understanding to detect or identify hazards and to make decisions about dose-response relationships (National-Research-Council, 2007).

In this context, we investigated the mechanisms that are responsible for fibroblast activation in response to direct exposure to CNT or indirectly, via macrophages and epithelial cells. To achieve this purpose, MLg, mouse alveolar epithelial cells (LA4) and mouse peritoneal macrophages (J774) were exposed to 7.5 - 30 µg MWCNT (NM400)/cm^2 in vitro. Effect on cell viability/proliferation was tested by the NM-adapted WST-1 assay. Production of collagen I and fibroblast differentiation, the two other critical processes of fibroblast activation besides proliferation, were assessed by quantitative RT-PCR on fibroblasts in both direct and indirect experimental conditions. Moreover, we also monitored MWCNT endocytosis by transmission electron microscopy (TEM). To identify the mechanism involved in the direct effect of CNT on fibroblast proliferation, we investigated different hypotheses regarding the possible involvement of PDGF and TGF-β, the two important growth factors in the development of fibrosis. These hypotheses include the implication of: i) PDGF and TGF-β secretion; ii) PDGF and TGF-β receptors; iii) PDGF and TGF-β intracellular

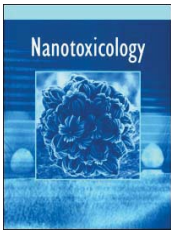
signaling pathway; iv) CNT endocytosis. Several MWCNT samples (differing in length and diameter) were tested in vivo and in vitro.

REFERENCES

National-Research-Council 2007. Application to the Study of Mechanisms of Action. *Applications of Toxicogenomic Technologies to Predictive Toxicology and Risk Assessment.* Washington (DC): National Academies Press (US).

3.3.2.

Towards predicting the lung fibrogenic activity of MWCNT: key role of endocytosis, kinase receptors and ERK 1/2 signaling.



Nanotoxicology

Taylor & Francis

ISSN: 1743-5390 (Print) 1743-5404 (Online) Journal homepage: http://www.tandfonline.com/loi/inan20

Towards predicting the lung fibrogenic activity of MWCNT: Key role of endocytosis, kinase receptors and ERK 1/2 signaling

Giulia Vietti, Saloua Ibouraadaten, Mihaly Palmai-Pallag, Yousof Yakoub, Jean-Pascal Piret, Etienne Marbaix, Dominique Lison & Sybille van den Brule

To cite this article: Giulia Vietti, Saloua Ibouraadaten, Mihaly Palmai-Pallag, Yousof Yakoub, Jean-Pascal Piret, Etienne Marbaix, Dominique Lison & Sybille van den Brule (2015): Towards predicting the lung fibrogenic activity of MWCNT: Key role of endocytosis, kinase receptors and ERK 1/2 signaling, Nanotoxicology, DOI: 10.3109/17435390.2015.1088588

To link to this article: http://dx.doi.org/10.3109/17435390.2015.1088588

Published online: 07 Oct 2015.

Submit your article to this journal

Article views: 9

View related articles

View Crossmark data

Full Terms & Conditions of access and use can be found at
http://www.tandfonline.com/action/journalInformation?journalCode=inan20

Download by: [Chelsea & Westminster NHS Trust Dept of Urology] **Date:** 15 October 2015, At: 04:43

http://informahealthcare.com/nan
ISSN: 1743-5390 (print), 1743-5404 (electronic)

Nanotoxicology

Nanotoxicology, Early Online: 1–13
© 2015 Taylor & Francis. DOI: 10.3109/17435390.2015.1088588

Taylor & Francis
Taylor & Francis Group

ORIGINAL ARTICLE

Towards predicting the lung fibrogenic activity of MWCNT: Key role of endocytosis, kinase receptors and ERK 1/2 signaling

Giulia Vietti[1], Saloua Ibouraadaten[1], Mihaly Palmai-Pallag[1], Yousof Yakoub[1], Jean-Pascal Piret[2], Etienne Marbaix[3], Dominique Lison[1], and Sybille van den Brule[1]

[1]*Louvain centre for Toxicology and Applied Pharmacology, Université Catholique de Louvain, Avenue E. Mounier, Brussels, Belgium,* [2]*Namur Nanosafety Center, Université de Namur, rue de Bruxelles, Namur, Belgium, and* [3]*De Duve Institute, Université Catholique de Louvain, Brussels, Belgium*

Abstract

Carbon nanotubes (CNT) have been reported to induce lung inflammation and fibrosis in rodents. We investigated the direct and indirect cellular mechanisms mediating the fibrogenic activity of multi-wall (MW) CNT on fibroblasts. We showed that MWCNT indirectly stimulate lung fibroblast (MLg) differentiation, via epithelial cells and macrophages, whereas no direct effect of MWCNT on fibroblast differentiation or collagen production was detected. MWCNT directly stimulated the proliferation of fibroblasts primed with low concentrations of growth factors, such as PDGF, TGF-β or EGF. MWCNT prolonged ERK 1/2 phosphorylation induced by low concentrations of PDGF or TGF-β in fibroblasts. This phenomenon and the proliferative activity of MWCNT on fibroblasts was abrogated by the inhibitors of ERK 1/2, PDGF-, TGF-β- and EGF-receptors. This activity was also reduced by amiloride, an endocytosis inhibitor. Finally, the lung fibrotic response to several MWCNT samples (different in length and diameter) correlated with their *in vitro* capacity to stimulate the proliferation of fibroblasts and to prolong ERK 1/2 signaling in these cells. Our findings point to a crosstalk between MWCNT, kinase receptors, ERK 1/2 signaling and endocytosis which stimulates the proliferation of fibroblasts. The mechanisms of action identified in this study contribute to predict the fibrogenic potential of MWCNT.

Keywords

Carbon nanotube, fibroblast proliferation, growth factor, lung fibrosis

History

Received 17 March 2015
Revised 12 August 2015
Accepted 12 August 2015
Published online 18 September 2015

Introduction

Carbon nanotubes (CNT) are widely developed for various industrial and biomedical applications due to their unique mechanical, electrical and thermal properties (De Volder et al., 2013). However, the manipulation of these materials and their release into the environment may lead to human exposure, especially through inhalation. Many experimental studies showed that CNT can induce lung fibrosis in rodents (Lam et al., 2004; Muller et al., 2008; Shvedova et al., 2005), but the mechanisms involved are not completely elucidated. Several cell types may contribute to induce pulmonary fibrosis in response to inhaled particles. While alveolar macrophages and epithelial cells are in the front line to defend the lung by secreting pro-inflammatory and fibrogenic mediators, fibroblasts are the final performers in the establishment of pulmonary fibrosis. Excessive proliferation of fibroblasts, their differentiation in myofibroblasts and the exaggerated production and deposition of extracellular matrix (ECM) proteins, including collagen, are the key features of pulmonary fibrosis. Platelet-derived growth factor (PDGF) and transforming growth factor (TGF)-β play a critical role in this fibrotic process, since they stimulate fibroblast recruitment, proliferation and activation (Wynn, 2011). The fibrogenic activity of inhaled particles (e.g. crystalline silica, asbestos fibers) is usually ascribed to an indirect effect on fibroblasts mediated by macrophages and/or epithelial cells (Mossman & Churg, 1998). Recent *in vitro* studies showed that multi-wall (MW) CNT are also able to activate the secretion of TGF-β and PDGF by macrophages and epithelial cells (Li et al., 2013; Wang et al., 2011, 2012, 2013). He et al. (2011) observed that MWCNT stimulated the production of TGF-β and PDGF by macrophages that acted as paracrine signals to stimulate fibroblast differentiation. Increased levels of TGF-β and PDGF were also reported in bronchoalveolar lavage fluid of mice instilled with CNT (Vietti et al., 2013; Wang et al., 2011).

Because inhaled CNT can distribute in distal areas, such as the alveolar interstitial space (Mercer et al., 2010), it has been suggested that they can also directly interact with fibroblasts and new studies were carried out to understand the direct molecular interactions between CNT and fibroblasts. Several *in vitro* studies showed an increased fibroblast proliferation in response to multiwall (MW), double-wall (DW) and single-wall (SW) CNT exposure (Azad et al., 2013; Vietti et al., 2013; Wang et al., 2010a, 2010b), suggesting that a direct stimulation of fibroblasts by CNT could contribute to exacerbate or even initiate the development of lung fibrosis. Only few studies provided information on the mechanism of interaction between CNT and fibroblasts. Azad et al. (2013) reported that SWCNT induced reactive oxygen species-regulated phosphorylation of p38 mitogen-activated protein kinase (MAPK), leading to TGF-β and vascular endothelial growth factor (VEGF) secretion by fibroblasts that induced their proliferation and collagen production.

Correspondence: Giulia Vietti, Louvain centre for Toxicology and Applied Pharmacology, Université Catholique de Louvain, Avenue E. Mounier, 52 – bte B1.52.12, 1200, Brussels, Belgium. Tel: 0032 (0)2 7645354. E-mail: giulia.vietti@uclouvain.be

Recent studies have also suggested an interaction between CNT and membrane receptors (Hirano et al., 2008; Yan, 2014). However, it is still unclear which cellular mechanisms and receptors are involved in the proliferative activity of CNT on fibroblasts.

Furthermore, data indicate that the physicochemical properties of CNT determine the severity of their lung toxicity. Diameter, length, impurities and defects have been reported to influence the fibrogenic activity of CNT (Fenoglio et al., 2012; Liu et al., 2012; Muller et al., 2008; Palomaki et al., 2011). Our previous study suggested that the proliferative activity of MWCNT on fibroblasts was predictive of their lung fibrotic potential (Vietti et al., 2013), as demonstrated with several MWCNT samples.

The aim of this study was to identify the direct and indirect mechanisms mediating the fibrogenic activities of MWCNT on fibroblasts. We first confirmed that macrophages and epithelial cells exposed to MWCNT-stimulated fibroblast differentiation. Secondly, we observed that, in the presence of low concentrations of growth factors (PDFG, TGF-β, epidermal growth factor (EGF)), MWCNT directly in contact with fibroblasts stimulated their proliferation. Kinase receptors for these growth factors, ERK 1/2 signaling pathway and MWCNT endocytosis were essential to this proliferative activity. Finally, we strengthened the association between CNT capacity to induce lung fibrosis and their *in vitro* fibroblast proliferative activity with MWCNT samples of varying length and diameter.

Methods

MWCNT

NM400 and NM402 MWCNT were obtained from the European Commission Joint Research Centre (Ispra, Italy) and originate from Nanocyl (Auvelais, Belgium). NM400c and MWCNTg 2400 were obtained as reported previously (Vietti et al., 2013). Briefly, a fraction of NM400 was crushed in an oscillatory agate ball mill (Fritsch, Idar-Oberstein, Germany), with a vertical vibration of 1 mm applied during 6 h to obtain NM400c. MWCNTg 2400 were obtained from another sample of MWCNT modified by grinding and then heating at 2400 °C for the elimination of metal clusters and ablation of structural defects (Fenoglio et al., 2008; Muller et al., 2008). MWCNT called long (MWNT 20–30 nm od), short (short MWNT 20–30 nm od) and thick (MWNT >50 nm od) were obtained from Cheap Tubes Company (Cambridgeport, VT). MWCNT physicochemical characteristics and dispersion are presented in the Supplementary material.

Cell culture and exposure

Mouse peritoneal macrophage cells (J774) and mouse type-II alveolar epithelial cells (LA-4) were seeded at a concentration of 150.000 cells/cm^2 (surface area of culture well) and mouse lung fibroblasts (MLg) at a concentration of 90.000 cells/cm^2 (Supplementary material). After 24 h at 37 °C in complete culture medium (10% FBS), cells were washed once with their basal medium (no FBS, no AA) and then supplied with 200 µL (96-well culture plate) or 500 µL (48-well culture plate) medium with 1% AA containing 1/10 stock material dilutions. Cells were exposed during 24 h or other specified time points to 7.5–30 µg MWCNT/cm^2. Depending on experiments, cells were also treated before MWCNT exposure with low concentrations of human platelet-derived growth factor (PDGF)-BB (3 ng/mL, R&D System, Minneapolis, MN) or transforming growth factor (TGF)-β1 (1 ng/mL, R&D System) during 2 h. Before or after this priming, cells were treated with inhibitors during 2 or 4 h: SIS3, LY294002, PD98059, LY364947 were from Merck Millipore (Darmstadt, Germany); SB431542 and IRESSA from R&D systems; AG1296 from Santa Cruz (Dallas, TX); amiloride from Sigma Aldrich and Gleevec, a gift from Pr. JB Demoulin (de Duve Institute, Brussels, Belgium). For fibroblasts treated with macrophage or epithelial cell conditioned medium, J774 or LA-4 were first exposed 24 h to MWCNT. Cell supernatants were collected and MLg were then treated for 24 h with 100 µL of this conditioned medium supplemented with 100 µL medium with 1% AA. Control, TGF-β and PDGF conditions also derived from LA-4 and J774 culture supernatants.

Proliferation/cytotoxicity assay

WST-1 is a colorimetric assay that quantifies mitochondrial activity and reflects cell viability. In this study, cell proliferation/cytotoxicity was measured by a NM-adapted WST-1 assay described by (Vietti et al., 2013) (Supplementary material). Cell viability results are presented as relative cell activity, that is, as a ratio to nontreated cells (Ctl), calculated as follows:

$$\text{Relative cell activity} = \frac{\text{Abs}_{\text{exposed}}}{\text{Abs}_{\text{non-exposed}}} \quad \text{where}$$

$$\text{Abs} = (\text{Abs}_{480} - \text{Abs}_{680})_{\text{no Triton}} - (\text{Abs}_{480} - \text{Abs}_{680})_{\text{Triton}}.$$

Immunoblotting

About 80 µL/well (48-well plate) of Laemmli Sample Buffer (BioRad, Hercules, CA) was added to cells for extracting proteins. About 25 µL extracts was run on a 4–20% sodium dodecyl sulfate-polyacrylamide gel electrophoresis (SDS-PAGE, BioRad, Hercules, CA), transferred to polyvinylidene difluoride (PVDF) membranes (Merck Millipore) and blocked with the Odyssey Blocking Buffer (Westburg, Leusden, the Netherlands). The membrane was blotted with the primary antibody at 4 °C overnight with shaking, followed by incubation with the secondary antibody for 1 h at room temperature protected from light. The primary antibodies used in this study were phospho-p44/42 MAPK (Thr 202/Tyr204) rabbit Ab (dilution 1:1000), p44/42 MAPK mouse mAb from Cell Signaling (dilution 1:1000, Danvers, MA) or β-actin from Sigma (dilution 1:2000) and the secondary antibodies IRDye 680 RD anti-mouse IgG or IRDye 800 anti-rabbit IgG from LI-COR (dilution 1:15000, Lincoln, NE). Detection was performed using an Odyssey LI-COR platform.

Real-time PCR

Tripure was added to cell cultures and RNA extraction was performed according to manufacturer's instructions (Roche). Total RNA was reverse transcribed with M-MLV reverse transcriptase (Invitrogen) with 350 pmol random hexamers (Eurogentec, Seraing, Belgium) in a final volume of 25 µL. Resulting cDNA was used as template in subsequent polymerase chain reaction (PCR). Sequences of interest were amplified using the following forward primers (Invitrogen): GGAGTAATGG TTGGAATGGGC (α-SMA), CCGGCTCCTGCTCCTCTT (procollagen I), CGGCTACCACATCCAAGGAA (18 S RNA), CTTGGTGGCACACCCTATCC (PDGF Rα), TCTATATCTTT GTGCCAGATCCCAC (PDGF Rβ), GAATGGTGAGCAAT GGRATAGTGG (TGF-β RI), CACGACCCCAAGCTCACCTA (TGF-β RI), CAAAGAAATCCTTGACGAAGCC (EGF R); and reverse primers: GCCTTAGGGTTCAGTGGTGC (α-SMA), GGGTTGGGACAGTCCAGTTCT (procollagen I), ATACGCTA TTGGAGCTGGAATTACC (18 S RNA), TCTCATAGACTTC ACTGGTGGCA (PDGF Rα), GCACGGAATTGTCGTCTCAGT (PDGF Rβ), TCTGTTAGGTATGTTTGGCCTCTG (TGF-β RI), GGTGGTGTATTCTTCCGAAAAGAT (TGF-β RI), TGTGTA

ATGAGCTGGACAGTGGA (EGF R). mRNA expression of these genes was quantified by real-time PCR using SYBR Green technology on an ABI Prism 7000 Sequence Detection System (Applied Biosystems, Foster City, CA) according to the following program: 10 min 95 °C, (15 s 95 °C, 1 min 60 °C) × 40. Five microliters of diluted cDNA or standards was amplified with 300 nM of the described primers using Power SYBR Green PCR Master Mix (Applied Biosystems) in a total volume of 25 µL. PCR product specificity was verified by taking a dissociation curve. The results were expressed as a ratio of gene expression to the expression of the reference gene (18 S rRNA).

Intracellular TEM analysis

After 24-h incubation with NM400, mouse lung fibroblasts, type-II alveolar epithelial cells and peritoneal macrophages were harvested by trypsinisation or scrapping, centrifuged and fixed for 150 min at 4 °C with 2.5% (w/v) glutaraldehyde (Agar Scientific) in 0.1 M cacodylate buffer (pH 7.4) in a pyramidal beem capsule (Agar Scientific). Cells were then washed 3 times with 0.2 M cacodylate buffer and postfixed in 1% (v/w) osmium tetroxide (Merck) in 0.1 M cacodylate buffer (pH 7.4) for 60 min at 4 °C. After fixation, cells were dehydrated in a graded series of ethanol solutions (30, 50, 70, 85 and 100%), infiltrated and embedded in epon resin LX 112 (LADD Research Industries). The samples were cut in 60–100 nm ultrathin sections with an ultramicrotome (Leica), placed on formvar coated copper/palladium grids (Agar) and contrasted with saturated lead citrate and uranyl acetate solutions. TEM images were taken using a transmission electronic microscope (Philips FEI Tecnai 10) at an acceleration voltage of 80 kV and a digital camera.

Animals and treatments

Eight-week-old C57BL/6 female mice were obtained from the local animal facility (Animalerie Centrale UCL, Brussels, Belgium), housed in positive pressure air-conditioned units (25 °C, 50% relative humidity) on a 12-h light/dark cycle with free access to water and laboratory animal food. MWCNT (NM400, long MWCNT, short MWCNT and thick MWCNT) were dispersed as previously described. MWCNT suspensions were diluted to 100 µg/50 µL H_2O with 1.4 mg/mL BSA. After anesthesia with a mix of Ketalar, 1 mg/mouse (Warner-Lambert, Zaventem, Belgium), and Rompun, 0.2 mg/mouse (Bayer, Leverkusen, Germany) given intraperitoneally, 50 µL of particle suspensions were introduced into the lungs by pharyngeal aspiration. Six mice were included per group. Control animals were treated with an equivalent volume of sterile water with the dispersant (control group). Mice were sacrificed 2 months after instillation with an overdose of sodium pentobarbital (15 mg/mouse intraperitoneally). The left lobe was isolated by clamping the corresponding bronchi. This lobe was recovered in 3.65% paraformaldehyde (Sigma-Aldrich) in PBS for later histological analysis. The remaining lobes were perfused with NaCl 0.9%, excised and then placed in 3 mL ice-cold PBS for the determination of lung hydroxyproline (OH-proline) content. The protocols of this investigation were approved by the local committee for animal research at the Université catholique de Louvain, Comité d'Ethique pour l'Expérimentation Animale, Secteur des Sciences de la Santé.

Lung homogenates and measurement of lung collagen content

Lungs were homogenized on ice with an Ultra-Turrax T25 homogenizer (Janke & Kunkel, Brussels, Belgium) and stored at −80 °C. Lung total collagen was estimated by measuring OH-proline, a specific component of collagen. Part of lung homogenate was hydrolyzed in HCl 6 N at 108 °C during 24 h and OH-proline was quantified by high-performance liquid chromatography (Biondi et al., 1997).

Histology

Paraffin-embedded sections were stained with Sirius Red (type-I collagen staining) for light microscopy examination.

Statistical analysis

Data are presented as means ± standard error on the mean (SEM). Differences were evaluated by using *t*-test between control conditions and high concentrations of growth factors or one-way analysis of variance (ANOVA), followed by Dunnett's multiple comparison or Newman–Keuls multiple comparison tests. Statistical significance was considered at $p \leq 0.05$. Data analysis was performed with GraphPad Prism 5.00 (GraphPad Software, San Diego, CA).

Results

MWCNT characterization

Physicochemical characteristics and morphology of the different MWCNT samples used in the present study are reported in Table 1. Long and short MWCNT are identical in diameter and impurity levels but differ by their length, while thick MWCNT have a similar length as long MWCNT but are thicker. NM400 are MWCNT selected as reference material by the JRC repository and present a similar diameter as long and short MWCNT with an intermediate length. NM400 contain high levels of Al impurity compared to the other MWCNT samples.

Indirect fibrogenic effects of MWCNT on lung fibroblasts

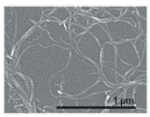
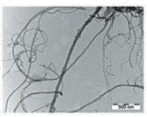
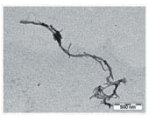
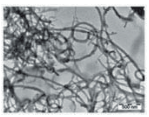
Indirect effects of MWCNT (NM400) on fibroblasts were assessed *in vitro* using macrophages and lung epithelial cells. We first assessed the effect of NM400 on the viability of mouse peritoneal macrophages (J774) and type-II alveolar epithelial cells (LA-4) by a nanomaterial (NM)-adapted WST-1 assay (Vietti et al., 2013). Cells were exposed for 24 h to 7.5–30 µg MWCNT/cm^2 (surface area of the culture well). NM400 significantly stimulated epithelial cell proliferation, while they were cytotoxic to macrophages in the same dose range (Figure 1A and B). Cells were also treated with the pro-fibrotic mediators PDGF and TGF-β. Both growth factors stimulated epithelial cell proliferation but had no effect on macrophages, as expected. Transmission electron microscopy (TEM) studies showed the presence of intracellular CNT: dispersed CNT were found in macrophage and epithelial cell endosomes, while aggregated MWCNT were also observed in macrophage cytoplasm (Figure 1C and D).

Next, we exposed mouse lung fibroblasts (MLg) 24 h to supernatants from J774 and LA-4 collected after 24-h exposure to MWCNT. Procollagen I and α-smooth muscle actin (SMA) were measured by quantitative RT-PCR as markers of collagen expression and fibroblast differentiation, respectively. Conditioned medium from both cell types increased fibroblast α-SMA expression (Figure 1E and F) significantly at the dose of 7.5 and 15 µg/cm^2 for LA-4 and J774 supernatant, respectively, while collagen expression was not altered (Figure 1G and H). These observations confirmed the indirect effects of CNT on fibroblasts, which might contribute to the establishment of lung fibrosis.

Direct fibrogenic effects of MWCNT on lung fibroblasts

In a previous study (Vietti et al., 2013), we demonstrated a direct proliferative activity of MWCNT on lung fibroblasts. This *in vitro*

Table 1. Physicochemical characteristics and morphology of MWCNT.

Characteristics	NM400	Long	Short	Thick
Diameter (nm)	5–35 [a]	11–59	10–47	15–74
Length (μm)	0.7–3[a]	10–30[b]	0.5–2[b]	10–30[b]
Impurities				
% Al	5.38[a]	0.01	0.01	0.01
% Co	0.24[a]	/	/	/
% Fe	0.58[a]	0.05	0.04	0.03
% Ni	/[a]	1.35	0.81	2
Morphology[c]				

[a]Refer to Vietti et al., 2013.
[b]Refer to CheapTubes Inc (http://www.cheaptubes.com).
[c]SEM (bar 1 μm) for NM400, TEM (bar 500 nm) for long, short and thick MWCNT.

response strongly reflected the lung fibrotic activity of several CNT samples in vivo. In the present experiments, we primed fibroblasts with low concentrations of pro-fibrotic growth factors (PDGF 3 ng/mL or TGF-β 1 ng/mL). These concentrations, contrary to the active doses used as positive controls (PDGF 30 ng/mL or TGF-β 10 ng/ml), were not observed to stimulate fibroblast proliferation. This priming represents a realistic scenario since PDGF and TGF-β are present in the CNT-exposed lung, potentially secreted by macrophages and/or epithelial cells (Cesta et al., 2010; Wang et al., 2013). When cells were additionally exposed to MWCNT (NM400), fibroblast proliferation was significantly and dose dependently increased (Figure 2A and B). The fact that MWCNT-stimulated fibroblast proliferation when primed with PDGF or TGF-β suggested the implication of their signaling pathways in this activity. These results were confirmed with other long MWCNT (NM402), whereas short MWCNT (NM400c and MWCNTg 2400) did not stimulate MLg proliferation (data not shown), in accordance with our previous results (Vietti et al., 2013). Like in macrophages and epithelial cells, we recorded loose MWCNT in fibroblast endosomes (Figure 2C).

Fibroblast collagen production and differentiation into myofibroblasts were also assessed after direct exposure to MWCNT. While TGF-β (10 ng/mL) increased both responses as expected (Wynn, 2011), procollagen I and α-SMA transcripts were not altered after direct exposure to MWCNT of cells primed with low concentrations of PDGF or TGF-β (Figure 2D–G). Interestingly, MWCNT even decreased α-SMA expression, similarly to PDGF 30 ng/mL (Figure 2D), as shown by other authors (Salabei et al., 2013). As our data confirmed that the tested MWCNT had a direct effect on fibroblast proliferation and suggested an involvement of PDGF and TGF-β as a mechanism of action, we next explored the impact of MWCNT at different levels of the PDGF/TGF-β stimulation axis.

PDGF or TGF-β secretion by fibroblasts and expression of their receptors in response to MWCNT

Several studies have reported an increased secretion of PDGF and TGF-β, and higher expression of TGF-β receptors after exposure to CNT, whereas other investigators did not record similar modifications (Azad et al., 2013; He et al., 2011; Lin et al., 2012; Wang et al., 2015). Thus, we investigated whether NM400 can alter PDGF and TGF-β secretion and the expression of their receptors. First, we assessed the basal level of PDGF and TGF-β receptor expression in the different cell lines used in this study. Figure S1A-D shows that PDGF (Rα and Rβ) and TGF-β (R1 and R2) receptors are significantly more expressed in MLg and LA-4 than in J774, which is consistent with the fact that both growth factors and MWCNT stimulated the proliferation of fibroblasts and epithelial cells but not of macrophages. Fibroblast exposure to MWCNT did not significantly modify PDGF and TGF-β secretion (Figure S1E-H) and receptor expression (data not shown).

MWCNT stimulate fibroblast proliferation via ERK 1/2 signaling pathway

Because PDGF and TGF-β signaling pathways appeared to play a role in the proliferative activity of MWCNT, we tested the possible implication of several intracellular signaling pathways known to be activated by these growth factors. Smad2/3 (TGF-β), PI3K (TGF-β and PDGF) and ERK 1/2 (TGF-β and PDGF) signaling were inhibited with SIS3, LY294002 and PD98059, respectively. Fibroblasts were first treated with inhibitors for 2 h, then primed with low concentrations of PDGF (3 ng/mL) or TGF-β (1 ng/mL) for two additional hours and finally exposed to MWCNT for 24 h. Smad3 and PI3K inhibitors had no effect on MWCNT proliferative activity (Figure 3A–D). On the contrary, the proliferative activity of MWCNT was inhibited by PD98059 when fibroblasts were primed with PDGF or TGF-β (Figure 3E and F). The effect of MWCNT on the ERK 1/2 signaling pathway was confirmed in a kinetic study where we showed that MWCNT prolonged ERK 1/2 phosphorylation induced by low concentrations of PDGF or TGF-β (Figure 4A and B). Two hours after the addition of PDGF 3 ng/mL (time 0), ERK 1/2 phosphorylation was increased. This phosphorylation decreased time-dependently in the absence of CNT, while after the addition of MWCNT, ERK 1/2 phosphorylation was prolonged compared to fibroblasts only treated with PDGF 3 ng/mL. Moreover, PD98059 (administered before or after priming, Figures 3 and 4, respectively) inhibited MWCNT-stimulated ERK 1/2 phosphorylation 2 h after exposure to MWCNT and also reduced the phosphorylation of ERK 1/2 induced by high concentration of PDGF and TGF-β. The inhibition of the proliferative activity of MWCNT by PD98059 was associated with a reduction of ERK 1/2 phosphorylation (Figure 3G and H). Our data suggest that MWCNT interfere with fibroblast proliferation at a level upstream of ERK 1/2 phosphorylation.

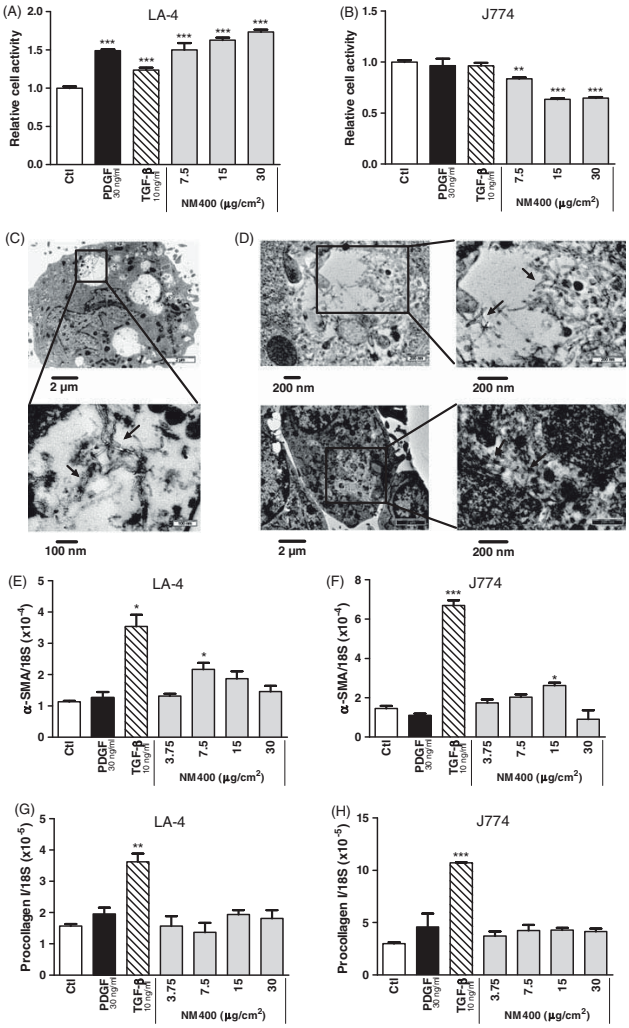


Figure 1. Indirect fibrogenic effect of MWCNT on lung fibroblasts via epithelial cells and macrophages. (A) Mouse type-II alveolar epithelial cells (LA-4) and (B) mouse peritoneal macrophages (J774) were exposed for 24 h to NM400 MWCNT (7.5–30 µg/cm^2). Cell viability was assessed by the adapted WST-1 assay. Results are presented as relative cell activity, that is, as a ratio to nontreated cells (Ctl). $^{**}p < 0.01$, $^{***}p < 0.001$ versus nontreated cells ($n = 4$, *t*-test or Dunnett's multiple comparison test, as appropriate). Intracellular localization of CNT was assessed by TEM 24 h after LA-4 (C) and J774 (D) exposure to MWCNT (30 µg/cm^2). Effect of conditioned medium collected 24 h after LA-4 (E, G) and J774 (F, H) exposure to MWCNT (3.75–30 µg/cm^2) on fibroblast differentiation and collagen production was assessed by quantifying α-SMA (E, F) and procollagen I (G, H) mRNA respectively by quantitative RT-PCR, 24 h after conditioned medium addition to fibroblasts. LA-4 and J774 were also treated with PDGF (30 ng/mL) and TGF-β (10 ng/mL). RT-PCR results are presented as a ratio of gene expression normalized on the expression of the reference gene, 18 S rRNA. $^{*}p < 0.05$, $^{**}p < 0.01$, $^{***}p < 0.001$ versus nontreated cells ($n = 3$, *t*-test or Dunnett's multiple comparison test as appropriate).

Implication of kinase receptors in the proliferative activity of MWCNT

To understand whether PDGF and TGF-β receptors (R) are involved in the fibrogenic activity of MWCNT, fibroblasts were treated with PDGF or TGF-β receptor kinase inhibitors after priming with low concentrations of PDGF or TGF-β before NM400 exposure. The stimulation of fibroblast proliferation by PDGF (30 ng/mL) and TGF-β (10 ng/mL) was inhibited by Gleevec and AG1296 (PDGF R inhibitors), and LY364947 and SB431542 (TGF-β R inhibitors), respectively (Figure 5A, C, E, and G). MWCNT-induced stimulation of fibroblast proliferation was reduced by these inhibitors except LY364947. Interestingly, PDGF R inhibitors did not reduce the proliferation of TGF-β-primed fibroblasts exposed to MWCNT, and SB431542 (TGF-β R inhibitor) of PDGF-primed fibroblasts exposed to MWCNT (data not shown). The absence of inhibitory activity of LY364947 on fibroblast proliferation in the presence of MWCNT could be explained by the fact that SB431542 reduced more efficiently ERK 1/2 phosphorylation compared to LY364947 when fibroblasts were treated with TGF-β 10 ng/mL (Figure 5H). None of TGF-β R inhibitors affected ERK 1/2 phosphorylation after fibroblast treatment with PDGF (30 ng/mL) (Figure 5).

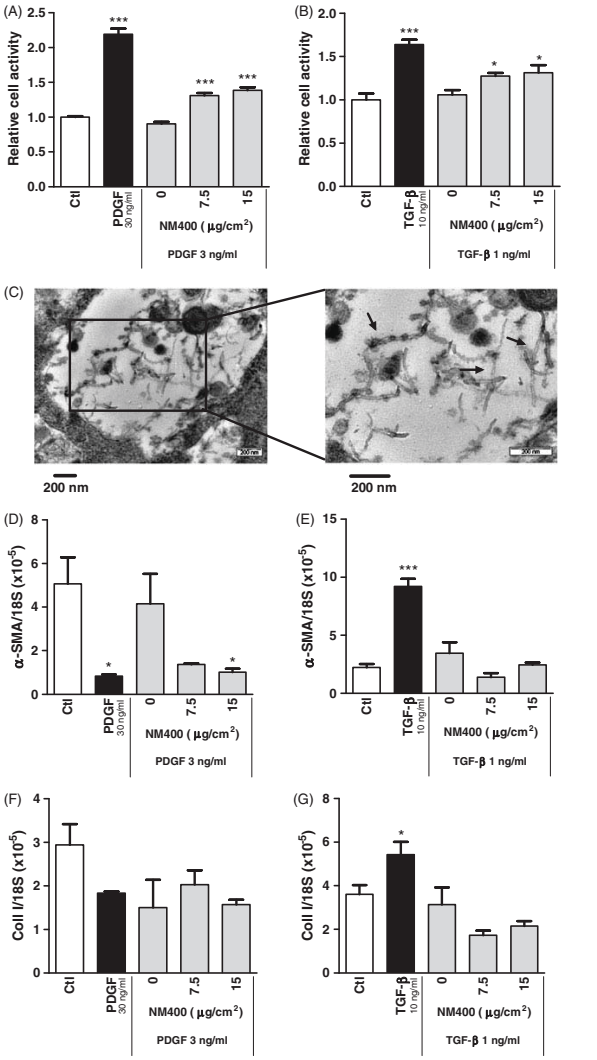


Figure 2. Direct fibrogenic effect of MWCNT on lung fibroblasts. Mouse lung fibroblasts (MLg) were exposed for 24 h to NM400 MWCNT (7.5–30 µg/cm^2) after cell priming with low concentrations of PDGF (A) or TGF-β (B) (3 and 1 ng/mL, respectively). Cell viability was assessed by the adapted WST-1 assay. PDGF (30 ng/mL) and TGF-β (10 ng/mL) were used as positive controls. Results are presented as relative cell activity, that is, as a ratio to nontreated cells (Ctl). $*p<0.05$, $***p<0.001$ versus nontreated cells ($n=4$, *t*-test or Dunnett's multiple comparison test as appropriate). (C) Intracellular localization of CNT was assessed by TEM 24 h after fibroblast exposure to MWCNT (30 µg/cm^2). Effect of MWCNT on fibroblast differentiation and collagen production was assessed by quantifying α-SMA (D, E) and pro-collagen I (F, G) mRNA, respectively, by quantitative RT-PCR. Fibroblasts were primed with low concentrations of PDGF (D, F) or TGF-β (E, G) (3 and 1 ng/mL, respectively) and then exposed to MWCNT (7.5–15 µg/cm^2) for 24 h. TGF-β (10 ng/mL) was used as positive control. RT-PCR results are presented as a ratio of gene expression normalized on the expression of the reference gene, 18 S rRNA gene. $*p<0.05$, $***p<0.001$ versus nontreated cells ($n=3$, *t*-test or Dunnett's multiple comparison test as appropriate).

PDGF R inhibitors or SB431542 (TGF-β R inhibitor) also reduced the prolonged ERK 1/2 phosphorylation induced by MWCNT after priming with PDGF or TGF-β, respectively (Figure 5B, D, and F). Thus, our observations suggested that PDGF and TGF-β receptors are implicated in the proliferative activity of MWCNT via the ERK 1/2 signaling pathway.

To determine whether kinase receptors, other than PDGF and TGF-β R, were involved in the proliferative activity of MWCNT, we investigated the role of the EGF R. We first compared the expression of the EGF R in the different cell types by quantitative RT-PCR and found that it was strongly expressed in fibroblasts compared to epithelial cells and macrophages (Figure S2A). Fibroblast proliferation was strongly stimulated by the addition of EGF (10 ng/mL, Figure 7B). As with PDGF and TGF-β, we primed fibroblasts with a low concentration of EGF (1 ng/mL), treated cells with an EGF R inhibitor (IRESSA) and finally exposed fibroblasts to MWCNT for 24 h. Figure S2B shows that CNT significantly stimulated fibroblast proliferation primed with a low concentration of EGF and this was inhibited by the EGF R inhibitor, suggesting that the EGF signaling pathway can also

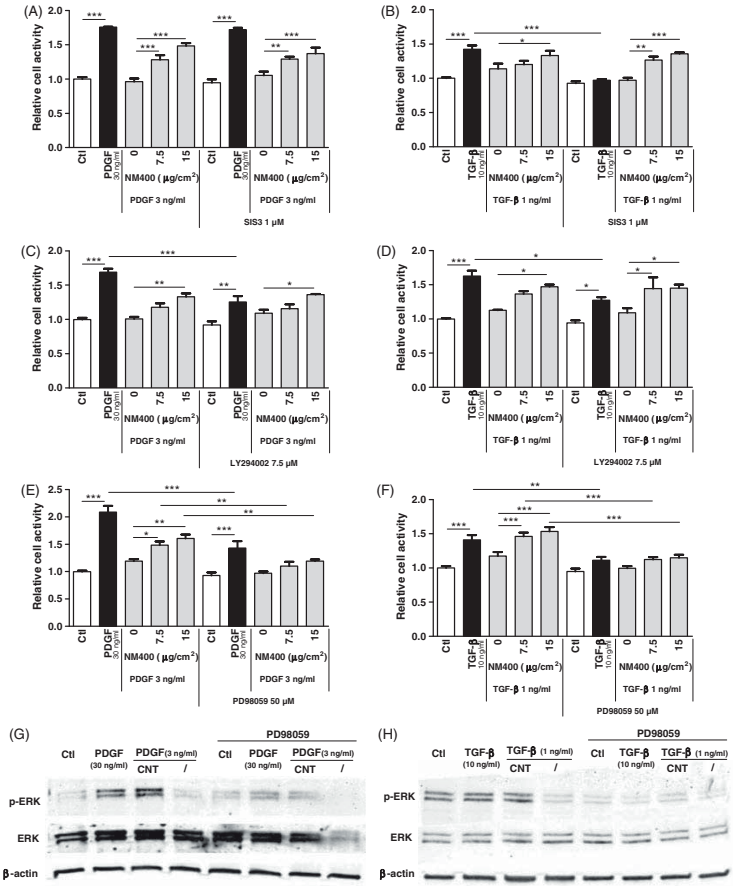


Figure 3. MWCNT stimulate fibroblast proliferation via ERK 1/2 signaling pathway. Fibroblasts (MLg) were treated with a Smad3 inhibitor, SIS3 (A, B), a PI3K inhibitor, LY294002 (C, D) or an ERK 1/2 inhibitor, PD98059 (E, F), primed with a low concentration of PDGF (A, C, E, G) or TGF-β (B, D, F, H) (3 or 1 ng/mL, respectively) and then exposed to MWCNT (7.5–15 μg/cm^2) for 24 h (WST-1 assay) or 2 h (immunoblotting). Cell viability was assessed by the adapted WST-1 assay 24 h after exposure to CNT (A-F) and ERK 1/2 phosphorylation by immunoblotting 2 h after exposure to CNT (G–H). PDGF and TGF-β (30 and 10 ng/mL, respectively) were used as positive controls. WST-1 results are presented as relative cell activity, that is, as a ratio to nontreated cells (Ctl). $*p<0.05$, $**p<0.01$, $***p<0.001$ versus nontreated cells ($n=4$, Newman–Keuls multiple comparison test).

participate to the fibrogenic activity of MWCNT. Of note, IRESSA completely inhibited EGF-stimulated (10 ng/mL), but not PDGF-stimulated proliferation of fibroblasts (data not shown).

Role of endocytosis in the proliferative activity of MWCNT

In a previous section, we showed that NM400 were endocytosed by fibroblasts (Figure 2C). To understand the role of MWCNT uptake in the stimulation of fibroblast proliferation, we used amiloride, a nonspecific inhibitor of endocytosis. Fibroblasts were treated during 2 h with amiloride, then primed with low concentrations of PDGF or TGF-β for two additional hours and finally exposed to MWCNT. Figure 6 shows that amiloride reduced the proliferative activity of MWCNT and the associated phosphorylation of ERK 1/2, while it did not alter PDGF- (30 ng/mL) or TGF-β- (10 ng/mL) induced proliferation or ERK 1/2 phosphorylation. These data indicate that the fibrogenic activity of MWCNT is also associated with the process of endocytosis in fibroblasts.

ERK 1/2 signaling as a mechanism-based predictor of the lung fibrogenic activity of MWCNT

We recently reported that the *in vitro* proliferative activity of a range of MWCNT on fibroblasts reflected their fibrotic activity *in vivo* (Vietti et al., 2013). Since the present study indicated that

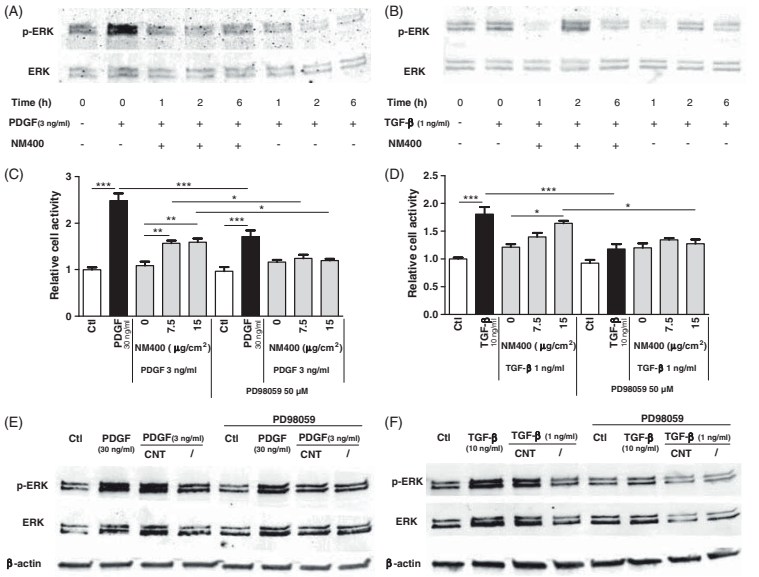


Figure 4. MWCNT prolong ERK 1/2 phosphorylation and act upstream of this signaling event. Fibroblasts (MLg) were primed with a low concentration of PDGF (A) or TGF-β (B) (3 and 1 ng/mL, respectively) and then exposed to MWCNT (15 μg/cm^2). ERK 1/2 phosphorylation was analyzed at different time points (0, 1, 2 and 6 h) by immunoblotting. The implication of ERK 1/2 in MWCNT activity was analyzed by the adapted WST-1 assay (C–D) and immunoblotting (E–F). MLg were primed with a low concentration of PDGF (C, E) or TGF-β (D, F) (3 or 1 ng/mL, respectively), then treated with an ERK 1/2 inhibitor, PD98059 (A–D) and finally exposed to MWCNT (7.5–15 μg/cm^2) for 24 h (WST-1 assay) or 2 h (immunoblotting). PDGF and TGF-β (30 and 10 ng/mL, respectively) were used as positive controls. WST-1 results are presented as relative cell activity, that is, as a ratio to nontreated cells (Ctl). *$p<0.05$, **$p<0.01$, ***$p<0.001$ versus nontreated cells ($n=4$, Newman–Keuls multiple comparison test).

the pro-fibrotic activity of CNT was correlated with the prolongation of ERK 1/2 phosphorylation promoted by growth factors, we verified this hypothesis with three other MWCNT samples. Thus, MWCNT with different physicochemical properties (such as length and diameter, described in Table 1) were selected to assess the potential predictive value of ERK 1/2 signaling phosphorylation in terms of lung fibrosis. We observed that long MWCNT, but not short and thick MWCNT, stimulated fibroblast proliferation and prolonged ERK 1/2 phosphorylation when primed with a low concentration of PDGF (Figure 7A and B). Fibroblast proliferation stimulated by long MWCNT was reduced by the ERK 1/2 inhibitor PD98059. Two months after administration of MWCNT by pharyngeal aspiration in mice, we observed a significant increase of lung collagen fibers and content with NM400 and long MWCNT, but not with short and thick MWCNT (Figure 7C and D). These data indicate that the MWCNT-induced prolongation of ERK 1/2 signaling *in vitro* correlates with their activity on fibroblast proliferation, and, most interestingly, may predict the lung fibrotic response to MWCNT.

Discussion

A number of studies have revealed that CNT can cause pulmonary fibrosis in rodents (Lam et al., 2004; Muller et al., 2008; Shvedova et al., 2005). As already mentioned, both indirect and direct mechanisms appear essential for the fibrogenic activity of CNT. Here, we show that CNT-exposed epithelial cells and macrophages are important mediators for fibroblast differentiation and that the additional direct proliferative activity of MWCNT on fibroblasts results from a prolonged activation of ERK 1/2 signaling mediated by kinase receptors and endocytosis. Moreover, the effect of different MWCNT samples on ERK 1/2 phosphorylation strongly reflected the proliferative activity of MWCNT on fibroblasts and the extent of lung fibrosis, suggesting that this in vitro mechanism of action is relevant for and predictive of the pulmonary fibrotic activity of MWCNT. Figure 8 depicts a schematic overview of the mechanisms identified in this study and participating in the indirect and direct fibrogenic activities of MWCNT on fibroblasts.

In the first part of our study, we confirmed the indirect effects of MWCNT on fibroblasts, via epithelial cells and macrophages. We found that, at equivalent doses, MWCNT induce a dose-dependent proliferative and cytotoxic effect on epithelial cells and macrophages, respectively. Furthermore, the intracellular localization analysis showed loose MWCNT in endosomes of both cell types and aggregated MWCNT in the macrophage cytoplasm. Macrophages are professional phagocytes highly specialized in the clearance of particles in the lung. The presence of aggregated MWCNT in their cytoplasm suggests a substantial endocytosis of CNT but an incapacity to clear them, leading to phagosome destabilization and cell death (Murphy et al., 2012). Conditioned media from epithelial cells and macrophages exposed to MWCNT were shown to upregulate α-SMA, suggesting a role of these cells in fibroblast differentiation via the secretion of (a) pro-fibrotic

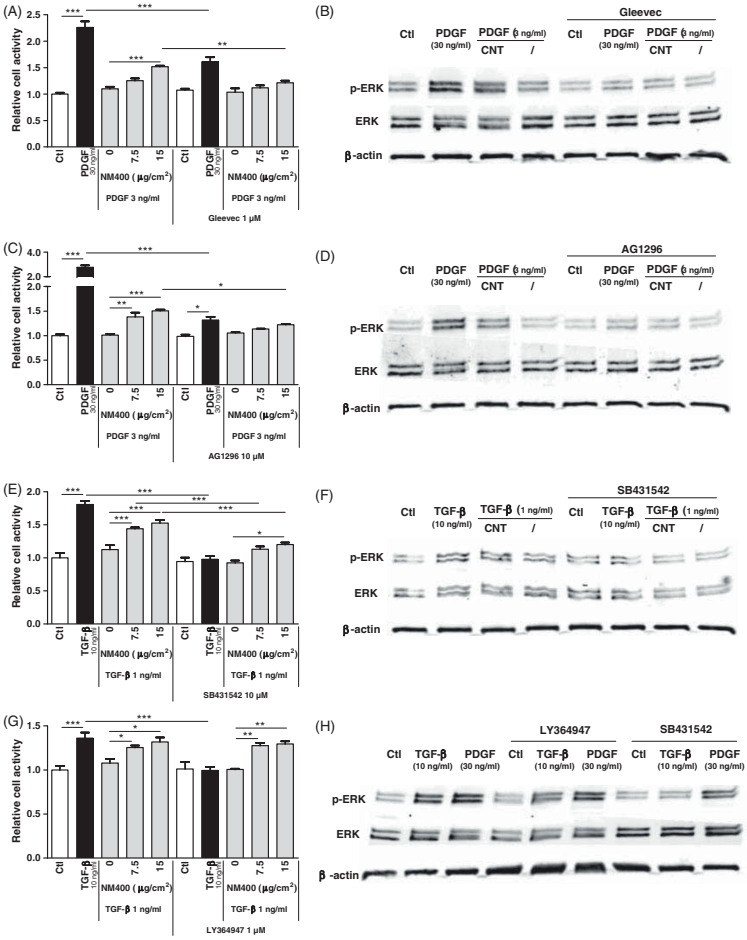


Figure 5. Implication of PDGF and TGF-β receptors in the fibrogenic activity of MWCNT in fibroblasts. MWCNT activity on fibroblast proliferation and ERK 1/2 phosphorylation in the presence of PDGF and TGF-β inhibitors were assessed by the adapted WST-1 assay (A, C, E, G) and immunoblotting (B, D, F), respectively. Fibroblasts (MLg) were primed with a low concentration of PDGF (A–D) or TGF-β (E–G) (3 or 1 ng/mL, respectively), treated with PDGF R inhibitors Gleevec (A, B) or AG1296 (C, D), TGF-β R inhibitors SB431542 (E, F) or LY364947 (G) and then exposed to MWCNT (7.5–15 μg/cm^2) for 24 h (WST-1 assay) or 2 h (immunoblotting). PDGF and TGF-β (30 and 10 ng/mL, respectively) were used as positive controls. WST-1 results are presented as relative cell activity, that is, as a ratio to nontreated cells (Ctl). $^*p < 0.05$, $^{**}p < 0.01$, $^{***}p < 0.001$ versus nontreated cells ($n = 4$, Newman–Keuls multiple comparison test). (H) Inhibitory activity of TGF-β receptor inhibitors on ERK 1/2 phosphorylation in fibroblasts was assessed by immunoblotting. MLg were treated with TGF-β R inhibitors LY364947 or SB431542 and then with active concentrations of PDGF or TGF-β (30 or 10 ng/mL, respectively).

mediator(s). Though conditioned medium might still contain CNT, we ascribed this effect to (a) factor(s) released by macrophages and epithelial cells, since NM400 did not directly increase α-SMA expression. Indeed, several investigators have amply shown that macrophages and epithelial cells exposed to CNT secrete key pro-fibrotic mediators such as PDGF, TGF-β and IL-1β (Cesta et al., 2010; Li et al., 2013; Wang et al., 2011). However, other mediators, such as EGF and fibroblast growth factor (FGF), could also contribute to the indirect effects of CNT on fibroblasts and further studies should be carried out to clarify this important issue. Our observations confirm, therefore, the indirect action of MWCNT on fibroblasts mediated by macrophages or epithelial cells that could contribute to the development of CNT-induced lung fibrosis.

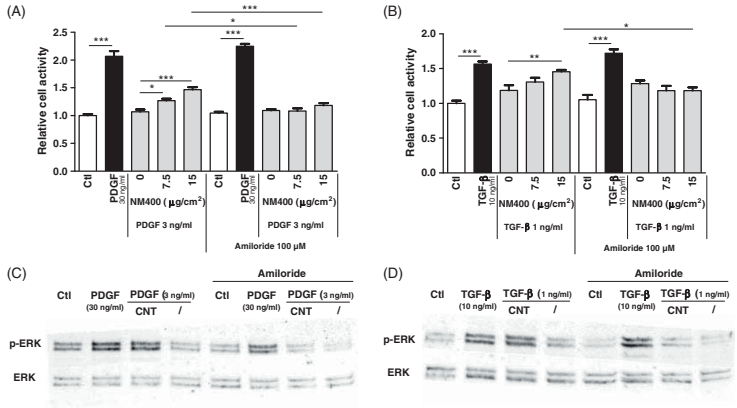


Figure 6. Implication of endocytosis in the fibrogenic activity of MWCNT in fibroblasts. MWCNT activity on fibroblast proliferation and ERK 1/2 phosphorylation in presence of the endocytosis inhibitor amiloride were assessed by the adapted WST-1 assay (A–B) and immunoblotting (C–D), respectively. Fibroblasts (MLg) were treated with the endocytosis inhibitor amiloride, primed with low concentrations of PDGF (A, C) or TGF-β (B, D) (3 and 1 ng/mL, respectively) and then exposed to MWCNT (7.5–15 µg/cm^2) for 24 h (WST-1 assay) or 2 h (immunoblotting). PDGF and TGF-β (30 and 10 ng/mL, respectively) were used as positive controls. WST-1 results are presented as relative cell activity, that is, as a ratio to nontreated cells (Ctl). *$p<0.05$, **$p<0.01$, ***$p<0.001$ versus nontreated cells ($n=4$, Newman–Keuls multiple comparison test).

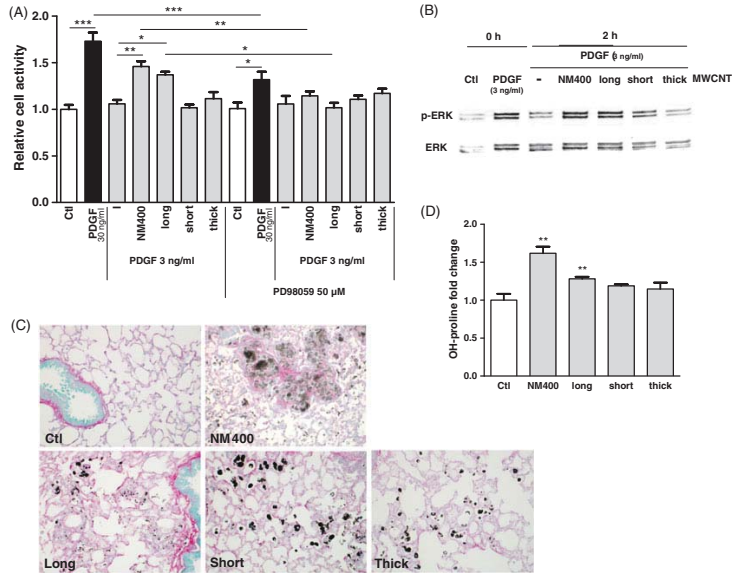


Figure 7. Activity of MWCNT on fibroblast proliferation and ERK 1/2 phosphorylation *in vitro* correlates with the induction of lung fibrosis. Fibroblasts (MLg) were exposed to different MWCNT samples (NM400, long, short or thick) in presence or absence of ERK 1/2 inhibitor, PD98059. Cell viability and ERK 1/2 phosphorylation were assessed by the adapted WST-1 assay (A) and immunoblotting (B), respectively. Fibroblasts were treated with ERK 1/2 inhibitor PD98059, primed with a low concentration of PDGF (3 ng/mL) and then exposed to MWCNT (15 µg/cm^2) for 24 h (WST-1 assay) or 2 h (immunoblotting). PDGF (30 ng/mL) was used as a positive control. WST-1 results are presented as relative cell activity, that is, as a ratio to nontreated cells (Ctl). *$p<0.05$, **$p<0.01$, ***$p<0.001$ versus nontreated cells ($n=4$, Newman–Keuls multiple comparison test). (C) Sirius red lung sections (12x) and (D) OH-proline lung content were analyzed 2 m after pharyngeal aspiration of 100 µg MWCNT/mouse (NM400, long, short, thick). **$p<0.01$ versus nontreated cells ($n=6$, Dunnett's multiple comparison).

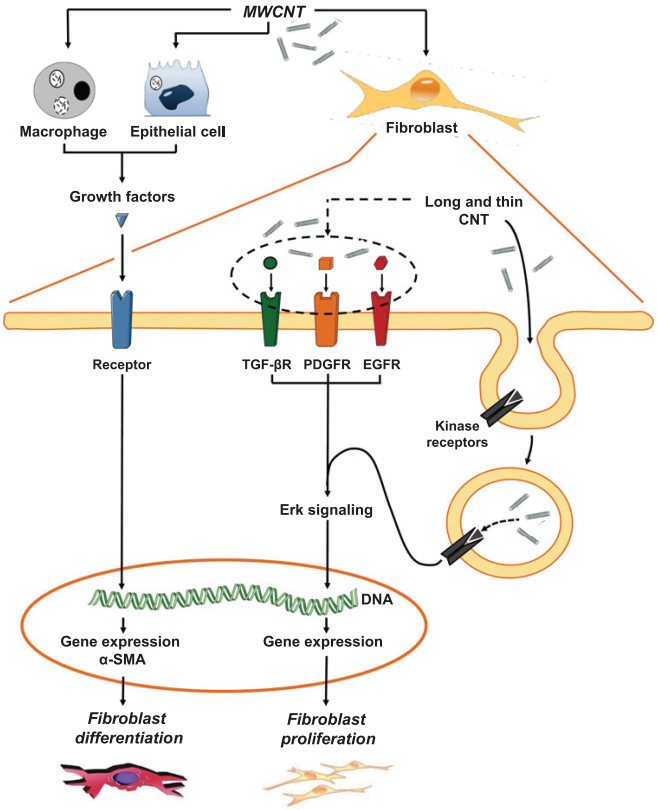


Figure 8. Potential direct and indirect mechanisms of MWCNT activity on fibroblasts to promote the development of lung fibrosis. Schematic illustration of the indirect and direct mechanisms of action of MWCNT on fibroblasts: (i) MWCNT stimulate macrophages and epithelial cells to secrete mediators that promote the differentiation of lung fibroblasts, (ii) in the presence of growth factors, long and thin MWCNT prolong ERK 1/2 phosphorylation in fibroblasts and directly stimulate their proliferation. We propose that MWCNT interact with kinase receptors and, through internalization, enhance their activation, which prolongs ERK 1/2 signaling and leads to fibroblast proliferation.

The ability of CNT to reach the alveolar interstitium and thus to directly interact with fibroblasts and stimulate their proliferation may also participate in the development of pulmonary fibrosis (Azad et al., 2013; Mercer et al., 2010; Vietti et al., 2013; Wang et al., 2010a; Wang et al., 2010b). In the present study, we showed that MWCNT stimulate fibroblast proliferation when cells are primed with low concentrations of PDGF or TGF-β. Interestingly, Wang et al. (2013) observed that MWCNT increased lung fibroblast number *in vivo* after intratracheal instillation by using the fibroblast-specific protein-1 (FSP-1) marker. Although it was not shown that increased fibroblasts number resulted solely from proliferation, these observations support the importance of this process in the development of fibrosis.

To explore the mechanisms responsible for fibroblast proliferation after MWCNT exposure, different hypotheses have been investigated. Some authors have reported increased TGF-βRII protein levels and the secretion of TGF-β by fibroblasts exposed to SWCNT (Azad et al., 2013; Lin et al., 2012; Manke et al., 2014). We did not observe increased PDGF or TGF-β secretion or expression of their receptors by fibroblast exposed to MWCNT. However, we observed a stronger expression of PDGF and TGF-β receptors in fibroblasts and epithelial cells compared to macrophages, suggesting the implication of their signaling pathway in the proliferative activity of MWCNT.

To assess this, several intracellular pathways of PDGF and TGF-β receptors (Smad3, PI3K and ERK 1/2) were probed by inhibitors. Results showed the involvement of ERK 1/2 in the proliferative activity of MWCNT. We also observed that MWCNT prolonged PDGF and TGF-β-induced ERK 1/2 phosphorylation in fibroblasts and that this effect was prevented by a ERK 1/2 inhibitor administered before or after priming, suggesting that MWCNT interfere with the signaling pathway upstream of the phosphorylation of ERK 1/2. The association between CNT exposure and activation of ERK 1/2 signaling was already shown in some studies but never in relation with the stimulation of

proliferation. For instance, phosphorylation of ERK 1/2 was detected in malignant human mesothelial cells after SWCNT exposure and during the induction of neoplastic-like transformation (Lohcharoenkal et al., 2014; Pacurari et al., 2008). Also, MWCNT were shown to activate ERK 1/2 in human skin fibroblasts, neuronal neurites and macrophages (Ding et al., 2005; Lee et al., 2012; Matsumoto et al., 2010).

Since we showed that MWCNT act upstream of ERK 1/2 in fibroblasts, we investigated whether PDGF and TGF-β receptors were involved in the proliferative activity of MWCNT. Inhibiting PDGF or TGF-β receptor after priming with their respective ligands drastically reduced MWCNT-induced fibroblast proliferation and ERK 1/2 phosphorylation. We observed that MWCNT also stimulated the proliferation of EGF-primed fibroblasts and the inhibitor of EGF R prevented this effect, suggesting that the proliferative activity of MWCNT on fibroblasts can be mediated by several kinase receptors. The EGF kinase R also regulates the activation of specific signaling pathways, including ERK 1/2 (Jorissen et al., 2003), and interacts with ultrafine carbon black particles and asbestos fibres to activate cells (Sydlik et al., 2006; Tamaoki et al., 2004; Taylor et al., 2013; Unfried et al., 2008). Currently, we ignore whether there is a direct interaction between the CNT and kinase receptors and further studies need to be performed. We can, however, conclude that the proliferative effect of MWCNT is mediated by kinase receptors.

As mentioned above, we observed the internalization of MWCNT in the endosomes of lung fibroblasts and, thus, decided to investigate whether the cellular uptake of CNT might play a role in their proliferative activity. We showed that an unspecific endocytosis inhibitor, amiloride, abolished the proliferative activity of MWCNT on primed fibroblasts as well as ERK 1/2 phosphorylation. Recent studies suggest that internalization of kinase receptors might act as a positive signal for their activation (Pahara et al., 2010; Wang et al., 2004). However, our data show that the inhibitor of endocytosis did not decrease fibroblast proliferation induced by high concentrations of PDGF and TGF-β, suggesting that receptor internalization alone is not sufficient to explain the pro-fibrotic activity of MWCNT.

Finally, we tested the proliferative activity of several MWCNT and found that their capacity to stimulate fibroblast proliferation was related to their lung fibrotic activity, as we already reported with other CNT samples (Vietti et al., 2013). Additionally, the proliferative activity of MWCNT was also associated with the prolongation of ERK 1/2 phosphorylation in fibroblasts in vitro, suggesting that this *in vitro* mechanism is predictive of a fibrogenic potential. We also confirmed the importance of MWCNT length and diameter in their fibrotic activity. Other studies also showed that MWCNT induce cytotoxic or fibrotic effects in a length-dependent manner and that thick MWCNT are less toxic than thinner ones both *in vivo* and *in vitro* (Fenoglio et al., 2012; Liu et al., 2012; Murphy et al., 2012; Nagai et al., 2011; Palomaki et al., 2011; Vietti et al., 2013). Thus, our data support the hypothesis that thin and long fibers can induce more chronic inflammation and lung fibrosis, as proposed in the fiber paradigm (Donaldson et al., 2010).

Conclusion

The present findings, summarized in Figure 8, demonstrate that MWCNT act both indirectly, via macrophages and epithelial cells, and directly on fibroblasts to stimulate their pro-fibrotic activities: (i) the interaction of MWCNT with macrophages and epithelial cells can promote the differentiation of lung fibroblasts, (ii) MWCNT interaction with fibroblasts can stimulate their proliferation. We showed that the proliferative activity of MWCNT is kinase receptor-, ERK 1/2 pathway- and endocytosis-dependent. As suggested in our previous study (Vietti et al, 2013), we confirmed with other MWCNT samples that the proliferative activity of MWCNT on fibroblasts strongly reflects their capacity to induce lung fibrosis. This was also associated with the prolongation of ERK 1/2 phosphorylation in fibroblasts, indicating that this *in vitro* mechanism of action is relevant for and predictive of the pulmonary fibrogenic activity of CNT. Other mechanisms of action have been shown to modulate the pro-fibrotic activity of CNT, and a better understanding of all pathways involved in the fibrotic potential of CNT is thus needed to better establish the value of our *in vitro* fibroblast proliferation assay to predict CNT lung fibrotic activity.

Declaration of interest

The authors declare that they have no competing interests.

GV is research fellow with the Fonds National de la Recherche Scientifique (FNRS, Belgium). This work has been supported by the Fonds de la Recherche Scientifique (FNRS) and the FP7 Risk Assessment of Engineered Nanoparticles (ENPRA) project.

References

Azad N, Iyer AK, Wang L, Liu Y, Lu Y, Rojanasakul Y. 2013. Reactive oxygen species-mediated p38 MAPK regulates carbon nanotube-induced fibrogenic and angiogenic responses. Nanotoxicology 7: 157–68.

Biondi PA, Chiesa LM, Storelli MR, Renon P. 1997. A new procedure for the specific high-performance liquid chromatographic determination of hydroxyproline. J Chromatogr Sci 35:509–12.

Cesta MF, Ryman-Rasmussen JP, Wallace DG, Masinde T, Hurlburt G, Taylor AJ, Bonner JC. 2010. Bacterial lipopolysaccharide enhances PDGF signaling and pulmonary fibrosis in rats exposed to carbon nanotubes. Am J Respir Cell Mol Biol 43:142–51.

De Volder MF, Tawfick SH, Baughman RH, Hart AJ. 2013. Carbon nanotubes: present and future commercial applications. Science 339: 535–9.

Ding L, Stilwell J, Zhang T, Elboudwarej O, Jiang H, Selegue JP, et al. 2005. Molecular characterization of the cytotoxic mechanism of multiwall carbon nanotubes and nano-onions on human skin fibroblast. Nano Lett 5:2448–64.

Donaldson K, Murphy FA, Duffin R, Poland CA. 2010. Asbestos, carbon nanotubes and the pleural mesothelium: a review of the hypothesis regarding the role of long fibre retention in the parietal pleura, inflammation and mesothelioma. Part Fibre Toxicol 7:5.

Fenoglio I, Aldieri E, Gazzano E, Cesano F, Colonna M, Scarano D, et al. 2012. Thickness of multiwalled carbon nanotubes affects their lung toxicity. Chem Res Toxicol 25:74–82.

Fenoglio I, Greco G, Tomatis M, Muller J, Raymundo-Pinero E, Beguin F, et al. 2008. Structural defects play a major role in the acute lung toxicity of multiwall carbon nanotubes: physicochemical aspects. Chem Res Toxicol 21:1690–7.

He X, Young SH, Schwegler-Berry D, Chisholm WP, Fernback JE, Ma Q. 2011. Multiwalled carbon nanotubes induce a fibrogenic response by stimulating reactive oxygen species production, activating NF-kappaB signaling, and promoting fibroblast-to-myofibroblast transformation. Chem Res Toxicol 24:2237–48.

Hirano S, Kanno S, Furuyama A. 2008. Multi-walled carbon nanotubes injure the plasma membrane of macrophages. Toxicol Appl Pharmacol 232:244–51.

Jorissen RN, Walker F, Pouliot N, Garrett TP, Ward CW, Burgess AW. 2003. Epidermal growth factor receptor: mechanisms of activation and signalling. Exp Cell Res 284:31–53.

Lam CW, James JT, Mccluskey R, Hunter RL. 2004. Pulmonary toxicity of single-wall carbon nanotubes in mice 7 and 90 days after intratracheal instillation. Toxicol Sci 77:126–34.

Lee JK, Sayers BC, Chun KS, Lao HC, Shipley-Phillips JK, Bonner JC, Langenbach R. 2012. Multi-walled carbon nanotubes induce COX-2 and iNOS expression via MAP kinase-dependent and -independent mechanisms in mouse RAW264.7 macrophages. Part Fibre Toxicol 9:14.

Li R, Wang X, Ji Z, Sun B, Zhang H, Chang CH, et al. 2013. Surface charge and cellular processing of covalently functionalized multiwall

carbon nanotubes determine pulmonary toxicity. ACS Nano 7: 2352–68.
Lin Z, Liu L, Xi Z, Huang J, Lin B. 2012. Single-walled carbon nanotubes promote rat vascular adventitial fibroblasts to transform into myofibroblasts by SM22-alpha expression. Int J Nanomedicine 7: 4199–206.
Liu D, Wang L, Wang Z, Cuschieri A. 2012. Different cellular response mechanisms contribute to the length-dependent cytotoxicity of multi-walled carbon nanotubes. Nanoscale Res Lett 7:361.
Lohcharoenkal W, Wang L, Stueckle TA, Park J, Tse W, Dinu CZ, Rojanasakul Y. 2014. Role of H-Ras/ERK signaling in carbon nanotube-induced neoplastic-like transformation of human mesothelial cells. Front Physiol 5:222.
Manke A, Luanpitpong S, Dong C, Wang L, He X, Battelli L, et al. 2014. Effect of fiber length on carbon nanotube-induced fibrogenesis. Int J Mol Sci 15:7444–61.
Matsumoto K, Sato C, Naka Y, Whitby R, Shimizu N. 2010. Stimulation of neuronal neurite outgrowth using functionalized carbon nanotubes. Nanotechnology 21:115101.
Mercer RR, Hubbs AF, Scabilloni JF, Wang L, Battelli LA, Schwegler-Berry D, et al. 2010. Distribution and persistence of pleural penetrations by multi-walled carbon nanotubes. Part Fibre Toxicol 7:28.
Mossman BT, Churg A. 1998. Mechanisms in the pathogenesis of asbestosis and silicosis. Am J Respir Crit Care Med 157:1666–80.
Muller J, Huaux F, Fonseca A, Nagy JB, Moreau N, Delos M, et al. 2008. Structural defects play a major role in the acute lung toxicity of multiwall carbon nanotubes: toxicological aspects. Chem Res Toxicol 21:1698–705.
Murphy FA, Schinwald A, Poland CA, Donaldson K. 2012. The mechanism of pleural inflammation by long carbon nanotubes: interaction of long fibres with macrophages stimulates them to amplify pro-inflammatory responses in mesothelial cells. Part Fibre Toxicol 9:8.
Nagai H, Okazaki Y, Chew SH, Misawa N, Yamashita Y, Akatsuka S, et al. 2011. Diameter and rigidity of multiwalled carbon nanotubes are critical factors in mesothelial injury and carcinogenesis. Proc Natl Acad Sci U S A 108:E1330–8.
Pacurari M, Yin XJ, Zhao J, Ding M, Leonard SS, Schwegler-Berry D, et al. 2008. Raw single-wall carbon nanotubes induce oxidative stress and activate MAPKs, AP-1, NF-kappaB, and Akt in normal and malignant human mesothelial cells. Environ Health Perspect 116: 1211–17.
Pahara J, Shi H, Chen X, Wang Z. 2010. Dimerization drives PDGF receptor endocytosis through a C-terminal hydrophobic motif shared by EGF receptor. Exp Cell Res 316:2237–50.
Palomaki J, Valimaki E, Sund J, Vippola M, Clausen PA, Jensen KA, et al. 2011. Long, needle-like carbon nanotubes and asbestos activate the NLRP3 inflammasome through a similar mechanism. ACS Nano 5: 6861–70.
Salabei JK, Cummins TD, Singh M, Jones SP, Bhatnagar A, Hill BG. 2013. PDGF-mediated autophagy regulates vascular smooth muscle cell phenotype and resistance to oxidative stress. Biochem J 451: 375–88.
Shvedova AA, Kisin ER, Mercer R, Murray AR, Johnson VJ, Potapovich AI, et al. 2005. Unusual inflammatory and fibrogenic pulmonary responses to single-walled carbon nanotubes in mice. Am J Physiol Lung Cell Mol Physiol 289:L698–708.
Sydlik U, Bierhals K, Soufi M, Abel J, Schins RP, Unfried K. 2006. Ultrafine carbon particles induce apoptosis and proliferation in rat lung epithelial cells via specific signaling pathways both using EGF-R. Am J Physiol Lung Cell Mol Physiol 291:L725–33.
Tamaoki J, Isono K, Takeyama K, Tagaya E, Nakata J, Nagai A. 2004. Ultrafine carbon black particles stimulate proliferation of human airway epithelium via EGF receptor-mediated signaling pathway. Am J Physiol Lung Cell Mol Physiol 287:L1127–33.
Taylor ES, Wylie AG, Mossman BT, Lower SK. 2013. Repetitive dissociation from crocidolite asbestos acts as persistent signal for epidermal growth factor receptor. Langmuir 29:6323–30.
Unfried K, Sydlik U, Bierhals K, Weissenberg A, Abel J. 2008. Carbon nanoparticle-induced lung epithelial cell proliferation is mediated by receptor-dependent Akt activation. Am J Physiol Lung Cell Mol Physiol 294:L358–67.
Vietti G, Ibouraadaten S, Palmai-Pallag M, Yakoub Y, Bailly C, Fenoglio I, et al. 2013. Towards predicting the lung fibrogenic activity of nanomaterials: experimental validation of an in vitro fibroblast proliferation assay. Part Fibre Toxicol 10:52.
Wang L, Mercer RR, Rojanasakul Y, Qiu A, Lu Y, Scabilloni JF, et al. 2010a. Direct fibrogenic effects of dispersed single-walled carbon nanotubes on human lung fibroblasts. J Toxicol Environ Health A 73: 410–22.
Wang P, Nie X, Wang Y, Li Y, Ge C, Zhang L, et al. 2013. Multiwall carbon nanotubes mediate macrophage activation and promote pulmonary fibrosis through TGF-beta/Smad signaling pathway. Small 9: 3799–811.
Wang P, Wang Y, Nie X, Braini C, Bai R, Chen C. 2015. Multiwall carbon nanotubes directly promote fibroblast-myofibroblast and epithelial-mesenchymal transitions through the activation of the TGF-beta/Smad signaling pathway. Small 11:446–55.
Wang X, Xia T, Duch MC, Ji Z, Zhang H, Li R, et al. 2012. Pluronic F108 coating decreases the lung fibrosis potential of multiwall carbon nanotubes by reducing lysosomal injury. Nano Lett 12:3050–61.
Wang X, Xia T, Ntim SA, Ji Z, George S, Meng H, et al. 2010b. Quantitative techniques for assessing and controlling the dispersion and biological effects of multiwalled carbon nanotubes in mammalian tissue culture cells. ACS Nano 4:7241–52.
Wang X, Xia T, Ntim SA, Ji Z, Lin S, Meng H, et al. 2011. Dispersal state of multiwalled carbon nanotubes elicits profibrogenic cellular responses that correlate with fibrogenesis biomarkers and fibrosis in the murine lung. ACS Nano 5:9772–87.
Wang Y, Pennock SD, Chen X, Kazlauskas A, Wang Z. 2004. Platelet-derived growth factor receptor-mediated signal transduction from endosomes. J Biol Chem 279:8038–46.
Wynn TA. 2011. Integrating mechanisms of pulmonary fibrosis. J Exp Med 208:1339–50.
Yan B. 2014. Reprogramming cellular signaling machinery using surface-modified carbon nanotubes. Chem Res Toxicol 28:296–305.

Supplementary material available at online

Supplementary Material

Figure S1

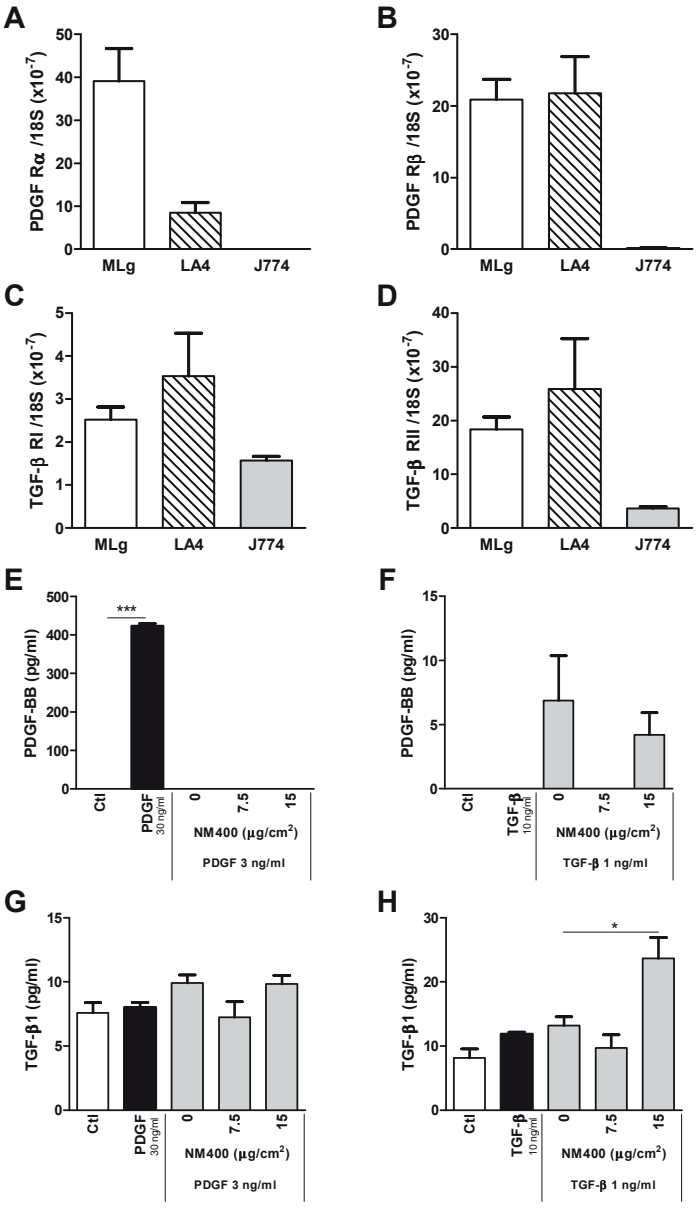


Figure S1. Effect of MWCNT on PDGF and TGF-β secretion by fibroblasts and expression of their receptors. Expression of PDGF Rα (A), PDGFRβ (B), TGF-β RI (C) and TGF-β RII (D) mRNA was assessed by quantitative RT-PCR on mouse lung fibroblasts (MLg), type II alveolar epithelial cells (LA-4) and peritoneal macrophages (J774). Results are presented as a ratio of gene expression normalized on the expression of the reference gene, 18S rRNA. Secretion of PDGF-BB (E,F) and TGF-β1 (G,H) was measured in MLg culture supernatants by ELISA. MLg were primed with low concentrations of PDGF (E,G) or TGF-β (F,H) (3 and 1 ng/ml, respectively) and then exposed to MWCNT (7.5-15 μg/cm^2) for 24 h. * $p < 0.05$, *** $p < 0.001$ vs non-treated cells (n = 3, t-test or Dunnett's Multiple Comparison test as appropriate).

Figure S2

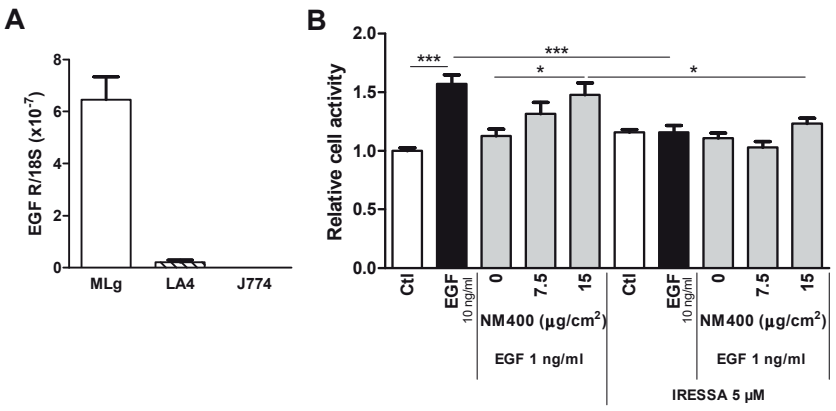


Figure S2. Implication of EGF R in the fibrogenic activity of MWCNT in fibroblasts. (A) Expression of EGF R mRNA was measured by quantitative RT-PCR in mouse lung fibroblasts (MLg), type II alveolar epithelial cells (LA-4) and peritoneal macrophages (J774). Results are presented as a ratio of gene expression normalized on the expression of the reference gene, 18S rRNA. (B) MWCNT activity on fibroblast proliferation in presence of the EGF R inhibitor IRESSA was assessed by the adapted WST-1 assay. Fibroblasts were primed with a low concentration of EGF (1 ng/ml), treated with IRESSA and then exposed to MWCNT (7.5-15 µg/cm^2) for 24 h. EGF (10 ng/ml) was used as a positive control. WST-1 results are presented as a ratio to non-treated cells (Ctl). * $p < 0.05$, *** $p < 0.001$ vs non-treated cells ($n = 4$, Newman-Keuls Multiple Comparison test).

3.3.3. How does this work contribute to nanotoxicology knowledge?

With this in vitro study we confirm that MWCNT NM400 directly increase fibroblast proliferation, and indirectly via macrophages and epithelial cells, stimulate fibroblast differentiation, both phenomena likely contributing to the establishment of lung fibrosis. These data also suggest that the mechanisms of action of CNT in inducing pro-fibrotic effects is mediated through specific signaling pathways, which were identified as kinase receptors, ERK 1/2 signaling and endocytosis in our manuscript.

Currently, there are few studies that clearly analyzed the direct effect of CNT on fibroblasts. Three studies have investigated this topic. Wang et al. (Wang et al., 2015) observed that long MWCNT (length 20-50 µm, doses 15-60 µg/ml) directly promote fibroblast differentiation into myofibroblasts through the activation of the TGF-β/Smad signaling. Another group observed that SWCNT (5-25 µg/ml) induce fibroblast proliferation and collagen production through a ROS-dependent p38 MAPK signaling leading to the production of vascular endothelial growth factor (VEGF) and TGF-β (Azad et al., 2013). Unfortunately, these studies did not investigate a possible correlation between their in vitro results on fibroblasts and in vivo findings. The group of Manke et al. (Manke et al., 2014) has simultaneously explored the direct mechanisms mediating the pro-fibrotic effect of CNT on fibroblasts and their in vivo fibrotic effect. Authors showed that the upregulation of TGF-β protein expression by fibroblasts in vitro upon CNT exposure was associated with the in vivo lung fibrosis outcome. The difference of mechanisms observed in all these studies may be not immediately obvious, but can probably be attributed to: i) the experimental conditions, such as cell lines, dispersion media and methods; and ii) the physico-chemical properties of CNT, suggesting that CNT can probably activate fibroblasts in different ways depending on their structure.

Principally fiber length and diameter have been shown to modulate CNT pro-fibrotic effects on fibroblasts.

Currently, even if it is probably difficult to draw definitive conclusions about the modes of action of CNT on fibroblasts, these results are useful to further investigate these issues and to find valid and relevant biomarkers predicting the fibrotic reaction induced by CNT in the lung. This knowledge will also be useful for industry and regulators to manufacture safe CNT and thus prevent their hazardous effects.

REFERENCES

Azad N, Iyer AK, Wang L, Liu Y, Lu Y, Rojanasakul Y. 2013. Reactive oxygen species-mediated p38 MAPK regulates carbon nanotube-induced fibrogenic and angiogenic responses. Nanotoxicology 7**,** 157-68.

Manke A, Luanpitpong S, Dong C, Wang L, He X, Battelli L, Derk R, Stueckle TA, Porter DW, Sager T, Gou H, Dinu CZ, Wu N, Mercer RR, Rojanasakul Y. 2014. Effect of fiber length on carbon nanotube-induced fibrogenesis. Int J Mol Sci 15**,** 7444-61.

Wang P, Wang Y, Nie X, Braini C, Bai R, Chen C. 2015. Multiwall Carbon Nanotubes Directly Promote Fibroblast-Myofibroblast and Epithelial-Mesenchymal Transitions through the Activation of the TGF-beta/Smad Signaling Pathway. Small 11**,** 446-55.

3.4. REVIEW ON CARBON NANOTUBES AND LUNG FIBROSIS MECHANISMS

3.4.1. Context and general review design.

The initial actor of fibrosis is still not clearly identified and, in the literature, few reviews have clearly organized and elucidated the key cells and mechanisms which lead to pulmonary fibrosis upon CNT exposure (Manke et al., 2013). In particle toxicology, fibrosis is generally interpreted as being the result of an inflammatory response that is driven by the inability to clear particles from the lungs via the usual protective mechanisms. In the lung, CNT can be cleared by responses such as coughing, mucociliary transport, and/or phagocytosis by alveolar macrophages (Gehr et al., 2000; Schurch et al., 1990). Instead, CNT that cannot be cleared by physiological processes are considered to be biopersistent (Donaldson et al., 2013), resulting in a chronic inflammatory response where immune cells, principally macrophages, and epithelial cells are excessively or inappropriately activated. Different types of CNT have been shown to induce diverse inflammatory responses, such as the release of mediators, both in vivo and in vitro. Interestingly, emerging evidences report that CNT can reach the interstitial space and, thus, be in contact with fibroblasts. In vitro and in vivo studies, including ours, have shown that CNT are able to activate fibroblasts, inducing their proliferation, differentiation and/or collagen production (Wang et al., 2010; Vietti et al., 2013; Vietti et al., 2015; Wang et al., 2015).

In this review, we have reorganized the mechanisms involved in CNT-induced lung fibrosis based on a new concept, i.e. we classified CNT activities in inducing lung fibrosis as “direct” and “indirect” effects on fibroblasts, as shown in Figure 6.

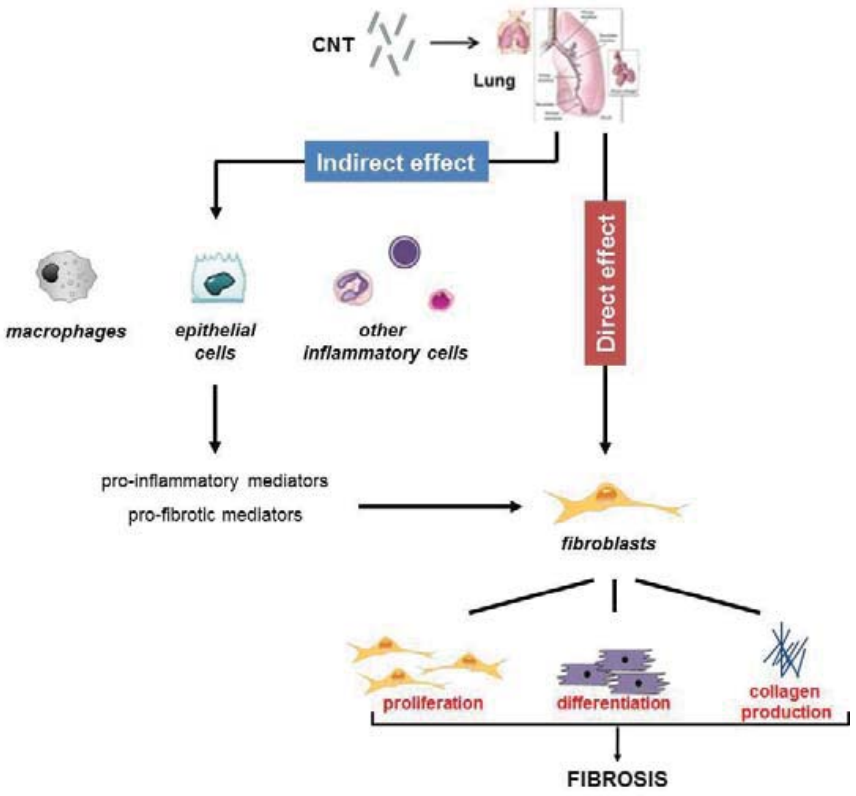


Figure 6. Direct and indirect effects of CNT on lung fibroblasts.

Macrophages and epithelial cells were principally investigated and analyzed for the indirect effects on fibroblasts. We also addressed the physico-chemical properties of CNT important for their toxic activities and the relationship between in vitro and in vivo findings. This knowledge allowed us to build an adverse outcome pathway (AOP) to guide further researches focusing on appropriate and priority toxic events and identify novel biomarkers, through which we can improve predictive approaches needed to advance regulatory nanotoxicology.

REFERENCES

Donaldson K, Poland CA, Murphy FA, Macfarlane M, Chernova T, Schinwald A. 2013. Pulmonary toxicity of carbon nanotubes and asbestos - similarities and differences. Adv Drug Deliv Rev 65**,** 2078-86.

Gehr P, Im Hof V, Geiser M, Schurch S. 2000. [The mucociliary system of the lung--role of surfactants]. Schweiz Med Wochenschr 130**,** 691-8.

Manke A, Wang L, Rojanasakul Y. 2013. Pulmonary toxicity and fibrogenic response of carbon nanotubes. Toxicol Mech Methods 23**,** 196-206.

Schurch S, Gehr P, Im Hof V, Geiser M, Green F. 1990. Surfactant displaces particles toward the epithelium in airways and alveoli. Respir Physiol 80**,** 17-32.

Vietti G, Ibouraadaten S, Palmai-Pallag M, Yakoub Y, Bailly C, Fenoglio I, Marbaix E, Lison D, Van Den Brule S. 2013. Towards predicting the lung fibrogenic activity of nanomaterials: experimental validation of an in vitro fibroblast proliferation assay. Part Fibre Toxicol 10**,** 52.

Vietti G, Ibouraadaten S, Palmai-Pallag M, Yakoub Y, Piret JP, Marbaix E, Lison D, Van Den Brule S. 2015. Towards predicting the lung fibrogenic activity of MWCNT: Key role of endocytosis, kinase receptors and ERK 1/2 signaling. Nanotoxicology**,** 1-13.

Wang L, Mercer RR, Rojanasakul Y, Qiu A, Lu Y, Scabilloni JF, Wu N, Castranova V. 2010. Direct fibrogenic effects of dispersed single-walled carbon nanotubes on human lung fibroblasts. J Toxicol Environ Health A 73**,** 410-22.

Wang P, Wang Y, Nie X, Braini C, Bai R, Chen C. 2015. Multiwall Carbon Nanotubes Directly Promote Fibroblast-Myofibroblast and Epithelial-Mesenchymal Transitions through the Activation of the TGF-beta/Smad Signaling Pathway. Small 11**,** 446-55.

3.4.2.

Mechanisms of carbon nanotube induced fibrosis: toward building an Adverse Outcome Pathway (AOP).

Vietti et al. Particle and Fibre Toxicology (2016) 13:11
DOI 10.1186/s12989-016-0123-y

Particle and Fibre Toxicology

REVIEW Open Access

Mechanisms of lung fibrosis induced by carbon nanotubes: towards an Adverse Outcome Pathway (AOP)

Giulia Vietti*, Dominique Lison and Sybille van den Brule

Abstract

Several experimental studies have shown that carbon nanotubes (CNT) can induce respiratory effects, including lung fibrosis. The cellular and molecular events through which these effects develop are, however, not clearly elucidated. The purpose of the present review was to analyze the key events involved in the lung fibrotic reaction induced by CNT and to assess their relationships. We thus address current knowledge and gaps with a view to draft an Adverse Outcome Pathway (AOP) concerning the fibrotic potential of CNT.

As for many inhaled particles, CNT can indirectly activate fibroblasts through the release of pro-inflammatory (IL-1β) and pro-fibrotic (PDGF and TGF-β) mediators by inflammatory cells (macrophages and epithelial cells) via the induction of oxidative stress, inflammasome or NF-kB. We also highlight here direct effects of CNT on fibroblasts, which appear as a new mode of toxicity relatively specific for CNT. Direct effects of CNT on fibroblasts include the induction of fibroblast proliferation, differentiation and collagen production via ERK 1/2 or Smad signaling. We also point out the physico-chemical properties of CNT important for their toxicity and the relationship between in vitro and in vivo effects. This knowledge provides evidence to draft an AOP for the fibrogenic activity of CNT, which allows developing simple in vitro models contributing to predict the CNT effects in lung fibrosis, and risk assessment tools for regulatory decision.

Keywords: Carbon nanotube, Lung fibrosis, AOP, Fibroblast, Macrophage, Epithelial cell, Mechanisms

Background

Carbon nanotubes (CNT) are cylinders with a diameter in the order of nanometers, constituted of one or several graphene layers named single walled (SW) or multi walled (MW) CNT, respectively. They attract wide interests because of their unique physico-chemical properties useful for a variety of applications. In the last few years, several studies have suggested diverse applications of CNT in consumer and industrial products, in fields such as electronics, structural engineering, manufacturing and medicine. Thus, determining the health hazards of CNT is of great importance in view of the increased potential for human exposure within occupational, environmental, medical and consumer environments. In particular, there is a great focus on inhalation exposure because the fibrous shape of CNT, similar to asbestos fibers, and their high surface area raise serious concerns for harmful respiratory effects [1]. Recent experimental studies have indicated that CNT can induce respiratory toxicity, including inflammatory and fibrotic reactions, and peritoneal mesothelioma in animals [2–7]. The National Institute for Occupational Safety and Health (NIOSH) has recommended an occupational exposure limit (REL) of 1 $\mu g/m^3$ together with other strategies for controlling workplace exposures to CNT and for implementing a medical surveillance program of exposed workers [8].

Table 1, 2, 3 shows that CNT can induce fibrotic lung reactions, whatever the mode of experimental administration (inhalation, aspiration or injection) or the animal species used. Depending on their physicochemical characteristics, the fibrogenic activity of CNT appear, however, to vary considerably, pointing out the necessity to identify which CNT property(ies) drive(s) their hazardous activities, and which mechanisms are involved. It is,

* Correspondence: giulia.vietti@uclouvain.be
Louvain centre for Toxicology and Applied Pharmacology, Université Catholique de Louvain, Avenue E. Mounier, 52 - bte B1.52.12, 1200 Brussels, Belgium

BioMed Central

© 2016 Vietti et al. **Open Access** This article is distributed under the terms of the Creative Commons Attribution 4.0 International License (http://creativecommons.org/licenses/by/4.0/), which permits unrestricted use, distribution, and reproduction in any medium, provided you give appropriate credit to the original author(s) and the source, provide a link to the Creative Commons license, and indicate if changes were made. The Creative Commons Public Domain Dedication waiver (http://creativecommons.org/publicdomain/zero/1.0/) applies to the data made available in this article, unless otherwise stated.

Table 1 In vivo lung fibrotic reaction of CNT administered via inhalation

Inhalation studies											
Duration	CNT					Dose	Experimental model			Fibrosis	References
	Type	Source	Length (m)	Diameter (nm)	Other		Species	Strain	Methods		
1-28d	SWCNT	CNI	0.1–1	0.8–1.2		5 mg/m^3, 5 h/d, 4d whole body	mouse	C57BL/6	SSCK, SRS	+	[81]
1y	SWCNT	U	1–3	65		5 mg/m^3, 5 h/d, 4d whole body	mouse	C57BL/6	SSCK	+	[83]
2-12d	MWCNT-7	HCC	/	/		10 mg/m^3, 5 h/d whole body	mouse	C57BL/6 J	MTS	+	[84]
1 to 336d	MWCNT-7	HCC	4.3	/		5 mg/m^3, 5 h/d, 12d whole body	mouse	C57BL/6 J	SRS	+	[27]
17 m	MWCNT-7	HCC	1–6	40–90		5 mg/m^3, 5 h/d, 5d/w whole body	mouse	B6C3F1	H&E	↑	[85]
90d	MWCNT-7	HCC	5.5–6.2	94–98		0.2–5 mg/m^3, 5 h/d, 4d whole body	rat	F344	MTS	++	[86]
1d-14w	MWCNT	HMS	0.3–50	30–50		1–30 mg/m^3, 6 h/d nose inh	mouse	C57BL/6	MTS	++	[87]
90d	MWCNT	N	0.1–10	5–15		0.1–2.5 mg/m3, 6 h/d, 5d/w, 13w nose inh	rat	Wistar	H&E	-	[88]
90d	MWCNT	N	0.1–10	5–15		0.1–2.5 mg/m^3 6 h/d, 5d/w, 13w nd inh	rat	SH	MTS, LS, GS	-	[89]

nd: not determined. *Duration:* d: day; w: week; y: year. *CNT type:* AP: as prepared; COOH: carboxyl; NH2: amino; PD: purified. Source: A: Arkema (France); CNI: Carbon Nanotechnologies Inc. (Houston, TX); CT: Cheap Tubes (Brattlebore, VT); HCC: Hodogaya Chemical Company; HMS: Helix Materials Solution (Richardson, TX); MC: Mitsui & Company (Tokio, Japan); N: Nanocyl (Sambreville, Belgium); NI: NanoIntegris (Skokie, IL); NP: Nanotech Port (Chengdu, China); PIH: produced in-house; SA: Sigma-Aldrich (Lyon, France); SN: Shenzhen Nanoharbor (Shenzhen, China); SNP: Shenzhen Nanotech Port (Shenzhen, China); U: Unidym (Sunnyvale, CA). *Other:* AD: acetone/sonication dispersed; ALD: atomic layer deposition; BSA: bovine serum albumin; cc-PEI: carboxyl converted PEI; D: dispersed; DPPC: dipalmitoylphosphatidylcholine; F: functionalized; ND: no dispersed; PABS: polyaminobenzene sulfonic acid group; PEG: polyethylene glycol; PEI: polyethyleneimine; PF108-C: cruder stock; PF108-HD: homogeneously dispersed; SD: survanta dispersed; swNH2: sidewall amine. *Methods:* GS: Gomori staining; H&E: Hematoxylin and eosin stain; hclll: histopathology collagen type III; LS: Ladewig staining; MTS: Masson's trichrome staining; OH-p: hydroxyl proline, SRS: Sirius red staining; SSCK: Sircol Soluble Collagen; WBc: western blot collagen. Fibrosis: $+p < 0.05$, $++p < 0.01$, $+++p < 0.001$ as reported in the respective paper; (#) $p < 0.05$ difference between particle responses as reported in the respective paper; ↑: increase of fibrosis suggested by authors but without statistical evidence

Table 2 In vivo lung fibrotic reaction of CNT administered via intratracheal injection

Intratracheal injection studies											
Duration	CNT					Dose	Experimental model			Fibrosis	References
	Type	Source	Length (m)	Diameter (nm)	Other		Species	Strain	Methods		
7-56d	short SWCNT	SN	0.35–0.7	10–20		60 g	Mouse	C57BL/6 J	SSCK, MTS	-	[65]
	long SWCNT		5–15	10–20		(3 mg/kg)				+	
14d	SWCNT AMIDE	/	0.7–1	4–6	F	10 mg/kg	Mouse	C57BL/6	MTS, hcl, hcIII, h -SMA	++	[90]
	SWCNT COOH		0.5–1.5	4–5	F					++	
	SWCNT PABS		0.5-1	1.1	F					++	
	SWCNT PEG		0.5–0.6	4.5	F					++	
1-180d	MWCNT	SA	0.5–2	20–50	BSA disp	1–100 g	Rat	Sprague–Dawley	SSCK, MTS	-	[91]
						(5–500 g/kg)					
1-91d	MWCNT-7	MC	5	88		40–160 g	Rat	F344	MTS	↑	[92]
						(0.2–0.8 mg/kg)					
1-30d	short MWCNT	NP	0.5–2	50		0.6 mg	Rat	SH	SRS, hcIII	-	[15]
	long MWCNT		20–50	50		(3 mg/kg)				++	
60d	MWCNT	PIH	5.9	9.7		0.5–5 mg	Rat	Sprague–Dawley	OH-p, MTS, ELISAc	+++	[2]
	MWCNTg		0.7	11.3		(2.5–25 mg/kg)				++	
60d	MWCNTg	PIH	0.7	20–50	defects +++	2 mg	Rat	Wistar	OH-p, MTS	++	[93]
	MWCNTg 600				defects ++	(10 mg/kg)				+++	
	MWCNTg 2400				defects +					+++	

nd: not determined. *Duration:* d: day; w: week; y: year. *CNT type:* AP: as prepared; COOH: carboxyl; NH2: amino; PD: purified. Source: A: Arkema (France); CNI: Carbon Nanotechnologies Inc. (Houston, TX); CT: Cheap Tubes (Brattlebore, VT); HCC: Hodogaya Chemical Company; HMS: Helix Materials Solution (Richardson, TX); MC: Mitsui & Company (Tokio, Japan); N: Nanocyl (Sambreville, Belgium); NI: NanoIntegris (Skokie, IL); NP: Nanotech Port (Chengdu, China); PIH: produced in-house; SA: Sigma-Aldrich (Lyon, France); SN: Shenzhen Nanoharbor (Shenzhen, China); SNP: Shenzhen Nanotech Port (Shenzhen, China); U: Unidym (Sunnyvale, CA). *Other:* AD: acetone/sonication dispersed; ALD: atomic layer deposition; BSA: bovine serum albumin; cc-PEI: carboxyl converted PEI; D: dispersed; DPPC: dipalmitoylphosphatidylcholine; F: functionalized; ND: no dispersed; PABS: polyaminobenzene sulfonic acid group; PEG: polyethylene glycol; PEI: polyethyleneimine; PF108-C: cruder stock; PF108-HD: homogeneously dispersed; SD: survanta dispersed; swNH2: sidewall amine. *Methods:* GS: Gomori staining; H&E: Hematoxylin and eosin stain; hcIII: histopathology collagen type III; LS: Ladewig staining; MTS: Masson's trichrome staining; OH-p: hydroxyl proline, SRS: Sirius red staining; SSCK: Sircol Soluble Collagen; WBc: western blot collagen. Fibrosis: $+p < 0.05$, $++p < 0.01$, $+++p < 0.001$ as reported in the respective paper; (#) $p < 0.05$ difference between particle responses as reported in the respective paper; ↑: increase of fibrosis suggested by authors but without statistical evidence

Table 3 in vivo lung fibrotic reaction of CNT administered via pharyngeal aspiration

Pharyngeal aspiration studies

Duration	CNT					Dose	Experimental model			Fibrosis	References
	Type	Source	Length (m)	Diameter (nm)	Other		Species	Strain	Methods		
2w	SD SWCNT	CNI	0.1–1	0.8–1.2	survanta acetone disp	10 g	mouse	C57BL/6 J	SSCK, WBc	+	[29]
	AD SWCNT					(0.5 mg/kg)				+	
1-28d	SWCNT	CNI	0.1–1	0.8–1.2		5–20 g	mouse	C57BL/6	SSCK, SRS	↑	[81]
						(0.25–1 mg/kg)					
1-60d	SWCNT	CNI	/	1–4		10–40 g	mouse	C57BL/6	SRS, MTS	+	[38]
						(0.5–2 mg/kg)					
28d	SWCNT	CNI	/	1–4		40 g	mouse	C57BL/6	SSCK	+	[17]
						(2 mg/kg)		C57BL/6gp91$^{phox-/-}$		-	
28d	SWCNT	CNI	0.7	1–4		40 g	mouse	C57BL/6	SRS, SSCK	+	[94]
						(2 mg/kg)		B6.129X1-MPO		+ (#)	
3w	SWCNT	CNI	0.5–2	0.4–1.2		40 g	mouse	C57BL/6	SSCK, MTS	+	[95]
						twice a week 3 weeks					
7d	SWCNT	CNI	1–3	1–4		40–80 g	mouse	C57BL/6	SSCK	+	[96]
						(2–4 mg/kg)					
28d	SWCNT	U	1–3	1–4		40 g	mouse	C57BL/6	SRS, SSCK	+	[19]
						(2 mg/kg)					
1y	SWCNT	U	1–3	65		40 g	mouse	C57BL/6	SSCK	+	[83]
						(2 mg/kg)					
21d	SWCNT BSA-AP-Hipco	NI	1000–5000	0.7–1.1	BSA-coated	2 mg/kg	mouse	C57BL/6	SSCK, MTS	+	[47]
	SWCNT PF108-Hipco		500–1500	0.7–1.1	PF-108-coated					-	
14-56d	SWCNT	/	5–15	<2		80 g/m	mouse	C57BL/6	OH-p, MTS	+	[64]
						(4 mg/kg)					
90d	Short SWCNT	CT	1	11		40 g/m	mouse	C57BL/6 J	SSCK, SRS	+	[31]
	Long SWCNT		13	11		(2 mg/kg)				+ (#)	
21d	MWCNT	CT	10–30	20–30		2 mg/kg	mouse	C57BL/6	SSCK, MTS	+	[54]
								P47$^{phox-/-}$ C57BL/6		-	

Table 3 in vivo lung fibrotic reaction of CNT administered via pharyngeal aspiration *(Continued)*

21d	MWCNT AP	CT	0.57		F					+	
	MWCNT NH2	From AP	0.45		F					+	
	MWCNT sw-NH2	From AP	0.58		F					+	
	MWCNT PEI	From AP	0.33	/	F	2 mg/kg	mouse	C57BL/6	SSCK, MTS	+ (#)	[45]
	MWCNT cc-PEI	From AP	-		F					+	
	MWCNT COOH	From AP	0.38		F					-	
	MWCNT PEG	From AP	0.27							-	
21d	AP MWCNT D	CT			BSA + DPPC					+	
	AP MWCNT ND	CT			/					-	
	PD MWCNT D	From AP	10–30	20–30	BSA + DPPC	2 mg/kg	mouse	C57BL/6	MTS, SSCK	+	[36]
	PD MWCNT ND	From AP			/					-	
	COOH MWCNT D	From AP			BSA + DPPC					+	
	COOH MWCNT ND	From AP			/					-	
21d	AP MWCNT	CT	1.97		BSA-dispersed					+	
	AP MWCNT	CT	1.16		PF108-C					-	
	AP MWCNT	CT	0.15		PF108-HD					-	
	PD MWCNT	From AP	2.11		BSA-dispersed					+	
	PD MWCNT	From AP	1.52	20–30	PF108-C	2 mg/kg	mouse	C57BL/6	SSCK, MTS	-	[97]
	PD MWCNT	From AP	0.14		PF108-HD					-	
	COOH MWCNT	From AP	1.96		BSA-dispersed					+	
	COOH MWCNT	From AP	1.8		PF108-C					-	
	COOH MWCNT	From AP	0.15		PF108-HD					-	
1-14d	MWCNT-7	MC	3.9	49		5–40 g (0.25–2 mg/kg)	mouse	C57BL/6 J	MTS, SRS	+++	[37]
1-56d	MWCNT-7	MC	3.86	49		10–80 g (0.5–4 mg/kg)	mouse	C57BL/6 J	SRS	+	[26]
1-56d	MWCNT-7	MC	3.86	49		10–80 g/m (0.5–4 mg/kg)	mouse	C57BL/6 J	SRS	+	[82]
1 to 56d	MWCNT-7	HCC	4.3	/		80 g/m (4 mg/kg)	mouse	C57BL/6 J	SRS	+	[27]
28d	MWCNT	HMS	0.5–40	10–30	Uncoated	4 mg/kg	mouse	C57BL/6	MTS	+++ (#)	[50]
					ALD-coated					+	

Table 3 in vivo lung fibrotic reaction of CNT administered via pharyngeal aspiration *(Continued)*

60d	MWCNT NM400	N	0.7–3	5–35					+++	
	MWCNT NM402	A	0.7–4	6–20	12.5–100 g/m	mouse	C57B6/6	OH-p, SRS	+++	[23]
	MWCNT NM400c	N	0.1–0.5	18–35	(0.6–5 mg/kg)				-	
	MWCNTg 2400	PIH	0.7	20–50					-	
60d	MWCNT NM400	N	0.7–3	5–35					++	
	MWCNT long	CT	10–30	11–59	100 g/m	mouse	C57BL/6	OH-p, SRS	++	[34]
	MWCNT short	CT	0.5–2	10–47	(5 mg/kg)				-	
	MWCNT thick	CT	10–30	15–74					-	

nd: not determined. *Duration:* d: day; w: week; y: year. *CNT type:* AP: as prepared; COOH: carboxyl; NH2: amino; PD: purified. Source: A: Arkema (France); CNI: Carbon Nanotechnologies Inc. (Houston, TX); CT: Cheap Tubes (Brattlebore, VT); HCC: Hodogaya Chemical Company; HMS: Helix Materials Solution (Richardson, TX); MC: Mitsui & Company (Tokio, Japan); N: Nanocyl (Sambreville, Belgium); NI: NanoIntegris (Skokie, IL); NP: Nanotech Port (Chengdu, China); PIH: produced in-house; SA: Sigma-Aldrich (Lyon, France); SN: Shenzhen Nanoharbor (Shenzhen, China); SNP: Shenzhen Nanotech Port (Shenzhen, China); U: Unidym (Sunnyvale, CA). *Other:* AD: acetone/sonication dispersed; ALD: atomic layer deposition; BSA: bovine serum albumin; cc-PEI: carboxyl converted PEI; D: dispersed; DPPC: dipalmitoylphosphatidylcholine; F: functionalized; ND: no dispersed; PABS: polyaminobenzene sulfonic acid group; PEG: polyethylene glycol; PEI: polyethyleneimine; PF108-C: cruder stock; PF108-HD: homogeneously dispersed; SD: survanta dispersed; swNH2: sidewall amine. *Methods:* GS: Gomori staining; H&E: Hematoxylin and eosin stain; hcIII: histopathology collagen type III; LS: Ladewig staining; MTS: Masson's trichrome staining; OH-p: hydroxyl proline, SRS: Sirius red staining; SSCK: Sircol Soluble Collagen; WBc: western blot collagen. Fibrosis: $+p < 0.05$, $++p < 0.01$, $+++p < 0.001$ as reported in the respective paper; (#) $p < 0.05$ difference between particle responses as reported in the respective paper; ↑: increase of fibrosis suggested by authors but without statistical evidence

therefore, important to study and investigate how CNT can exert their pro-fibrotic activities and to initiate prevention strategies to avoid the development of diseases in humans like asbestosis.

Regulatory toxicology currently moves towards the mode of action concept, aligned with so-called adverse outcome pathways (AOP). AOP refers to a conceptual structure that portrays existing knowledge concerning a series of key events (KE) along a biological pathway from the molecular initial event (MIE) to the adverse outcome (AO) [9]. Organization of these data in an AOP provides a systematic and transparent knowledge that may help elucidating and identifying the key mechanisms of toxicity, and the strength of their relationship, which lead to the progression of the AO. This knowledge can guide researchers to focus on key toxic events and assays or, where data gaps exist, this might provide an incentive to identify and highlight new mechanisms of action. Additionally, AOPs can facilitate the development of simple and fast test methods to predict the potential hazard of CNT, thus reducing the use and costs of animal and time-consuming experiments. The present review focuses on mechanisms of the lung fibrotic reaction induced by CNT with a view to developing an AOP.

Lung fibrotic reactions and CNT

In response to prolonged tissue injury or chronic inflammation, fibroblasts can be activated, resulting in three KE involved in the development of lung fibrosis: i) cell proliferation, ii) differentiation into myofibroblasts and iii) exaggerated production of extracellular matrix (ECM) proteins, leading to ECM accumulation in the lung parenchyma, modification of the lung architecture, organ dysfunction and, eventually, severe respiratory insufficiency [10]. Fibroblasts can derive from different sources, including lung resident fibroblasts, epithelial cells undergoing epithelial-mesenchymal transition (EMT) and bone marrow progenitors called fibrocytes. Numerous studies have

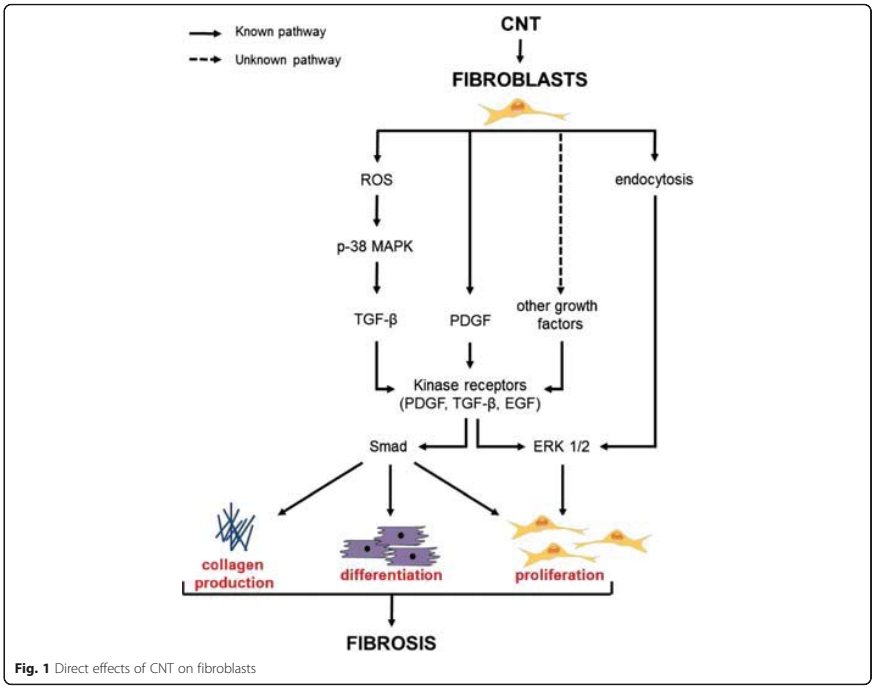


Fig. 1 Direct effects of CNT on fibroblasts

aimed at identifying how CNT can promote pro-fibrotic responses, based on the current paradigm in particle toxicology that considers particle-inflammation as key player in inducing fibrosis [11, 12].

CNT can induce the release of pro-inflammatory and pro-fibrotic growth factors by macrophages and epithelial cells [13–16], which are in the frontline in lung alveoli. The release of these mediators can induce the recruitment, proliferation and differentiation of fibroblasts, which then produce the ECM components. In this context, interstitial fibroblasts, epithelial cells undergoing EMT and fibrocytes can be involved. Additionally, other cell types seem to be involved in fibrogenic responses induced by CNT, such as T and B cells, polymorphonuclear neutrophils (PMN), mast and endothelial cells [17–21]. However, there is no evidence on how these cells can activate fibroblasts upon CNT exposure and lead to fibrosis.

In addition, scientists recently started to scrutinize the potential interaction of CNT with fibroblasts. CNT can activate fibroblasts in vitro, resulting in increased proliferation, differentiation and collagen production [22–24]. Interestingly, only fiber-shape particles such as asbestos [25] and CNT seem to have the capacity to induce fibroblast activation, suggesting a new mechanism of action for these particles.

After reviewing recent advances in this area we propose an AOP, focusing on CNT and lung fibrosis. In agreement with the observations reported above, we classified the effects of CNT in two different ways: i) direct effects on fibroblasts and ii) pro-inflammatory and pro-fibrotic effects on macrophages and epithelial cells, which we call “indirect” effects on fibroblasts. For the indirect effect on fibroblasts, we focused on macrophages and epithelial cells, because of their central role and extensive literature published in this area. To have a clear overview of the pathways involved in the development of fibrosis we further structured the review in multiple sections for each cell type analyzed (CNT localization, effects, mechanisms, relevance of in vitro CNT activities for in vivo effects) in order to design a structured AOP. We summarize here evidences of a close cooperation between fibroblasts, macrophages and epithelial cells in the development of pulmonary fibrosis upon CNT exposure.

The direct effects of CNT on fibroblasts

Fibroblasts and CNT lung localization

To support the new paradigm that CNT can have a direct effect on fibroblasts, we first need to address the localization of CNT deposited in the lung. Recent studies have shown the localization of CNT in the alveolar interstitium after pharyngeal aspiration or inhalation exposure using light microscopy, field emission electron microscopy (FESEM) and a new technique based on enhanced-darkfield illumination optics and imaging [26, 27]. These studies support the idea that CNT are able to reach the alveolar interstitium rapidly after exposure and get in close contact with fibroblasts, suggesting that these particles can act directly on these cells possibly contributing to fibrosis development. This observation is further supported by a previous paper by Mercer et al. [28], who observed that dispersed SWCNT (average equivalent diameter 0.69 μm) reached the deep lung and rapidly penetrated in the alveolar interstitium causing after 7 days an increase of thickness of alveolar walls and collagen content after pharyngeal aspiration of 10 μg CNT/mouse (corresponding to 0.5 mg/kg b.w., considering a mouse weight of 20 g). On the contrary, agglomerates and poorly dispersed SWCNT (average equivalent diameter 15.2 μm) were principally deposited in the proximal alveolar region and formed granuloma, confirming that CNT aggregation plays a role in their tissue distribution and thus fibrogenic activity. These studies used doses of CNT equivalent to a human exposure scenario for a person performing a light work, based on average daily CNT workplace exposure. Also the group of Wang et al. [24] showed that MWCNT can directly interact with fibroblasts in vivo. Long MWCNT (length 20–50 μm), which were not phagocytosed by macrophages, were found at the surface and also inside cells stained positively for FSP-1 (fibroblast specific marker) contrary to short MWCNT (length 0.5-2 μm) after intratracheal instillation of 0.6 mg/rat (3 mg/kg b.w., considering a rat weight of 200 g). This dose is similar to that used by Mercer et al. [28] as 80 μg CNT/mouse corresponds to 4 mg/kg b.w. Taken together, these data confirm the relevance of investigating the direct activities of CNT on lung fibroblasts.

CNT activities on fibroblasts

Effects

In this section, we focus on in vitro studies that addressed the activation of fibroblasts by CNT, as illustrated in Fig. 1. As mentioned above, the ultimate events in fibrogenesis are fibroblast proliferation, differentiation and ECM production. The first study that demonstrated a direct effect of CNT on fibroblasts was published by the group of Wang et al. [22]. Low concentrations of dispersed SWCNT (0.02–0.24 μg/cm^2), extrapolated from in vivo doses (10–40 μg/mouse, corresponding to 0.5–2 mg/kg b.w.), stimulated cell proliferation, collagen production and matrix metalloproteinases (MMP)-9 expression in human lung fibroblast (CRL-1490). Other in vitro studies observed that both SWCNT and MWCNT were able to directly stimulate fibroblast proliferation, differentiation and collagen production [14, 23, 24, 29–31]. In general, these studies

demonstrated that CNT have a direct and rapid effect on different types of fibroblasts, only after 24 or 48 h exposure to doses of CNT relevant for in vivo and human exposure scenarios. These results also show that CNT activity on fibroblasts is not species-specific and that the types of fibroblast tested, such as CRL-1490 and mouse lung fibroblast (MLg), are useful cell models, providing support to extrapolate in vitro data to in vivo and human exposures. However, some CNT have also been observed to be cytotoxic to fibroblasts [13, 32] and it appears that this effect is related to the production of reactive oxygen species (ROS) by fibroblasts exposed to CNT, which we will describe in more details in the next section. MWCNT (20 μg/ml) were also found to increase transforming growth factor (TGF)- and platelet-derived growth factor (PDGF) mRNA and proteins in lung fibroblasts after 24 h exposure [13]. Both growth factors are well known as key mediators in the pathogenesis of pulmonary fibrosis. PDGF stimulates fibroblast proliferation and acts as a potent chemoattractant for fibroblasts and myofibroblasts, thereby promoting fibrosis. TGF- stimulates the differentiation of mesenchymal cells and the synthesis of collagen. Also, pro-inflammatory mediators could mediate the release of TGF- and PDGF and thus potentially exacerbate fibrosis development [13]. However, the release of pro-inflammatory mediators by fibroblasts after CNT exposure has not been observed so far.

Mechanisms

Few studies investigated the specific mechanisms of action by which CNT can directly promote fibroblast activation. A recent study observed that long MWCNT (length 20–50 μm, doses 15–60 μg/ml) directly promote fibroblast differentiation into myofibroblasts through the activation of TGF- /Smad signaling [24]. This pathway is largely known to drive myofibroblast differentiation, but explored for the first time in the context of CNT-induced fibroblast activation. The mechanisms involved in fibroblast proliferation were investigated in two other studies. Azad et al. [14] observed that SWCNT (5–25 μg/ml) induce fibroblast proliferation and collagen production through a ROS-dependent p38 MAPK signaling leading to the production of TGF- and vascular endothelial growth factor (VEGF). Oxidative stress reflects an imbalance between the production of different reactive metabolites, including ROS and antioxidant defenses. CNT have been shown to induce ROS production both in vitro and in vivo, directly via physico-chemical reactivity, for example through active residual metal catalysts present on the surface of CNT (discussed in section: "Indirect effects of CNT on fibroblasts"), or indirectly, via the activation of enzymatic pathways leading to release of oxidative species. Oxidative stress has been identified as an initiating factor in the pathogenesis of fibrosis as it can increase pro-fibrotic growth factors production leading to the activation of fibroblasts, as described by Azad et al. [14]. Interestingly, Manke et al. [31] also observed that SWCNT (0.06 μg/cm^2) induced collagen and TGF- production via ROS generation in normal human lung fibroblasts (NHLF) and these effects were inhibited in the presence of N-acetyl cysteine (NAC). MWCNT-induced oxidative response was also related to a cytotoxic activity of CNT on fibroblasts [32, 33]. We showed the implication of TGF- , PDGF and epidermal growth factor (EGF) receptors in MWCNT-induced fibroblast proliferation. In presence of low concentrations of different growth factors, we observed that long and thin MWCNT (MWCNT length 10–30 μm and diameter 10–60 nm; doses 15 μg/cm^2, corresponding to 24 μg/ml by considering a well surface area of 0.32 cm^2), but not short or thick CNT (MWCNT short: length 0.5-2 μm and diameter 10–50 nm; MWCNT thick: length 10–30 μm and diameter 15–75 nm), directly stimulated fibroblast proliferation via kinase receptors, ERK 1/2 signaling and endocytosis pathways [34]. Some other studies have shown that CNT can be taken up by fibroblasts [24]. However, for the first time it was shown that endocytosis is required for the activation of fibroblasts [34]. Moreover, kinase receptors have been found to be involved in the proliferative activity of MWCNT by using receptor inhibitors, which also inhibited ERK 1/2 signaling pathway [34]. Currently, no data is available on how CNT could interact with these receptors. Asbestos fibers have been shown to directly bind and activate EGF receptor [35], suggesting that CNT could somehow interact with kinase receptors. Azad et al. [14] and Vietti et al. [34] have identified different mechanisms leading to CNT-induced fibroblast proliferation. This may be related to the physico-chemical properties of CNT, suggesting that CNT can activate fibroblast in different ways depending on their structure and possibly their potential to generate ROS. However, these differences can also reflect different experimental procedures, such as cell lines, dispersion medium and methods used. It should be noted that the doses able to activate fibroblasts are in the same range of 5–60 μg/ml, which has been calculated to be relevant for in vivo and human exposure scenarios.

Relevance of in vitro CNT activities for in vivo effects

Exploring correlations between in vitro results and pulmonary fibrotic responses in vivo is helpful to derive in vitro assays suitable for predicting the lung fibrogenic activity of CNT. Several studies observed a relationship between in vitro results on fibroblasts and in vivo findings [23, 30, 31, 36]. The capacity of a range of CNT to induce fibroblast proliferation and collagen production has been shown to correlate with their in vivo fibrotic activity. Moreover, the upregulation of TGF- expression

by fibroblasts in vitro upon CNT exposure has been associated with the in vivo lung fibrosis outcome [31]. More recently, MWCNT-induced prolongation of ERK 1/2 signaling pathway in vitro was reported as a mechanism correlated with their activity on lung fibroblast proliferation and, most interestingly, with their lung fibrotic activity in vivo [34]. Taken together, these results show that in vitro responses of lung fibroblasts to CNT correlate to their pro-fibrogenic potential in vivo. Assessing the activity of CNT in fibroblast proliferation and collagen production assays may therefore contribute to refine, reduce and/or replace conventional in vivo animal tests for predicting pulmonary fibrotic responses.

Indirect effects of CNT on fibroblasts

The fibrogenic activity of inhaled particles, such as asbestos and crystalline silica, is usually ascribed to an indirect effect on fibroblasts mediated by macrophages and epithelial cells. In this section, we focus on the role of these cells in promoting, indirectly, fibroblast activation upon CNT exposure.

The role of macrophages

Macrophages are inflammatory cells involved in innate and adaptive immunity, present in alveoli as front line immune defense. Their primary role is to remove or sequester offending agents. They play an essential role in intercellular communication through the release of growth factors and cytokines promoting lung fibrosis including the pro-fibrotic growth factors PDGF and TGF- , and pro-inflammatory cytokines, such as interleukin (IL) -1 .

Macrophage recruitment and CNT phagocytosis

Traditionally, particle-induced fibrosis (asbestosis and silicosis) has been associated with sustained inflammatory recruitment and responses as a first step in fibrogenesis. Dong et al. [37] have shown a rapid infiltration of macrophages in lung tissues and alveoli after pharyngeal aspiration of CNT (40 μg/mouse, corresponding to 2 mg/kg b.w.). They observed a macrophage infiltration at day 1 post-exposure that was maintained till day 7 and then reduced but significantly higher than in controls through day 14 in both the interstitial and alveolar spaces. The early macrophage infiltration was also confirmed in other studies with an up-regulated number until day 28, accompanied by an early increase of pro-inflammatory cytokines [18, 38]. Mangum et al. [39] did not observe an inflammatory response upon SWCNT exposure (2 mg/kg rat b.w.) after 21 days, although interstitial fibrotic lesions were observed near clusters of macrophages that had engulfed aggregates of SWCNT. However, it should be noted that lung histology may not be sufficiently sensitive to exclude SWCNT-induced inflammatory responses. Interestingly, the authors observed that CNT were able to form intercellular structures that bridged alveolar macrophages at 21 days post-exposure, while these structures were not observed in the lungs of rats exposed to carbon black (CB). Rats were exposed to equivalent doses of SWCNT and CB (2 mg/kg b.w.), with similar specific surface area (about 300–600 m^2/g), thus suggesting that the intercellular structures that bridged alveolar macrophages were probably due to particle shape. How CNT bridges form and their functional consequences have yet to be determined. They observed that a major portion of CNT was engulfed by macrophages. Others papers have also observed the uptake and long-term persistence of CNT within macrophages [2, 40]. Mercer et al. [27, 28, 40] documented the presence of CNT within alveolar and interstitial macrophages and the pulmonary persistence of these particle was associated with toxicity. However, in the study of Kobayashi et al. [41], fibrotic responses were not observed, though MWCNT (0.04-1 mg/kg rat b.w.) were present in alveolar macrophages until 6 month post-exposure. Authors suggested that MWCNT were being processed and cleared by alveolar macrophages probably due to their short length (1.5 μm). It could also be due to the lower doses used compared to other studies (Table 1, 2, 3).

Collectively, these observations show that CNT interact with macrophages. We discuss below the activities of CNT on macrophages and their mechanisms of action and how this may impact on fibroblast activation, thus contributing to the indirect pro-fibrotic effects of CNT on fibroblasts as part of the AOP.

CNT activities on macrophages

Effects Macrophages can, in response to CNT, produce pro-inflammatory and pro-fibrotic mediators that play important roles in inflammation and establishment of pulmonary fibrosis. Among pro-inflammatory mediators, IL-1 has been reported to play a key role in fibrosis pathogenesis. MWCNT (25–100 μg/ml) were shown to induce the release of IL-1 and IL-18 by cultured alveolar macrophages isolated from naive C57BL/6 mice and by human monocytic cell line (THP-1), and their secretion was suppressed by inhibitors of caspase-1 and cathepsin B [42]. Several other in vitro studies observed that CNT enhanced IL-1 release in macrophages via inflammasome activation, nuclear factor-kappa B (NF-kB) and oxidative stress [13, 35, 36, 43–47], which we discuss in the mechanisms section. Moreover, IL-1 has also been shown to induce the release of the pro-fibrotic mediators TGF- and PDGF from different cell types, thus highlighting the importance of the pro-inflammatory mediators released by macrophages [13]. Tumor necrosis factor (TNF)- is also known to upregulate the expression of TGF- by epithelial cells [48]. Increased levels of TNF-

were observed in murine lung after CNT administration and secreted by macrophages after in vitro exposure to CNT [2, 38, 49, 50]. However, the role of TNF- in CNT-induced fibrosis is less well documented than for IL-1 .
Both SWCNT and MWCNT have also been shown to induce the secretion of TGF- and PDGF from macrophages in vitro and in vivo [13, 15, 38, 45, 51]. Conditioned media from macrophages exposed to CNT, in which TGF- and PDGF was measured, acted as paracrine signals on fibroblasts by inducing their activation, thus potentially contributing to the development of CNT-induced lung fibrosis [13, 15]. Recent reports also demonstrated the release of osteopontin (OPN), MMP and tissue inhibitors of matrix metalloproteinase (TIMP) by macrophages [50, 52]. The pro-fibrotic activity of OPN is known to involve proliferation and migration of fibroblasts and, like MMP and TIMP, modulation of ECM. However, evidence for the role of OPN in CNT-induced fibroblast activation is currently lacking.

Thus, we identified IL-1 , TGF- and PDGF released by macrophages as relevant paracrine signals to stimulate fibroblasts via alteration of several signal transduction pathways that may contribute to the AOP.

Mechanisms Recent studies have reported the role of inflammasome activation in inducing pulmonary inflammation and fibrosis. Inflammasome is a multiprotein oligomer that mediates activation of caspase-1 which promotes the maturation of the pro-inflammatory cytokines IL-1 and IL-18. Members of the Nod-like receptor family, including NLRP1, NLRP3 or NLRC4, and the adaptor ASC are critical components of the macrophage inflammasome. Several studies observed that CNT enhance IL-1 release by macrophages via inflammasome activation [42–46].

Nuclear factor-kappa B (NF-kB), a key mediator of inflammatory responses, is another player implicated in the release of IL-1 . He et al. [13] showed that MWCNT (2–20 μg/ml) increased the secretion of different pro-inflammatory cytokines and chemokines, such as IL-1 , TNF- , IL-6, IL-10 and MCP1, through the activation of the NF- B signaling pathway in mouse leukaemic monocyte macrophage cell line (RAW 264.7). However, authors did not provide data linking the release of pro-inflammatory mediators with the activation of NF-kB. Thus, it remains critical to elucidate the mechanisms by which CNT affect NF-kB activity and the downstream

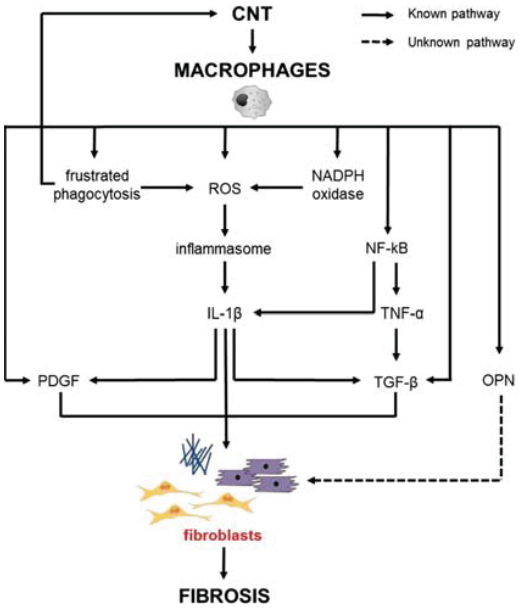


Fig. 2 Indirect effects of CNT on fibroblasts via macrophages

responses, as the release of IL-1 . Similar observations were obtained after THP-1 exposure to SWCNT (0.05 mg/ml), which led to the activation of NF-kB and the secretion of different cytokines [53].

Activation of the inflammasome and release of IL-1 have also been associated with oxidative stress induced by CNT. Nicotinamide adenine dinucleotide phosphate (NADPH) oxidase is an important regulator of inflammasome and fibrotic development in response to CNT. NADPH oxidase is a membrane-bound enzyme complex that generates superoxide by transferring electrons from NADPH and coupling these to molecular oxygen to produce superoxide anion. NADPH oxidase is composed of transmembrane ($gp91^{phox}$ and $p22^{phox}$), cytosolic ($p40^{phox}$, $p47^{phox}$ and $p67^{phox}$) and GTPase (Rac 1/2) subunits. Sun et al. [54] observed that NADPH oxidase-induced oxidative stress was involved in the generation of lung fibrosis upon MWCNT exposure, via NLRP3 inflammasome activation and IL-1 production. These responses were obtained in wild-type and $p22^{phox}$-deficient THP-1 macrophage cells, $p47^{phox}$-deficient primary bone marrow-derived macrophages and in vivo models (C57BL/6 and $p47^{phox-/-}$ C57BL/6 mice) exposed to 50 μg/ml and 50 μg/mouse (corresponding to 2.5 mg/kg b.w.) MWCNT, respectively. These data were also confirmed by treating wild type mice with NAC, a thiol antioxidant, confirming a significant reduction of IL-1 , TGF- and collagen deposition in vivo. Another study showed that long, needle-like CNT (100 μg/ml, length of about 13 μm) induced NLRP3 inflammasome activation via ROS production [43]. Thus, oxidative stress plays a role in the activation of the inflammasome by CNT and release of IL-1 , which can contribute to the induction of pro-fibrotic growth factors and fibrosis development.

Phagocytosis of CNT has also been implicated in the release of reactive species, mainly associated with frustrated phagocytosis, which is a pro-inflammatory condition [55]. This occurs when particles are physically too long for the macrophages to engulf them. CNT which undergo frustrated phagocytosis or were taken up by macrophages induced oxidative stress [56, 57]. Further studies should be conducted to investigate the direct relationship between CNT phagocytosis, oxidative stress and their impact on the release of IL-1 , for example by using endocytosis inhibitors. Moreover, frustrated phagocytosis also led to CNT biopersistence, as the clearance of inhaled material is hampered, and to the release of pro-inflammatory (IL-6 and IL-8) and pro-fibrotic mediators (TGF-) [58, 59]. These data suggest a relevant role of oxidative stress in CNT-induced IL-1 release and fibrosis development.

In conclusion and in the context of the AOP, inflammasome, NF-kB and oxidative stress induced by CNT in macrophages can be identified as important mechanisms of action since these can induce the release of pro-inflammatory and pro-fibrotic mediators regulating fibroblast activation and fibrotic responses.

Relevance of in vitro CNT activities for in vivo effects

We found fewer studies that investigated the relationship between the response of macrophages in vitro and in vivo data regarding the development of lung fibrosis, compared to the direct effect of CNT on fibroblasts. CNT able to trigger the release of IL-1 by THP-1 or alveolar macrophages in vitro were observed to induce an increase of this cytokine and collagen deposition in the alveolar region of mice [36, 45, 47, 54]. Sun et al. [54] observed the implication of NADPH oxidase in the activation of the NLRP3 inflammasome and the release of IL-1 both in vitro and in vivo and thus the development of lung fibrosis. Unfortunately, these authors have investigated only one type of MWCNT in vivo whereas several CNT were used in the in vitro tests. Thus, the relevance of these in vitro data should be confirmed with a wider range of CNT. The release of TGF- and PDGF has also been observed in a co-culture of THP-1 with human bronchial epithelial cells (BEAS-2B) exposed to CNT and associated with an increase of collagen and of these growth factors in vivo [45].

Taken together, these results suggest that the release of TGF- , PDGF and IL-1 (that can also act as autocrine signals) by macrophages exposed to CNT can act as paracrine signals for the activation of fibroblasts, supporting an indirect mechanism of CNT to activate fibroblasts, as illustrated in Fig. 2. This knowledge is used for establishing the AOP, as in vitro studies on macrophages were identified as another potentially effective model for assessing the pro-fibrogenic potential of CNT. To investigate the indirect effect of CNT on fibroblast via macrophages, TGF- , PDGF and IL-1 are relevant mediators and inflammasome, NF-kB and oxidative stress are relevant pathways.

The role of epithelial cells

The alveolar epithelium comprises two main cell types: type I and type II pneumocytes. Type I cell represents the gas exchange surface in the alveolus and cover about 97 % of the total alveolar surface area, while type II cells mainly release pulmonary surfactant to optimize conditions for gas exchange. In case of tissue injury, type I cells can be damaged, causing a loss of epithelial barrier and type II cells can i) be activated to release inflammatory mediators, ii) proliferate or differentiate in type I cells to restore the injured basement membranes, iii) undergo epithelial-mesenchymal transition (EMT) as an alternative source of fibroblasts to repair injured tissue. Also the epithelial cells in the trachea or bronchi region have a role in the pulmonary system. These cells secrete

mucus, which helps to maintain epithelial moisture and traps particulate material and pathogens moving through the airway. Several evidences show that the effect of CNT on epithelial cells can play an important role in fibrosis development. CNT can induce the indirect activation of fibroblasts via the release of pro-inflammatory and pro-fibrotic mediators by epithelial cells and, additionally, CNT have been found to induce the transformation of epithelial cells through EMT.

Epithelial surface and CNT localisation

Alveolar epithelial cells are one of the first targets of CNT once inhaled, and CNT were observed to directly interact with alveolar epithelial cells in vivo few days after particle exposure. CNT (0.6 mg/rat, corresponding to 3 mg/kg b.w.) accumulated and were taken up by epithelial cells stained positively for E-cadherin in vivo, and these data were confirmed in vitro in a rat alveolar type II cell line [24]. Mercer et al. [40] observed a rapid and direct penetration of MWCNT (80 μg/mouse, corresponding to 4 mg/kg b.w.) in type I epithelial cells only one day after mice exposure. In contrast, they rarely observed the penetration of MWCNT in type II epithelial cells. However, several in vitro studies showed the capacity of different type II epithelial cell lines to take up CNT [36, 60–62].

The above data highlight that CNT are able to rapidly enter in contact with epithelial cells, thus potentially inducing a variety of adverse effects on these cells, which can contribute to promote a fibrotic process. In the following sections we will discuss CNT activities on epithelial cells, including the process of EMT, and release of pro-inflammatory and pro-fibrotic mediators, and their impact on fibroblasts. This knowledge contributes to the development of the AOP.

CNT activities on epithelial-mesenchymal transition

Epithelial injury can lead to EMT, a process characterized by the transition of epithelial cells to mesenchymal features, by which epithelial cells lose their cell polarity and cell-cell adhesion, and gain migratory and invasive properties. EMT has been suggested to play an important role in fibrosis development, providing an alternative source of fibroblasts and causing a loss of epithelial barrier [63].

Currently, few studies have analyzed the effect of CNT on EMT and its effective role in fibrosis induced by CNT is still unclear. Chang et al. [64] showed that in vivo SWCNT exposure (80 μg/mouse, corresponding to 4 mg/kg b.w.) induced EMT of lung epithelial cells, identified by surfactant protein C (SPC) and N-cadherin (N-cad) markers. Moreover, these epithelial derived fibroblasts have been shown to produce collagen. Authors suggested that this process was induced by the activation of TGF- /p-Smad2 and -catenin in epithelial cells. Two other studies confirmed the importance of TGF- /Smad2 signaling in CNT-induced EMT [24, 65]. Chen et al. exposed mice (60 μg/mouse, corresponding to 3 mg/kg b.w.) and A549 cells (1.4–16 μg/cm^2, corresponding to 2–26 μg/ml considering a well surface area of 0.32 cm^2) to long (length 5–15 μm) and short (length 350–750 nm) MWCNT. Wang et al. tested long (length 20–50 μm) and short (0.5–2 μm) MWCNT in rats (0.6 mg/rat, corresponding to 3 mg/kg b.w.) and the rat alveolar type II cell line (RLE-6TN; 30 μg/ml). Both in vivo studies showed that only long MWCNT, but not short fibers, directly interacted with epithelial cells, were taken up by endocytosis and promoted EMT. In vitro data confirmed that only long MWCNT induced EMT through the activation of TGF- /Smad2 signaling in epithelial cells and CNT were shown to downregulate E-cadherin and upregulate -SMA, cell-cell adhesion and myofibroblast markers, respectively.

In summary, CNT-induced EMT was confirmed in different species and in epithelial cells of various origins. The mechanism of CNT-induced EMT is similar to that identified for CNT-induced fibroblast differentiation, TGF- /Smad2 signaling playing a key role in cell transformation in response to CNT. On the other hand, asbestos was found to induce EMT in A549 cells via the MAPK/ERK pathway, not associated with TGF- signaling activity [66]. Thus, CNT have been shown to increase fibroblast population via the induction of EMT.

CNT activities on epithelial cells

Effects Activation of epithelial cells after CNT exposure can result in the release of pro-inflammatory and pro-fibrotic mediators. Hussain et al. [16] demonstrated that the internalization of MWCNT (1.5–24 μg/ml) in primary human bronchial epithelial cells (HBE) induced the release of IL-1 and IL-18, which have been identified as key modulators of pro-fibrotic responses in fibroblasts, including the expression of tenascin (TN)-C (an extracellular matrix glycoprotein), TIMP-1 and OPN. Authors also observed a release of IL-8 from epithelial cells upon CNT exposure, which contributed to the expression of TN-C by fibroblasts. Sweeney et al. [67] observed a release of IL-8, and IL-6, upon exposure to MWCNT (1–50 μg/ml) in a human alveolar type-I like epithelial cell line and primary human alveolar type-II epithelial cells, showing that both type I and II cells can play an active role in pulmonary responses to CNT. Several studies showed that both SWCNT (100 μg/ml) and MWCNT (10–100 μg/ml), were able to trigger the release of TGF- from BEAS-2B cells [36, 47] that is able to stimulate fibroblasts and induce EMT. In addition, MWCNT (20 μg/ml) were found to increase the expression and protein levels of the pro-fibrogenic growth factor PDGF in BEAS-2B, as well as TGF- [13].

Another study also analyzed the impact of CNT on ciliated tracheobronchial epithelium, as these cells play a role in the clearance of inhaled particles by ciliary transport [68]. These authors showed that MWCNT with a length of 3 and 8 μm damaged the ciliated epithelium in the trachea of rats (250 μg/ml in rat, corresponding to 75 μg/rat considering that rats were treated with 0.3 ml) and mouse tracheal epithelial cells in vitro (10 μg/ml) and suggested that these lesions can prevent the clearance of inhaled CNT in the lung and thus lead to a chronic inflammatory process. Moreover, long MWCNT and SWCNT (100 μg/ml; length of 5–9 μm and 0.5–100 μm, respectively) have been shown to cause an impairment of airway epithelium barrier, as demonstrated by a decrease of the trans-epithelial electrical resistance (TEER) on human epithelial Calu-3 cells, contrary to short CNT (length 0.5–2 μm) and CB [69]. As reported by Snyder et al. [70], this reduction in barrier functions can be related to the interference of MWCNT with the cytoskeleton on lung epithelium. Further studies should investigate the effects of CNT on epithelial barrier and ciliated epithelium as this could have a role in CNT biopersistence and lung damage.

In summary, CNT stimulate the secretion of relevant pro-fibrotic and pro-inflammatory mediators, including TGF- , PDGF, IL-1 and IL-8, by epithelial cells that can indirectly promote the activation of fibroblasts and induce EMT, two relevant sources of pulmonary fibroblasts. Moreover, the loss of epithelial barrier and ciliated epithelium can contribute to CNT biopersistence, resulting in chronic damage and permanence of CNT in the lung. It necessary to note that the majority of these studies, regarding the effect of CNT on epithelial cells, have been performed on bronchial cell type, while few authors have focused on alveolar epithelial cells, which, however, represent one of the first target in CNT exposure.

Mechanisms Few studies investigated the mechanism involved in the release of pro-inflammatory and pro-fibrotic mediators by epithelial cells. Hussain et al. have demonstrated that MWCNT (1.5–24 μg/ml) activated the NLRP3 inflammasome in HBE cells and induced the release of IL-1 and IL-18. Conditioned medium from MWCNT-treated HBE added on human lung fibroblasts increased the expression of OPN, TIMP-1, pro-collagen 1 and TN-C, which were decreased in the presence of IL-1 and IL-18 antibodies and siRNA against NLRP3 inflammasome. These results point out the importance of inflammasome activation and derived mediators in epithelial cells to induce fibroblast activation.

The release of IL-6 and IL-8 has also been investigated and has been found to be associated to JNK, p38 and ERK 1/2 MAPK signaling pathways in transformed human alveolar type-I-like epithelial cells (TT1) and primary human alveolar type-II epithelial cells (ATII) cells upon MWCNT (50 μg/ml) exposure [67]. This result was further confirmed by Hirano et al. [71], who observed NF- B activation, enhanced MAP kinase phosphorylation and increased IL-6 and IL-8 release in BEAS-2B cells after MWCNT (2–10 μg/ml) exposure.

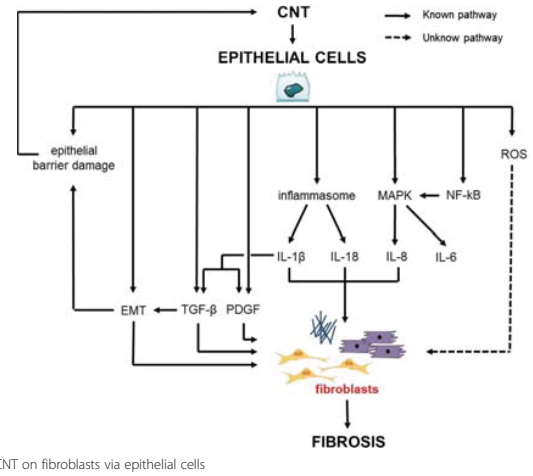


Fig. 3 Indirect effects of CNT on fibroblasts via epithelial cells

Table 4 In vitro CNT activities on fibroblast, macrophage or epithelial cell

Cell		CNT					Concentrations	Effects	Mechanisms	References
Type	Name	Type	Source	Length (m)	Diameter (nm)	Other				
Fibroblast	CRL1490	AP MWCNT D				BSA + DPPC		P		
		AP MWCNT ND				/		/		
		PD MWCNT D	CT	10–30	20–30	BSA + DPPC	5 g/ml	P	nd	[30]
		PD MWCNT ND				/		/		
		COOH MWCNT D				BSA + DPPC		/		
		COOH MWCNT ND				/		/		
Fibroblast	MLg, HFL-1,	MWCNT NM400	N	0.7–3	5–35		7.5–30 g/cm^2	P		
	BALB-3 T3,	MWCNT NM402	A	0.7–4	6–20		(12–48 g/ml)	P	nd	[23]
	PMF	MWCNT NM400c	N	0.1–0.5	18–35			/		
		MWCNTg 2400	PIH	0.7	20–50			/		
Fibroblast	MLg	MWCNT NM400	N	0.7–3	5–35		7.5–15 g/cm^2	P	KR, End, Erk 1/2	
		MWCNT long	CT	10–30	11–59		(12–24 g/ml)	P	Erk 1/2	[34]
		MWCNT short	CT	0.5–2	10–47			/		
		MWCNT thick	CT	10–30	15–74			/		
Fibroblast	NIH-3 T3	MWCNT	NP	20–50	50		15–60 g/ml	P, C, D	Smad	[24]
Fibroblast	CRL1490	SWCNT	CNI				0.02–0.24 g/cm^2	P, C, MMP-9	nd	[22]
							(0.03–0.4 g/ml)			
Fibroblast	CRL1490	SD SWCNT	CNI	0.1–1	0.8–1.2	SD	0.02 g/cm^2	C	nd	[29]
		AD SWCNT				AD	(0.03 g/ml)	C		
Fibroblast	CRL1490	SWCNT	CNI	0.1–1	0.8–1.2		5–25 g/ml	P, C, TGF-β, VEGF	ROS, p38	[14]
Fibroblast	NHLF	Short SWCNT	CT	1	11		0.02–0.2 g/cm^2	C, TGF-β	ROS	[31]
		Long SWCNT		13	11		(0.03–0.4 g/ml)	C, TGF-β		
Fibroblast	WI38-VA13	MWCNT	SA	2.5–20	6–13		1–20 g/ml	cyt, TGF-β, PDGF	ROS	[13]
Fibroblast	L929	MWCNT	SA		5.5		10–300 g/ml	cyt	ROS	[32]
Macrophage	THP-1	SWCNT	NI	1–5	0.8–1.2		50 g/ml	IL-1β	IFM, ROS, End	[54]
		MWCNT	CT	10–30	20–30			IL-1β		
Macrophage	THP-1	SWCNT BSA-AP-Hipco	NI	1000–5000	0.7–1.1	BSA coated	50–100 g/ml	IL-1β	IFM	[47]
		SWCNT BSA-PD-Hipco		500–1500	0.7–1.1	BSA coated		IL-1β	IFM	

Table 4 In vitro CNT activities on fibroblast, macrophage or epithelial cell *(Continued)*

		SWCNT PF108-Hipco		500–1500	0.7-1.1	PF108 coated		/		
		SWCNT BSA-AP-Arc		100–1000	1.2–2	BSA coated		IL-1β	nd	
		SWCNT BSA-PD-Arc		100–1000	1.2–2	BSA coated		IL-1β	nd	
		SWCNT PF108-Arc		100–1000	1.2–2	PF108 coated		/		
		SWCNT BSA-PD-SG65		450–2000	0.7–1	BSA coated		IL-1β	nd	
		SWCNT PF108-SG65		450-2000	0.7–1	PF108 coated		/		
Macrophage	THP-1	MWCNT	BNR		67		2–10 g/ml	IL-1β	IFM, ROCK, End	[46]
Macrophage	THP-1	AP MWCNT D	CT			BSA + DPPC	10–100 g/ml	IL-1β	nd	
		AP MWCNT ND	CT			/				
		PD MWCNT D	From AP	10–30	20–30	BSA + DPPC				[36]
		PD MWCNT ND	From AP			/				
		COOH MWCNT D	From AP			BSA + DPPC				
		COOH MWCNT ND	From AP			/				
Macrophage	PM, PBMC	short MWCNT	BMS	1–10	5–20			/		
		long tangled MWCNT	CT	10–50	8–15		10–100 g/ml	/		[43]
		long needle-like MWCNT (Mitsui MWCNT-7)	MC	13	>50			IL-1β, IL-	IFM, ROS, Src, Syc, P2X7 R	
Macrophage	PAM	raw MWCNT				/		IL-1β, IL-18	IFM	
	THP-1	pure MWCNT				PD		IL-1β, IL-18	IFM	
		raw MWCNT COOH	NAM			COOH F	25–100 g/ml	/		[42]
		pure MWCNT COOH				COOH F - PD		/		
Macrophage	PHM	DWCNT	PIH	0.1–100	1.2–3.2		25 g/ml	IL-1β, IL-18	IFM, End, K efflux	[44]
Macrophage	RAW 264.7	MWCNT	SA	2.5–20	6–13		2–20 g/ml	IL-1β, TNF- , IL-6, IL-10, MCP-1	NF-kB	[13]
Macrophage	THP-1, PBMC	MWCNT	HMS	0.5–40	10–30	Uncoated	10–100 g/ml	IL-1β, TNF- ,	nd	[50]
						ALD-coated		IL-6, OPN		
								IL-1β		
Macrophage	PAM	Short MWCNT	Nth	1.1	30		10 g/ml	/		[58]
		Long MWCNT		20	28			IL-6, IL-8	ROS	
Macrophage	THP-1	MWCNT AP	CT	0.57		F		IL-1β, TGF-β, PDGF		
		MWCNT NH2	From AP	0.45		F		IL-1β, TGF-β, PDGF		

Table 4 In vitro CNT activities on fibroblast, macrophage or epithelial cell *(Continued)*

		MWCNT sw-NH2	From AP	0.58		F		IL-1β, TGF-β, PDGF		
		MWCNT PEI	From AP	0.33		F	60 g/ml	IL-1β, TGF-β, PDGF	for IL-1β: IFM, End	[45]
		MWCNT PEG	From AP	0.27		F		IL-1β, TGF-β		
		MWCNT cc-PEI	From AP	0.38		F		/		
		MWCNT COOH	From AP					/		
Macrophage	RAW 264.7	SWCNT	CNI		1–4		100 g/ml	TGF-β	nd	[38]
Macrophage	RAW 264.7	Short MWCNT	NP	0.5–2	50		15 g/ml	/		[15]
		Long MWCNT		20–50	50			TGF-β, TNF-	nd	
Macrophage	NR8383	MWCNT	HMS	0.3–50	10–30		10 g/cm^2	PDGF	nd	[51]
							(16 g/ml)			
Epithelial cell	A549	Short MWCNT	SN	0.35–0.7	10–20		1–16 g/cm^2	/		[65]
		Long MWCNT		5–15	10–20		(1.6–25.6 g/ml)	EMT	TGF-β/Smad	
Epithelial cell	RLE-6TN	MWCNT	NP	20–50	50		30 g/ml	EMT	TGF-β/Smad	[24]
Epithelial cell	HBE	MWCNT	HMS	0.5–40	10–30		1.5–24 g/ml	IL-1β, IL-18	IFM, ROS	[16]
								IL-8		
Epithelial cell	BEAS-2B	MWCNT	BNR		67		1–10 g/ml	IL-6, IL-8, MIF	NF-kB, p38,	[71]
									ERK 1/2, HSP27	
Epithelial cell	TT1, ATII	MWCNT 0.6 m	Nth	1.1	30			IL-6, IL-8, MCP-1		
		MWCNT 3 m		4.3	33		1–50 g/ml	IL-8, MCP-1	JNK, p38, ERK 1/2	[67]
		MWCNT 20 m		20	28			MCP-1		
Epithelial cell	BEAS-2B	SWCNT BSA-AP-Hipco	NI	1000–5000	0.7–1.1	BSA coated		TGF-β		
		SWCNT BSA-PD-Hipco		500–1500	0.7–1.1	BSA coated		TGF-β		
		SWCNT PF108-Hipco		500–1500	0.7–1.1	PF108 coated		/		
		SWCNT BSA-AP-Arc		100–1000	1.2–2	BSA coated	100 g/ml	TGF-β	nd	[47]
		SWCNT BSA-PD-Arc		100–1000	1.2–2	BSA coated		TGF-β		
		SWCNT PF108-Arc		100–1000	1.2–2	PF108 coated		TGF-β		
		SWCNT BSA-PD-SG65		450–2000	0.7–1	BSA coated		TGF-β		
		SWCNT PF108-SG65		450–2000	0.7–1	PF108 coated		/		
Epithelial cell	BEAS-2B	AP MWCNT D	CT	10–30	20–30	BSA + DPPC	10–100 g/ml	TGF-β		[36]
		AP MWCNT ND	CT			/		/		
		PD MWCNT D	From AP			BSA + DPPC		TGF-β		

Table 4 In vitro CNT activities on fibroblast, macrophage or epithelial cell *(Continued)*

		PD MWCNT ND	From AP			/			/	nd	
		COOH MWCNT D	From AP			BSA + DPPC			Few TGF-β		
		COOH MWCNT ND	From AP			/			Few TGF-β		
Epithelial cell	BEAS-2B	MWCNT	SA	2.5–20	6–13		2–200	g/ml	TGF-β, PDGF	ROS	[13]

nd: not determined. *Cell name:* A549: human lung adenocarcinoma alveolar epithelial cell line; ATII: primary human alveolar type-II epithelial cells; BALB-3 T3: mouse embryonic fibroblast cell line; BEAS-2B: human bronchial epithelial cell line; CRL1490: human lung fibroblast cell line; HBE: primary human bronchial epithelial cells; HFL-1: human lung fibroblast cell line; L929: mouse fibroblast cell line; MLg: mouse lung fibroblast cell line; NHLF: normal human lung fibroblast cell line; NIH-3 T3: mouse embryonic fibroblast cell line; NR8383: rat alveolar macrophage cell line; PAM: primary alveolar macrophages; PBMC: peripherial blood mononuclear cells; PHM: primary human monocytes; PMF: primary mouse fibroblasts; RAW 264.7: mouse leukemic monocyte macrophage cell line; RLE-6TN: rat alveolar type II epithelial cell line; THP-1: human leukemia monocytic cell line; TT1: transformed human alveolar type-I-like epithelial cells; WI38-VA13: human normal lung fibroblast cell line immortalized with SV40. *CNT type:* AP: as prepared; COOH: carboxyl; NH2: amino; PD: purified. Source: A: Arkema (France); BMS: Bayer Material Science (Leverkusen, Germany); BNR: Bussan Nanotech Research (Ibaraki, Japan); CNI: Carbon Nanotechnologies Inc. (Houston, TX); CT: Cheap Tubes (Brattlebore, VT); HMS : Helix Materials Solution (Richardson, TX); MC: Mitsui & Company (Tokio, Japan); N: Nanocyl (Sambreville, Belgium); NAM: Nanostructured & Amorphous Materials Inc. (Houston, TX); NI: NanoIntegris (Skokie, IL); NP: Nanotech Port (Chengdu, China); Nth: Nanothinx (Rio Patras, Greece); PIH: produced in house; SA: Sigma-Aldrich (Lyon, France); SN: Shenzhen Nanoharbor (Shenzhen, China). *Other:* AD: acetone/sonication dispersed; BSA: bovine serum albumin; cc-PEI: carboxyl converted PEI; D: dispersed; DPPC: dipalmitoylphosphatidylcholine; F: functionalized; ND: no dispersed; PEG: polyethylene glycol; PEI: polyethyleneimine; PF108: Pluronic F108; SD: survanta dispersed; swNH2: sidewall amine. *Effects:* C: collagen; cyt: cytotoxic; D: differentiation of fibroblasts into myofibroblasts; EMT: epithelial mesenchymal transition; IL: interleukin; MCP: monocyte chemoattractant protein; MIF: migration inhibitory factor; MMP-9: matrix metallopeptidase 9; OPN: osteopontin; P: proliferation; PDGF: platelet derived growth factor; TGF: transforming growth factor; TNF: tumor necrosis factor; VEGF: vascular endothelial growth factor. *Mechanisms:* End: endocytosis; ERK 1/2: extracellular signal-regulated kinase; HSP27: heat shock protein 27; IFM: inflammasome; JNK: c-Jun N-terminal kinase; K: potassium; KR: kinase receptor; NF-kB: nuclear factor-kappa B; ROCK: Rho-kinases; ROS: reactive oxygen species

Signs of oxidative stress have also been observed in epithelial cells and several studies reported free radical formation and antioxidant depletion in this cell system after CNT exposure [60, 61, 72–74]. Interestingly, Nymark et al. [75], observed the formation of a unique and yet unidentified radical in both absence and presence of BEAS-2B by two types of long MWCNT (average of lengths 4 and 6 μm). However, contrary to macrophages, there is no evidence of a correlation between oxidative stress and the release of pro-inflammatory mediators. Additional analysis showed that early intracellular uptake of MWCNT (length 1–5 μm; 24 μg/cm^2 corresponding to 38 μg/ml, considering a well surface area of 0.32 cm^2) in BEAS-2B correlated with the generation of ROS measured by DCF-DA [37]. Authors suggested that this can lead to different variations in the cellular homeostasis, including cell proliferation, differentiation and motility. SWCNT and MWCNT induced epithelial cell proliferation [29, 34]. However it is still not possible to determine whether this effect is related to CNT-induced ROS and more studies have to be carried out to understand the mechanisms. Moreover, Hussain et al. [16] showed that CNT-induced ROS were also associated to cytotoxic effects as these authors observed a reduction of human bronchial epithelial death after antioxidant treatment.

Regarding the indirect effect of CNT on fibroblasts via epithelial cells, inflammasome, NF- B and oxidative stress appear as mechanisms altering signal transduction pathways, as previously indicated for macrophages, by inducing the release of different mediators able to activate fibroblasts.

Relevance of in vitro CNT activities for in vivo effects

As for macrophages, few studies investigated the correlation between in vitro and in vivo results regarding the development of fibrosis via epithelial cells. Two studies observed a good correlation between the release of the pro-fibrogenic TGF- from BEAS-2B exposed to CNT in vitro and the induction of a fibrotic response in vivo [36, 47]. Moreover, CNT-induced EMT in vitro correlated with in vivo studies, suggesting that some fibroblasts involved in the lung fibrosis originate from epithelial cells. Further investigation is, however, required to understand the critical role of epithelial cells in fibrosis.

For the AOP we identify the release of TGF- from epithelial cells as a key mediator of the indirect effect of CNT on fibroblasts via epithelial cells. However, other relevant mediators, PDGF, IL-1 and IL-8, and pathways, such as inflammasome, NF-kB and oxidative stress, have been shown in vitro to play a role in the complex fibrotic process. Collectively, these data are summarized in Fig. 3.

Determinants of the fibrotic activities of CNT

Physico-chemical properties of CNT appear to determine their capacity to induce fibroblast, macrophages and epithelial cell activation. The length has been

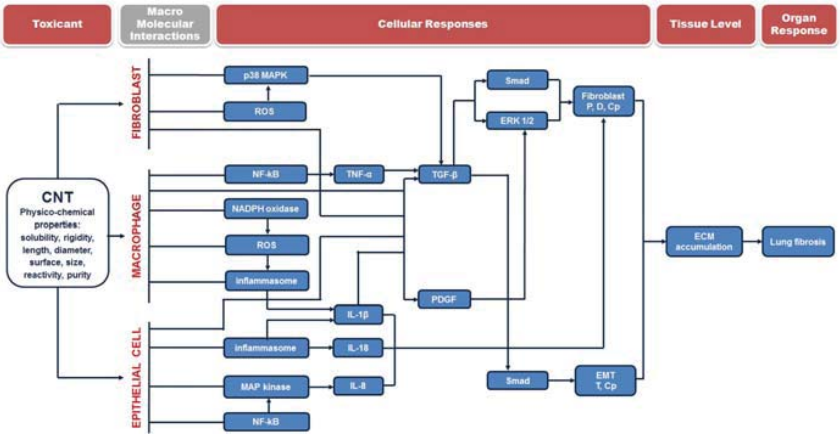


Fig. 4 AOP for CNT and lung fibrosis. Legend: Cp: collagen production; D: differentiation; P: proliferation; T: transition in fibroblasts

identified as an important factor. Manke et al. [31] showed that long SWCNT (13 μm) were more potent than short SWCNT (1 μm) to elicit a ROS response, collagen production and TGF- release by fibroblasts in vitro as well as to induce fibrosis in vivo. Several studies confirmed that the length of CNT constitutes an important determinant in the capacity of these materials to induce the activation of fibroblasts and lung fibrosis [24, 34]. Regarding macrophages, Wang et al. [15] showed that only long MWCNT (0.6 mg/rat, corresponding to 3 mg/kg b.w.; length 20–50 μm and diameter 50 nm) stimulated the release of TGF- in vivo, as measured by immunohistochemistry, contrary to short CNT (length 0.5-2 μm and diameter 50 nm). Long MWCNT (10 μg/ml; length 20 μm), but not short fibers (length 0.6 μm), were also shown to affect alveolar macrophage function, including cell death, ROS generation and pro-inflammatory (IL-6 and IL-8) mediator release [58]. A stronger ROS generation was also observed in A549 epithelial cells exposed to long CNT (length 5–30 μm; doses 5–20 μg/ml) compared to short fiber (length 0.5–2 μm) [76]. Poland et al. [3] reported frustrated phagocytosis in the peritoneal lavage of mice exposed to long MWCNT (50 μg/mouse, corresponding to 2.5 mg/kg b.w.), whereas short and tangled MWCNT were completely phagocytosed by macrophages. An accelerated rate of clearance of short CNT by macrophages has been reported, suggesting that these particles could be taken up by inflammatory cells leading to their translocation from the lung and, possibly, biodegradation, while long CNT seem to be biopersistent [77, 78]. Long MWCNT and SWCNT (length of 5–9 μm and 0.5–100 μm, respectively) have been shown to cause an impairment of airway epithelium barrier contrary to short particles. However, short MWCNT (length 0.6 μm) were shown to induce greater IL-6, IL-8 and MCP-1 levels than long MWCNT (length 20 μm) in TT1 and ATII cells [67].

CNT diameter also appeared critical since CNT with a thin diameter have been shown to stimulate fibroblast proliferation and to induce fibrosis compared to CNT with a thicker diameter [34].

The presence of residual metals from the synthesis of CNT has been shown to be associated to oxidative stress. Aldieri et al. [79] observed that only Fe-rich MWCNT were significantly cytotoxic and genotoxic in murine alveolar macrophages and induced a severe oxidative stress, contrary to the Fe-free MWCNT, suggesting that metals can be important factors in promoting CNT-induced toxicity. These data were further confirmed in another study, in which two types of SWCNT with different iron content, 26 wt. % and 0.23 wt. % (0.12–0.5 mg/ml), generated different amount of hydroxyl radicals in RAW 264.7 macrophages, confirming that iron can act as a catalyst of oxidative stress [80].

Finally, CNT dispersion was also found as another critical factor. Several evidences show that well dispersed CNT stimulate proliferation and collagen production by lung fibroblasts [29, 30], induce the release of IL-1 from macrophages [13, 35, 36, 43–47] and TGF- from epithelial cells [36, 47], compared to not dispersed CNT. The extent and localization of CNT and inflammatory cells in the lung was also related to the particle dispersion and agglomeration state before administration. Agglomerated CNT form granulomatous inflammation and fibrosis in larger airways, while, in general, well-dispersed CNT are able to penetrate alveoli and interstitial space leading to alveolar fibrosis, as discussed in the section on fibroblasts [15, 28, 29, 81].

Conclusion

The observations summarized in this review highlight indirect and direct effects of CNT on fibroblasts, which both contribute to their fibrogenic activity on the lung. In vitro studies indicate that a dose range of CNT between 1 and 100 μg/ml induced effects on the different cell types, as shown in Table 4, which summarizes in vitro data reported in this review. The dose range used in in vivo experiments (10–100 μg/mouse, corresponding to 0.5–5 mg/kg) is relevant for human exposure scenari, following the approach suggested by Porter et al. [82], and shown to exert a fibrotic activity in the lung of experimental animals. We propose in Fig. 4 a linear flow diagram based on an AOP structure describing the processes by which CNT have been shown to lead to fibroblast activation and pulmonary fibrosis. Physico-chemical properties of CNT, such as length and diameter are relevant for their fibrogenic activity. Therefore, an accurate analysis of these characteristics can already suggest whether a material may have or not a pro-fibrotic activity. The exact macromolecular interactions (MMI) between CNT and cells have currently not been identified and we can only hypothesize that this probably occurs at the surface of membranes in fibroblasts, macrophages and epithelial cells. CNT have been observed to induce several cellular responses, which can be stratified according to 5 levels: i) initial signaling, ii) pro-inflammatory mediators, iii) pro-fibrotic mediators, iv) distal signaling in response to mediators and finally v) activation of key cells in fibrosis (fibroblasts and epithelial cells for EMT). ROS, MAPK, NF-kB, NADPH oxidase and inflammasome have been identified as the most important initial signals, with some differences depending on the cell type. Only macrophages and epithelial cells have been observed to release pro-inflammatory mediators with pro-fibrotic activities (IL-1 , IL-18, IL-8 and TNF-) upon exposure to CNT. IL-1 seems to play a major role by promoting the secretion of pro-fibrotic mediators. PDGF and TGF- can also be released directly from fibroblasts, macrophages or epithelial

cells after CNT exposure and have been shown to activate the second signaling (ERK1/2 and Smad). Additionally, CNT prolonge ERK 1/2 activation in fibroblasts exposed to PDGF. ERK 1/2 and Smad phosphorylation was also prolonged by CNT in presence of TGF- . ERK 1/2 and Smad signalings stimulated fibroblast proliferation, while Smad can also increase fibroblast differentiation, promote EMT and increase collagen production. This sequence of key events eventually causes collagen accumulation and ECM alteration and leads to the development of lung fibrosis.

These data will be useful to guide researchers to focus on relevant mechanisms of action induced by CNT, or to investigate underlined knowledge gaps. The proposed AOP can help proposing or developing simple and fast test methods for predicting the potential hazard of CNT. Most importantly, it will help identifying how a mechanistic information obtained from one specific assay contributes to obtaining a global picture of the fibrogenic activity of a test sample.

Abbreviations

A549: human lung adenocarcinoma epithelial cell line; AM: alveolar macrophages; AO: adverse outcome; AOP: adverse outcome pathway; ATII: primary human alveolar type-II epithelial cells; BEAS-2B: bronchial epithelial cells; BEAS-2B: human bronchial epithelial cells; BSA: bovine serum albumin; CB: carbon black; CNT: carbon nanotube; CRL-1490: human lung fibroblast; DCFH-DA: dichlorodihydrofluorescein diacetate; DHE: dihydroethidium; ECM: extracellular matrix; EGF: epidermal growth factor; EMT: epithelial-mesenchymal transition; EPR: electron spin resonance; FBS: foetal bovine serum; FESEM: field emission electron microscopy; FSP: fibroblast specific marker; GSH: glutathione; HBE: human bronchial epithelial cells; IL: interleukin; MIE: molecular initial event; MLg: mouse lung fibroblast; MMI: macro-molecular interactions; MMP: matrix metalloproteinases; MW: multi walled; NAC: N-acetyl cysteine; NADPH: nicotinamide adenine dinucleotide phosphate; N-cad: N-cadherin; NF-kB: nuclear factor-kappa B; NHLF: normal human lung fibroblasts; NIOSH: National Institute for Occupational Safety and Health; OPN: osteopontin; PDGF: platelet-derived growth factor; PMN: polymorphonuclear neutrophils; RAW 264.7: mouse leukaemic monocyte macrophage cell line; REL: reccomended exposure limit; RLE-6TN: rat alveolar type II cell line; ROS: reactive oxygen species; SMA: smooth muscle actin; SPC: surfactant protein C; SW: single walled; TBARS: thiobarbituric reactive substances; TEER: trans-epithelial electrical resistance; TGF: transforming growth factor; THP-1: human monocytic cell line; TIMP: tissue inhibitors of matrix metalloproteinase; TN: tenascin; TNF: tumor necrosis factor; TT1: transformed human alveolar type-I-like epithelial cells; VEGF: vascular endothelial growth factor.

Competing interests

The authors declare that they have no competing interests.

Authors' contributions

GV drafted and designed the manuscript. DL and SV revised the manuscript. All authors read and approved the final manuscript.

Funding

Giulia Vietti is a Research Fellow of the Fonds de la Recherche Scientifique (FNRS), Belgium.

Received: 18 November 2015 Accepted: 12 February 2016
Published online: 29 February 2016

References

1. Donaldson K, Poland CA, Murphy FA, MacFarlane M, Chernova T, Schinwald A. Pulmonary toxicity of carbon nanotubes and asbestos - similarities and differences. Adv Drug Deliv Rev. 2013;65:2078–86.
2. Muller J, Huaux F, Moreau N, Misson P, Heilier JF, Delos M, Arras M, Fonseca A, Nagy JB, Lison D. Respiratory toxicity of multi-wall carbon nanotubes. Toxicol Appl Pharmacol. 2005;207:221–31.
3. Poland CA, Duffin R, Kinloch I, Maynard A, Wallace WA, Seaton A, Stone V, Brown S, Macnee W, Donaldson K. Carbon nanotubes introduced into the abdominal cavity of mice show asbestos-like pathogenicity in a pilot study. Nat Nanotechnol. 2008;3:423–8.
4. Xu J, Futakuchi M, Shimizu H, Alexander DB, Yanagihara K, Fukamachi K, Suzui M, Kanno J, Hirose A, Ogata A, et al. Multi-walled carbon nanotubes translocate into the pleural cavity and induce visceral mesothelial proliferation in rats. Cancer Sci. 2012;103:2045–50.
5. Nagai H, Okazaki Y, Chew SH, Misawa N, Yamashita Y, Akatsuka S, Ishihara T, Yamashita K, Yoshikawa Y, Yasui H, et al. Diameter and rigidity of multiwalled carbon nanotubes are critical factors in mesothelial injury and carcinogenesis. Proc Natl Acad Sci U S A. 2011;108:E1330–1338.
6. Rittinghausen S, Hackbarth A, Creutzenberg O, Ernst H, Heinrich U, Leonhardt A, Schaudien D. The carcinogenic effect of various multi-walled carbon nanotubes (MWCNTs) after intraperitoneal injection in rats. Part Fibre Toxicol. 2014;11:59.
7. Sargent LM, Porter DW, Staska LM, Hubbs AF, Lowry DT, Battelli L, Siegrist KJ, Kashon ML, Mercer RR, Bauer AK, et al. Promotion of lung adenocarcinoma following inhalation exposure to multi-walled carbon nanotubes. Part Fibre Toxicol. 2014;11:3.
8. NIOSH D. Current Intelligence Bulletin 65: Occupational Exposure to Carbon Nanotubes and Nanofibers. vol. 145; 2013.
9. Ankley GT, Bennett RS, Erickson RJ, Hoff DJ, Hornung MW, Johnson RD, Mount DR, Nichols JW, Russom CL, Schmieder PK, et al. Adverse outcome pathways: a conceptual framework to support ecotoxicology research and risk assessment. Environ Toxicol Chem. 2010;29:730–41.
10. Wynn TA. Integrating mechanisms of pulmonary fibrosis. J Exp Med. 2011;208:1339–50.
11. Sanchez VC, Pietruska JR, Miselis NR, Hurt RH, Kane AB. Biopersistence and potential adverse health impacts of fibrous nanomaterials: what have we learned from asbestos? Wiley Interdiscip Rev Nanomed Nanobiotechnol. 2009;1:511–29.
12. Manke A, Wang L, Rojanasakul Y. Pulmonary toxicity and fibrogenic response of carbon nanotubes. Toxicol Mech Methods. 2013;23:196–206.
13. He X, Young SH, Schwegler-Berry D, Chisholm WP, Fernback JE, Ma Q. Multiwalled carbon nanotubes induce a fibrogenic response by stimulating reactive oxygen species production, activating NF-kappaB signaling, and promoting fibroblast-to-myofibroblast transformation. Chem Res Toxicol. 2011;24:2237–48.
14. Azad N, Iyer AK, Wang L, Liu Y, Lu Y, Rojanasakul Y. Reactive oxygen species-mediated p38 MAPK regulates carbon nanotube-induced fibrogenic and angiogenic responses. Nanotoxicology. 2013;7:157–68.
15. Wang P, Nie X, Wang Y, Li Y, Ge C, Zhang L, Wang L, Bai R, Chen Z, Zhao Y, Chen C. Multiwall Carbon Nanotubes Mediate Macrophage Activation and Promote Pulmonary Fibrosis Through TGF-beta/Smad Signaling Pathway. Small. 2013
16. Hussain S, Sangtian S, Anderson SM, Snyder RJ, Marshburn JD, Rice AB, Bonner JC, Garantziotis S. Inflammasome activation in airway epithelial cells after multi-walled carbon nanotube exposure mediates a profibrotic response in lung fibroblasts. Part Fibre Toxicol. 2014;11:28.
17. Shvedova AA, Kisin ER, Murray AR, Kommineni C, Castranova V, Fadeel B, Kagan VE. Increased accumulation of neutrophils and decreased fibrosis in the lung of NADPH oxidase-deficient C57BL/6 mice exposed to carbon nanotubes. Toxicol Appl Pharmacol. 2008;231:235–40.
18. Park EJ, Roh J, Kim SN, Kang MS, Han YA, Kim Y, Hong JT, Choi K. A single intratracheal instillation of single-walled carbon nanotubes induced early lung fibrosis and subchronic tissue damage in mice. Arch Toxicol. 2011;85:1121–31.
19. Murray AR, Kisin ER, Tkach AV, Yanamala N, Mercer R, Young SH, Fadeel B, Kagan VE, Shvedova AA. Factoring-in agglomeration of carbon nanotubes and nanofibers for better prediction of their toxicity versus asbestos. Part Fibre Toxicol. 2012;9:10.
20. Snyder-Talkington BN, Dong C, Zhao X, Dymacek J, Porter DW, Wolfarth MG, Castranova V, Qian Y, Guo NL. Multi-walled carbon nanotube-induced gene expression in vitro: concordance with in vivo studies. Toxicology. 2015;328:66–74.
21. Katwa P, Wang X, Urankar RN, Podila R, Hilderbrand SC, Fick RB, Rao AM, Ke PC, Wingard CJ, Brown JM. A carbon nanotube toxicity paradigm driven by mast cells and the IL-(3)(3)/ST(2) axis. Small. 2012;8:2904–12.

22. Wang L, Mercer RR, Rojanasakul Y, Qiu A, Lu Y, Scabilloni JF, Wu N, Castranova V. Direct fibrogenic effects of dispersed single-walled carbon nanotubes on human lung fibroblasts. J Toxicol Environ Health A. 2010;73:410–22.
23. Vietti G, Ibouraadaten S, Palmai-Pallag M, Yakoub Y, Bailly C, Fenoglio I, Marbaix E, Lison D, van den Brule S. Towards predicting the lung fibrogenic activity of nanomaterials: experimental validation of an in vitro fibroblast proliferation assay. Part Fibre Toxicol. 2013;10:52.
24. Wang P, Wang Y, Nie X, Braini C, Bai R, Chen C. Multiwall Carbon Nanotubes Directly Promote Fibroblast-Myofibroblast and Epithelial-Mesenchymal Transitions through the Activation of the TGF-beta/Smad Signaling Pathway. Small. 2015;11:446–55.
25. Lasky JA, Coin PG, Lindroos PM, Ostrowski LE, Brody AR, Bonner JC. Chrysotile asbestos stimulates platelet-derived growth factor-AA production by rat lung fibroblasts in vitro: evidence for an autocrine loop. Am J Respir Cell Mol Biol. 1995;12:162–70.
26. Mercer RR, Hubbs AF, Scabilloni JF, Wang L, Battelli LA, Friend S, Castranova V, Porter DW. Pulmonary fibrotic response to aspiration of multi-walled carbon nanotubes. Part Fibre Toxicol. 2011;8:21.
27. Mercer RR, Scabilloni JF, Hubbs AF, Battelli LA, McKinney W, Friend S, Wolfarth MG, Andrew M, Castranova V, Porter DW. Distribution and fibrotic response following inhalation exposure to multi-walled carbon nanotubes. Part Fibre Toxicol. 2013;10:33.
28. Mercer RR, Scabilloni J, Wang L, Kisin E, Murray AR, Schwegler-Berry D, Shvedova AA, Castranova V. Alteration of deposition pattern and pulmonary response as a result of improved dispersion of aspirated single-walled carbon nanotubes in a mouse model. Am J Physiol Lung Cell Mol Physiol. 2008;294:L87–97.
29. Wang L, Castranova V, Mishra A, Chen B, Mercer RR, Schwegler-Berry D, Rojanasakul Y. Dispersion of single-walled carbon nanotubes by a natural lung surfactant for pulmonary in vitro and in vivo toxicity studies. Part Fibre Toxicol. 2010;7:31.
30. Wang X, Xia T, Ntim SA, Ji Z, George S, Meng H, Zhang H, Castranova V, Mitra S, Nel AE. Quantitative techniques for assessing and controlling the dispersion and biological effects of multiwalled carbon nanotubes in mammalian tissue culture cells. ACS Nano. 2010;4:7241–52.
31. Manke A, Luanpitpong S, Dong C, Wang L, He X, Battelli L, Derk R, Stueckle TA, Porter DW, Sager T, et al. Effect of fiber length on carbon nanotube-induced fibrogenesis. Int J Mol Sci. 2014;15:7444–61.
32. Alarifi S, Ali D. Mechanisms of Multi-walled Carbon Nanotubes-Induced Oxidative Stress and Genotoxicity in Mouse Fibroblast Cells. Int J Toxicol. 2015;34:258–65.
33. Yang H, Liu C, Yang D, Zhang H, Xi Z. Comparative study of cytotoxicity, oxidative stress and genotoxicity induced by four typical nanomaterials: the role of particle size, shape and composition. J Appl Toxicol. 2009;29:69–78.
34. Vietti G, Ibouraadaten S, Palmai-Pallag M, Yakoub Y, Piret JP, Marbaix E, Lison D, van den Brule S. Towards predicting the lung fibrogenic activity of MWCNT: Key role of endocytosis, kinase receptors and ERK 1/2 signaling. Nanotoxicology. 2015;7:1–13
35. Taylor ES, Wylie AG, Mossman BT, Lower SK. Repetitive dissociation from crocidolite asbestos acts as persistent signal for epidermal growth factor receptor. Langmuir. 2013;29:6323–30.
36. Wang X, Xia T, Ntim SA, Ji Z, Lin S, Meng H, Chung CH, George S, Zhang H, Wang M, et al. Dispersal state of multiwalled carbon nanotubes elicits profibrogenic cellular responses that correlate with fibrogenesis biomarkers and fibrosis in the murine lung. ACS Nano. 2011;5:9772–87.
37. Dong J, Porter DW, Batteli LA, Wolfarth MG, Richardson DL, Ma Q. Pathologic and molecular profiling of rapid-onset fibrosis and inflammation induced by multi-walled carbon nanotubes. Arch Toxicol. 2015;89:621–33.
38. Shvedova AA, Kisin ER, Mercer R, Murray AR, Johnson VJ, Potapovich AI, Tyurina YY, Gorelik O, Arepalli S, Schwegler-Berry D, et al. Unusual inflammatory and fibrogenic pulmonary responses to single-walled carbon nanotubes in mice. Am J Physiol Lung Cell Mol Physiol. 2005;289:L698–708.
39. Mangum JB, Turpin EA, Antao-Menezes A, Cesta MF, Bermudez E, Bonner JC. Single-walled carbon nanotube (SWCNT)-induced interstitial fibrosis in the lungs of rats is associated with increased levels of PDGF mRNA and the formation of unique intercellular carbon structures that bridge alveolar macrophages in situ. Part Fibre Toxicol. 2006;3:15.
40. Mercer RR, Hubbs AF, Scabilloni JF, Wang L, Battelli LA, Schwegler-Berry D, Castranova V, Porter DW. Distribution and persistence of pleural penetrations by multi-walled carbon nanotubes. Part Fibre Toxicol. 2010;7:28.
41. Kobayashi N, Naya M, Ema M, Endoh S, Maru J, Mizuno K, Nakanishi J. Biological response and morphological assessment of individually dispersed multi-wall carbon nanotubes in the lung after intratracheal instillation in rats. Toxicology. 2010;276:143–53.
42. Hamilton Jr RF, Xiang C, Li M, Ka I, Yang F, Ma D, Porter DW, Wu N, Holian A. Purification and sidewall functionalization of multiwalled carbon nanotubes and resulting bioactivity in two macrophage models. Inhal Toxicol. 2013;25:199–210.
43. Palomaki J, Valimaki E, Sund J, Vippola M, Clausen PA, Jensen KA, Savolainen K, Matikainen S, Alenius H. Long, needle-like carbon nanotubes and asbestos activate the NLRP3 inflammasome through a similar mechanism. ACS Nano. 2011;5:6861–70.
44. Meunier E, Coste A, Olagnier D, Authier H, Lefevre L, Dardenne C, Bernad J, Beraud M, Flahaut E, Pipy B. Double-walled carbon nanotubes trigger IL-1beta release in human monocytes through Nlrp3 inflammasome activation. Nanomedicine. 2012;8:987–95.
45. Li R, Wang X, Ji Z, Sun B, Zhang H, Chang CH, Lin S, Meng H, Liao YP, Wang M, et al. Surface charge and cellular processing of covalently functionalized multiwall carbon nanotubes determine pulmonary toxicity. ACS Nano. 2013;7:2352–68.
46. Kanno S, Hirano S, Chiba S, Takeshita H, Nagai T, Takada M, Sakamoto K, Mukai T. The role of Rho-kinases in IL-1beta release through phagocytosis of fibrous particles in human monocytes. Arch Toxicol. 2015;89:73–85.
47. Wang X, Duch MC, Mansukhani N, Ji Z, Liao YP, Wang M, Zhang H, Sun B, Chang CH, Li R, et al. Use of a pro-fibrogenic mechanism-based predictive toxicological approach for tiered testing and decision analysis of carbonaceous nanomaterials. ACS Nano. 2015;9:3032–43.
48. Warshamana GS, Corti M, Brody AR. TNF-alpha, PDGF, and TGF-beta(1) expression by primary mouse bronchiolar-alveolar epithelial and mesenchymal cells: tnf-alpha induces TGF-beta(1). Exp Mol Pathol. 2001;71:13–33.
49. Di Giorgio ML, Di Bucchianico S, Ragnelli AM, Aimola P, Santucci S, Poma A. Effects of single and multi walled carbon nanotubes on macrophages: cyto and genotoxicity and electron microscopy. Mutat Res. 2011;722:20–31.
50. Taylor AJ, McClure CD, Shipkowski KA, Thompson EA, Hussain S, Garantziotis S, Parsons GN, Bonner JC. Atomic layer deposition coating of carbon nanotubes with aluminum oxide alters pro-fibrogenic cytokine expression by human mononuclear phagocytes in vitro and reduces lung fibrosis in mice in vivo. PLoS One. 2014;9:e106870.
51. Cesta MF, Ryman-Rasmussen JP, Wallace DG, Masinde T, Hurlburt G, Taylor AJ, Bonner JC. Bacterial lipopolysaccharide enhances PDGF signaling and pulmonary fibrosis in rats exposed to carbon nanotubes. Am J Respir Cell Mol Biol. 2010;43:142–51.
52. van Berlo D, Wilhelmi V, Boots AW, Hullmann M, Kuhlbusch TA, Bast A, Schins RP, Albrecht C. Apoptotic, inflammatory, and fibrogenic effects of two different types of multi-walled carbon nanotubes in mouse lung. Arch Toxicol. 2014;88:1725–37.
53. Chou CC, Hsiao HY, Hong QS, Chen CH, Peng YW, Chen HW, Yang PC. Single-walled carbon nanotubes can induce pulmonary injury in mouse model. Nano Lett. 2008;8:437–45.
54. Sun B, Wang X, Ji Z, Wang M, Liao YP, Chang CH, Li R, Zhang H, Nel AE, Xia T. NADPH Oxidase-Dependent NLRP3 Inflammasome Activation and its Important Role in Lung Fibrosis by Multiwalled Carbon Nanotubes. Small. 2015;11:2087–97.
55. Donaldson K, Murphy FA, Duffin R, Poland CA. Asbestos, carbon nanotubes and the pleural mesothelium: a review of the hypothesis regarding the role of long fibre retention in the parietal pleura, inflammation and mesothelioma. Part Fibre Toxicol. 2010;7:5.
56. Rothen-Rutishauser B, Brown DM, Piallier-Boyles M, Kinloch IA, Windle AH, Gehr P, Stone V. Relating the physicochemical characteristics and dispersion of multiwalled carbon nanotubes in different suspension media to their oxidative reactivity in vitro and inflammation in vivo. Nanotoxicology. 2010;4:331–42.
57. Fenoglio I, Aldieri E, Gazzano E, Cesano F, Colonna M, Scarano D, Mazzucco G, Attanasio A, Yakoub Y, Lison D, Fubini B. Thickness of multiwalled carbon nanotubes affects their lung toxicity. Chem Res Toxicol. 2012;25:74–82.
58. Sweeney S, Grandolfo D, Ruenraroengsak P, Tetley TD. Functional consequences for primary human alveolar macrophages following treatment with long, but not short, multiwalled carbon nanotubes. Int J Nanomedicine. 2015;10:3115–29.
59. Boyles MS, Young L, Brown DM, MacCalman L, Cowie H, Moisala A, Smail F, Smith PJ, Proudfoot L, Windle AH, Stone V. Multi-walled carbon nanotube induced frustrated phagocytosis, cytotoxicity and pro-inflammatory

conditions in macrophages are length dependent and greater than that of asbestos. Toxicol In Vitro. 2015;29:1513–28.
60. Snyder-Talkington BN, Pacurari M, Dong C, Leonard SS, Schwegler-Berry D, Castranova V, Qian Y, Guo NL. Systematic analysis of multiwalled carbon nanotube-induced cellular signaling and gene expression in human small airway epithelial cells. Toxicol Sci. 2013;133:79–89.
61. Visalli G, Bertuccio MP, Iannazzo D, Piperno A, Pistone A, Di Pietro A. Toxicological assessment of multi-walled carbon nanotubes on A549 human lung epithelial cells. Toxicol In Vitro. 2015;29:352–62.
62. Maruyama K, Haniu H, Saito N, Matsuda Y, Tsukahara T, Kobayashi S, Tanaka M, Aoki K, Takanashi S, Okamoto M, Kato H. Endocytosis of Multiwalled Carbon Nanotubes in Bronchial Epithelial and Mesothelial Cells. Biomed Res Int. 2015;2015:793186.
63. Kalluri R, Weinberg RA. The basics of epithelial-mesenchymal transition. J Clin Invest. 2009;119:1420–8.
64. Chang CC, Tsai ML, Huang HC, Chen CY, Dai SX. Epithelial-mesenchymal transition contributes to SWCNT-induced pulmonary fibrosis. Nanotoxicology. 2012;6:600–10.
65. Chen T, Nie H, Gao X, Yang J, Pu J, Chen Z, Cui X, Wang Y, Wang H, Jia G. Epithelial-mesenchymal transition involved in pulmonary fibrosis induced by multi-walled carbon nanotubes via TGF-beta/Smad signaling pathway. Toxicol Lett. 2014;226:150–62.
66. Tamminen JA, Myllarniemi M, Hyytiainen M, Keski-Oja J, Koli K. Asbestos exposure induces alveolar epithelial cell plasticity through MAPK/Erk signaling. J Cell Biochem. 2012;113:2234–47.
67. Sweeney S, Berhanu D, Misra SK, Thorley AJ, Valsami-Jones E, Tetley TD. Multi-walled carbon nanotube length as a critical determinant of bioreactivity with primary human pulmonary alveolar cells. Carbon N Y. 2014;78:26–37.
68. Ohba T, Xu J, Alexander DB, Yamada A, Kanno J, Hirose A, Tsuda H, Imaizumi Y. MWCNT causes extensive damage to the ciliated epithelium of the trachea of rodents. J Toxicol Sci. 2014;39:499–505.
69. Rotoli BM, Bussolati O, Barilli A, Zanello PP, Bianchi MG, Magrini A, Pietroiusti A, Bergamaschi A, Bergamaschi E. Airway barrier dysfunction induced by exposure to carbon nanotubes in vitro: which role for fiber length? Hum Exp Toxicol. 2009;28:361–8.
70. Snyder RJ, Hussain S, Rice AB, Garantziotis S. Multiwalled carbon nanotubes induce altered morphology and loss of barrier function in human bronchial epithelium at noncytotoxic doses. Int J Nanomedicine. 2014;9:4093–105.
71. Hirano S, Fujitani Y, Furuyama A, Kanno S. Uptake and cytotoxic effects of multi-walled carbon nanotubes in human bronchial epithelial cells. Toxicol Appl Pharmacol. 2010;249:8–15.
72. Sharma CS, Sarkar S, Periyakaruppan A, Barr J, Wise K, Thomas R, Wilson BL, Ramesh GT. Single-walled carbon nanotubes induces oxidative stress in rat lung epithelial cells. J Nanosci Nanotechnol. 2007;7:2466–72.
73. Jacobsen NR, Pojana G, White P, Moller P, Cohn CA, Korsholm KS, Vogel U, Marcomini A, Loft S, Wallin H. Genotoxicity, cytotoxicity, and reactive oxygen species induced by single-walled carbon nanotubes and C(60) fullerenes in the FE1-Mutatrade markMouse lung epithelial cells. Environ Mol Mutagen. 2008;49:476–87.
74. Ravichandran P, Periyakaruppan A, Sadanandan B, Ramesh V, Hall JC, Jejelowo O, Ramesh GT. Induction of apoptosis in rat lung epithelial cells by multiwalled carbon nanotubes. J Biochem Mol Toxicol. 2009;23:333–44.
75. Nymark P, Jensen KA, Suhonen S, Kembouche Y, Vippola M, Kleinjans J, Catalan J, Norppa H, van Delft J, Briede JJ. Free radical scavenging and formation by multi-walled carbon nanotubes in cell free conditions and in human bronchial epithelial cells. Part Fibre Toxicol. 2014;11:4.
76. Patel HJ, Kwon S. Length-dependent effect of single-walled carbon nanotube exposure in a dynamic cell growth environment of human alveolar epithelial cells. J Expo Sci Environ Epidemiol. 2013;23:101–8.
77. Porter AE, Gass M, Bendall JS, Muller K, Goode A, Skepper JN, Midgley PA, Welland M. Uptake of noncytotoxic acid-treated single-walled carbon nanotubes into the cytoplasm of human macrophage cells. ACS Nano. 2009;3:1485–92.
78. Kolosnjaj-Tabi J, Hartman KB, Boudjemaa S, Ananta JS, Morgant G, Szwarc H, Wilson LJ, Moussa F. In vivo behavior of large doses of ultrashort and full-length single-walled carbon nanotubes after oral and intraperitoneal administration to Swiss mice. ACS Nano. 2010;4:1481–92.
79. Aldieri E, Fenoglio I, Cesano F, Gazzano E, Gulino G, Scarano D, Attanasio A, Mazzucco G, Ghigo D, Fubini B. The role of iron impurities in the toxic effects exerted by short multiwalled carbon nanotubes (MWCNT) in murine alveolar macrophages. J Toxicol Environ Health A. 2013;76:1056–71.
80. Kagan VE, Tyurina YY, Tyurin VA, Konduru NV, Potapovich AI, Osipov AN, Kisin ER, Schwegler-Berry D, Mercer R, Castranova V, Shvedova AA. Direct and indirect effects of single walled carbon nanotubes on RAW 264.7 macrophages: role of iron. Toxicol Lett. 2006;165:88–100.
81. Shvedova AA, Kisin E, Murray AR, Johnson VJ, Gorelik O, Arepalli S, Hubbs AF, Mercer RR, Keohavong P, Sussman N, et al. Inhalation vs. aspiration of single-walled carbon nanotubes in C57BL/6 mice: inflammation, fibrosis, oxidative stress, and mutagenesis. Am J Physiol Lung Cell Mol Physiol. 2008;295:L552–565.
82. Porter DW, Hubbs AF, Mercer RR, Wu N, Wolfarth MG, Sriram K, Leonard S, Battelli L, Schwegler-Berry D, Friend S, et al. Mouse pulmonary dose- and time course-responses induced by exposure to multi-walled carbon nanotubes. Toxicology. 2010;269:136–47.
83. Shvedova AA, Yanamala N, Kisin ER, Tkach AV, Murray AR, Hubbs A, Chirila MM, Keohavong P, Sycheva LP, Kagan VE, Castranova V. Long-term effects of carbon containing engineered nanomaterials and asbestos in the lung: one year postexposure comparisons. Am J Physiol Lung Cell Mol Physiol. 2014;306:L170–182.
84. Porter DW, Hubbs AF, Chen BT, McKinney W, Mercer RR, Wolfarth MG, Battelli L, Wu N, Sriram K, Leonard S, et al. Acute pulmonary dose-responses to inhaled multi-walled carbon nanotubes. Nanotoxicology. 2013;7:1179–94.
85. Snyder-Talkington BN, Dong C, Sargent LM, Porter DW, Staska LM, Hubbs AF, Raese R, McKinney W, Chen BT, Battelli L, et al. mRNAs and miRNAs in whole blood associated with lung hyperplasia, fibrosis, and bronchiolo-alveolar adenoma and adenocarcinoma after multi-walled carbon nanotube inhalation exposure in mice. J Appl Toxicol. 2016;36(1):161-74.
86. Kasai T, Umeda Y, Ohnishi M, Kondo H, Takeuchi T, Aiso S, Nishizawa T, Matsumoto M, Fukushima S. Thirteen-week study of toxicity of fiber-like multi-walled carbon nanotubes with whole-body inhalation exposure in rats. Nanotoxicology. 2015;9:413–22.
87. Ryman-Rasmussen JP, Cesta MF, Brody AR, Shipley-Phillips JK, Everitt JI, Tewksbury EW, Moss OR, Wong BA, Dodd DE, Andersen ME, Bonner JC. Inhaled carbon nanotubes reach the subpleural tissue in mice. Nat Nanotechnol. 2009;4:747–51.
88. Ma-Hock L, Treumann S, Strauss V, Brill S, Luizi F, Mertler M, Wiench K, Gamer AO, van Ravenzwaay B, Landsiedel R. Inhalation toxicity of multiwall carbon nanotubes in rats exposed for 3 months. Toxicol Sci. 2009;112:468–81.
89. Treumann S, Ma-Hock L, Groters S, Landsiedel R, van Ravenzwaay B. Additional histopathologic examination of the lungs from a 3-month inhalation toxicity study with multiwall carbon nanotubes in rats. Toxicol Sci. 2013;134:103–10.
90. Zhang Y, Deng J, Zhang Y, Guo F, Li C, Zou Z, Xi W, Tang J, Sun Y, Yang P, et al. Functionalized single-walled carbon nanotubes cause reversible acute lung injury and induce fibrosis in mice. J Mol Med. 2013;91:117–28.
91. Elgrabli D, Abella-Gallart S, Robidel F, Rogerieux F, Boczkowski J, Lacroix G. Induction of apoptosis and absence of inflammation in rat lung after intratracheal instillation of multiwalled carbon nanotubes. Toxicology. 2008;253:131–6.
92. Aiso S, Yamazaki K, Umeda Y, Asakura M, Kasai T, Takaya M, Toya T, Koda S, Nagano K, Arito H, Fukushima S. Pulmonary toxicity of intratracheally instilled multiwall carbon nanotubes in male Fischer 344 rats. Ind Health. 2010;48:783–95.
93. Muller J, Huaux F, Fonseca A, Nagy JB, Moreau N, Delos M, Raymundo-Pinero E, Beguin F, Kirsch-Volders M, Fenoglio I, et al. Structural defects play a major role in the acute lung toxicity of multiwall carbon nanotubes: toxicological aspects. Chem Res Toxicol. 2008;21:1698–705.
94. Shvedova AA, Kapralov AA, Feng WH, Kisin ER, Murray AR, Mercer RR, St Croix CM, Lang MA, Watkins SC, Konduru NV, et al. Impaired clearance and enhanced pulmonary inflammatory/fibrotic response to carbon nanotubes in myeloperoxidase-deficient mice. PLoS One. 2012;7:e30923.
95. Teeguarden JG, Webb-Robertson BJ, Waters KM, Murray AR, Kisin ER, Varnum SM, Jacobs JM, Pounds JG, Zanger RC, Shvedova AA. Comparative proteomics and pulmonary toxicity of instilled single-walled carbon nanotubes, crocidolite asbestos, and ultrafine carbon black in mice. Toxicol Sci. 2011;120:123–35.
96. Shvedova AA, Kisin ER, Murray AR, Mouithys-Mickalad A, Stadler K, Mason RP, Kadiiska M. ESR evidence for in vivo formation of free radicals in tissue of mice exposed to single-walled carbon nanotubes. Free Radic Biol Med. 2014;73:154–65.
97. Wang X, Xia T, Duch MC, Ji Z, Zhang H, Li R, Sun B, Lin S, Meng H, Liao YP, et al. Pluronic F108 coating decreases the lung fibrosis potential of multiwall carbon nanotubes by reducing lysosomal injury. Nano Lett. 2012;12:3050–61.

3.4.3. How does this work contribute to nanotoxicology knowledge?

In the previous manuscripts (Vietti et al., 2013; Vietti et al., 2015) we showed that the proliferative activity of MWCNT on fibroblasts strongly reflects their capacity to induce lung fibrosis and, in this review, we placed the importance of the direct effect of CNT on fibroblast activation in a broader context. We highlighted that other indirect mechanisms of action, via macrophages and epithelial cells, also contribute and are probably essential to the pro-fibrotic activity of CNT.

Based on the AOP we developed, we recently started to systematically investigate pro-inflammatory and pro-fibrotic responses to a series of CNT samples (Table 1) on cells indirectly involved in the development of fibrosis (macrophages and lung alveolar epithelial cells). For this purpose, we collaborated with the group of Prof. T. Tetley (Imperial College of London, UK) to test the responses of a unique transformed human alveolar type-I-like epithelial cells (TT1) developed in their laboratory (Sweeney et al., 2014), as well as primary human alveolar type II epithelial cells (ATII) to CNT.

Sample	OD (nm)	Length (µm)	Functionalisation	Walls
NM400	5 - 35	3	-	MW
MWCNT long	20 - 30	10 - 30	-	MW
MWCNT short	20 - 30	0.5 - 2	-	MW
MWCNT thick	50 - 80	10 - 30	-	MW
MWCNT thin	< 8	10 - 30	-	MW
MWCNT OH	20 - 30	10 - 30	OH	MW
MWCNT COOH	20 - 30	10 - 30	COOH	MW
MWCNT NH2	13 - 18	1 - 12	NH2	MW
SWCNT	1 - 2	3 - 30	-	SW

Table 1: Physico-chemical characteristics of CNT. OD: outer diameter.

Our purpose was to test an additional series of in vitro endpoints vs fibroblast proliferation to predict the lung fibrotic activity of CNT and to understand which one or which set of endpoints could be the most relevant. We explored the effect of 9 different CNT with different physico-chemical properties, including length, diameter and functionalization groups (Table 1), on MLg for their proliferative effect, as well as on differentiated monocytes (THP-1), human lung epithelial type II cells (A549), TT1 and ATII cells focusing on their potential to release pro-inflammatory (IL-1β, IL-6 and IL-8) and pro-fibrotic (TGF-β1 and PDGF) mediators after 24h exposure to CNT (7.5-30 μg/cm^2). These mediators were measured by ELISA on the collected supernatant of cells exposed to CNT. Several CNT directly stimulated fibroblast proliferation or induced the release of IL-1β, IL-6, IL-8 and TGF-β1 from macrophages or epithelial cells as summarized and reported in Table 2.

	Mouse	Fibroblasts	Macrophages			Epithelial cells								
	C57BL/6	MLg	THP-1			A549			TT1			ATII		
	OH-proline	*Proliferation*	*IL-1β*	*TGF-β1 activated*	*PDGF*	*IL-8*	*IL-6*	*TGF-β1 activated*	*IL-8*	*IL-6*	*TGF-β1 activated*	*IL-8*	*IL-6*	*TGF-β1 activated*
NM400	+	+	+	/		-/		/	+	/	+	/	+	
MWCNT long	+	+	+	+/		-		+	+	+	/	+	+	
MWCNT short	/	/	+	/		/		+	+	/	/	/	/	
MWCNT thick	/	/	+	+		/		+	/	/	/	/	+	No release
MWCNT thin	+	-	/	+		-		+	+	+	/	/	+	
MWCNT OH	+	+	+	+		-		/	/	+	/	/	+	
MWCNT COOH	+	-	/	+		-		+	/	+	+	/	+	
MWCNT NH2	+	+	+	+		-		/	/	/	/	+	+	
SWCNT	+	+	+	+		-		+	/	+	/	/	+	
Accuracy		7/9	5/9	6/9		?		4/9	4/9	7/9	4/9	4/9	8/9	

Table 2: Comparison of in vivo lung fibrogenic activity (100 μg CNT pharyngeal aspiration) with in vitro (MLg, THP-1, A549, TT1 and ATII) data (exposure to CNT 30 μg/cm^2). Statistically significant positive changes compared to control were marked as "+", negative as "-", and no significant changes were noted as "/". Accuracy represents to the closeness of in vitro data to in vivo result.

Further experiments, such as the release of PDGF or TGF-β, have to be (re)-performed in order to complete and confirm the present data. Finally, we compared these preliminary in vitro results with the in vivo lung fibrotic responses. Briefly, in vivo data were obtained 2 months after pharyngeal aspiration of the different CNT (100 µg/mouse) and the lung fibrotic response was quantified by measuring OH-proline lung content, as a marker of collagen, and by sirius red staining of lung sections. Only short and thick MWCNT did not induce lung fibrosis, while the other CNT showed a significant increase of OH-proline (Figure 7).

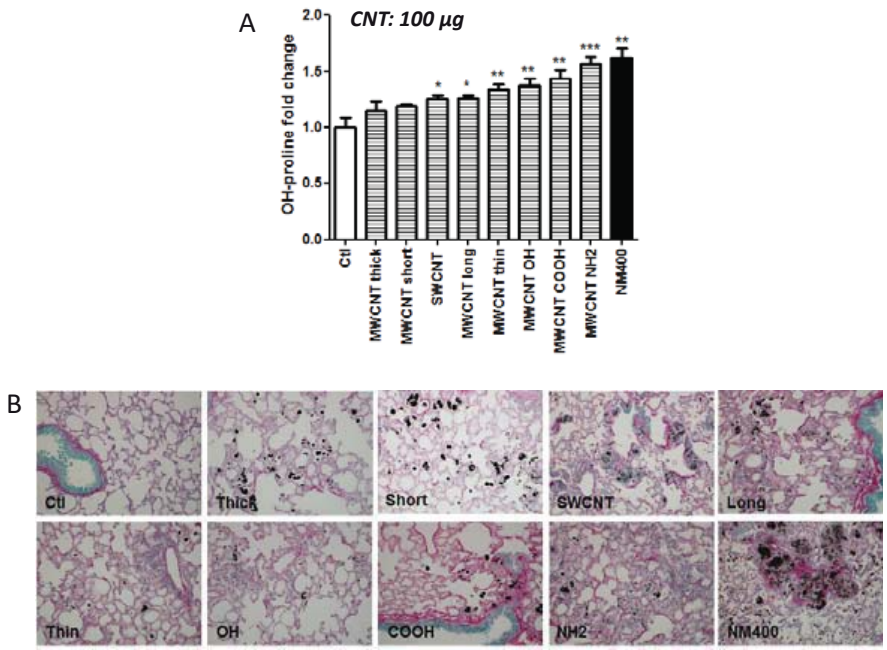


Figure 7. In vivo lung fibrotic response to several CNT assessed by (A) OH-proline and (B) Sirius red staining of lung sections 2 months after pharyngeal aspiration of CNT (100 µg/mouse).

We observed that the release of IL-6 from both TT1 and ATII cells upon CNT exposure highly correlated with the in vivo findings, like the vitro proliferative assay on fibroblasts (Table 2). Thus, IL-6 could be selected as another useful biomarker, in addition to the proliferative activity of CNT on fibroblasts, to investigate and predict the toxic potential of CNT.

In conclusion, these results enable to fill some of the gaps identified in the review. Regarding the AOP, this contributed to identify mechanism-based biomarkers to investigate the toxicity of CNT. In this way, IL-6 could be added to the AOP as another pro-inflammatory mediator relevant for the development of fibrosis in response to CNT exposure and/or for the identification of potentially pro-fibrotic CNT.

REFERENCES

Sweeney S, Berhanu D, Misra SK, Thorley AJ, Valsami-Jones E, Tetley TD. 2014. Multi-walled carbon nanotube length as a critical determinant of bioreactivity with primary human pulmonary alveolar cells. Carbon N Y 78**,** 26-37.

Vietti G, Ibouraadaten S, Palmai-Pallag M, Yakoub Y, Bailly C, Fenoglio I, Marbaix E, Lison D, Van Den Brule S. 2013. Towards predicting the lung fibrogenic activity of nanomaterials: experimental validation of an in vitro fibroblast proliferation assay. Part Fibre Toxicol 10**,** 52.

Vietti G, Ibouraadaten S, Palmai-Pallag M, Yakoub Y, Piret JP, Marbaix E, Lison D, Van Den Brule S. 2015. Towards predicting the lung fibrogenic activity of MWCNT: Key role of endocytosis, kinase receptors and ERK 1/2 signaling. Nanotoxicology**,** 1-13.

IV. GENERAL CONCLUSIONS, PERSPECTIVES AND RECOMMENDATIONS

Some respirable CNT exhibit pathogenic potentials similar to asbestos fibers, including a capacity to induce lung fibrosis. As a result, there is an urgent need to evaluate and prevent these adverse health impacts by developing in vitro assays suitable for predicting the lung fibrogenic activity of CNT. Thus, a comprehensive understanding of the physico-chemical characteristics of pathogenic CNT and of the cellular mechanisms of action by which CNT trigger these adverse effects is required.

When this project was initiated, information about these issues was almost absent. In our working hypotheses we assumed that fibroblast proliferation could play a key role in lung fibrosis induced by CNT and that a fibroblast proliferation assay could allow predicting the in vivo fibrotic response. We addressed these needs by developing a predictive in vitro model that allows rapidly assessing of a critical endpoint for the development of lung fibrosis. The in vitro fibroblast proliferation assay strongly correlates with in vivo fibrosis findings, supporting a predictive value of this in vitro assay. We also identified cellular mechanisms involved in the proliferative activity of CNT on fibroblasts, by pointing out a crosstalk between CNT, kinase receptors, ERK 1/2 signaling and endocytosis to stimulate the proliferation of fibroblasts. A key point of our studies was the correlation between the in vitro and in vivo data, indicating the potential usefulness of the in vitro model as a predictive screening tool for fibrogenicity testing of CNT. Thus, in a near future, this model could be useful to reduce animal experiments. Compared to animal experiments, in vitro assays are also more rapid, less expensive and can be performed with a limited amount of CNT sample. Thus, we were able to confirm our hypotheses based on these results.

We highlighted that the length and the diameter of CNT constitute important physico-chemical determinants for their capacity to induce lung fibrosis. However, it has to be underlined that other physico-chemical properties can also contribute to the biological activity of CNT. The influence of

morphology, purity, surface properties, defects, functionalization and number of walls generally appear to strongly determine CNT toxicity (Rittinghausen et al., 2014; Kagan et al., 2006; Li et al., 2013; Muller et al., 2008), although it remains unclear how exactly these parameters contribute because experimental data are conflicting.

Another step in which we have contributed came with the organization of the mechanisms involved in CNT-induced lung fibrosis through the development of a tentative AOP. We highlighted that both direct and indirect mechanisms of action on fibroblasts contribute to the pro-fibrotic activities of CNT. In this context, we found that different signaling pathways and in vitro assays could be predictors of in vivo activity and, in our opinion, a combination of these, such as fibroblast proliferation and the release of IL-6 from epithelial cells, can probably better predict the pro-fibrotic activity of CNT. Thus, these available assays could be considered as key starting points for evaluating the toxic potential of CNT.

Regarding the hazard evaluation of CNT, it is necessary to underline that lung fibrosis is only one toxicity endpoint relevant for CNT. When assessing risks associated with a material, especially when this has structural characteristics resembling fibers, it is crucial to address its potential carcinogenic effects. Currently, different observations indicate that CNT are able to develop mesothelioma in murine model (Nagai et al., 2011; Xu et al., 2012; Rittinghausen et al., 2014), thus carcinogenic activity should also be taken into account for a global assessment of the health hazard posed by CNT exposure.

The American federal agency that provides guidance on occupational safety and human health issues, i.e. NIOSH, proposed in 2013 to lower the REL for CNT from 7, as proposed in 2010, to 1 $\mu g/m^3$, to assure safe and healthful working conditions. According to these recommendations, all types of CNT are considered as a respiratory hazard and exposure should

be controlled below the REL, or at least until results from research can fully explain the physical-chemical properties of CNT that define their inhalation toxicity. A number of knowledge gaps are still open and additional data and information are needed to assist evaluating the occupational safety and health concerns of working with CNT.

Among the main issues that have to be addressed and investigated we can consider the following:

- *Need to focus on mechanistic studies.*

Knowledge of the mechanism of toxicity of a substance enhances the ability of preventing toxicity and of designing safer materials. However, understanding mechanisms, such as the development of lung fibrosis, is a complex task and presumes a general knowledge of fundamental biological processes. We contributed in this area by proposing a draft AOP, which reports and highlights cellular response relationships across specific biological levels, allowing a general overview of the sequence of events identified as important in the development of pulmonary fibrosis. According to these observations, we suggest to deeply investigate on the mode of action of CNT with different physico-chemical properties in lung fibrosis, by focusing on new targets that we underlined in the AOP. For example, it appears important to investigate the mechanisms involved in the release of pro-fibrotic mediators TGF-β and PDGF from lung cells, as there is still no data concerning these important proximal effects of CNT in the development of fibrosis.

- *Need to validate in vitro studies with in vivo findings.*

A majority of mechanistic studies in the literature have been performed in cultured cells without parallel in vivo studies, as discussed in chapter 3.4. However, to validate in vitro observations and to define their value, it is necessary to confirm in vitro results in vivo. Thus, we recommend to

systematically integrate animal data to validate the relevance of in vitro findings.

- *Need to study representative CNT exposure levels.*

Researchers involved in mechanistic studies have to focus more attention on CNT materials that can be found in workplace environments. There is, therefore, a need to develop more efforts for monitoring the potential emission of CNT and potential exposure of workers. Lee et al. (Lee et al., 2010) found full-shift total gravimetric mass concentrations in personal breathing zone measurements between 7.8 to 320.8 μg/m^3 by visiting 13 facilities ranging from industrial to lab scale settings, i.e. much higher doses than those recommended by NIOSH at 1 μg/m³. In a more recent study conducted on 13 sites to assess exposure to CNT, it has been shown that, although the majority of samples were below the NIOSH REL, 30% of the inhalable samples were found to be >1 μg/m³ (Dahm et al., 2015). However, information on workplace exposure is still very limited. In this context, we would recommend deeply investigating the exposure scenarios for the production, use and release of CNT in workplace environments to provide knowledge on real exposure that can be used for in vivo and in vitro studies. Moreover, also qualitative characterization of CNT released during the machining (cutting, drilling, boring) of composite polymers containing CNT or from products or articles containing CNT-composites could be useful to investigate, in order to evaluate and assess the toxic impact of modified material. Nowack et al. (Nowack et al., 2012) have evaluated how different environmental conditions affect the alteration of composite material, as well as the transformation of the CNT once they are released from the composite. They concluded that the release of CNT from products or articles containing CNT-composites may occur over a long time scale and thus that this material will probably alter at a slow rate. These transformation processes are thought to change CNT aggregation,

dispersibility, and interaction with biota in the environmental compartment. In conclusion, quantitative and qualitative exposure studies in this area should be conducted to provide further knowledge about this topic for in vitro and in vivo studies.

- *Need to develop chronic in vitro studies.*

Fibrosis is a multi-step process requiring long-term exposure to a toxicant. Indeed, the latency period (time period between harmful contact and emergence of the actual resulting illness) for fiber materials, such as asbestos, to induce fibrosis in humans, is of about 12 to 20 years, and potentially up to 40 years (Mossman and Churg, 1998). Moreover, correlating acute (24-72 h) in vitro CNT exposure findings to one-time exposure over a longer time period (1-2 months) in vivo models is problematic, underlining the need for a new approach to assess chronic effects such as CNT pro-fibrotic effects in cell cultures. Few studies have been published concerning the chronic exposure of mesothelial cells to low-doses of non-cytotoxic concentrations of CNT in order to investigate mesothelioma pathogenesis (Lohcharoenkal et al., 2013; Luanpitpong et al., 2014). Chronic in vitro studies focusing on fibrosis have not been reported. In view of all these considerations, we recommend to explore and implement chronic in vitro exposure models and compare them with acute in vitro assays to understand which can be the most realistic to use for predicting the fibrotic activities of CNT.

REFERENCES

Dahm MM, Schubauer-Berigan MK, Evans DE, Birch ME, Fernback JE, Deddens JA. 2015. Carbon Nanotube and Nanofiber Exposure Assessments: An Analysis of 14 Site Visits. Ann Occup Hyg 59**,** 705-23.

Kagan VE, Tyurina YY, Tyurin VA, Konduru NV, Potapovich AI, Osipov AN, Kisin ER, Schwegler-Berry D, Mercer R, Castranova V, Shvedova AA. 2006. Direct and indirect effects of single walled carbon nanotubes on RAW 264.7 macrophages: role of iron. Toxicol Lett 165**,** 88-100.

Lee JH, Lee SB, Bae GN, Jeon KS, Yoon JU, Ji JH, Sung JH, Lee BG, Lee JH, Yang JS, Kim HY, Kang CS, Yu IJ. 2010. Exposure assessment of carbon nanotube manufacturing workplaces. Inhal Toxicol 22**,** 369-81.

Li R, Wang X, Ji Z, Sun B, Zhang H, Chang CH, Lin S, Meng H, Liao YP, Wang M, Li Z, Hwang AA, Song TB, Xu R, Yang Y, Zink JI, Nel AE, Xia T. 2013. Surface charge and cellular processing of covalently functionalized multiwall carbon nanotubes determine pulmonary toxicity. ACS Nano 7**,** 2352-68.

Lohcharoenkal W, Wang L, Stueckle TA, Dinu CZ, Castranova V, Liu Y, Rojanasakul Y. 2013. Chronic exposure to carbon nanotubes induces invasion of human mesothelial cells through matrix metalloproteinase-2. ACS Nano 7**,** 7711-23.

Luanpitpong S, Wang L, Manke A, Martin KH, Ammer AG, Castranova V, Yang Y, Rojansakul Y. 2014. Induction of stemlike cells with fibrogenic properties by carbon nanotubes and its role in fibrogenesis. Nano Lett 14**,** 3110-6.

Mossman BT, Churg A. 1998. Mechanisms in the pathogenesis of asbestosis and silicosis. Am J Respir Crit Care Med 157**,** 1666-80.

Muller J, Huaux F, Fonseca A, Nagy JB, Moreau N, Delos M, Raymundo-Pinero E, Beguin F, Kirsch-Volders M, Fenoglio I, Fubini B, Lison D. 2008. Structural defects play a major role in the acute lung toxicity of multiwall carbon nanotubes: toxicological aspects. Chem Res Toxicol 21**,** 1698-705.

Nagai H, Okazaki Y, Chew SH, Misawa N, Yamashita Y, Akatsuka S, Ishihara T, Yamashita K, Yoshikawa Y, Yasui H, Jiang L, Ohara H, Takahashi T, Ichihara G, Kostarelos K, Miyata Y, Shinohara H, Toyokuni S. 2011. Diameter and rigidity of multiwalled carbon nanotubes are critical factors in mesothelial injury and carcinogenesis. Proc Natl Acad Sci U S A 108**,** E1330-8.

Nowack B, Ranville JF, Diamond S, Gallego-Urrea JA, Metcalfe C, Rose J, Horne N, Koelmans AA, Klaine SJ. 2012. Potential scenarios for nanomaterial release and subsequent alteration in the environment. Environ Toxicol Chem 31**,** 50-9.

Rittinghausen S, Hackbarth A, Creutzenberg O, Ernst H, Heinrich U, Leonhardt A, Schaudien D. 2014. The carcinogenic effect of various multi-walled carbon

nanotubes (MWCNTs) after intraperitoneal injection in rats. Part Fibre Toxicol 11**,** 59.

Xu J, Futakuchi M, Shimizu H, Alexander DB, Yanagihara K, Fukamachi K, Suzui M, Kanno J, Hirose A, Ogata A, Sakamoto Y, Nakae D, Omori T, Tsuda H. 2012. Multi-walled carbon nanotubes translocate into the pleural cavity and induce visceral mesothelial proliferation in rats. Cancer Sci 103**,** 2045-50.